Lawrence Berkeley National Laboratory
Recent Work

Title
STATUS OF THE DOE BATTERY AND ELECTROCHEMICAL TECHNOLOGY PROGRAM III

Permalink
https://escholarship.org/uc/item/2km1d92p

Author
Roberts, R.

Publication Date
1982-02-01

eScholarship.org Powered by the California Digital Library
University of California

LBL-14438
UC-94cb

Lawrence Berkeley Laboratory
UNIVERSITY OF CALIFORNIA

ENERGY & ENVIRONMENT DIVISION

STATUS OF THE DOE BATTERY AND ELECTROCHEMICAL TECHNOLOGY PROGRAM III

R. Roberts

February 1982

RECEIVED
LAWRENCE
BERKELEY LABORATORY
JUN 15 1982
LIBRARY AND
DOCUMENTS SECTION

TWO-WEEK LOAN COPY
This is a Library Circulating Copy which may be borrowed for two weeks. For a personal retention copy, call Tech. Info. Division, Ext. 6782.

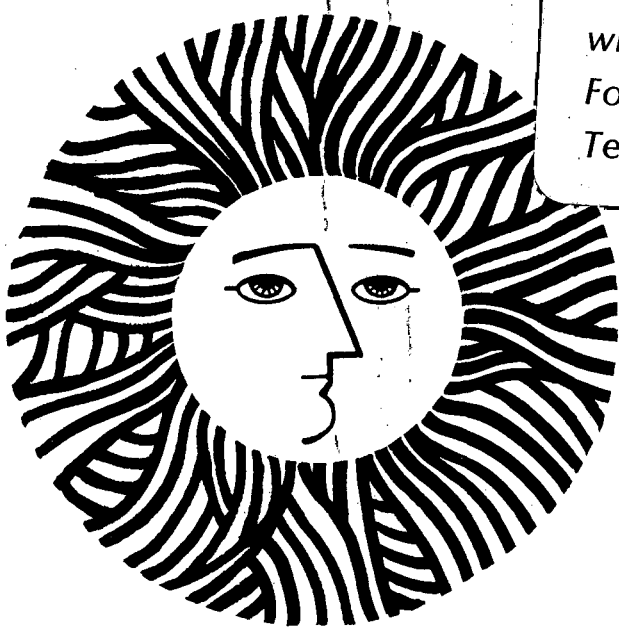

Prepared for the U.S. Department of Energy under Contract DE-AC03-76SF00098

DISCLAIMER

This document was prepared as an account of work sponsored by the United States Government. While this document is believed to contain correct information, neither the United States Government nor any agency thereof, nor the Regents of the University of California, nor any of their employees, makes any warranty, express or implied, or assumes any legal responsibility for the accuracy, completeness, or usefulness of any information, apparatus, product, or process disclosed, or represents that its use would not infringe privately owned rights. Reference herein to any specific commercial product, process, or service by its trade name, trademark, manufacturer, or otherwise, does not necessarily constitute or imply its endorsement, recommendation, or favoring by the United States Government or any agency thereof, or the Regents of the University of California. The views and opinions of authors expressed herein do not necessarily state or reflect those of the United States Government or any agency thereof or the Regents of the University of California.

Status of the DOE Battery and Electrochemical Technology Program III

R. Roberts

February 1982

MTR-81W223

Sponsor: Lawrence Berkeley Laboratory
University of California
Berkeley, CA 94720
Purchase Order: 4513810

The MITRE Corporation
Metrek Division
1820 Dolley Madison Boulevard
McLean, Virginia 22102

ABSTRACT

This report reviews the status of the Department of Energy Subelement on Electrochemical Storage Systems. It emphasizes material presented at the Fourth U.S. Department of Energy Battery and Electrochemical Contractors' Conference, held June 2-4, 1981. The conference stressed secondary batteries, however, the aluminum/air mechanically rechargeable battery and selected topics on industrial electrochemical processes were included.

The potential contributions of the battery and electrochemical technology efforts to supported technologies: electric vehicles, solar electric systems, and energy conservation in industrial electrochemical processes, are reviewed. The analyses of the potential impact of these systems on energy technologies as the basis for selecting specific battery systems for investigation are noted.

The battery systems in the research, development, and demonstration phase discussed include:

Aqueous Mobile Batteries (near term): lead-acid, iron/nickel-oxide, zinc/nickel-oxide.

Advanced Batteries: aluminum/air, iron/air, zinc/bromine, zinc/ferricyanide, chromous/ferric, lithium/metal sulfide, sodium/sulfur.

Exploratory Batteries: lithium organic electrolyte, lithium/polymer electrolyte, sodium/sulfur(IV) chloroaluminate, calcium/iron disulfide, lithium/solid electrolyte.

Supporting research on electrode reactions, cell performance modeling, new battery materials, ionic conducting solid electrolytes, and electrocatalysis is reviewed. Potential energy saving processes for the electrowinning of aluminum and zinc, and for the electrosynthesis of inorganic and organic compounds are included.

ACKNOWLEDGEMENT

The author wishes to express his appreciation to the participants in the Fourth U.S. Department of Energy Battery and Electrochemical Contractors' Conference (June 1981) for their cooperation in furnishing supplemental information and commenting on the initial draft of this report. The advice and suggestions of Dr. Frank McLarnon, the contract monitor at the Lawrence Berkely Laboratory, and Dr. Albert R. Landgrebe of the Department of Energy have been of great help.

Mr. Ernest P. Krajeski, Associate Department Head, Ms. Vivian Aubuchon, editor, and Ms. Susan Armstrong and Ms. Sharon Hill, secretaries of the Metrek Division of the MITRE Corporation, have contributed much to the preparation of this report. Their assistance is gratefully acknowledged.

This work was supported by the Assistant Secretary for Conservation and Renewable Energy, Office of Energy Systems Research, Energy Storage Division of the U.S. Department of Energy under Contract No. DE-AC03-76SF00098; through Subcontract PO 4513810.

EXECUTIVE SUMMARY

This report is the third in a series entitled Status of the DOE Battery and Electrochemical Technology Program. The material emphasizes progress and changes in direction of the Electrochemical Storage Systems (ECS) Program from December 1979 to June 1981. The primary sources of information were publications associated with the Fourth U.S. Department of Energy Battery and Electrochemical Contractors' Conference held June 2-4, 1981.

Although the policies of the Reagan administration had not impacted on the program reviewed at the fourth Contractors' Conference, they will affect future efforts. The Federal role in energy research and development under the Reagan Administration was described by Dr. M. Savitz, the Department of Energy's Deputy Assistant Secretary for Conservation:

> "The Federal government should continue to support long-term, generic and high-risk, but potentially high-payoff research, that private industry will not undertake. However, it is the Administration's conviction that the marketplace can, and will, perfect and commercialize new energy technologies more efficiently and effectively than government, especially if energy prices are allowed to reflect their true replacement costs. Accordingly, industry is to expect to support development and demonstration of promising near-term technology and to be responsible for their ultimate market or commercial development."

The immediate reported effect of the above description of the Federal government's role has been the curtailment of further purchases of electric vehicles for in-fleet testing and the dropping

of plans to proceed with the Storage Battery Electrical Energy Demonstration (SBEED). The intent of SBEED was to demonstrate the battery load-leveling concept to electric utilities.

Simulation testing of advanced vehicle propulsion systems has been initiated. Simulation testing has been utilized to estimate propulsion efficiencies of 76% and increased energy efficiency through the use of regenerative braking. The results of electric vehicle systems studies emphasize the importance of high specific energy for high market penetration. A hybrid gasoline/battery vehicle propulsion system is undergoing dynamometric and track testing. The applicability of fuel cells in transportation has been evaluated and the fuel cell/battery hybrid power plant provides performance equivalent to an internal combustion engine, but with greater fuel economy.

The Battery Energy Storage Test (BEST) facility was dedicated during May 1981. The purpose of the facility, partially supported by the Electric Power Research Institute and the host utility, the Public Service Electric and Gas Company, is to test and evaluate the operating characteristics of battery systems and power conversion equipment in an operating utility environment. Initial tests will use lead-acid batteries. Later tests will employ zinc/chlorine batteries being produced in a pilot plant operated by Energy Development Associates, a subsidiary of Gulf and Western.

Along with performance evaluation, researchers are conducting economic assessments on the use of storage batteries in optimally expanded utility systems. As an alternative to utilities using battery storage, batteries may be installed on the customer side of the meter. This has been evaluated at the Battelle Columbus Laboratories. The economic viability of this type of storage is highest for customers with large time-of-day rate differentials. The New York Energy Research and Development Authority's study of the use of battery storage to meet peak loads in the New York City subway system has been projected to offer several benefits:

- Reduced demand charges;
- A receptor for electricity produced by regenerative braking;
- Increased operational safety; and
- Improved utility load management, petroleum conservation, and deferment of new generation capacity.

The evaluation of battery requirements for use in photovoltaic/battery energy storage systems is continuing at Sandia National Laboratories. The SOLSTOR computer program is being used. It was shown that the state-of-charge profile for the battery is highly sensitive to time-of-day electricity pricing. A study at Argonne National Laboratory on the optimum battery location concluded that, for utility connected photovoltaic systems, there was no advantage in distributing the battery storage units below the substation level.

Studies on the selection of batteries for photovoltaic electrical energy storage favored the zinc/bromine battery. Other continuous feed batteries were not as broadly compatible with solar photovoltaics. However, work to improve these and selected non-flow batteries to satisfy specific solar photovoltaic system requirements continues. A facility for testing batteries for solar system application is being established at Sandia National Laboratory. Various testing procedures, to meet variations in photovoltaic battery system performance requirements, are to be used.

The advanced lead-acid battery development has led to success in increasing the specific energy and cycle life of the lead-acid battery. The use of grid designs which give more uniform current distributions together with electrolyte circulation has led to a longer cycle life. Contributing to the higher specific energy has been the development of lighter weight battery containers. To further improve the specific energies of lead-acid batteries, researchers are exploring the use of conducting plastic and metal-coated plastic grids, lead-plated copper grids, and graphite fibers in the active material of the positive electrode. Improved lead-acid batteries, to meet the requirements for dispersed electrical systems and stand-alone solar systems, are being investigated. Sealed batteries are being emphasized for stand-alone solar applications.

Iron/nickel-oxide battery modules meeting most of the 1980 performance goals have been demonstrated. Laboratory-produced batteries have given an in-vehicle performance approximately 200% greater than the state-of-the-art lead-acid battery. The ability to reduce the cost of manufacturing these batteries to that projected as necessary for high market penetration of the electric vehicle is still to be established. Progress has also been made in the zinc/nickel-oxide battery but reliable battery cycle life remains to be proven, even though the U.S. Army Electronics Research and Development Command has achieved 500 cycles in single-cell tests. One contractor has withdrawn from the program because of the high projected cost of mass-produced sintered-nickel positive electrodes. Studies on the production of nickel electrodes without sintering of the nickel plaque continue, as projections indicate this approach is capable of meeting cost goals.

Considerable progress is being made in the development of continuous and semicontinuous reactant feed batteries. Much progress has been made on the iron/air cell, especially in improving the cycling of the bifunctional air electrode (i.e., one that can be used for both charge and discharge). Over 500 cycles have been demonstrated in laboratory cells. Advances in air-electrode research include better definition of the function and requirements for electrocatalysts during charge and discharge. Advances have also been made in the aluminum/air battery. Full-scale electrodes

have shown the desired performance and the concept of rapid mechanical recharging has been demonstrated in full-scale cells.

Life testing of components of the zinc/bromine system has not identified any life-limiting mechanism. Parasitic losses have been decreased through improved design of the electrolyte system. Stable performance has been demonstrated in 3 and 10kWh sub-modules. A stand-alone battery is scheduled to be delivered to the Sandia National Laboratories for evaluation as the battery energy storage component of a solar-photovoltaic system. There is, however, a large variance in the projected manufacturing cost of the zinc/bromine battery by the two development groups: $28/kWh by Exxon and $88/kWh by Gould, Inc. The difference between these cost estimates requires resolution.

Progress has also been made on the zinc/ferricyanide battery, which has been transferred from the exploratory to the advanced battery program, as well as the National Aeronautic and Space Administration's chromous/ferric redox battery. Both are being considered for potential applications in solar-photovoltaic and dispersed energy systems.

The failure of one of the Mark I lithium-aluminium/iron sulfide batteries led to a thorough evaluation of possible causes. The primary failure mechanism was cell shorting due to electrolyte transport within the cell. This has led to greater emphasis on cell reproducibility and changes in the separator to reduce electrolyte

mobility. Pressed, powdered mixtures of magnesium oxide and electrolyte, as the separator, have yielded engineering cells achieving 300 to 400 deep discharge cycles. A group of 10 cells has operated for over 170 cycles without failure. A cell design producing 100Wh/kg has also been demonstrated.

Efforts on sodium/sulfur batteries have led to improved reproducibility of cell components. Battery modules have been designed that permit bypassing of failed cells and have sufficient redundancy to compensate for cell failures. 25kWh modules of load-leveling batteries have been constructed and demonstrated to have capacities equal to or greater than the design capacity. A 100kWh battery, consisting of four 25kWh modules in series, has been constructed and it met design performance. A number of safety tests have been conducted on nine-cell sodium/sulfur batteries without runaway temperatures being observed. The sodium/sulfur battery technology has been advanced to pilot plant production of cells.

Supporting research activities have provided valuable guidance to battery developers. These research activities have revealed details of chemical and structural changes in secondary batteries and devised mathematical models of cell performance. As has been noted, the zinc/bromine and zinc/ferricyanide batteries have been transferred from this category to exploratory research and are now being evaluated for specific applications. The sodium/sulfur(IV) chloroaluminate cell has demonstrated excellent specific energy

and reversibility in laboratory size cells. It is approaching readiness for evaluation in large cells and modules. Studies on high temperature battery materials suggest the possible use of a lithium-tin negative electrode matrix for improving the cycle life of the lithium-aluminum/iron sulfide cells. The reversibility of the lithium/thionylchloride cell and an all solid state lithium cell has also been demonstrated. The application of advanced laser Raman spectroscopy and other methods to the study of electrode behavior has shed light on the fundamental requirements for reversibility of electrode reactions.

Studies on energy conservation in electrochemical technology have been limited to the most promising areas selected from previous studies. Oxygen cathodes developed specifically to permit reduced energy use in the chlor-alkali industry have been evaluated in pilot plant cells and further evaluation is scheduled in commercial cells. The use of a hydrogen anode for reducing overall energy consumption in zinc electrolysis has been demonstrated and is ready for commercialization. The possibility of low energy-consuming electrochemical synthetic routes to organic compounds is being explored.

Overall, the various research efforts have resulted in marked improvements in many battery systems, spurred the advancement of several systems to the point of technology transfer to the commercial sector, and pointed the way to reduced energy consumption in selected electrochemical technologies.

TABLE OF CONTENTS

TABLE OF CONTENTS (Continued)

TABLE OF CONTENTS (concluded)

LIST OF ILLUSTRATIONS

LIST OF ILLUSTRATIONS (continued)

LIST OF ILLUSTRATIONS (continued)

LIST OF ILLUSTRATIONS (continued)

LIST OF ILLUSTRATIONS (concluded)

LIST OF TABLES

LIST OF TABLES (continued)

LIST OF TABLES (concluded)

1.0 INTRODUCTION

The Department of Energy (DOE) program on batteries and electrochemical technologies is carried out by the Electrochemical Energy Storage Branch (ECS) in the Office of Energy Storage Research, which is under the administration of the Assistant Secretary, Conservation and Renewable Energy.

Two earlier reports[1][2] reviewed the status of the ECS program as of June 1978 and December 1979. The first of these status reports (SR-I) includes background information on the battery and other technologies of interest as well as their status.[1] The second report (SR-II) emphasizes technical progress and the results of system studies.[2] SR-II includes background information concerning cell systems not described in SR-I and electrochemical technologies. This status report, the third in the series, will again emphasize both progress and changes in program direction. The primary information source for this report is the material presented at the Fourth U.S. Department of Energy Battery and Electrochemical Contractors' Conference (BECC), held 2-4 June 1981.[3] The conference program is included as Appendix A. Information gleaned from conference presentations is supplemented by material included in the Electrochemical Storage Systems Program Summary (ECPS),[4] contractor reports, and contractor publications since June 1979. Reports presented at the BECC and information

contained in the ECPS will not be specifically cited; all other references are appropriately cited.

1.1 Current Program Guidance

Before reviewing the ECS program, this report includes a brief review of the anticipated impact of the Reagan Administration policies on energy research and development. Although the policies have not affected the electrochemical energy storage program reviewed, they are expected to effect changes in the future program structure, the types of efforts supported, and funds available.

The administration's policies within which these adjustments are to be made were reviewed by Dr. Maxine Savitz, Deputy Assistant Secretary for Conservation.[5] She noted that the issues and solutions over the coming decade will be carried out within the following context:

- Reducing the nation's vulnerability to oil supply disruption;
- Attaining economic efficiency in the supply and use of energy; and
- Making the transition to domestically abundant fuels and renewable domestic energy sources.

Savitz further noted that the projected contribution of conservation to energy savings has been from 20% to 45% without introducing advanced conservation technologies. Current research and development efforts are expected to lead to the achievement of even greater energy savings.

Savitz reported that the current Administration's energy policy and revised budget request are based on the following underlying assumptions:

- The nation's energy problems will be solved primarily by the American people themselves--by consumers, workers, managers, inventors, and investors in the private sector--not by government.
- The government's role is to establish sound public policies based on economic principles, so that individuals and firms in the private sector have incentives to produce and conserve energy efficiently.
- The government's role is not to select and promote favored sources of energy.

With respect to the Federal role in energy research and development, Dr. Savitz stated:

> "The Federal government should continue to support long-term, generic and high-risk (but potentially high-payoff) research, that private industry will not undertake. However, it is the Administration's conviction that the marketplace can, and will, perfect and commercialize new energy technologies more efficiently and effectively than government, especially if energy prices are allowed to reflect their true replacement costs. Accordingly, industry is to expect to support development and demonstration of promising near-term technologies and to be responsible for their ultimate market or commercial development."

Conservation, according to the Deputy Assistant Secretary, "means developing use patterns that reflect the true marginal cost of additional energy production and use. This includes improving the efficiency of energy use as well as developing less energy-intensive technologies for producing goods and services."

Within the guidelines of the current administration and the goals of the conservation program, the role of the electrochemical energy storage program is the support of long-term, high risk, generic research. This emphasis will decrease the role of the ECS branch in the demonstration and commercialization of batteries and other electrochemical technologies. This decreased role is reflected in the FY 1982 budget for the ECS branch program (Table I).

1.2 ECS Program Organization

The organizational structure of the Office of the Deputy Assistant Secretary for Conservation is shown in Figure I. The Electrochemical Energy Storage Branch is part of the Office of Energy Systems Research. The ECS research and development efforts are strongly supportive of other activities within and outside of the Office of Conservation. The applications research activities, included in SR-II as "missions," are end-use oriented and are supported by ECS within its own budget or with funds transferred from other activities. The applications research includes system studies to help guide the selection of specific investigations. The applied research areas include:

- Mobile applications--electric and hybrid vehicles;
- Solar applications--photovoltaic and wind systems;
- Dispersed battery applications--battery storage of electricity for utilities, industry, and buildings; and
- Industrial energy conservation--commercial electrolytic processes.

TABLE I

ECS PROGRAM FUNDING

Program Element Program Subelement	Funding ($1,000)						
	FY 1980			FY 1981			FY 1982
	Pass-Thru	ECS	Total	Pass-Thru	ECS	Total	Estimated
Technology Base Research		7,100	7,100		7,900	7,900	11,000
Electrochemical Systems Research		2,600	2,600		3,300	3,300	
Supporting Research		3,000	3,000		3,400	3,400	
Electrolytic Processes		1,500	1,500		1,200	1,200	
Technology Development							
Advanced Batteries		13,900	13,900		10,700	10,700	11,300[a]
Applications Research	8,100	12,100	20,200	7,500	8,600	8,600	2,850[b]
Mobile Applications	7,600	1,600	9,200	7,100	2,300	9,400	
Solar Applications	500	4,900	5,400	400	3,600	4,000	
Dispersed Battery Applications		4,500	4,500		2,300	2,300	
Capital Equipment		1,100	1,100		400	400	
Total	8,100	33,100	41,200		27,200	34,700	25,150[b]

[a] Includes exploratory technology development.
[b] Does not include pass-through funds.

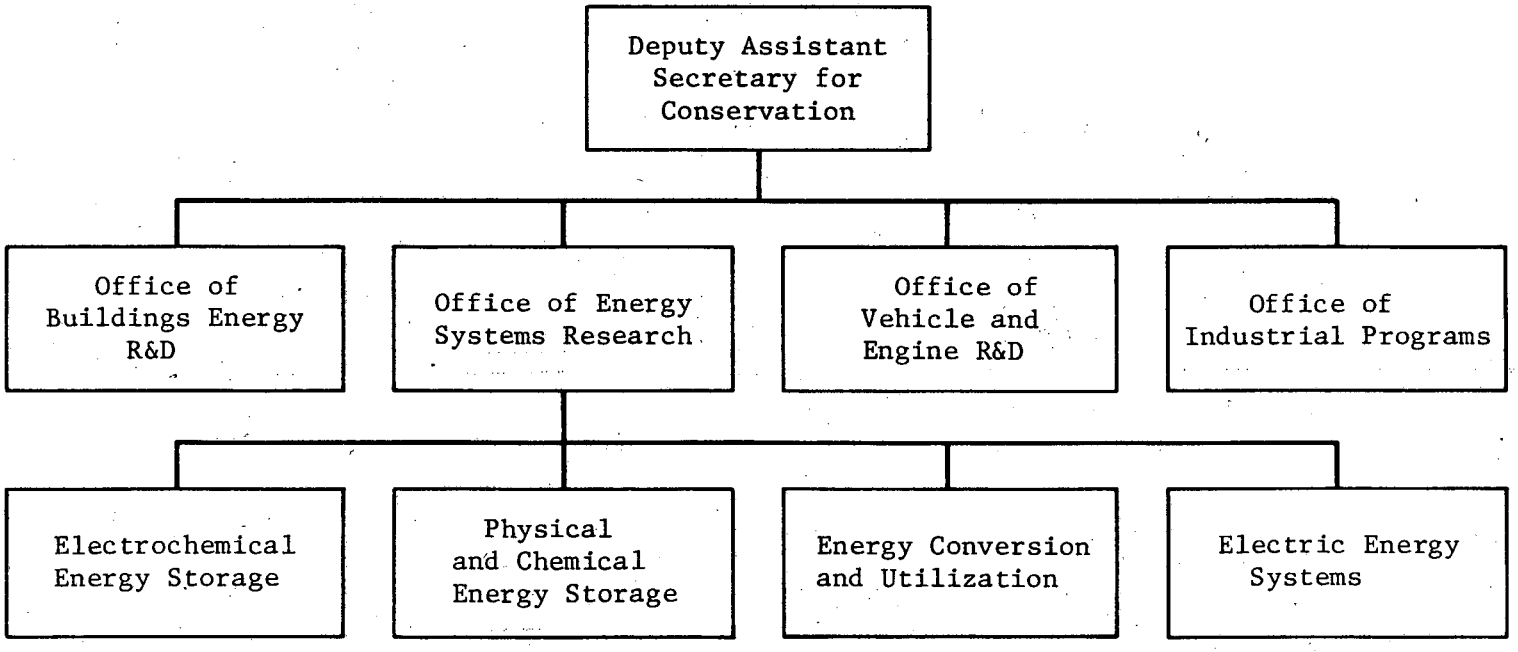

FIGURE 1
ORGANIZATION OF THE OFFICE OF THE DEPUTY ASSISTANT SECRETARY FOR CONSERVATION

The support of the program for FY 1980 and 1981, and the projected budget for 1982, as described in Savitz' remarks, are listed in Table I. The table reveals increased emphasis on the technology base and advanced and exploratory technology with a marked decrease in support of applied (mission) efforts. This reflects the deemphasis on demonstration and commercialization efforts with a higher priority being placed on more exploratory research and development. Also note that the ECS activities related to conservation in industry are included within the electrolytic processes subprogram element.

Except for the relatively small effort on electrolytic processes (i.e., industrial electrochemistry), the remaining activities included in Table I emphasize battery technology. Figure 2 shows the FY-1981 distribution of the ECS effort among various battery components and operating temperatures. The share of funds dedicated to alkali-metal negative electrodes, sulfur and sulfide positive electrodes, high operating temperatures, and non-aqueous electrolytes indicates the exploratory aspects of battery research and development activities.

1.3 Report Structure

Before discussing specific battery and electrochemical processes, this report reviews the battery technology goals, as defined by the various applications research subelements. These mission studies provide guidance to the battery system performance

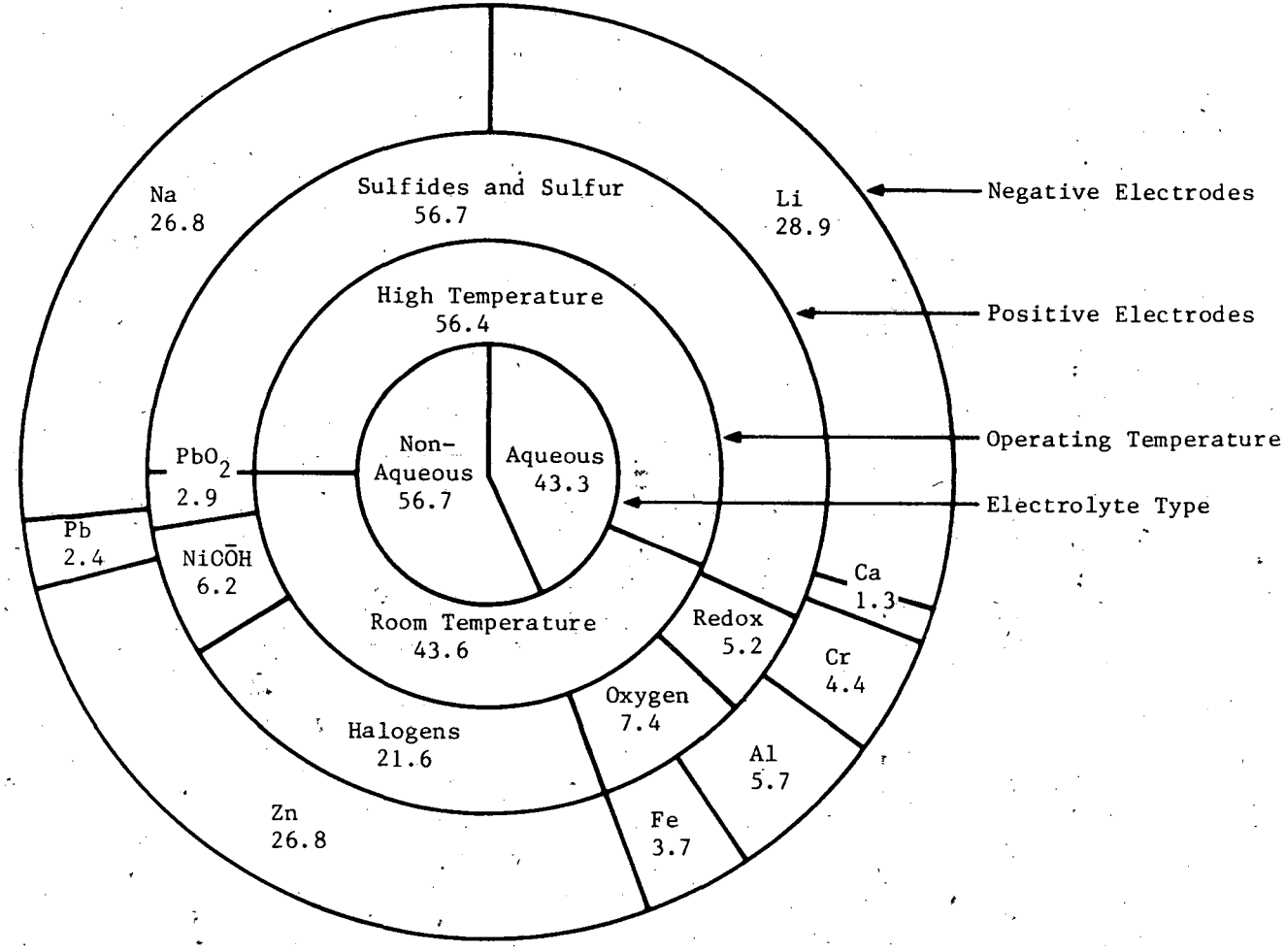

FIGURE 2
BATTERY STORAGE PROGRAM: FUNDING BREAKDOWN BY TECHNOLOGY

requirements and affect battery research and development emphasis. However, the R&D efforts on a particular battery system are reviewed in the technology sections of the report. This permits comparison of technology differences and commonalities for a given battery system. The research supporting a specific couple is described with that couple. Other supporting research is included in Section 6. The battery couples will be written negative/positive. When the electrolyte is included the components will be written: negative/electrolyte/positive. A major exception is the lead-acid battery for which the common name is used.

2.0 APPLICATIONS RESEARCH: SYSTEMS STUDIES

The status of the studies supporting the applications research program element is discussed in this section. As noted in the introduction, the system studies are intended to provide guidance for establishing research goals and to assist in the selection of critical research problems. The applied research areas reviewed in this section include:

- Electric and hybrid vehicles;
- Dispersed electrical systems; and
- Solar (photovoltaic) systems.

Studies supporting the electrolytic processes program subelement are discussed in Section 6 on electrolytic processes.

2.1 Mobile Applications

Paul J. Brown, acting director of the DOE Electric and Hybrid Vehicles Division, presented an update on the status of the DOE program being conducted to implement P.L. 94-413, The Electric and Hybrid Vehicle Research, Development, and Demonstration Act of 1976. The Administration and Congress have agreed not to fund the addition of any electric vehicles to the demonstration fleet in FY 1982. However, the current demonstration program will continue for 3 more years in accordance with the cost-shared contracts from previous years' funding. The demonstration fleet currently includes 1,415 electric vehicles at 94 different sites. Electric vehicles are being used at these sites by telephone companies, public

utilities, government agencies (Federal, state, and local), commercial organizations, and universities.

In addition to the road testing demonstration program, experimental electric test vehicles with advanced technology are being developed. These include the Electric Test Vehicle (ETV-1), developed by the GE/Chrysler/Globe team for DOE, which has demonstrated an overall propulsion efficiency of 76%. The regenerative braking system of the ETV-1 increased the energy efficiency of the battery by 19%, based on energy input during the charging cycle. Another vehicle, the ETV-2, developed for DOE by the Garrett Corporation, has been delivered and is under dynamometer laboratory and road track testing at the Jet Propulsion Laboratory (JPL). The propulsion system includes a composite flywheel for regenerative braking. The dynamometer tests indicated a top vehicle speed of 60 mph and an urban driving range of 70 miles. The power source is an Eagle Picher tubular positive lead-acid battery with a specific energy of 40Wh/kg.

A Hybrid Integrated Test Vehicle (HTV-1) is being developed for DOE by a GE/VW team. It consists of an internal combustion engine and a small battery pack. An 80-HP Volkswagen engine with a quick on and off capability is utilized. The hybrid concept results in a vehicle that is not range limited, but conserves petroleum in urban use when operating on battery power.

Advanced vehicle concepts such as fuel cells, aluminum/air and zinc/bromine batteries, and electrified roadways are also being investigated. In addition, propulsion system components such as advanced technology motors and controllers are under development. A complete alternating current propulsion system including the traction motor, controller, transaxle, and charger has been developed in the program in a cost-shared contract with the Eaton Corporation.

Experimental aqueous battery technology development for electric vehicle application continues to be a top priority in the program. Battery types under development include improved lead-acid, iron/nickel-oxide, zinc/nickel-oxide, and zinc/chlorine. The integration of complete vehicle sets of iron/nickel-oxide and advanced lead-acid experimental batteries into test vehicles is being carried out by JPL. Goals for batteries for improved ETVs are illustrated in Figure 3.

Walsh and coworkers at Argonne National Laboratory (ANL) have undertaken the development of a method for establishing battery research and development goals which are optimum for electric vehicle applications. The method has the following features:

- Comprehensive modeling of key battery relationships;
- Avoidance of premature specification of battery or vehicle characteristics;
- Identification of range, acceleration, and payload which match electric vehicle mission requirements; and
- Optimization using minimum ownership-cost criterion.

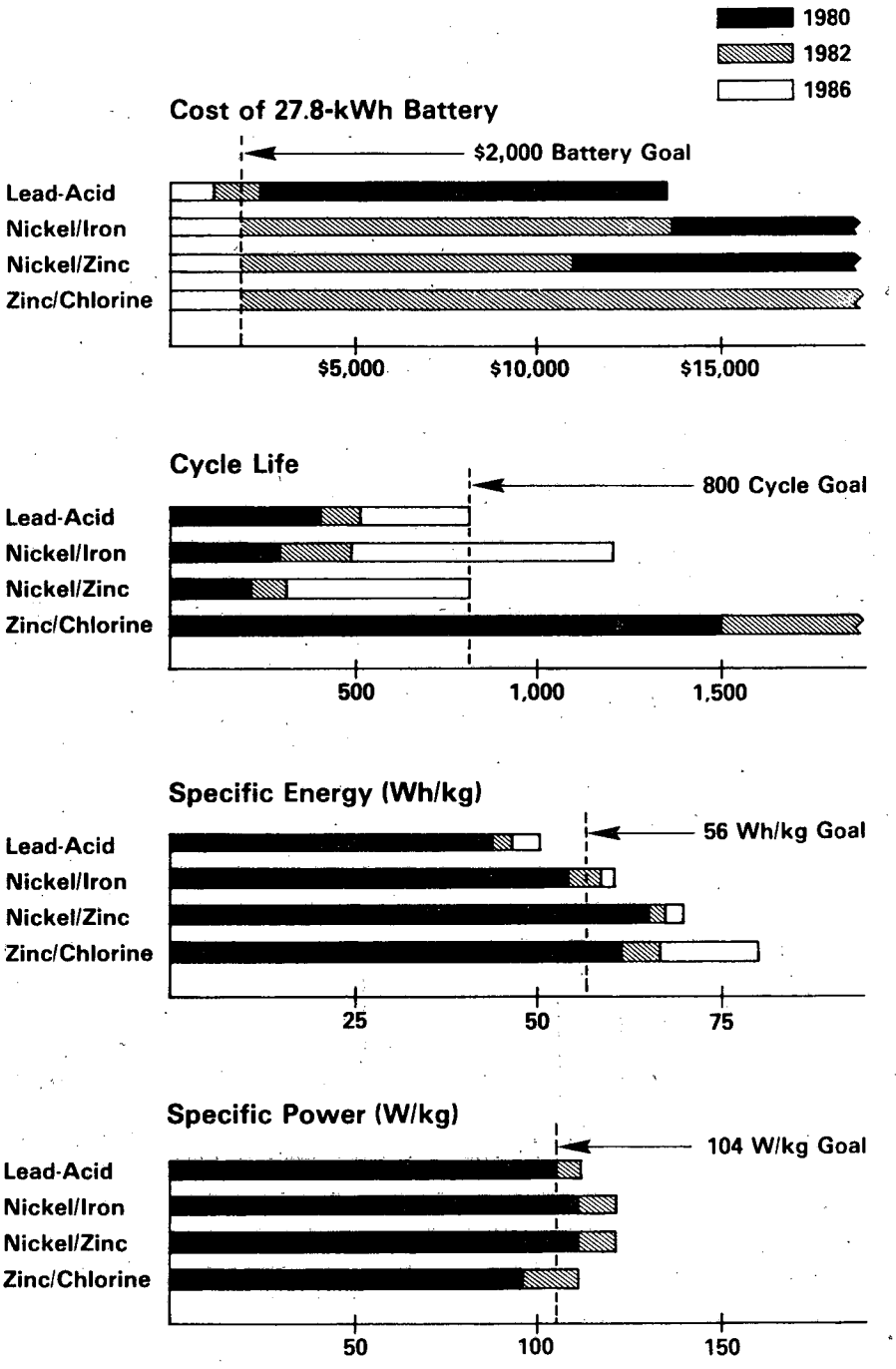

Source: Reference 3.

FIGURE 3
PROJECTED GOALS FOR BATTERY TECHNOLOGY

The output of the analytical method, the battery characteristics, enables the identification of battery goals which match DOE objectives.

A closed-form mathematical solution has been developed and sample computations were compiled to illustrate the technique. The battery system selected was sodium/sulfur for application in fleets of light trucks and autos. The total discounted user cost per km was the minimization parameter selected. Figure 4 illustrates the results of the computation. The results emphasize the importance of specific energy for achieving long-range electric vehicles and a high market penetration.

Further improvements in the analysis are anticipated by including the:

- National Personal Transportation Study data base;
- Cost/power/energy inter-relationships; and
- Cycle life/depth-of-discharge relationship.

2.1.1 Future Vehicle Requirements

Forrest of the Aerospace Corporation is analyzing the vehicle requirements for third-generation electric vehicles. The objective of his study is to define the vehicle characteristics that will be required to accommodate advanced batteries. This is to help determine the need for vehicle research and development in order to realize the full capability of advanced battery propulsion systems

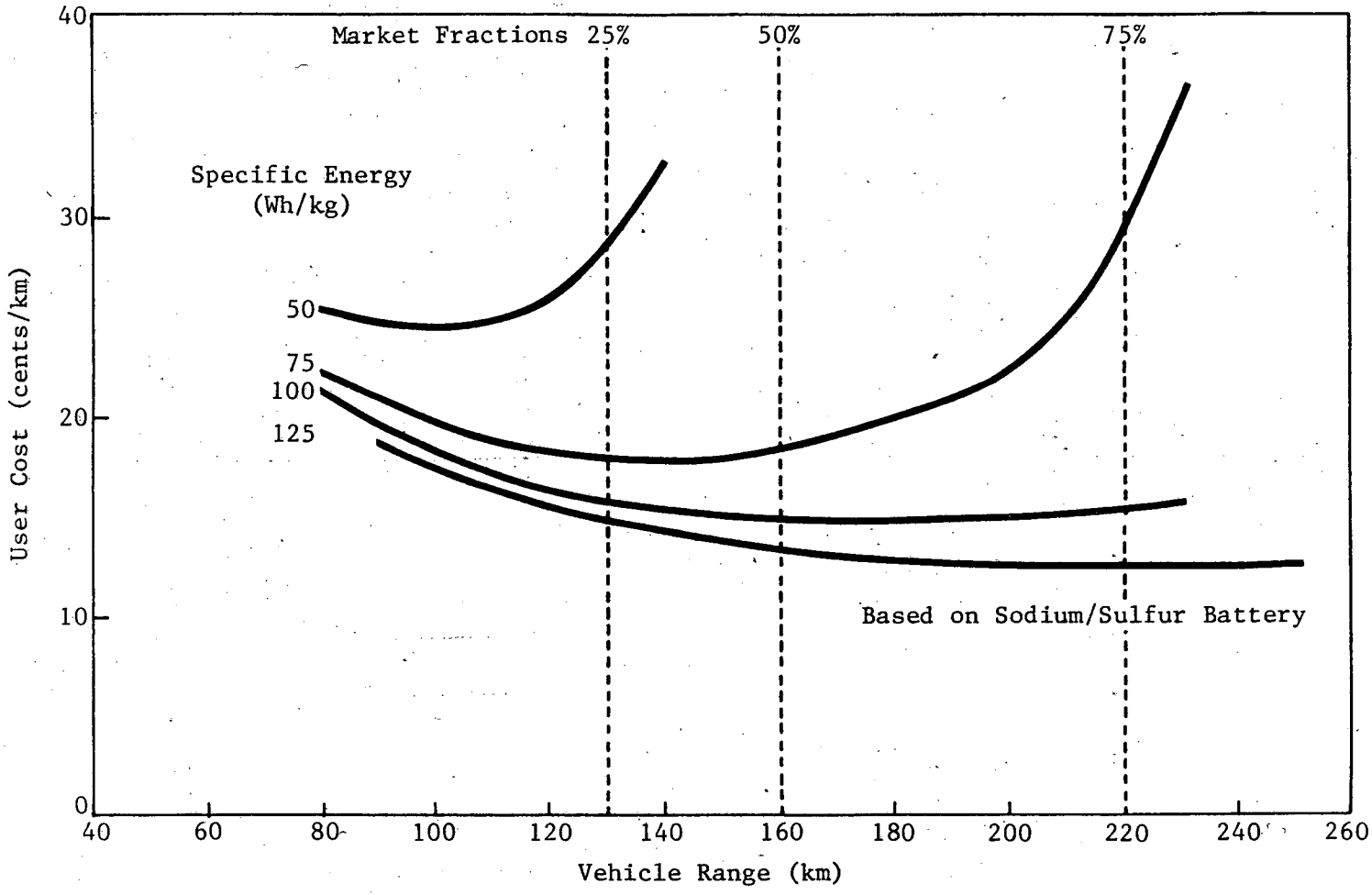

Source: Reference 3.

FIGURE 4
FLEET AUTO COST

for electric vehicles. The batteries included in this study are: sodium/sulfur, lithium/metal-sulfide, and aluminum/air.

The focus of the study has been on four-passenger vehicles using the Chevrolet Citation as the reference vehicle. A lower weight or smaller size vehicle will further restrict packaging volume and lowering the trunk or tray to accommodate the battery will substantially reduce the ground clearance. The feasibility of packaging the lithium/iron-sulfide battery between the seats' console arrangement by piercing the fire-wall and extending into the engine compartment was examined. This battery space configuration could accomodate a 45-inch long battery tunnel and enable a 50% increase in battery capacity relative to the front battery module packaged in a modified-Citation electric vehicle.

The study of the accommodation of the zinc/chlorine battery in the Citation vehicle found that the maximum feasible battery size is 36kWh. The resulting vehicle would be significantly heavier than the stock Citation. The electric vehicle also would have an undesirable front-to-rear weight distribution.

2.1.2 Electric Vehicle Battery Resource Availability

Future resource availability is important to all battery applications. A study of the materials impacts of battery development has been conducted by Hittman Associates. The firm's estimates of future battery production show that lead-acid batteries will account for most of the battery production between 1980 and

2000 even if vehicle and load-leveling markets grow at high rates (Figure 5). In addition to the market projection, the study evaluated:

- The supplies of mineral resources for batteries;
- The manufacturing investments required for battery production; and
- The effects of supply interruptions on battery commercialization.

The results of the study, in addition to the projected accumulated demand for batteries, included:

- Investments for battery manufacture are likely to be between $10 and $30/kWh/yr of production.
- The most critical materials affecting battery production are lead, nickel, titanium, and lithium.

A more detailed analysis of nickel availability was carried out by Tuffnell of International Nickel Co. This study was not sponsored by DOE but is included because of the potential importance of nickel in future battery systems such as Fe/NiO(OH) and Zn/NiO(OH). Production scenarios were based on 4%, 10%, and 20% electric vehicle (EV) penetration in world markets by 2010. Other assumptions included:

- An initial (1985) nickel battery penetration of 50% decreasing to 30% (1995) and to 15% (2005);
- An average nickel content of 200 lbs per EV battery;
- Battery life of 5 years;
- Vehicle life of 15 years; and
- Nickel recovery from spent batteries of 95%.

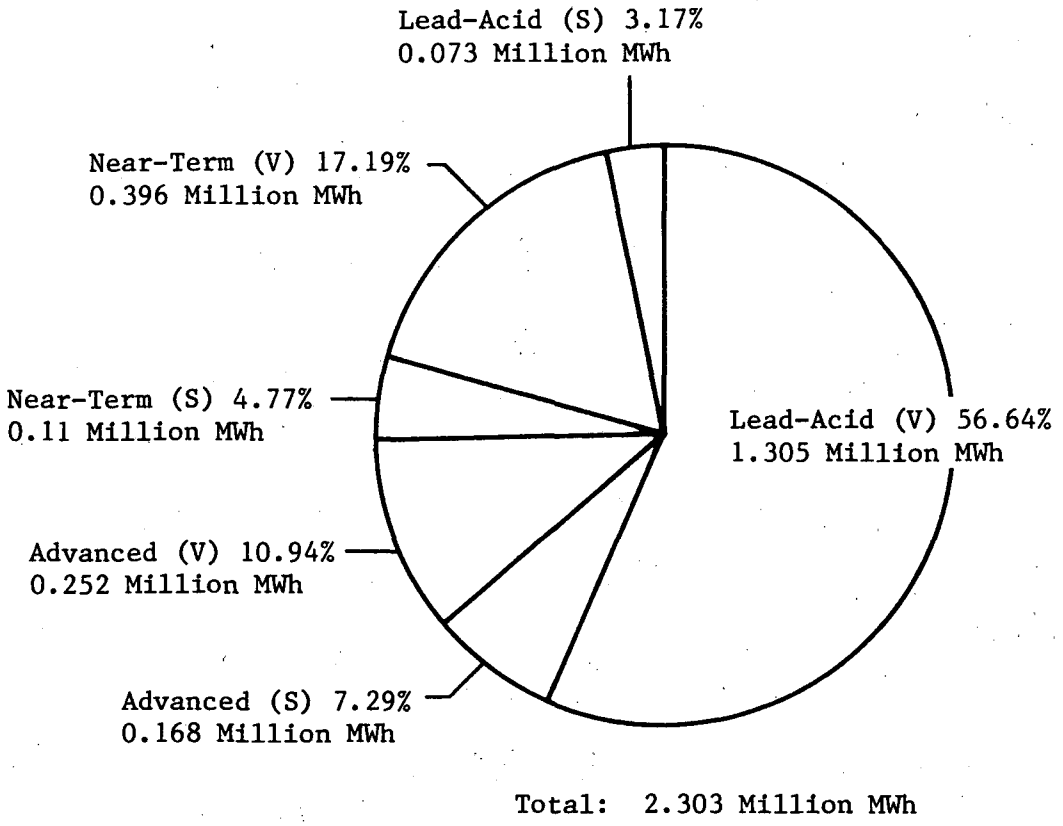

FIGURE 5
CUMULATIVE DEMAND FOR STORAGE BATTERIES (1980-2000)

Depending on the EV penetration, the scenario led to an annual nickel production peaking at 60, 150, and 250 million pounds between the years 2000 and 2005 for the three penetration rates. The reclamation of nickel from spent batteries was found to be a highly important factor in limiting demand. The three scenarios required 0.7%, 2.4%, and 4.2%, respectively, of the world nickel reserves. It was concluded that world nickel reserves were adequate to meet these demands, but the nickel industry would require an adequate lead time to meet the increased nickel demand.

The status of DOE-supported studies on technology for the recovery of spent battery materials is reviewed in Section 6.

2.1.3 Electric Vehicle Energy Analysis

The dominance of the electrical energy required for the cycling of secondary batteries in the life-cycle energy demand was noted in SR-II. The study, by Sullivan of Hittman Associates, of the energy demand over the battery lifetime has been extended to additional systems. The analysis included a detailed consideration of materials and energy requirements for each of the systems studied. The results for the energy used for component materials, battery manufacture, lifetime cycling energy, and energy saved through materials recovered are included in Table II. For the secondary batteries there is a greater variation in operating energy than in total energy. The high energy cost in the production and recovery

TABLE II

BATTERY ENERGY REQUIREMENTS FOR 100,000 MILES OF OPERATION

(Btu x 10^3 per 10^5 miles)[a]

	Lead-Acid	Zinc/ Nickel-Oxide	Iron/ Nickel-Oxide	Zinc/ Chlorine	Sodium Sulfur Ceramic	Lithium/ Metal Sulfide	Aluminum Air
Materials Production	6,181	27,928	17,933	11,652	30,290	28,598	24,514
Battery Manufacture	3,108	1,829	8,293	3,885	10,098	9,534	8,169
Operating Energy	293,400	278,900	308,800	338,600	289,200	256,800	923,600
Recycling Energy	-	(5,282)	(3,592)	(552)	(4,243)	(3,509)	(3,815)
Total Energy	302,689	303,375	331,434	353,585	325,345	291,423	952,468

[a]Replacement batteries not included in energy estimate.

[b]Not a secondary battery, recharged mechanically.

of aluminum accounts for the much higher lifetime energy required by the aluminum/air battery system.

The conclusions reached in this study were:

- The shift in fuel sources--from petroleum to coal and natural gas--made possible by batteries far exceeds the energy invested to produce the batteries;
- Life cycle battery energy use is highly sensitive to overall battery efficiency; and
- The investment energy (materials production and battery manufacture) is highly dependent on cycle life.

2.1.4 Health and Environmental Impact of Batteries for Electric Vehicles

The studies of Argonne National Laboratory concerning the ecological and biomedical effects of commercialization of electric vehicles, reported in SR-II, have been extended. The scenario used has remained the same:

- Market penetration by the year 2000, 3 million lead-acid batteries and 8 million Zn/NiO(OH) or Fe/NiO(OH); and
- One megawatt of installed power required for each 40 EVs.

The complete lead-acid battery production process, from mining through spent battery recovery, is depicted in Figure 6.[6] The stages during the process leading to emissions which could cause health and/or environmental concerns are indicated. The estimated emissions, based on a 66% increase in lead mining and milling needed to meet the increased lead-acid battery demand, would increase markedly. The lead, arsenic, and antimony aerial and wastewater discharges could cause adverse health and ecological impacts within

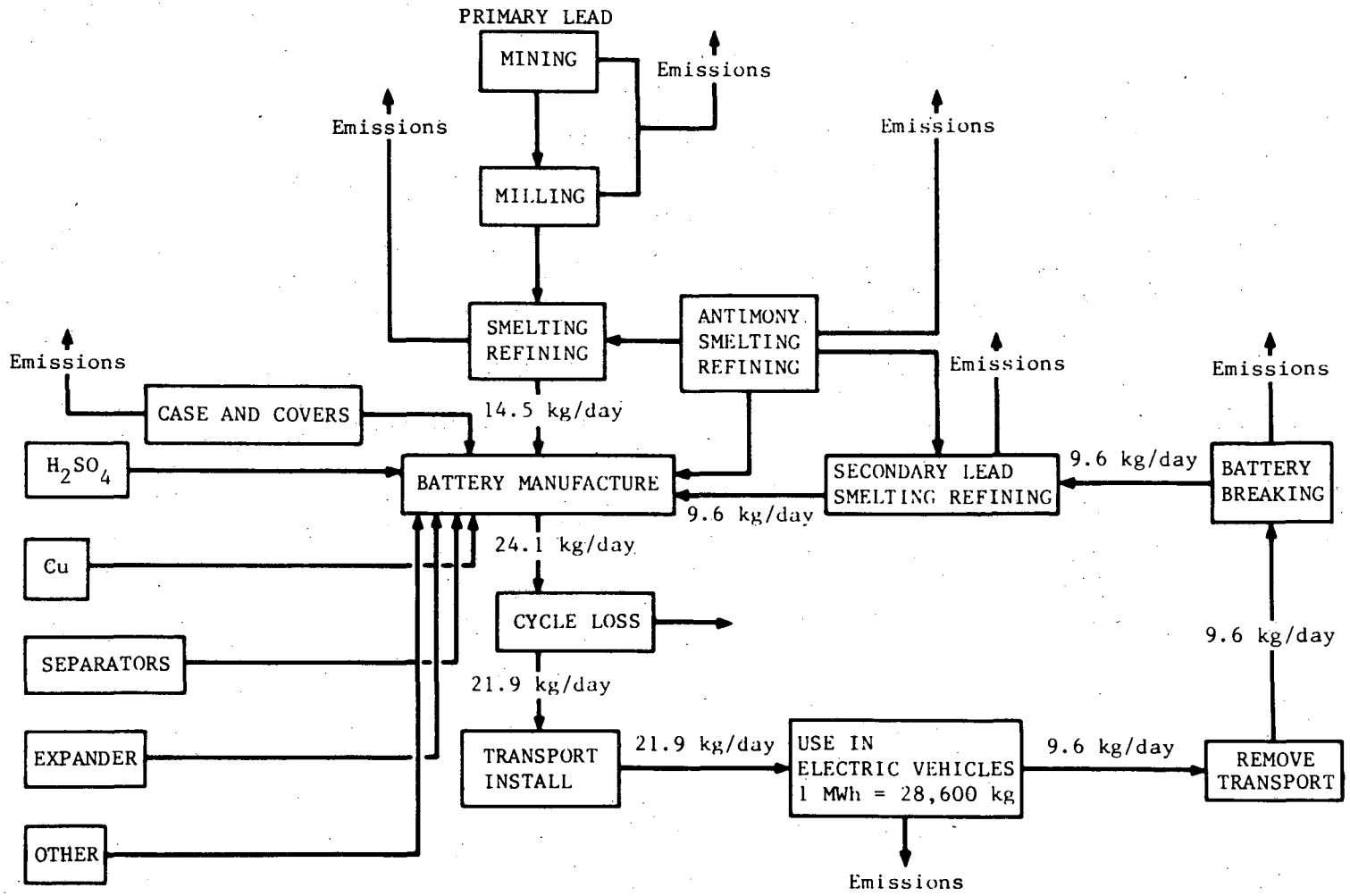

Source: Reference 6.

FIGURE 6
THE STATE-OF-THE-ART LEAD-ACID BATTERY CYCLE FOR ELECTRIC VEHICLES

several kilometers of operations. The closed-space recharging of lead-acid batteries could create hazardous amounts of stibine and arsine in closed garages used in home recharging. However, the trend toward calcium alloyed grids and decreased arsenic and antimony in the cell components can lead to a marked decrease in the potential hazard of arsenic and antimony. The increased production of lead will also lead to an increase in sulfur dioxide emissions. The increased production of nickel and zinc will further increase sulfur dioxide emissions. With the exception of zinc anode sludge, formed during the electrolytic recovery of zinc, the metal/nickel-oxide batteries emit few materials that are classified as hazardous wastes under Section 2001 of the Resource Conservation and Recovery Act. However, exposure to nickel and its compounds during nickel recovery and processing has been to shown to cause an increased incidence of various ailments.

To obtain more specific information on possible health effects, the ANL staff has developed a non-interactive dispersion model for the various potential pollutants in the total battery production and use process.[6] The pollutants considered were lead, sulfur, copper, nickel, cadmium, zinc, and antimony. Based on this model, there is a greater potential for adverse responses to lead over background levels at distances of 5 to 15 km from the mine-mill complex. The model projects that electric vehicles may penetrate

the market to the point at which an increasing number of persons suffer a greater risk of exposure to lead, antimony, and cadmium.

Hazard assessment of electric vehicle batteries has been continued at Factory Mutual Engineering Corporation. Zalosh has extended the fault-tree analysis, described for hydrogen-oxygen explosions in SR-II, to other hazards. These include electrical shocks, acid/caustic electrolyte burns, thermal contact burns, halogen releases, and sodium-sulfur fires.

Based on the analysis of the hydrogen-oxygen systems, the most popular alternative protection measures are hydrogen-oxygen recombiners and vent lines equipped with flame arresters. The hydrogen venting option has also been evaluated.

Hazards from hypothetical sodium and sodium-sulfur fires were also evaluated. It was assumed that the dominant hazard outside of the immediate fire vicinity was due to the dispersal of toxic combustion products, such as sodium oxide aerosols and sulfur dioxide. The generation of these two agents was calculated for various pool sizes and spray fire configurations.

2.1.5 Fuel Cells for Transport

The use of fuel cells for transportation has been considered from time to time for more than a quarter of a century.[7] McCormick et al. reviewed the application of fuel cells to transportation in 1979,[8] evaluating their technical and economic feasibility. The specific applications considered were city and

highway buses, delivery vans, and passenger cars. Using a Los Alamos-developed computer simulation model, they concluded that these applications are technically feasible. The computer modeling was assisted by the design and instrumentation of a fuel-cell-powered golf cart.

The fuel-cell power plant schematic used is shown in Figure 7. It is based on reforming methanol to produce hydrogen. The hydrogen and air are reacted in a 15kW phosphoric-acid fuel cell (PAFC). Supplementing the fuel cell is a battery pack containing four 24-volt batteries. The inclusion of the fuel cell and battery in an automobile is shown in Figure 8.

The Los Alamos vehicle simulation model, as reported by Lynn, described the vehicle in terms of measureable input/output variables such as voltage, current, fuel consumption, torque, and angular velocity. Measured values were used to describe each variable in the simulation program. The schematic of the vehicle configuration and some of the resultant vehicle performance characteristics are shown in Figure 9.

In addition to having the potential for producing vehicles with performance comparable to that of vehicles with internal combustion engines, the fuel-cell battery hybrid vehicle offers higher efficiency, lower pollution, and the use of fuels that can be derived from non-petroleum sources, such as methanol from coal.

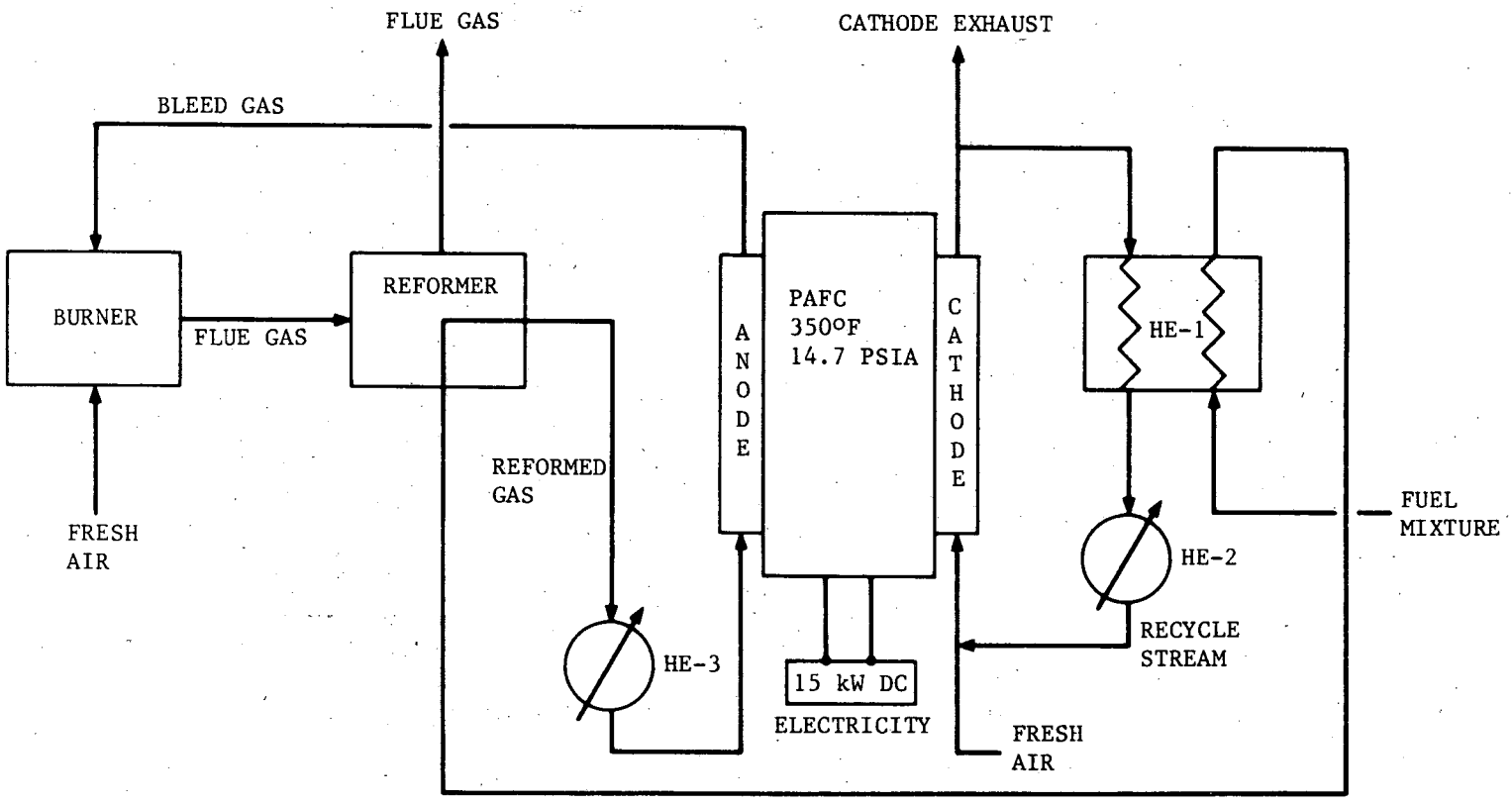

HE - Heat Exchanger
PAFC - Phosphoric Acid Fuel Cell

FIGURE 7
15-kW FUEL CELL POWER PLANT SYSTEM

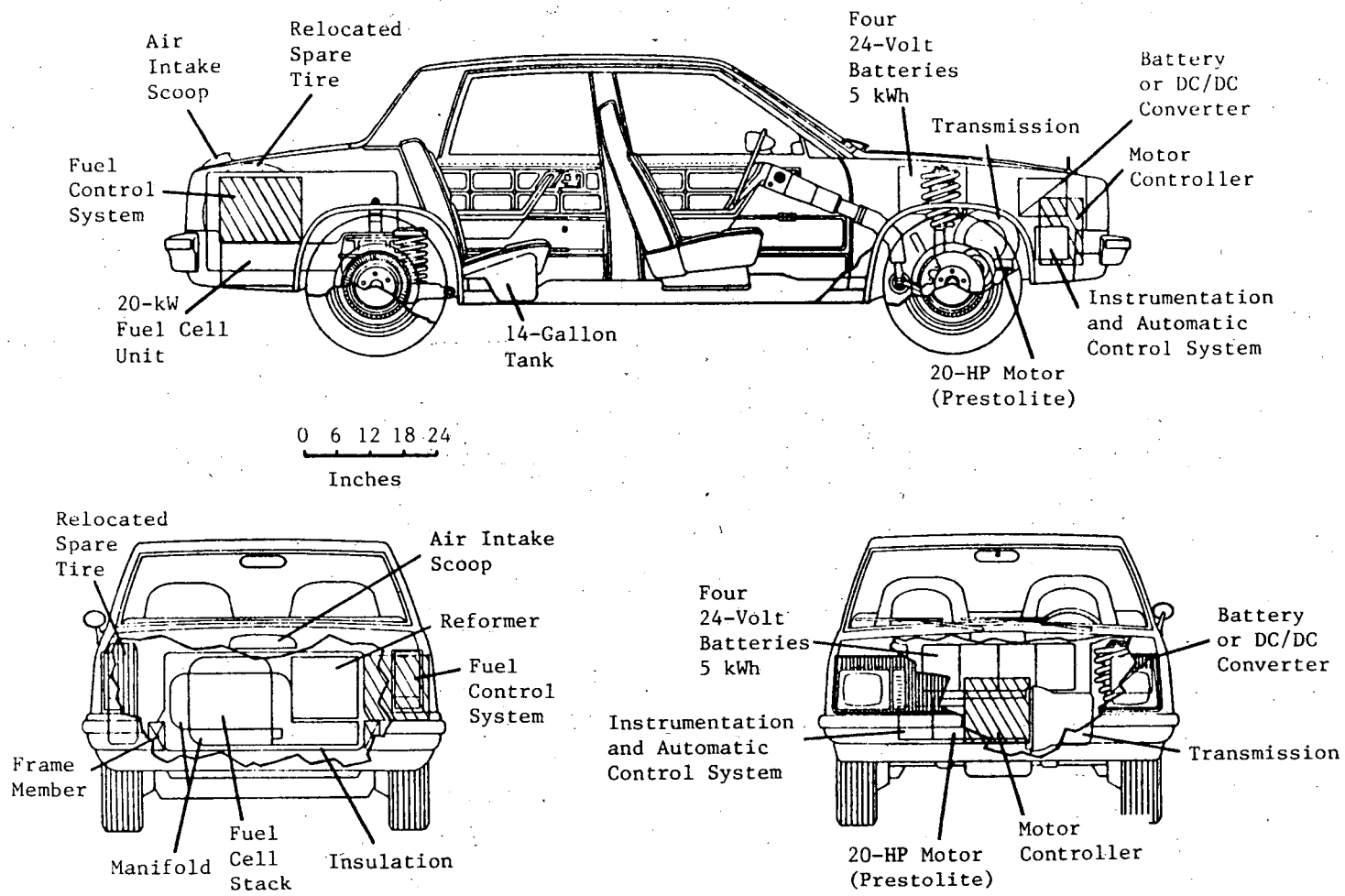

FIGURE 8
NEAR-TERM HYBRID FUEL CELL VEHICLE
(GM X-BODY, OLDSMOBILE OMEGA)

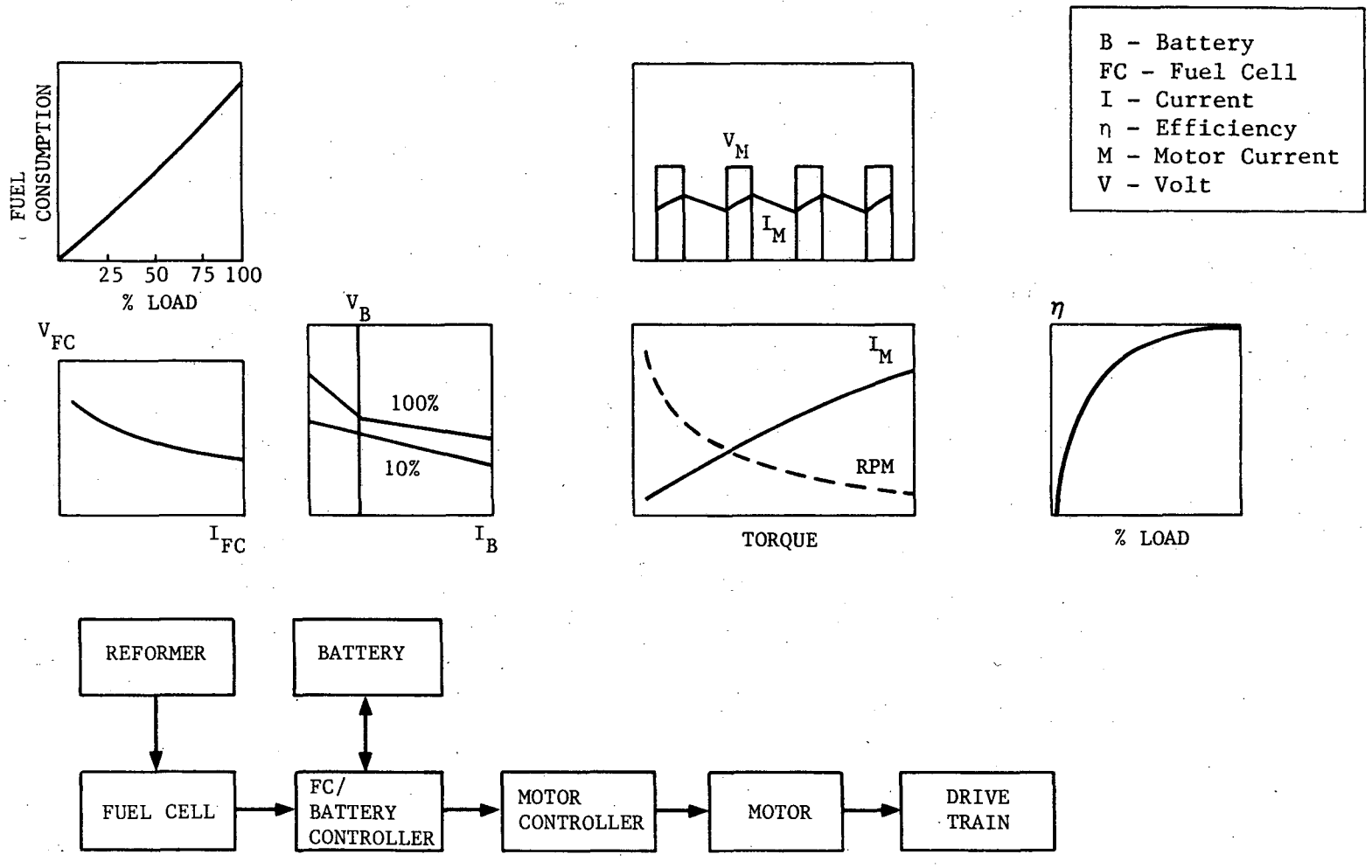

FIGURE 9
FUEL-CELL-POWERED VEHICLE CONFIGURATION

Srinivasan and coworkers at Los Alamos have reviewed the current status of fuel cells which are being developed or have been investigated for other applications. Of these they considered the fuel, fuel-cell combinations, shown in Table III, as the most promising for transport applications. The most highly developed of these is the methanol PAFC which has been emphasized by the Department of the Army. In addition, the PAFC has been highly developed under the joint efforts of DOE, the Electric Power Research Institute (EPRI), the Gas Research Institute (GRI), and cooperating utilities for utility and other applications. The review of Srinivasan also outlines areas of research on fuel cells for electric vehicles. The major activity which has greatest relevance to fuel cells, because of its potential for decreasing cell operating temperature, is that of superacid fuel cells. The potential for cell performance improvement through the use of one of these acids, trifluoromethane sulfonic acid, was first shown by Adams and Foley in research sponsored by the Department of the Army.[9]

2.2 Distributed Energy Systems

The use of storage batteries at distributed sites to decrease electric peak-load generating capacity requirements is a joint effort of the DOE, EPRI, and Public Service Electric and Gas Company. Within DOE it is a collaborative effort of the ECS and the Electric Energy Systems (EES) Programs. The overall EES program was

TABLE III

PROMISING TYPES OF FUEL CELLS FOR ELECTRIC VEHICLES

Fuel	Electrolyte	Operating Temperature	Electrocatalysts
Methanol	85%-100% H_3PO_4	150-225 C	Pt; Intermetallics; Non-metals (organic, inorganic)
Hydrogen	25%-50% KOH	60-90 C	Pt; Ni; Ag with and without additives: alloys, intermetalics, non-metals (inorganic, organic)
Methanol	NAFION	80-150 C	Pt; Intermetallics; Non-metals (organic, inorganic)
Methanol	Superacid TFMSA, Higher Homologs	60-150 C	Pt; Intermetallics; Non-metals (organic, inorganic)

Note: TFMSA = Trifluormethanesulfonic acid.

described at the conference by L. Rogers, the former program director. The major effort related to the utilization of batteries in electrical utility systems is the BEST (Battery Energy Storage Test) facility. This facility, designed, built, and to be operated by the Public Service Electric and Gas Company, was dedicated in May 1981. The purpose of the BEST facility is to test and evaluate the operating characteristics of battery systems and power conversion equipment in a utility environment. The components of the system and the test plan were detailed in SR-II.

Public Service Electric and Gas is continuing to assess technical and economic aspects of electrochemical energy storage systems. The company is working on the development and application of a consistent methodology for analytical, technical, and economic assessments of electrochemical energy storage systems.[4] The four battery systems included in the assessment are:

- Zinc/chlorine;
- Sodium/sulfur;
- Lithium-alloy/iron-sulfide; and
- Advanced lead-acid.

Each system is to be examined for the balance of plant requirements to satisfy major environmental, safety, regulatory, and construction issues. As part of the overall technical assessment a generic electrochemical energy storage system has been defined. This baseline system would cost approximately $600/kW (in 1979 dollars),

have 5 hours of storage, be approximately 70% efficient, and require approximately 7 hours to recharge. This analysis treats the battery system as a "black box" and takes into account the battery system costs but not costs for the plant, land, or land preparation. This baseline system is being redefined and was expected to be completed in January 1982. The technology of the batteries for the BEST facility are discussed below in Sections 3 to 5, which concern battery research and development. Their characteristics are compared with system goals.

A system stability impact assessment to examine the dynamic interaction of dispersed storage devices and power systems has been initiated. Battery and converter models are being defined for use in the stability model. The EPRI transient stability computer program is being modified to accommodate the battery and converter models. In the future, extensive computer analysis will be utilized to thoroughly assess the impact of battery energy storage on system stability and performance.

Economic assessments are being conducted to identify the impact of battery systems on generation system dispatch for an optimally expanded (excluding energy storage) reference utility system. This is being used to estimate the system production cost benefits for varying levels of market penetration of advanced battery storage. To accomplish this, advanced batteries are substituted in the reference system for intermediate and peaking duty in the generation

mix. In addition, capital costs or equivalent savings attributable to the following advanced battery parameters for the reference system are to be identified:

- Storage system life and salvage value;
- Battery availability;
- Transmission and distribution savings resulting from dispersed siting;
- Participation in carrying system spinning reserve; and
- Effective battery capacity.

A simplified analysis of the impact of battery systems on two extreme expansions of the reference utility system has been completed for an all base-load unit expansion and a soft-technology expansion.

Public Service Electric and Gas Company was to initiate, during the 1981 fiscal year, a review of existing battery cost estimating techniques as a basis for estimating battery manufacturing costs. The goal is to develop a standard computerized battery cost methodology for estimating the capital cost of a battery system, including costs for the plant. This methodology will determine sensitivities to changes in the cost of credit, labor, and raw materials, as well as battery manufacturing process considerations and plant parameters.

An alternative method of using battery storage is on the customer side of the meter. This has been evaluated by Bates and

coworkers at Battelle Columbus Laboratories. The study was directed toward evaluation of the following:

- The issues of battery system design;
- The economics of battery storage for electricity customers;
- Institutional and environmental concerns for battery users; and
- Market potential on the customer side of the meter.

The baseline system used in the study was the lead-acid battery because of its availability for near-term evaluation. The battery characteristics used are shown in Table IV. Baseline systems costs were calculated using power level as a parameter. A power range of 2 to 20,000kW was used. The results are shown in Table V. The DOE cost goal, $65/kWh-ac, is lower than that calculated for the baseline case. The economic viability of the baseline storage system was found to be greatest for customers with large rate differentials associated with present rate schedules. The economic viability was also found to be impacted by the level of demand charges (capital utilization charge), the duration of the battery system discharge, and the cost of the battery storage system. It was further concluded that the achievement of the DOE battery cost goals will significantly improve economic viability. Several organizations were identified as potential demonstration program participants.

Strnisa of the New York Energy Research and Development Authority (NY ERDA) is studying a specific customer-side-of-

TABLE IV

DISPERSED APPLICATIONS FOR THE BASELINE BATTERY SYSTEM

Type:	Lead-Acid
Energy:	100 MWh
Charge:	7-hr + 2- to 3-hr Taper
Design Rate:	5-hr Discharge
Voltage:	1,505 Volts DC (minimum)
Power:	20 MW (constant)
Life:	2,000 Cycles
Cost Status:	Mature Plant

Source: Reference 3, Battelle.

TABLE V

BATTERY SYSTEM CHARACTERISTICS FOR VARIOUS CUSTOMERS

Example	Power (kW)	Energy (kWh)	Line Voltage (volts-AC)	System Cost ($/kWh-AC)	Possible Customer Application
1	20,000	100,000	15,000	140	Large industrial
1	1,000	5,000	15,000	162	Small industrial
3	40	200	440	194	Small commercial
4	2	10	220	241	Small residential

the-meter battery storage application. This is to meet the morning and evening peak loads of the New York City subway systems. Figure 10 shows the estimated effect of battery storage on the electricity demand of the subway system. Note the projected impact of peak shaving by means of batteries on the power demand curve (heavy black line). The high power peaks of present day operations lead to high demand charges which represent 40% to 60% of the transit system power cost. The reduced demand charge is one of the potential benefits to the NYC Transit Authority of battery storage. Other projected benefits to the subway system are the provision of a receptor for regenerative braking, if this should be applied to subway trains, and increased safety by providing limited train operation in the event of a utility power failure. The major benefit forseen for the utility is load management with the resulting potential for petroleum conservation and the deferment of new generation capacity.

2.3 Solar Applications

Santopietro of the DOE Photovoltaics Program of the Office of the Deputy Assistant for Renewable Energy described current photovoltaic (PV) energy demonstration projects. Some of these include battery storage systems. The following are some examples:

- A 25kW power source for irrigation;
- A 3.5kW power source for an Indian village;
- Telecommunications;

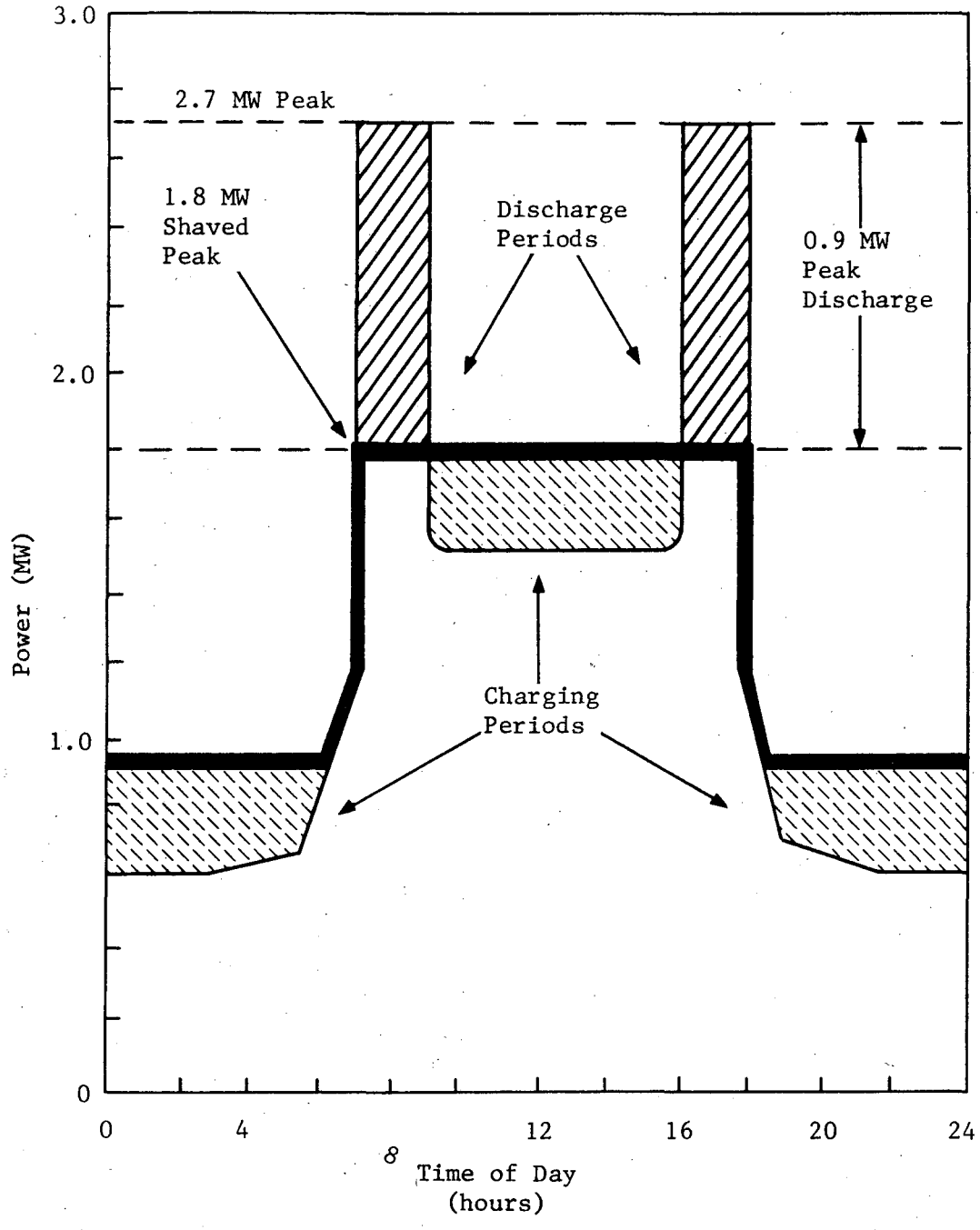

FIGURE 10
NEW YORK SUBWAY SUBSTATION LOAD PROFILE

- Navigational aids; and
- Cathodic protection.

Developments in present technology silicon photovoltaic solar cells are continuing to reduce the cost of PV energy sources. The projected ultimate cost is of the order of 70 cents per peak watt.

Program responsibility for efforts concerning Batteries for Specific Solar Applications (BSSA) is centered at the Sandia National Laboratories (SNL). Clark, director of SNL activities, said, in his overview at the 1981 conference, that the BSSA program goal is to develop storage battery technology in support of various DOE solar missions. Initial emphasis is on PV systems, however, there is an increasing interest in wind systems. The program plan includes:

- Analyzing battery requirements;
- Surveying the current battery state-of-the-art;
- Conducting laboratory verification of requirements analysis;
- Engaging in research and development; and
- Develop the resulting technology.

In this section emphasis is placed on the first three parts of the program. The research and development activities will be reviewed in the sections devoted to specific battery systems.

2.3.1 Battery Requirements Analysis for Solar Applications

The objectives of the battery requirements analysis program are to determine the economic feasibility of system battery storage and

to define specific battery requirements. To aid in achieving these objectives the SOLSTOR (solar energy storage) computer program was developed. The SOLSTOR program and some of its initial results were described in SR-II. Some of the PV battery system features included in the model are:

- PV only or combined PV thermal system;
- Residential or commercial loads;
- Utility connected or stand-alone PV-battery combinations;
- Variable utility pricing including time-of-day (TOD) pricing, seasonal pricing, and sell-back to the utility;
- Hourly simulation over 1 year;
- Minimization parameter of the level annual cost; and
- Collector size, storage size, and power conditioning rating varied to obtain least cost.

Included in SR-II were results for PV battery systems in the case of grid-connected residences. The primary requirements with respect to the batteries for the grid-connected residence scenario were:

- Low cost $100/kWh;
- Long life (20 yrs); and
- Low maintenance costs ($1 to $2/kWh/yr).

These requirements cannot be met with present day batteries.

The SOLSTOR program was also used to help define monthly performance factors such as the expected charge-discharge profile. Depending on the scenario used, the computations showed large differences in the battery average state-of-charge (SOC) profile.

More specifically, when low sell-back ratios were assumed, the average SOC is low, with long periods when the SOC is essentially zero. Conversely, with high TOD price ratios, the average SOC is quite high because the battery is charged every night with cheap off-peak electricity. The sell-back and TOD price considerations require development of a battery that is quite insensitive to the SOC.

The SOLSTOR code has been expanded with the addition of a stand-alone model. In this version, the backup energy is supplied by an on-site, fossil-fueled generator rather than by the utility grid. Since on-site generators are subject to wear and replacement, different operating strategies were required for the stand-alone systems.

The computational capability has been extended to explore how knowledge of weather and load benefits the system. The inclusion in the model of an assumed prediction of weather data for an arbitrary period of time was used to calculate an upper bound on system performance. Even the use of expected weather patterns based on past patterns gave improved performance predictions. However, the prediction only benefits systems where the utility offers TOD rates.(9)

Mueller and coworkers at ANL are cooperating with Sandia on photovoltaic (PV) battery energy systems assessments. The ANL group, using the ANL SIMSTOR (simulated storage computer program)

have compared customer owned PV battery storage with utility owned PV battery storage. This was done for PV battery storage market penetrations of up to 30%. At low PV penetrations, battery discharge periods of 4 to 6 hours were optimum and storage capacities were relatively insensitive to the PV level of penetration. In several utility systems, high penetration of PV systems tended to significantly narrow peak loads, increasing the need for batteries with higher discharge capabilities.

A cost trade-off to determine optimum battery location--substation, commercial, or residential customer--was conducted. The economy of scale for both batteries and AC/DC conversion equipment was used in the analysis. The projected battery costs, especially for flow batteries, were found to increase sharply at the smaller sizes appropriate to residential-scale systems. The analytical results showed no conclusive reason for dispersing batteries beyond the substation level.

2.3.2 Battery Requirements for Solar Applications

Although the studies of PV battery storage systems are still incomplete, they have provided guidance concerning battery requirements and testing procedures. Particular classes of applications have battery requirements reflecting their particular duty cycles. In spite of these differences, some generalizations have been made.

Generally, battery storage systems must have shallow and deep discharge operating capabilities. The shallow discharges are more typical of stand-alone systems that need a large capacity-to-load ratio. The longer the storage system must be capable of power delivery, the shallower is the average individual cycle. These shallow daily or short time cycles are superimposed on deeper seasonal cycles. On the other hand, deep discharge cycles are typical of grid-connected operations.

In spite of the above differences, the two operations have some commonalities. Both undergo fluctuations in the charge and discharge characteristics due to variations in insolation and load. As noted in Section 2.3.1, these variations, which are weather dependent, are presently not predictable with the needed accuracy.

Like utility batteries, solar storage systems should have a long lifetime; on the order of 20 years. Estimates of acceptable battery costs are approximately $100 to $150/kWh for grid-connected systems and $200/kWh for stand-alone systems. The battery systems must also have low maintenance costs and, for stand-alone remote applications, be virtually maintenance free and capable of a high degree of automation.

The above and related studies led to the selection of batteries for further study. The work of Chamberlin at Sandia strongly favors flow type batteries, such as the zinc/bromine batteries being developed by Exxon and Gould, which appear to be suitable for numerous

applications. Sandia is also providing funding for the National Aeronautics and Space Administration's (NASA's) iron/chromium redox battery. Only limited applications have been identified for this system. Initial battery screening studies at ANL have identified a number of batteries as attractive candidates. Grouped by general application, they are:

- Residential
  - Lead-acid
  - Zinc/bromine
- Commercial and utility scale
  - Zinc/bromine
  - Zinc/chlorine
  - Sodium/sulfur
  - Lead-acid
  - Lithium/metal-sulfide
- Slow discharge applications
  - Redox batteries

Hittman Associates has reviewed battery systems for their compatability with various applications. Eleven battery systems were included in six applications scenarios. Three factors were considered in making the battery selection:

- Cost;
- Safety and health; and
- Reliability and maintainability.

Table VI summarizes the results of the study for non-military applications.

While there are differences in the various battery system selections, ANL, Hittman, and Sandia all appeared to select the zinc/bromine system for further development for PV battery systems. The lead-acid battery is a general choice for use, especially in near-term systems evaluations. The studies which produced these tentative results have not yet been published in detail and the assumptions leading to the variation in conclusions should be thoroughly analyzed.

2.3.3 Battery Test Program

SNL is establishing a facility for testing batteries under simulated PV battery system conditions for various solar applications. The test programs are to be computer controlled. The batteries will be exposed to one or more of the following:

- Long-term performance testing;
- Accelerated life testing; and
- Simulated photovoltaic power system operational testing.

The initial test program involves four types of batteries:

- Commercially available lead-acid;
- Deep-discharge sealed lead-acid;
- Zinc/bromine circulating electrolyte; and
- Chromium/iron redox.

TABLE VI

BATTERIES FOR PHOTOVOLTAIC SYSTEMS APPLICATIONS

Application	Residential	Village	Dairy Farm	Utility	Office
Location	Denver, Colorado (single family)	Africa	Howard County, Maryland	Arizona (Population 10,000)	Washington, D.C. (50,000 ft^2)
Installation	Grid-Connected	Stand-Alone	Onsite, Generator Backup	Grid-Connected	Onsite, Generator Backup
Battery					
Lead-Acid	X	X	X	X	X
Redox		X			
Zinc/Bromine	X		X		X
Zinc/Chlorine				X	
Calcium/Metal Sulfide					X
Zinc/Ferricyanide			X		

Test programs have been set for deep-discharge, full state-of-charge; deep-discharge, partial state-of-charge; and shallow-discharge, partial state-of-charge testing. The test cycle for the deep-discharge, partial state-of-charge test is shown in Figure 11.

2.4 Technology Information System

The Technical Information System (TIS) at the Lawrence Livermore National Laboratory (LLNL) provides nationwide information concerning management, modeling, communications, and networking for the DOE conservation technology activities. TIS is a new-generation information machine that stores programmatic information. It connects automatically to other information centers and computers when additional information and models are needed. Authorized users simply specify the name of the desired resource.

As of June 1981, information was available concerning transportation statistics, data from the National Battery Test Laboratory (described in SR-I and SR-II), and the BEST facility. TIS electric vehicle models include the LLNL hybrid systems model, the EXXON electric vehicle econometric model, and the JPL electric vehicle performance model. Additional battery and electrochemical information can be included to provide a common base for the ongoing programs.

TIS also offers services such as electronic mail, polling, conferencing, and report writing or editing. TIS interconnects to

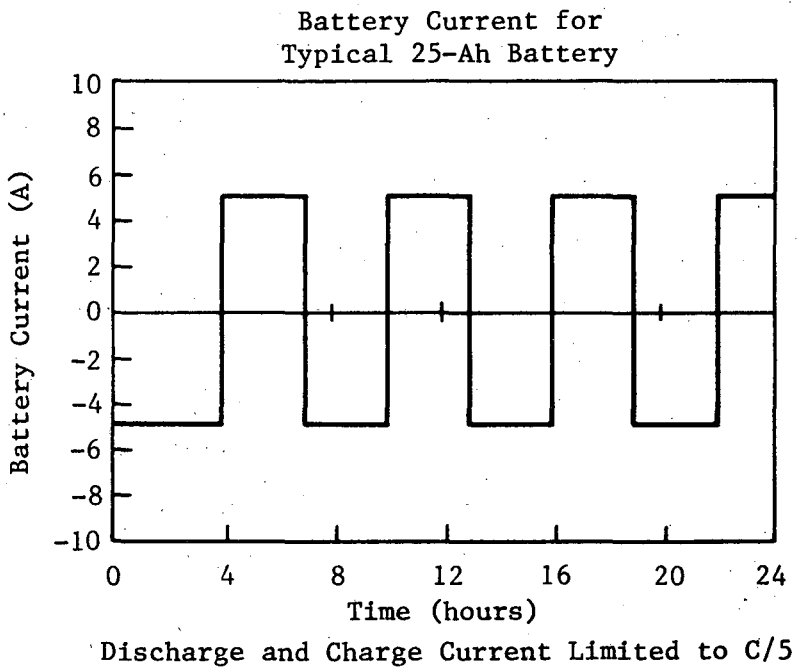

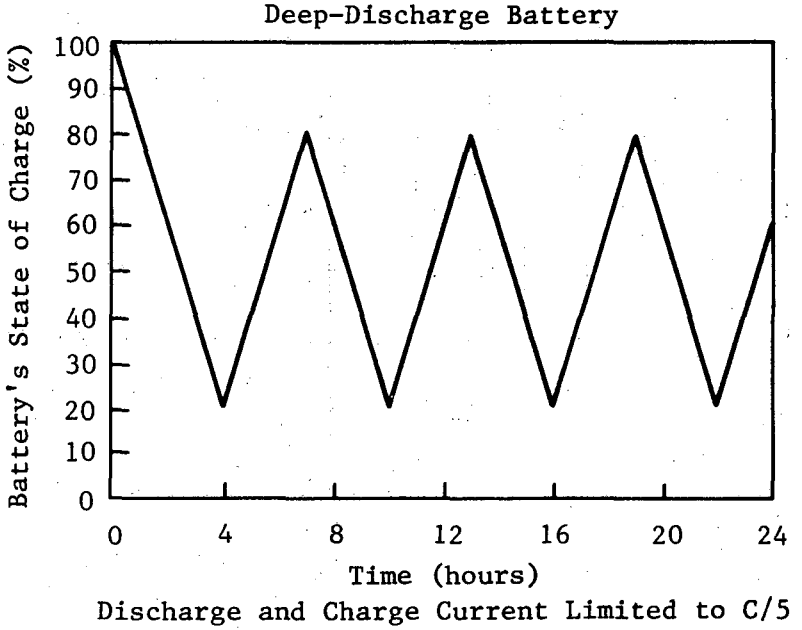

FIGURE 11
TYPICAL DEEP-DISCHARGE PARTIAL STATE-OF-CHARGE CYCLE TEST

electronic text processors, making it possible to transfer memoranda, illustrations, and reports. It is available by regular national and other telephone services.

2.5 The National Battery Advisory Committee

The National Battery Advisory Committee (NBAC) was formed in 1976 to serve in an advisory capacity to the battery elements of the ECS program. Members are battery experts representing industry, universities, the national laboratories, and government. The NBAC functions through five subcommittees:

- Planning;
- Demonstration and commercialization;
- Standards and specifications;
- Data and communications; and
- Resources and conservation.

ECS has a member on each subcommittee who is responsible for transmitting results of subcommittee deliberations to the program directors. The activities of the subcommittees are coordinated by an executive committee. A general meeting of the committee is held annually for a review of activities and to discuss matters of overall concern.

3.0 AQUEOUS MOBILE BATTERY RESEARCH AND DEVELOPMENT

The major effort concerning aqueous mobile batteries (formerly called near-term batteries) is in response to the needs of the electric vehicle (EV) program. Included are battery systems which, when the EV program was initiated under the Electric and Hybrid Vehicle Research, Development, and Demonstration Act of 1976, were projected as being available for demonstration around 1985. The relationship of the Mobile Applications Subelement, for which the aqueous batteries are being developed, and the EV program is indicated by the large fraction of the subelement effort that is funded by the EV program (see Table I above). The batteries included in this effort are:

Lead-acid;

Iron/nickel-oxide; and

Zinc/nickel-oxide.

The zinc/chlorine or zinc-chloride EV battery, which was described in SR-I and SR-II, will not be included in this review. The present effort is being continued by Energy Development Associates (EDA). That company has elected to continue its efforts without government funding.

The aqueous battery research and development technology efforts for the mobile and dispersed battery applications subelements are under the management of the Argonne National Laboratory (ANL). The

solar applications battery development activities are being managed by the Sandia National Laboratories (SNL).

Table VII lists the participants in the Mobile Applications Subelement technology program, the contract period, and the contract value (industrial and governmental support). Table VIII lists the aqueous mobile (formerly near-term EV) battery development goals and expected vehicle performance. The lead-acid battery contractors and the battery performance goals for the dispersed and solar applications are included in the review of the specific battery investigations. Figure 12 shows the progress from 1977 to March 1981 toward meeting the EV battery performance goals. Note that the batteries included are in an earlier stage of development than those described in the following sections.

3.1 The Lead-Acid Batteries

Improved state-of-the-art (ISOA) lead-acid batteries are being developed for all three applications technologies. Most of the emphasis on the advanced lead-acid battery is related to the mobile application, the most demanding in terms of specific energy and specific power. In this section, the status of the ISOA and advanced battery developments and the related supporting research are reviewed.

3.1.1 ISOA Lead-Acid Batteries for Mobile Applications

The various contractors' approaches to improved state-of-the-art (ISOA) and advanced lead-acid batteries for mobile

TABLE VII

MOBILE APPLICATIONS PROGRAM CONTRACTORS

Battery Type	Contractor	Contract Period	Contract Value[a] ($1,000)
Lead-Acid	Eltra	04/78-05/81	2,580
	Exide	02/78-01/82	3,386
	Globe	03/78-09/81	4,633
Nickel/Iron	Eagle-Picher/SU	03/78-09/81	2,988
	Westinghouse	12/77-09/81	3,022
Nickel/Zinc	Exide	04/79-03/82	1,200
	Energy Research Corp.	02/78-09/81	3,608
	Gould	01/78-01/81[b]	6,736
	Yardney	07/77-05/79[b]	1,000
Zinc/Chloride	EDA	11/79-12/80[b]	1,433

[a]Includes contractor's share.

[b]Terminated by mutual agreement.

TABLE VIII

NEAR-TERM MOBILE APPLICATIONS PERFORMANCE GOALS

Battery Parameters	Development Goals	Expected Vehicle Performance[a]
Specific Energy	56 Wh/kg (C/3 rate)	100 miles/charge (SAE J227 aD urban driving)
Specific Power[b]	104 W/kg (30-sec peak)	Acceleration 0 to 30 mph in 8 secs
Cycle Life	800 cycles (to 80% DOD)	>60,000 miles (life)
OEM[c] Price	$70/kWh	~$2,000 battery cost

[a] Based on DOE/ETV-1 vehicle with regenerative braking.

[b] Specific power is measured at 50% DOD.

[c] OEM = Original Equipment Manufacturer.

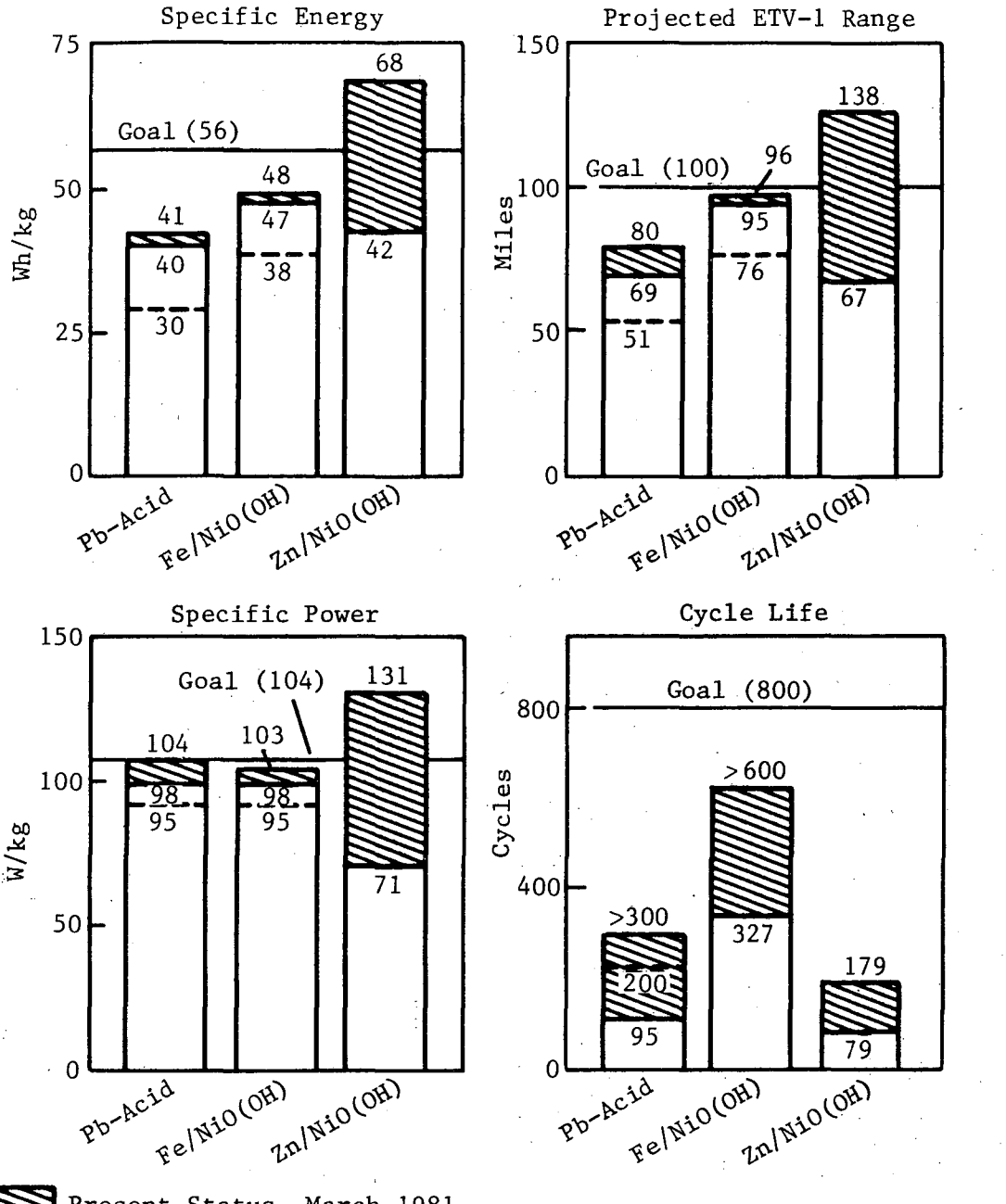

Measurements conducted at the Argonne National Laboratory's National Test Laboratory.

FIGURE 12
PERFORMANCE AND LIFE OF IMPROVED ELECTRIC VEHICLE BATTERIES

applications vary, and the greatest differences lie in their efforts to develop advanced batteries.

The approach of Globe to the ISOA battery has been the simultaneous optimization of cell design, materials selection, and the manufacturing process. This has led to the successful design and molding of large, lightweight, polypropylene containers and covers contributing to an improved battery specific energy. Molding techniques required to permit penetration of the cover for the battery terminals and the vent/water and air manifolds (for the electrolyte circulation system) were developed. The grid design was based on the resistance minimization computer models reported earlier.[1][2] Based on cell testing, a low-corrosion grid-alloy was selected. The positive paste density was determined from the performance testing of machine pasted plates which revealed an optimum positive plate active material density. Positive plate formation variables were also investigated and evaluated in terms of lead dioxide and lead sulfate content at the end of formation. Evaluation of the six best formation conditions is continuing.

The negative-to-positive weight ratio was decreased. This contributed to the reduction of the module weight by 1.18 kg and the thickness of the element by 0.092 cm per cell. The electrolyte volume was also reduced. An independent electrolyte circulation system was developed and this has contributed to the improved battery performance. The Globe ISOA battery design was frozen as of

April 1980 and five test modules with peripheral equipment have been submitted to the National Battery Test Laboratory (NBTL) for testing.(10)

Exide's approach to the ISOA EV battery has been based on investigation of the interrelationships among the following design variables:(11)

- Four different positive paste formulations;
- Two commercially available microporous separators in conjunction with a glass mat;
- Two concentrations of sulfuric acid, sp gr 1.285 and 1.315; and
- Two cell construction variations (12 negative and 11 positive plates and 11 positive and 12 negative plates).

Based on study of the resulting 32 cell variations, it was concluded that:

- Batteries containing Daramic separators operate at a higher discharge voltage, providing a higher specific energy;
- The use of 1.315 sp gr sulfuric acid does not provide sufficient additional capacity to compensate for the increase in weight;
- It will be necessary to increase the separator rib thickness to provide increased electrolyte circulation. Battery design adjustments must be made to accommodate the increased spacing;
- Cycle life improvement is required and is to be obtained by increasing positive plate thickness; and
- Radial design grids should be used to decrease internal voltage drop.

The last of these changes is based on the results of a study at Battelle Columbus Laboratories on improved grid design. Features of the Exide radial negative, R, which are similar to those of the Globe radial grid and the Battelle nonorthogonal grid, B, are shown in Figure 13.[11] The comparison of the capacity of cells with grids having the two plate designs is shown in Figure 14. The cells were tested at higher rates of discharge (6 to 9 minutes) than is required for mobile applications. Cycling of the cells at rates of discharge corresponding to mobile batteries is required to determine the extent to which the observed capacity improvement, approximately 85% at a cutoff of 1.5 volts, will occur at the lower rates of discharge in EVs.

The Exide effort is also evaluating cells with tubular positive plates. The cell variables are similar to those used in the flat plate investigations. The cells with tubular positives had greater cycle life than did the flat plate cells. However, the best specific energy achieved, 37.7Wh/kg, was below the goal of 40 Wh/kg. Design changes are being made which are expected to yield a tubular-positive battery with a specific energy of 40Wh/kg.

The Eltra (C&D Batteries Division) approach to the ISOA is based on the expanded grid technology developed by that corporation and reported in SR-II. Studies to evaluate different battery parameters were also conducted by Eltra. The factors included were:

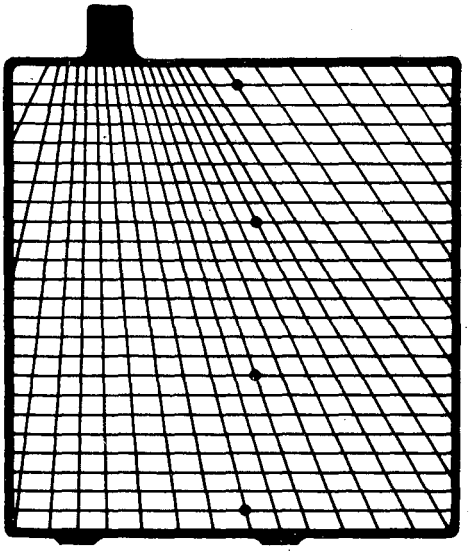

Radial Grid

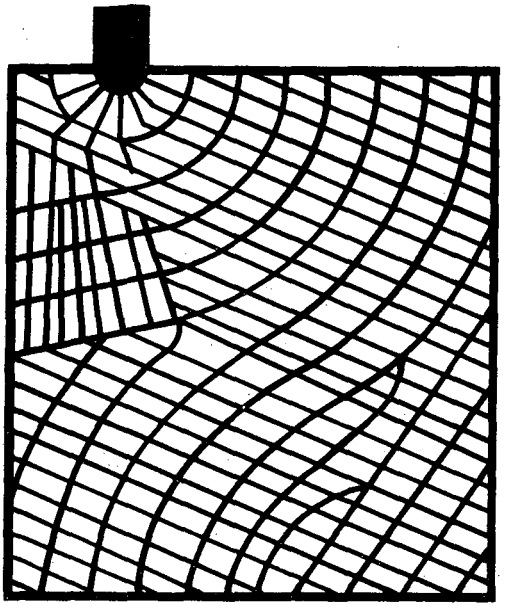

Battelle Grid

FIGURE 13
COMPARISON OF RADIAL AND BATTELLE GRID STRUCTURES

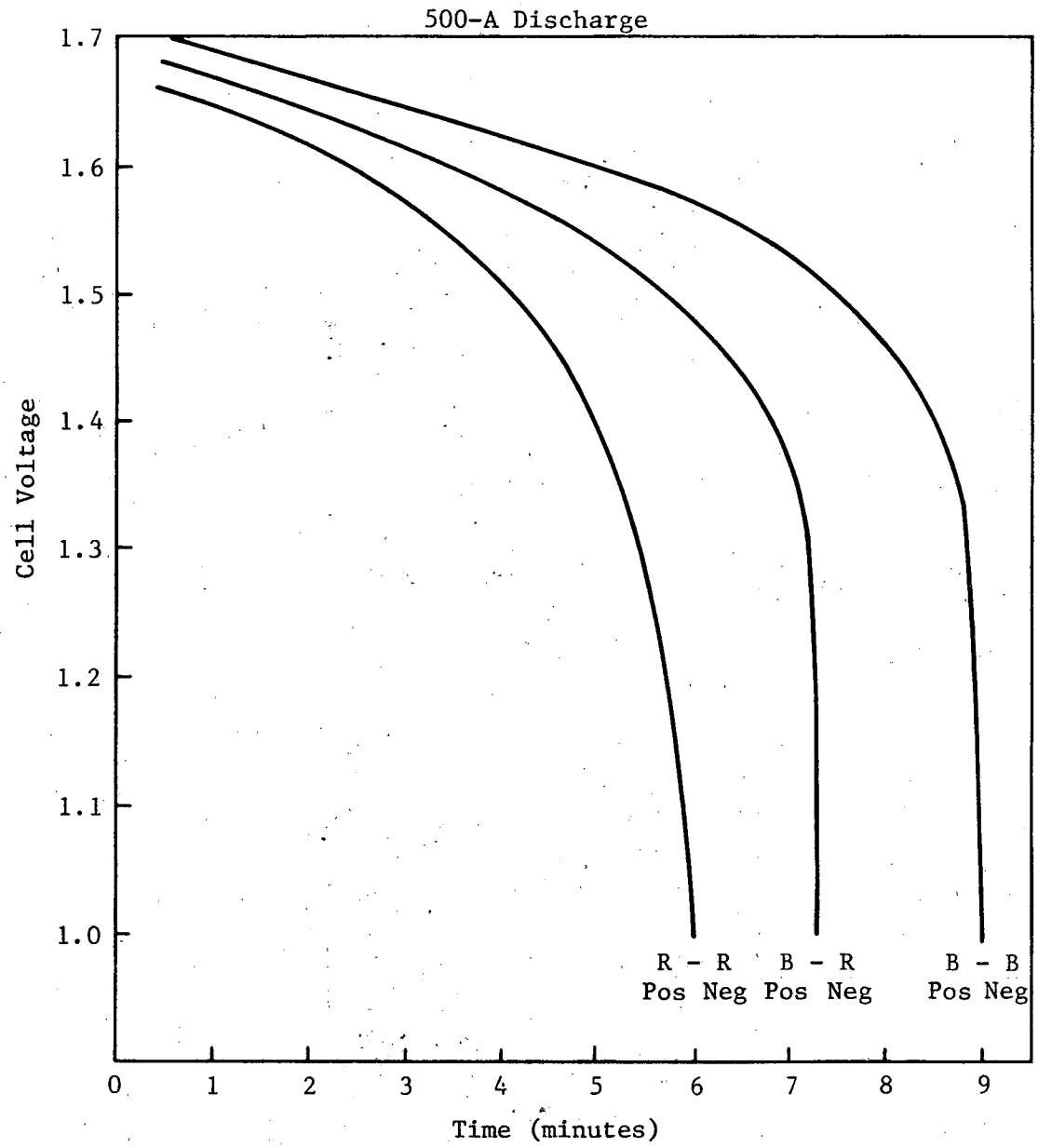

FIGURE 14
COMPARISON OF PERFORMANCE OF RADIAL AND BATTELLE GRIDS

- Two different paste densities;
- Two different electrolyte gravities;
- Two types of glass mat retainers; and
- Two types of separators.

The above parameters were tested in 19 plate cells (10 negatives, 9 positives) in three-cell, golf-cart battery containers. Positive and negative grids were cast from a lead alloy containing 0.07% Ca and 0.7% Sn. A specially formulated negative expander was used in the negative plate. The active material in the paste was a mixture of tetrabasic lead sulfate (TTB) and leady oxide.

Within the constraints of the experimental results, which revealed small differences in the effect of the variables on performance, the following conclusions were considered to be valid:

- Paste density--There is some advantage to higher paste density for both greater energy density and longer cycle life.
- Acid gravity--Higher gravity provided higher energy density but lower gravity provided higher cycle life.
- Separator--No marked advantage was observed for either of the separators studied.
- Retainers--The parallel fiber Slyver glass mat was distinctly better than a random fiber mat.

The post-mortem analysis of the cells, after cycling, showed that failure was primarily due to loosening and washing of active material from the positive plates.

A comparative study of the Pb-Ca-Sn grid modules and 4.56% antimony-lead alloy grids showed the latter provided for a cycle

life that was four times longer. Some of the cells with the Pb-Ca-Sn grids showed severe grid corrosion.

The Eltra group has prepared a series of ISOA batteries for NBTL examination. The performance of these and the Globe and Exide ISOA batteries are included in Table IX along with the ANL 1980 lead-acid battery goals.

3.1.2 Advanced Lead-Acid Batteries for Mobile Applications

The Globe approach to advanced lead-acid batteries is a combination of design refinements and technology improvements. A process for the manufacture of lead-plastic composite grids has been developed and the grids are under test in three-plate cells. Work has continued on the study of expanders by cyclic voltammetry. This is discussed in Section 3.1.5 under lead-acid battery supporting research.

An electrolyte pumping system has been developed which is reported to increase the cycle life of batteries. Based on accelerated C/3, 70% depth-of-discharge (DOD) cycling tests, with a cutoff voltage of 1.75, a cycle life of over 1,000 was obtained. For laboratory evaluation, air-actuated lift pumps were placed in each cell compartment to maintain a uniform acid concentration. A single 3-watt, aquarium-type air pump was used to activate 12 cells. The pumps operated during charge and discharge. The use of pumping enables the use of a gentle and simple equalization charge mode. This resulted in a coulombic efficiency of 95% and energy

TABLE IX

STATUS OF ISOA LEAD-ACID BATTERIES

Battery Parameter	ANL ISOA Goal (Pb-Acid)	Globe ISOA 9/80	Exide ISOA		Eltra ISOA
			Flat Plate	Tubular	
Battery Capacity (kWh)	20-30	--	--	--	--
Specific Energy (Wh/kg)	40	41	40	35	40
Specific Power (W/kg)	20	104	128	100	98
Sustaining Peak (15 sec)	100	111	--	--	128
Cycle Life (cycles)	800	508	295	>450	95
OEM Price[a] ($/kWh)	50	--	--	--	20
Energy Efficiency	60	80-85	--	--	--

[a]OEM = Original equipment manufacturer.

Figures are based on 1978 lead prices and a production rate of 10,000 batteries/yr.

efficiencies of between 80% and 85%, well above the goals for advanced lead-acid batteries. The electrolyte pumping system, mentioned in Section 3.1.1, has been included in the total package submitted to NBTL for testing of the Globe ISOA lead-acid batteries. Although the electroyle circulation uses energy, the net result, due to improved battery performance, is an increase in specific energy, specific power, and round-trip efficiency.

The Exide advanced battery group is also investigating lower weight grids. The approach is to use a plastic negative grid for strength and weight reduction, a copper coating on the plastic for conductivity, and a lead coating to protect the copper from corrosion. This approach, if successful, can give a 50% to 60% reduction in grid weight and a 5% to 6% reduction in battery weight. All cells tested as of September 1980 showed cycle lives of over 500 at a 100% depth of discharge. Some loss of copper from the grid was observed on an electrode from an operating cell terminated for the purpose of diagnostics. Testing of plastic grids has been extended to the Battelle radial grid design.

Electrolyte agitation to improve battery performance is also being explored by Exide. Initially, air bubbling through the electrolyte is being investigated. The air is introduced at the bottom of the cell container through the sediment ribs via a manifold exit pipe. With air bubbling, the average voltage during discharge and charge was decreased 0.01 and 0.09 volt, respectively.

The light-weight, plastic-metal grid, electrolyte agitation, and flat (Battelle radial design) and tubular positive plates are included in the advanced battery design. Methods for increasing the utilization of the active material are also being explored.

Eltra also is working on advanced lead-acid batteries. The isopotential lines of grids with active material have been experimentally determined. Grids with varying aspect ratio, high width-to-height, and with multiple or different lug positions have been examined. These measurements are being used to help improve active material utilization. Lead-plastic composite positive plates are being investigated to decrease cell weight. A cycle life of 210 was achieved in September 1980 with the three-cell module test continuing. The calculated energy density for a cell with ISOA construction was 41Wh/kg.

The addition of graphite fibers to improve positive active material conductivity is under investigation at Eltra. Concentrations of graphite fiber in the range of 0.5% have been shown to produce benefits. Thick positive plates with graphite fibers show an improved rate of conversion to lead dioxide during formation. Thin plates with graphite fibers have shown an increase in active material utilization as high as 16%. Other studies on active material formulation and other cell components have been noted as part of the ISOA effort. The circulation of electrolyte is

also included in the Eltra studies and resulted in improved cycle life of the advanced battery design. Reported advanced battery designs have achieved a specific energy of 41Wh/kg but cycle life still requires improvement. The similarity to and differences among the above approaches and advanced electric vehicle batteries are shown in Table X.

Several of the state-of-the-art (SOA), ISOA, and advanced lead-acid batteries have been tested at the ANL National Battery Test Laboratory (NBTL). The results reported at the fourth BECC are summarized in Figure 15. The results show steady, but not dramatic, improvement in the lead-acid battery technology. However, these reported tests cover only part of the testing procedure and do not include the results of advanced battery concepts not yet developed to the point of demonstration.

3.1.3 Lead-Acid Batteries for Dispersed Applications

The development of lead-acid batteries for dispersed electrical storage applications is being monitored by ANL. The battery performance goals are listed in Table XI. Although earlier studies have shown that the adaptability of SOA batteries to utility systems is questionable, SOA batteries are being procured for initial testing in the BEST facility. The major thrust of the ANL-monitored effort is the development of an advanced lead-acid battery which will better fulfill utility requirements. In the interim, a 15kWh

TABLE X

APPROACHES TO ADVANCED LEAD-ACID BATTERIES

Battery Component	Globe	Exide	Eltra
Grid Structure	Radial ribs	Radial and Battelle nonorthogonal	Equipotential grids, aspect ratio and lug position
Grid Material	Lead-plastic composite	Plastic coated with copper and lead negative	Lead-plastic positive composites
Electrolyte	Circulation	Agitation	Agitation
Active Material	---	---	Graphite fibers in positive active materials

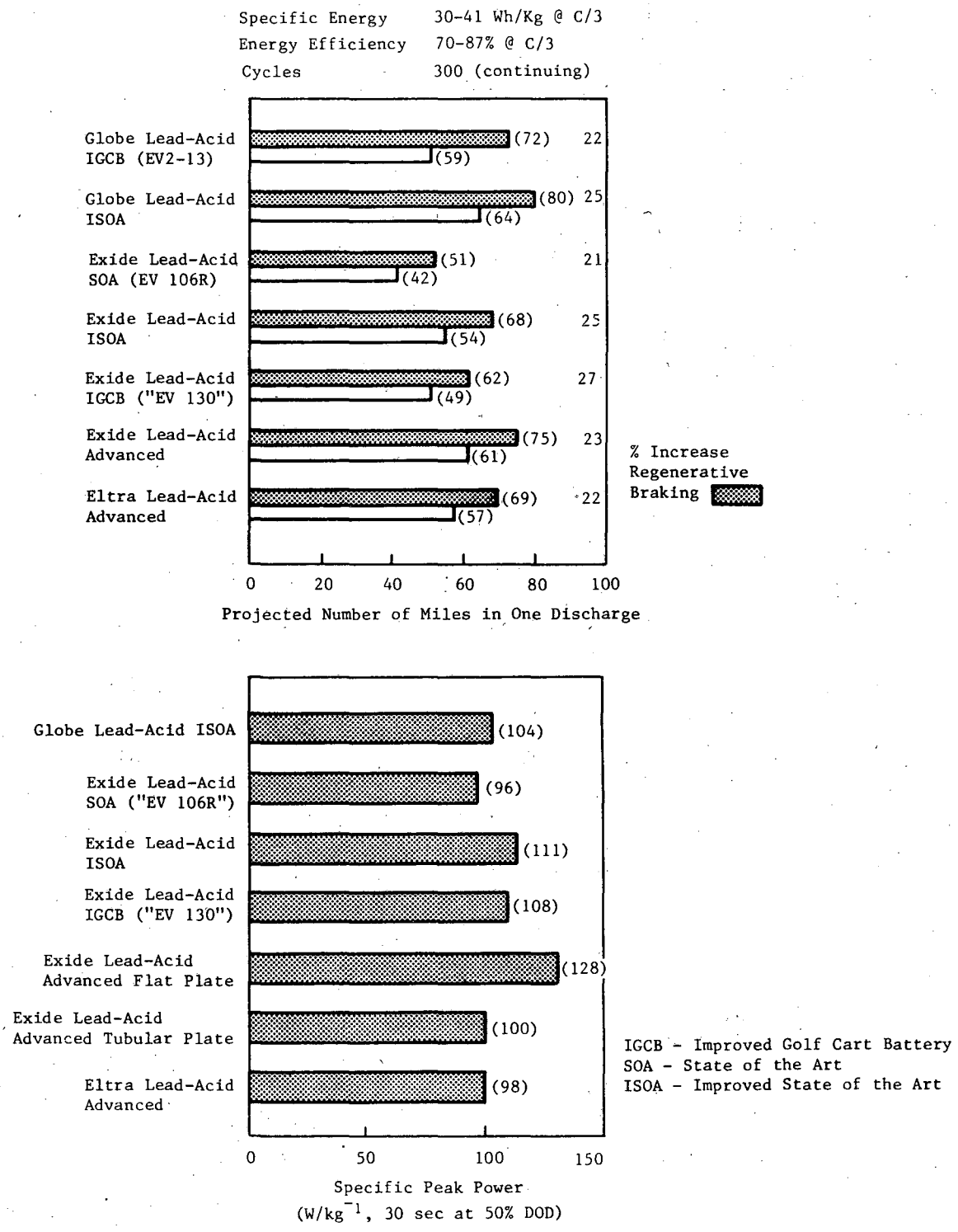

FIGURE 15
NBTL LEAD-ACID BATTERY TEST RESULTS

TABLE XI

ADVANCED LEAD-ACID LOAD-LEVELING BATTERY DEVELOPMENT GOALS

Goal		Unit	State of the art	Advanced Battery
Battery for BEST Facility Test		MWh	5	5
Life	Stand	Yr	10	20
	Cycles (80%)	Each	2,000	4,000
Energy Efficiency, Turn Around		%	76-85	80
Energy Foot Print		kWh/m^2	43-54	75
Initial Battery Price		$/kWh		
Lead	25¢/lb		42-58	37-50
	58¢/lb		75-100	50-75
Battery Rebuild Price		% of initial	46-79	50
Operating Temperature		°C	4-50	4-50
Cycle	Discharge	Hr	5	5
	Recharge	Hr	7-10	5-7
	Depth	% 5-hr rated	80	80

Source: Reference 3.

SOA module, most closely meeting the development objectives, is being tested at NBTL.

Phase 1 of the ANL-managed effort is the study of battery design and cost and the development and testing of concepts to be integrated into the advanced battery. The C&D Batteries Division of Eltra Corporation and Exide Management and Technology Corporation are the two contractors working on development of the advanced batteries for dispersed applications.

Eltra has initiated a multi-variable, 40-battery testing program using factory-prepared, motive-power (industrial truck) batteries (400Ah). This test program uses two cycles per day with 80% DOD. The cell variables included:

- Positive grid thickness;
- Grid alloy composition;
- Active material paste composition and density;
- Positive material affecting additives;
- Acid concentration;
- Separators;
- Negative grid configuration; and
- Operating temperature.

The program to test the above variables was initiated in March 1980 and, as of September 1980, all test cells had completed 250 cycles with tests continuing. The process improvement activities included the development of a positive active material formulation

based on a low density paste containing a high percentage of tetrabasic lead sulfate (TTB). Seeding to decrease the formation time of the TTB pastes was successful. The crystalline structure and the α/β PbO_2 ratio in the formed plate are being determined. Cell cooling requirements are also being investigated.

Based on the preliminary data, it has been estimated that the resulting advanced load-leveling batteries will achieve the cycle life goals and reduced battery cost goals.

The group at Exide is investigating accelerated cell testing in order to obtain a reliable correlation between these tests and battery performance. Testing at 70 ± 3°C is being evaluated as a means of accelerating the determination of the cycle life. Earlier correlations by Exide personnel have shown that one cycle at 70°C and 80% DOD is equivalent to six cycles at 25°C.[14] At the time of the cited report (approximately mid-summer 1981), 52 of 60 cells, each having 17 plates and a capacity of 1,785Ah, completed 450 plus accelerated cycles. The eight cells that failed (loss of 20% of rated capacity), had low-density negative active materials and low negative-to-positive active material ratios. This ruled out the low-density negative electrode as a means for cost reduction.

Accelerated corrosion testing of flat-plate positive grids is also being conducted at Exide.[15] Five-plate, 400A cells, differing only in the composition of the positive-grid alloy, were anodically polarized at 4.5 and 3 times the finishing rate at 50 to

55°C. Residual capacity was periodically determined by conducting a discharge at the 5-hour rate. It was shown that the grid corrosion rate was a linear function of the overcharge current density. The tests showed little variation in the corrosion rate of antimony-alloy grids with antimony concentrations of 4% and 2.5%. The effect of arsenic concentration (0.03 and 0.05%) was unclear. It was also found that the corrosion rates in the 70°C cycling tests were 1.4 times those in the overcharge tests. The tests enabled the identification of at least one grid alloy which should be suitable for the 1,000-hour test.

Arsine and stibine evolution were determined during the overcharge test; the method of Varma, Cook, and Yao[16] was used for the determination. X-ray diffraction studies at Exide on the positive materials in the overcharge tests showed a trend toward higher levels of α-PbO_2, with increasing cumulative overcharge. The effect is greater in materials without additives. The higher rate of α-PbO_2 accumulation indicated a greater rate of capacity loss. This was verified in the catch-out deep cycle data.[15]

A third accelerated test being developed at Exide is to determine the shedding of positive-plate active material. Following an initial series of experiments involving active material formation, capacity buildup cycles, and catch-out cycles, the accelerated testing was initiated.[17] This consisted of 36 shallow cycles/day with controlled overcharge for 18 to 20 days.

This was followed by a set of catch-out cycles. The procedure was repeated until cell failure. The accelerated testing revealed several important factors related to positive electrode design including:

- Maintenance of cell stack pressure;
- Optimum positive plate wrap and retainer;
- Effect of paste density;
- Effect of electrolyte specific gravity; and
- Optimum separation between plates.

Eight pre-prototype cells have been designed from a combination of accelerated cycle and deep-cycle data. These cells were under test (mid-summer 1981) using a two-cycles/day regime at ambient conditions.(16)

The Varta study on the fabrication and testing of a prototype gas recombination device for utility lead-acid cells has been successfully completed. The device is based on the decomposition of stibine and arsine by a charcoal bed followed by the catalytic recombination of the hydrogen with oxygen. Figure 16 provides a view of the interior of the device, showing the active components and thermocouples for monitoring the device. The charcoal hydride decomposer is in a replaceable canister. The catalyst matting is composed of palladium, polytetrafluoroethylene, infusorial earth, and activated charcoal. The matting is about 4 mm thick. Tests of the device were conducted on a 9kAh, lead-acid cell. The hydrogen-

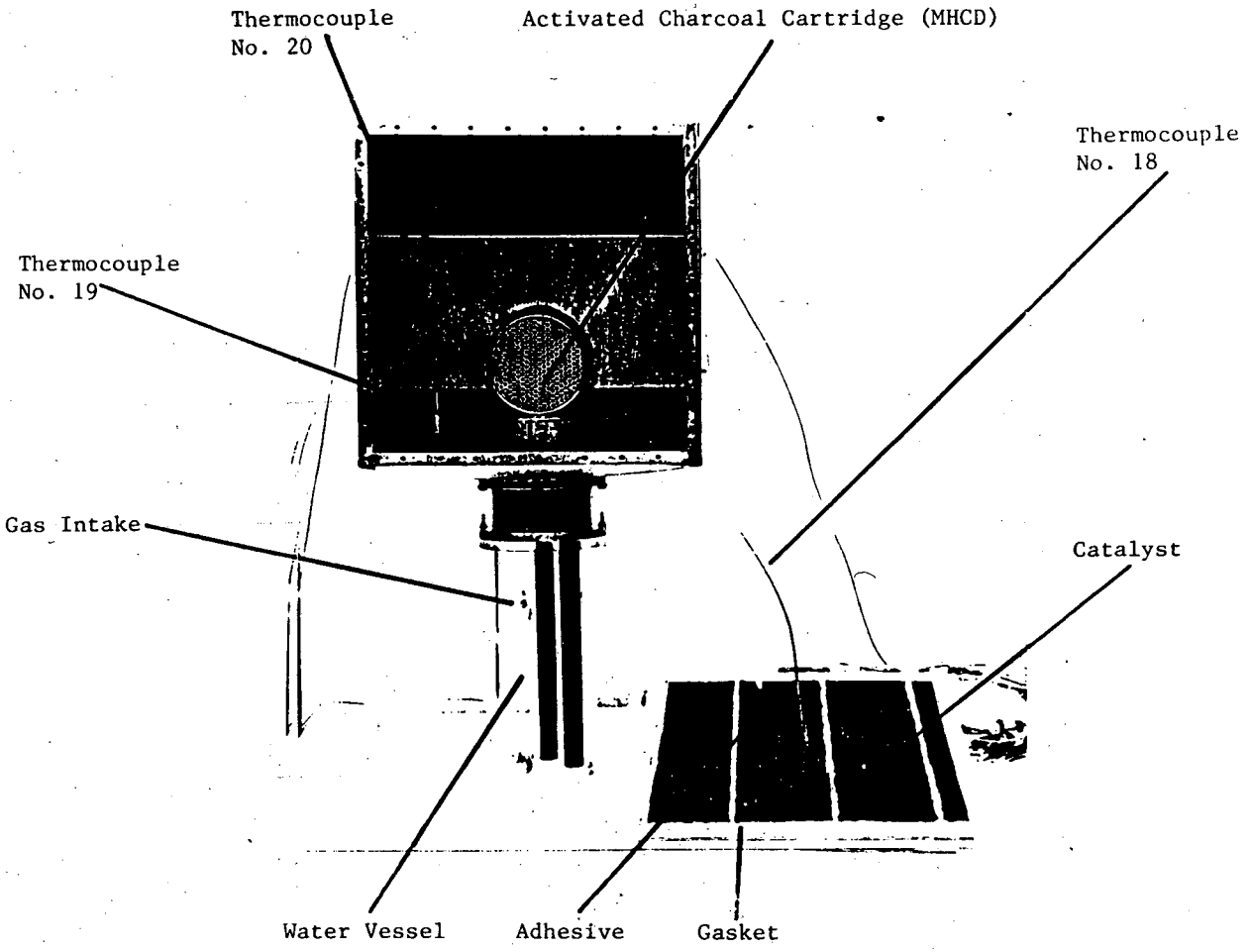

FIGURE 16
INTERIOR OF THE HYDROGEN-OXYGEN RECOMBINATION DEVICE

oxygen recombination was 97%. It was shown that the device operates effectively during overcharge. The cost of the hydrogen-oxygen recombination device was estimated to range from $4 to $10/kWh of cell capacity for production of more than 10,000 units.

3.1.4 Lead-Acid Batteries for Solar Applications

Remote solar systems require essentially maintenance-free batteries. In addition, the use of residential, on-site battery storage with solar photovoltaics makes a battery which does not require specially ventilated charging rooms a worthy objective. The Sandia National Laboratories has undertaken the development of sealed, maintenance-free, lead-acid batteries. The battery performance goals for a 6-volt, 100Ah battery are listed in Table XII. Two contractors, Eagle Picher and Gould, have been selected to develop batteries which meet these goals. The approaches of the two contractors are very different.

Eagle Picher has initiated a program of component studies. This includes the study of nonantimonial grids and the development of methods for processing wrought-lead grids, including grids prepared by expansion. Various active material formulations, including formulations based on tetrabasic lead sulfate as well as more conventional lead-oxide based formulations, are being evaluated. Various separator materials (both the retainer mats and the microporous polymers) are being examined. The use of an immobilized electrolyte and of a horizontal plate design is being

TABLE XII

GOALS FOR SEALED LEAD-ACID BATTERIES

Discharge Rate:	1 hr maximum, 6 hrs nominal
Duty Cycle:	Discharge to 80% of rated capacity
Charge Rate:	2 hrs maximum, 6 hrs nominal
Life:	5 yrs (approximately 2,000 cycles)
Energy Efficiency:	80% roundtrip
Self Discharge:	<1% per week
Temperature Range:	0-50°C
Maintenance:	None

explored. Early results of studies of the effect of plate position on battery performance appear in Figure 17. Based on the evaluation of the above and other cell design variables, a 100Ah battery is to be constructed and tested.

The Gould approach is to design cells that only evolve oxygen during charge. Cells are being studied that have an excess negative capacity and highly porous separators, permitting ready access of the oxygen to the negative plate. The oxygen-negative plate reaction rate is high enough to keep the oxygen buildup below one atmosphere. Even with this design feature, it is desirable to take precautions against oxygen pressure buildup. This is achieved with a low pressure vent that has been designed to permit the escape of excess gas. The batteries are to be tested on an open-circuit stand at various states of discharge for: short time exposures to various temperatures, cycle life, and reduced state-of-charge performance. Gould has fabricated cells and batteries with a capacity of over 100Ah and these have been delivered to Sandia for testing.

3.1.5 Lead-Acid Battery Supporting Research

Cell studies which can be used for guidance in accelerated testing of batteries are described above in Section 3.1.3. Research is also in progress to better understand lead-acid battery performance at the microscopic level, to aid in material selection, and in controlling potential hazards from lead-acid batteries.

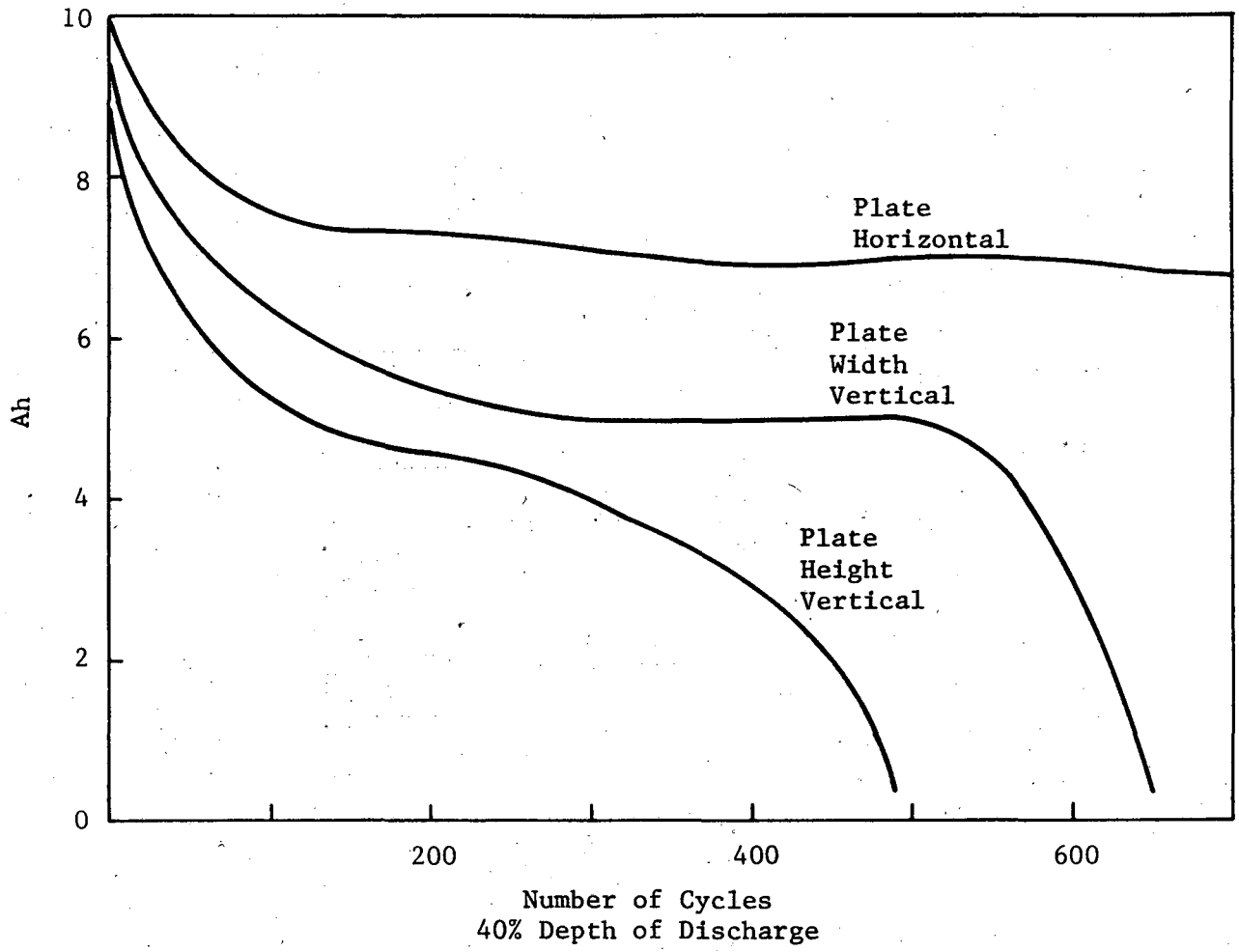

FIGURE 17
EFFECT OF BATTERY POSITION ON PERFORMANCE

Varma, Cook, and Yao have extended their studies of in-situ laser Raman scattering (LRS) to the anodization and sulfidation of tetrabasic lead sulphate in 0.1N H_2SO_4.[18]. In addition, they determined the laser Raman spectra of various basic lead sulfates for reference. The LRS spectra were taken at intervals during the anodic formation of a tetrabasic lead sulfate positive plate. The spectra strongly suggested the presence of $PbSO_4$, $PbO.PbSO_4$, and $3PbO.PbSO_4$ in the surface layers of the PbO_2 formed. Lead sulfate was the major one of the three surface compounds. The initial tetrabasic lead sulfate was partially transformed into a mixture of $PbSO_4$ and $PbO.PbSO_4$. The presence of $PbO.PbSO_4$ and $3PbO.PbSO_4.H_2O$ is consistent with the Pourbaix diagram of the pH-lead sulfate thermodynamics at a pH above 8. It was concluded that the high pH range could only exist in the case of electrolyte starvation at the electrode surface during plate formation. The experimental limitations of acid concentration, because of light absorption by the acid ions, makes the extension of these results to the higher acid concentrations of battery technology uncertain.

The relationship of the high current demand of an electric vehicle to the negative electrode microstructure of a lead-acid battery has been investigated by Wales, Caulder, and Simon.[19] Discharge rates of 18, 125, 500, and 2,000A/m^2 were used. Samples of the negative plates were removed and examined by light

and electron microscopy, image analysis, and surface area measurements. It was observed that the size of the lead sulfate crystal in the discharged plates decreased with the increased current density. This roughly corresponded to the decrease in plate capacity with increased current density. The authors concluded that this behavior suggests passivation of the lead as the proximate cause for the capacity loss since passivation becomes more critical as the crystallite size of $PbSO_4$ decreases. Based on the observed polarization curves, it was suggested that limited electrolyte diffusion rates and decreased contact of active material crystals, the result of the porosity that developed with cycling, also contributed to the reduction of plate capacity.

Mahato of Johnson Controls Incorporated (Globe) has continued studies of lead-acid negative plate expanders using a microelectrode with a cyclic linear potential sweep.[10][20][21] Figure 18 compares the curves obtained with a highly reversible electrode and one that has poor capacity recovery on charge. Note that the anodic portion of the potential sweep for the electrode with poor capacity recovery has a much smaller area than does the potential sweep for the reversible electrode. This higher reversibility was shown to be a function of the amount of expander in solution, as shown in Figure 19. Note that the capacity after cycling increases with concentrations up to 20 ppm of lignosulfonate in solution and then decreases This decrease in capacity at the higher concentration is attributed,

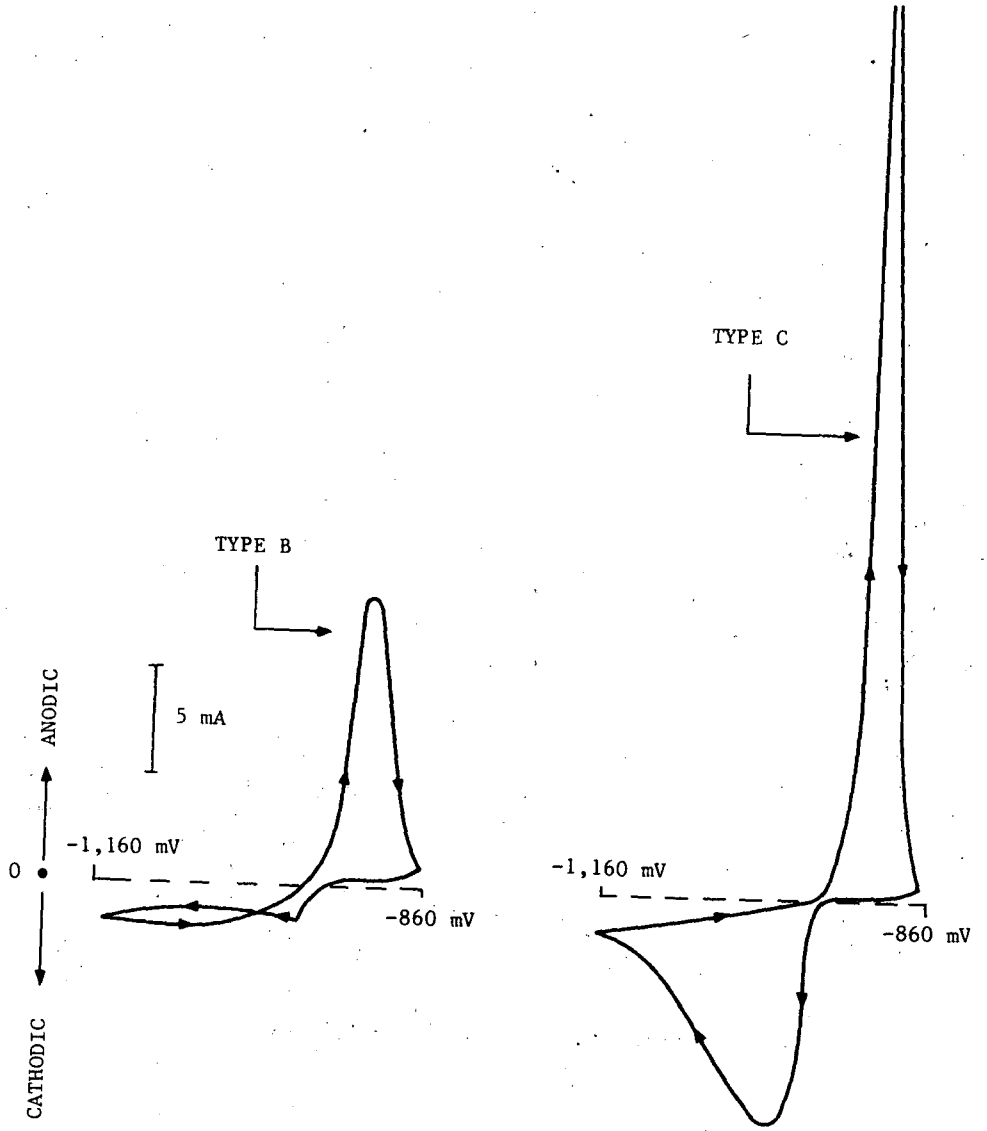

Reference Electrode: Hg/Hg_2SO_4
Sweep Rate: 5 mV/sec
Cycle No: 145
Electrolyte: H_2SO_4, 1.250 sp. gr.

FIGURE 18
VOLTAMMOGRAM OF EXPANDERS IN LEAD ELECTRODE

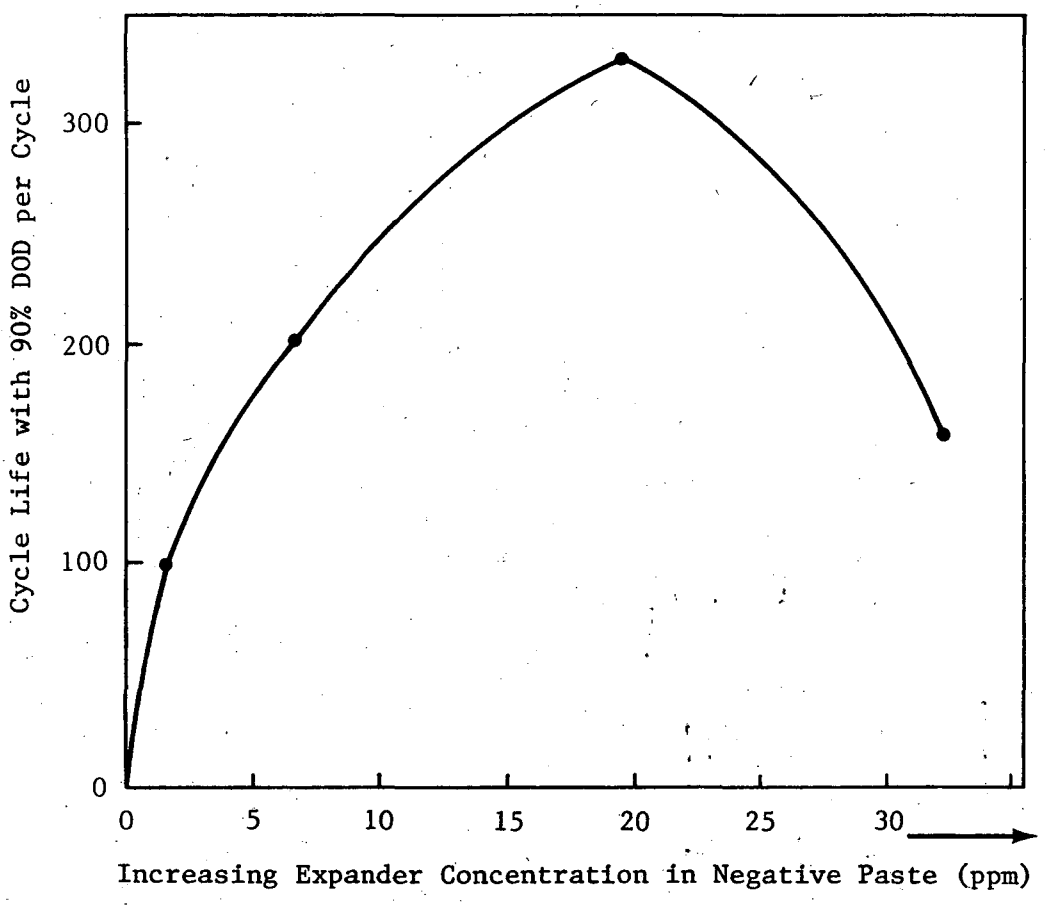

- Lignosulfonate Expander, Actual Concentration Not Provided

FIGURE 19
EXPANDER CONCENTRATION AND LEAD-NEGATIVE CAPACITY

at least in part, to surface coverage by adsorbed lignosulfonate. The use of different lignosulfonates showed that expander activity varied with the composition and concentration of the expander. It was concluded that the microelectrode probe technique is a valid research tool for expander material evaluation.

3.1.6 Lead-Acid Battery Status Overview

The status of lead-acid battery technology makes it the system of choice for proof-of-concept even in those cases which require battery properties that advanced lead-acid batteries have not been demonstrated as fulfilling. Extending the usefulness of lead-acid batteries, especially for mobile applications which require high specific energy and power, is a potential interim solution until alternative battery systems prove to have performance exceeding the lead-acid battery at a competitive price.

The broad scope of applications for which lead-acid is being considered, both for demonstration of concept and commercialization, has led to varied approaches to lead-acid battery technology. For mobile systems, emphasis on decreased weight is leading to the exploration of alternative negative grid materials such as metal-coated plastics, conducting plastics, tailoring of expanders for improved active material utilization without decreased cycle life, lower resistant separators, and the addition of conducting fibers to the positive active material to lower resistance and improve material utilization. Attempts are also being made to eliminate

antimony from the negative plate to decrease stibine formation. The use of forced convection in the electrolyte can give more uniform consumption of active material with improved cell performance and cycle life.

The advanced batteries for dispersed applications emphasize cycle life and lower cost. Weight is not as great a concern as in the case of the mobile, especially private vehicle, applications. The solar batteries, for remote unattended use, require the development of closed-system batteries. This has led to considering high purity lead electrodes in spite of their more difficult processing. This avoids the problems of stibine and arsine formation. The electrodes will require operation without water loss through recombining hydrogen and oxygen. The use of wrought lead should increase the lifetime of hydrogen-oxygen recombination catalysts through the avoidance of catalyst poisoning by stibine and arsine. There is no question that the projected applications of batteries have encouraged a broader approach to lead-acid battery development.

Supporting research, basic and applied, is providing information leading to a greater depth of understanding of the physical and chemical processes in the lead-acid battery. The further development and increased application of techniques for the in-situ study of electrode changes during charge and discharge can lead to improved material selection. Attempts to develop rapid

laboratory tests for projecting battery lifetimes, if proven to be reliable, can accelerate the rate of progress in advancing battery technology. The lead-acid battery, in spite of its long history, still shows the potential for performance increases which will extend its utility.

3.2 Iron/Nickel-Oxide Electric Vehicle Batteries

The development goals set by ANL for the iron/nickel-oxide [NiO(OH)] alkaline electrolyte battery are listed in Table XIII. To be noted are the higher specific energy and longer cycle-life goals than for the lead-acid battery. Two organizations are involved in the development of iron/nickel-oxide batteries: Westinghouse and Eagle Picher Industries. The latter has a subcontract with the National Development Corporation of Sweden for work on the iron electrode and the separator. Reference 2 (SR-II) contained a comparison of the two batteries. The battery features are repeated in Table XIV, along with the performance reported at the BECC.[3] Cycle life information is the major new input in Table XIV. The Eagle Picher program has achieved 2,000 cycles with tests proceeding on individual cells indicating the potential for meeting the 1984 cycle life goal.

Additional descriptive information on the Eagle Picher positive plate production was included in the company's FY 1980 annual report.[22] An expanded nickel grid with very thin ribbing is used as the supporting structure. A highly porous, approximately

TABLE XIII

IRON/NICKEL-OXIDE DEVELOPMENT GOALS

Goal	Year 1980	Year 1984
Specific Energy[a] (Wh/kg)	54	56
Specific Power[b] (W/kg)	110	140
Cycle Life[c]	300	800
OEM/Price[d] (1977$/kWh)	--	70

[a]At C/3 discharge rate.

[b]30-second average at 50% DOD.

[c]Cycled at 80% DOD.

[d]At a production level of 100,000 units/yr.

TABLE XIV

COMPARISON OF IRON/NICKEL-OXIDE BATTERIES

	Eagle Picher	Westinghouse
Component Structure		
Iron electrode	Proprietary NRC Sweden sintered iron	Sintered-steel fiber with pasted active material
Ah/gm_3	0.27	0.23
Ah/cm^3	0.93	-
Positive electrode	Sintered nickel plaque with electrochemical impregnation	Sintered nickel plated steel fiber with paste or electrochemical impregnation
Ah/gm_3	0.106	0.12
Ah/cm^3	0.383	-
Separator	Ribbed, sintered PVC separator	Multilayer polypropylene
Electrolyte	Lithiated KOH	Lithiated KOH with circulation during charge
Performance Characteristics[a]		
Cells		
Size, width, length, height (cm)	6.9, 18, 27	
Capacity (Ah @ C/3)	280	250
Specific Energy (Wh/kg)	50	57-61
Energy Density (Wh/l)	105	120
Specific Power (W/kg)	107	105
Cycle Life[a] (100% DOD)	2,300 electrodes 800	1,000 (80% DOD) >457
Cycle Efficiency	70	55
Modules		
Voltage (volts)	6	7.26
Capacity (Ah)	270	240
Specific Energy (Wh/kg)	45	53
Energy Density (Wh/l)	90	120
Specific Power (W/kg)	103	-
Cycle Life	800 (100% DOD) 650 (80% DOD) NBTL	325 (80% DOD)
Project Commercial Production Costs		$80

[a]As of fourth DOE Battery and Electrochemical Contractors' Conference.

Source: Reference 3.

80% nickel plaque is sintered onto the supporting grid. This is then impregnated by an electrochemical process with nickel hydroxide precipitate. A single impregnation suffices to achieve a cell with a specific energy of 54Wh/kg. Plaque processing improvements contributed to the improved positive plate. The improvements included control of slurry preparation and sintering.

The Swedish National Development Corporation iron electrode is a sintered-iron plaque. It is manufactured by sintering iron powder on an expanded iron substrate. No further processing is required; the plaque is the active material. Trace elements which significantly affect electrode performance have been identified. Although small amounts of sulfide improved negative electrode performance in individual plates, this improvement was not shown in complete cells.(22)

Eagle Picher has developed a semi-automatic battery watering system. The necessary equipment has been fabricated and the assembly tested. The system consists of a single filling reservoir, a flow indicator, a manifold reservoir, and control valves; all the components are external to the battery. Each cell serviced by the watering system has an automatic shut-off device.

Prototype 36-volt electric vehicle batteries have been assembled. These consisted of six, 6-volt modules with a theoretical capacity of 341kWh and a measured capacity of 269kWh after 20 cycles of conditioning. Table XV compares the performance

TABLE XV

EAGLE PICHER IRON/NICKEL-OXIDE BATTERY IN VEHICLE PERFORMANCE

Vehicle	Test Cycle	Lead-Acid Miles	Fe/NiO(OH) Miles
Converted F-100	"C"	18.7 (Varta)[b]	62.5
(Electric Vehicle Assoc.)[a]	Urban	23.4	71.5
Converted VW Rabbit	"C"	22.1 (Oldham)[b]	74.8
(South Coast Technology)[a]	Urban	35.3	91.0
VW Transporter Van	"C"	Not tested	71.0
(Volkswagen)[a]	Urban	36 (EV-106) (Exide)[b]	103.0

[a]Vehicle manufacturer.
[b]Battery manufacturer.

of these batteries with commercially available lead-acid batteries in comparable electric vehicles. The results of the test showed that the vehicle range can be increased by a factor of two to three by substituting Eagle Picher iron/nickel-oxide batteries for currently available lead-acid batteries.

The Westinghouse positive electrode starts with a plaque of nickel-plated steel wool. The plaque contains two vertical grooves that serve as electrolyte flow channels. Two levels of nickel hydroxide impregnation have been found to consistently give better electrode performance. This involves a high-current step followed by a low-current one. The high-current step is rapid; the low-current step to complete the impregnation is slow, taking from 16 to 20 hours. The complete electrode processing time in the pilot plant is 48 hours.[23]

The current effort is aimed at further increasing the capacity of the nickel electrode from 0.12 to 0.14Ah/gm. Improvement in the nickel electrode dimensional stability is also a development objective. Higher fiber density in the steel wool for the positive plaques is being investigated to decrease the loss of performance due to positive plate swelling. The higher fiber density plate technology is being evaluated in a six-cell module. Shorting in one of the cells also damaged the adjacent cells. Tests were continued on the remaining three cells. Also being investigated is the ozonization of $Ni(OH)_2$ to the black oxide. This can lead to a

decrease in the time needed for electrochemical formation of the plate. Several substitutes for $Co(OH)_2$ as an additive to the active nickel oxide have been investigated but none has provided the same performance improvement.

The iron oxide used for the negative electrode is obtained by the thermal decomposition of ferric sulfate. There is a small sulfate residue (0.05 wt %). Corn starch has been found to be an effective paste additive for electrode preparation. These iron electrodes improved performance over the earlier technology, as shown in Figure 20. This resulted in an electrode with a capacity of 0.25Ah/gm.

Improvements have also been made in various battery components, such as separators, through the use of Celgard IC-501 manufactured by the Celanese Corporation, the electrical connectors, and an electrolyte management system (EMS). This EMS features a single-point water replenishment, charge temperature control, and safe gas handling. Electrolyte circulation permits temperature control during charge, permitting more rapid charging.

Pilot plant operations have been developed for fabricating plaque, nickel-oxide and iron electrodes, cells, modules, and batteries. The cell components are tested in full size cells with electrolyte circulation. Among the best cells, the specific energy varied from 45 to 61Wh/kg, with the longest-duration cell having a

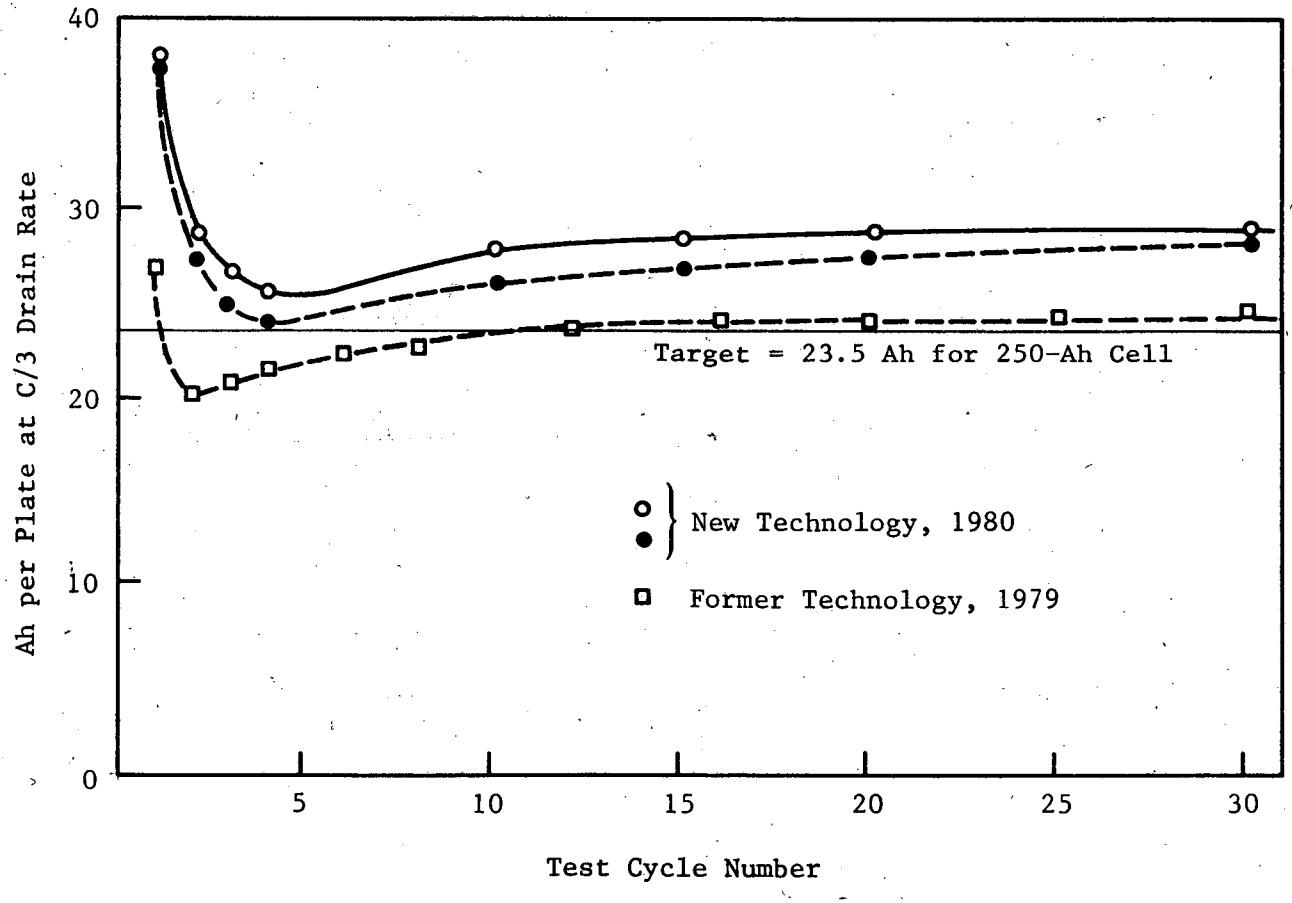

FIGURE 20
WESTINGHOUSE IRON ELECTRODE PERFORMANCE

capacity of 50Wh/kg and a cycle life of 511 to a capacity loss of 20%.

For use in the Jet Propulsion Laboratory (JPL) in-vehicle battery test program, two full-sized batteries and spare cells were fabricated. All were delivered to the JPL by the end of calendar year 1980. Post-mortems were carried out on the defective cells from modules returned by JPL. Two cells had shorts due to the accidental folding of the separators and three cells had high charge voltages due to inlet tubes being blocked by epoxy cement. These and other observations have led to changes in cell construction. The results of the NBTL tests on iron/nickel-oxide batteries are shown in Figure 21.

Supporting research has emphasized the investigation of the nickel-oxide electrode. This is discussed below.

3.3 Zinc/Nickel-Oxide Electric Vehicle Batteries

The zinc/nickel-oxide couple has the inherent capability of producing the battery most readily fulfilling the performance requirements of aqueous mobile batteries. Figure 3, above, shows that it has exceeded the specific energy and specific power that was the 1980 goal for near-term batteries. However, it falls far short of the cycle life goal.

Four groups were participating in the zinc/nickel-oxide technology program during the period included in the BECC--December 1979 to June 1981. Those participating included the Energy Research

Specific Energy: 38-48 Wh/kg
Energy Efficiency: 48-66%
Cycle Life: ≥600 (testing continuing)

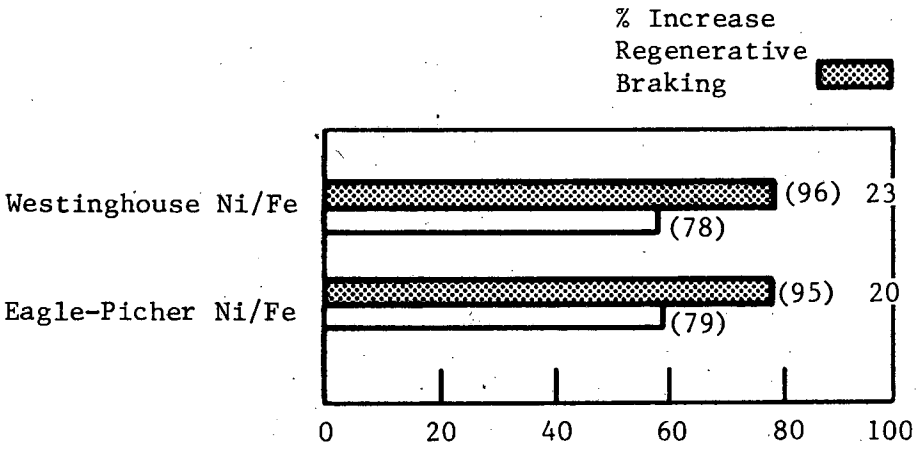

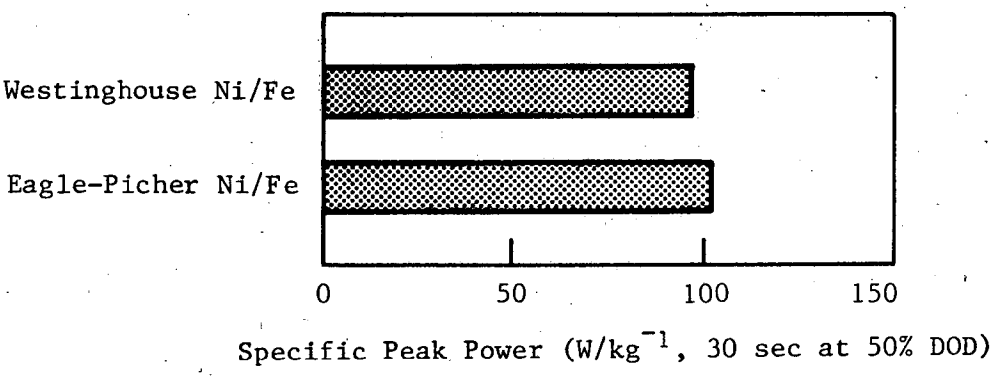

Source: Reference 3.

FIGURE 21
NBTL IRON/NICKEL-OXIDE BATTERY TEST RESULTS

Corporation (ERC), Exide, Gould, and the U.S. Army Electronics Research and Development Command (ERADCOM). The Yardney effort, which was included in SR-II, was discontinued during 1979 because the Yardney Company elected to withdraw from the program. ERADCOM is primarily concerned with the development of a battery with improved performance. Although ERADCOM is planning to build batteries, these are not for in-vehicle testing. The ERADCOM effort is receiving support from the Department of the Navy and DOE. The section below reviews the current status of the zinc/nickel-oxide battery and provides a discussion of on-going supporting research. The Exide approach will be discussed last as it has fewer features in common with the other developments.

The zinc/nickel-oxide development contractors, other than ERADCOM, are listed in Table VII above. As noted in the earlier status reports (SR-I and SR-II), the major problem in this battery is the lack of cycle life due to the limited reversibility of the zinc electrode. This is the result of shape change of the zinc electrode, dendrite formation, and the deposition of zinc oxide in separators and on the positive plate. The zinc electrode also has a tendency to become passivated. The resolution of the zinc reversibility problem is the major thrust of the current efforts. In addition to the reversibility of the zinc electrode, attention is being placed on the dynamics of the system and the separator.

The Energy Research Corporation is continuing to develop the roll-bonded electrode structures. To overcome the zinc electrode problems, ERC is emphasizing the use of additives, electrode design, and improved separators. Basic studies are also being conducted.

A combination of additives to the zinc electrode has been identified which is reported to have resulted in an improved cycle life, reduced shape change, and reduced dendritic shorting. Single negative electrode cells with a theoretical capacity of 24.3Ah were reported to have a cycle life of over 200 at a 20% loss of the initial capacity, 18Ah. This represents almost double the single-cell cycle life reported in December 1979.(2)

Much effort has been expended on improving the separator. ERC developments have shown that a cross-linked, polyvinyl-alcohol (PVA) separator increases the failure of cells by shape change and decreases the incidence of zinc shorting. On the other hand, ERC composite separators result in a substantial reduction in shape change but poor stopping ability for dendrite formation. The polymer blend composite separators are nylon based.(24)

The polymer blend separator was compared with one made from Celgard K-307, which is cellulose acetate coated Celgard 2400. Cells with the two separators failed at between 120 and 135 cycles, with the polymer blend showing the greater lifetime. Combination polymer blend and PVA separators are also being investigated.(24)

Evaluation of commercially available materials, along with further development of polymer blended separators, is continuing.

The roll-bonded nickel-oxide positives have been tested for cycle life in cadmium/nickel-oxide cells. These experienced a 20% loss of capacity after 900 cycles, showing the long life of the nickel-oxide positive. Cycle life expectations for the positive electrode in the zinc/nickel-oxide cells cannot be inferred from these tests because there is no zinc oxide accumulation in the positive plate of the Cd/NiO(OH) cell.

Full size zinc/nickel-oxide cells have been tested using a simulated J227 aD pulsed discharge profile and a mix of discharge depths derived from vehicle data. Zn/NiO(OH) cells have been tested for the equivalent of 13,000 cumulative miles before the estimated mileage range decreasd from 100 to 60 miles.

The Gould effort also emphasizes zinc electrode reversibility and separator development. The approach to improved negative reversibility has been the immobilization of the zinc discharge product, primarily the zincate ion, through solubility reduction and the use of mechanical barriers. Solubility suppression has been approached through a decrease in potassium hydroxide concentration with replacement of the KOH with an ionizable substance to maintain the electrolyte conductivity. The addition of solubility suppressants to 31% KOH solution is an alternative approach. Mobility suppression is being approached through the use of

colloid-forming additives. Other approaches included the improvement of current density distribution and the optimization of charging characteristics. These approaches have resulted in demonstrating a decrease in the rate of shape change. Small 5Ah cells, with additives, have shown an increase in cyclelife of 2.5 to 3 times that of control cells. These studies have been extended to 50Ah batteries with similar results.[25]

Gould has also attempted immobilization by microencapsulating the zinc oxide of the negative electrode. An electroporous polymer was used. A cell based on this approach lasted for 115 cycles with a 20% decrease in its maximum delivered capacity (MDC) and at the end of 300 cycles had a 30% decrease in its MDC. The reproducibility of this electrode has been poor and improvement in reproducibility was investigated.

The separator development has centered on the use of Electroporous and microporous separators. The Electroporous separator is preferred.[25] The membrane is fabricated by casting an aqueous dispersion of the polymer substrate onto a strippable support film in a continuous process. The film thickness is built up by the consecutive deposition of a series of layers. The final laminate, four to six layers, is 0.002 to 0.0025 inch (0.051 to 0.063 mm) thick. The film can be cross-linked by high energy irradiation to prevent swelling and extraction of film components.

Melt extrusion is being investigated as an alternative to the process of casting and cross-linking.

To further improve the zinc electrode, an "electrode wicker" which absorbs electrolyte but decreases electrolyte transport has been investigated. The latest reported wicker performed better than earlier ones and tests were still under way at the time of the fourth BECC.[25]

The positive electrode uses a porous sintered-nickel plaque on a thin, expanded-nickel support. The active material is chemically deposited. The need for high porosity and electrode strength has led to the development of a thick positive electrode.

During the program, a large number of various sized cells, 225Ah modules, and batteries have been constructed and tested. Table XVI summarizes the results of these tests.

Gould has estimated the cost of electric vehicle batteries based on the technology developed by that laboratory. Analysis of the material costs indicated that the lower power density battery has a materials cost of over $170/kWh, at February 1981 production levels. Seventy three percent of this cost was due to nickel components. Material costs for the more practical higher power density EV battery were estimated as $204/kWh. Gould's most optimistic projection of the manufacturing cost, for production of 50,000 batteries per year, was $106/kWh for the low power design. It was concluded that, based on Gould technology, the zinc/nickel-

TABLE XVI

SUMMARY OF GOULD ZINC/NICKEL-OXIDE BATTERY TESTS

	Cycle Life[a]
Battery	125(2)
225-Ah Module	189
225-Ah Cells	200
50-Ah Cells	300
5-Ah Cells	400

[a]Figure for battery is as of 1978. Other figures are as of January 1981.

oxide batteries will have a high cycle life cost compared to alternative EV batteries. On the basis of these estimates, Gould has elected to terminate its efforts on the zinc/nickel-oxide battery for electric vehicles.

The investigations at ERADCOM emphasize the use of a separator which uses nickel within its structure and cell charge control to overcome the problem of the reversibility of the zinc electrode. Earlier efforts on separator development were described in SR-II. The best separator system developed in the ERADCOM program, as of January 1981, consisted of a layer of 5-mil polyamide felt on the nickel positives, a layer of 1-mil Aldex paper on the zinc negatives, and a main separator wrap in an accordion configuration. This wrap consisted of a layer of Celgard K-317, which contains nickel powder, and a layer of 1-mil cellophane facing the anodes. Both layers were sandwiched between two layers of Celgard 3500. The best of the binary additives to the zinc negative consisted of 2% to 5% CdO plus 1% to 5% PbO.[26]

Wagner and coworkers at ERADCOM have developed a rapid test procedure for the determination of zinc penetration of the separator. The cell design is shown in Figure 22. The test subjects the separator to extreme overcharge conditions and the time it takes for a short to develop by zinc penetration is determined. Reference 26 includes a description of cell design and operation.

SZ - SHEET ZINC
SN - SHEET NICKEL
NR(+) - NICKEL REFERENCE ELECTRODE
C - CELGARD
NC - NICKEL COATED CELGARD
P - POLYAMIDE FELT (PELLOW)
SB - SUPPORTING BLOCKS
CC - CELL CASE
CCC - CELL CASE COVER
AC - ANOLYTE COMPARTMENT
PE - HEATED SEALED POLYETHYLENE BAL
FSC - LAYER OF FIBROUS
SAUSAGE CASING

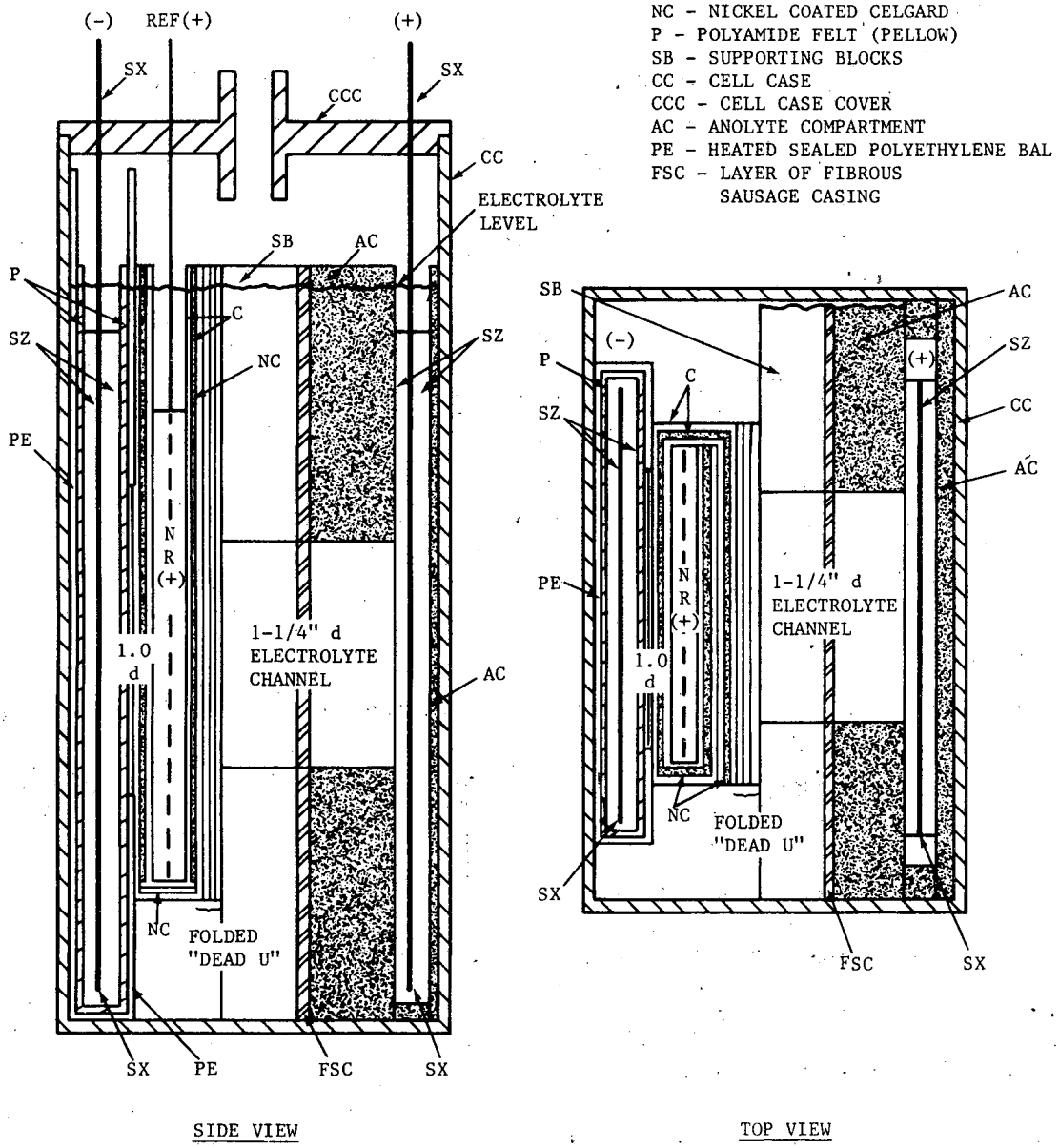

FIGURE 22
ZINC PENETRATION CELL DESIGN

The best charging mode found was the interrupted current mode at a frequency of 10 Hz, a rest-to-pulse ratio of 5:1 to 10:1 and an average charging rate of C/15 to C. It was found that effective charge control was achieved by mounting a pressure cutoff switch set to 8 psig, with venting means at 10 psig, to each cell of the zinc/nickel-oxide battery. The switches are series connected on a separate circuit to the charger.[26]

Among the nickel-oxide electrodes were ones prepared by the staff of the Naval Surface Weapons Center.[27] These are sintered-nickel-graphite plaques which are electrochemically impregnated with active material by the method of Pickett.[28]

Single- and four-cell, 5Ah capacity units have been tested. The best of the single-cell units attained over 600 cycles at C/3 and 80% DOD. Four-cell batteries have delivered 425 cycles under the same operating conditions. A contract with a battery manufacturer was to be established during the third quarter of 1981 for the construction and testing of 150Ah units. This effort is to be part of the DOD program without DOE participation.

Exide development of the Vibrocel was briefly described in SR-II.[2] Figure 23 compares the principle of the operation of the Vibrocel and the conventional zinc/nickel-oxide cell. Use of the vibrating electrode during charge avoids shape change and dendrite growth, eliminating the need for a separator. As previously reported,[1][2] the zinc electrode is highly reversible

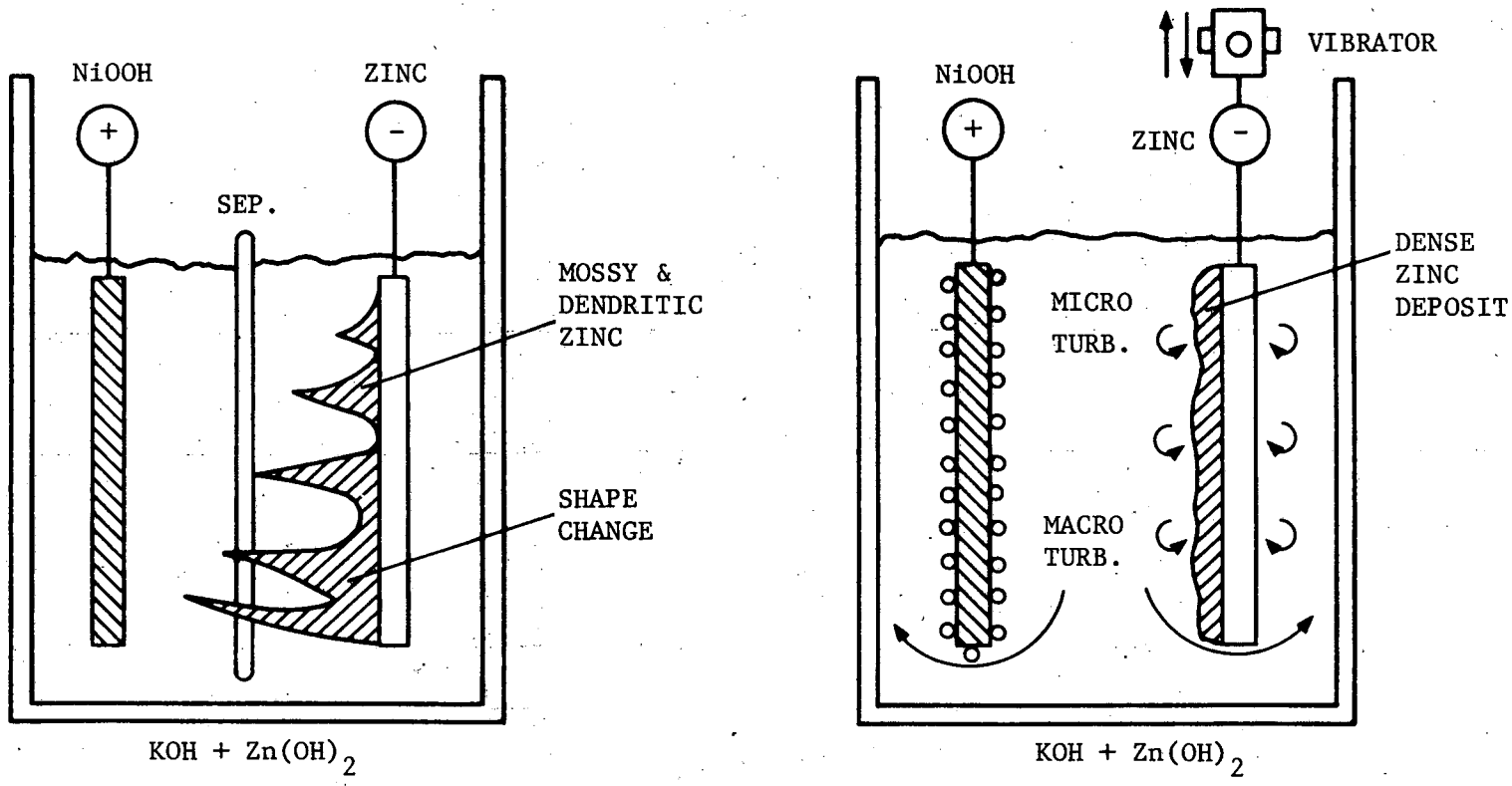

FIGURE 23
COMPARISON OF CONVENTIONAL ZINC/NICKEL-OXIDE CELL AND VIBROCEL

under operating conditions. During the period since June 1979, it has been observed that the transfer of nickel shed from the nickel-oxide positives can lead to accelerated self discharge of the zinc. The free-standing nickel electrode has a greater tendency to lose nickel than do those with separators. To overcome this, Exide has been investigating the shedding characteristics of the following commercially available nickel-oxide positive electrodes:[29]

- INCO controlled micro-geometry (CMG) layered nickel foil--slurry coated with active material;
- Exide plastic bonded;
- Sintered-carbonyl-nickel powder--impregnated with nickel hydroxide;
- Perforated, nickel-plated steel pockets--active material contained in briquette; and
- Sintered-nickel-plated steel wool--impregnated with nickel hydroxide.

Screening tests of the above positive electrode structures were conducted in a Vibrocel. The results of the tests are listed in Table XVII. The Exide plastic bonded electrode showed higher swelling and little or no shedding.

The initial cells had an interelectrode spacing of 2.5 mm. Through the development of special charging techniques the interelectrode distance has been decreased to 1.5 mm. The completed cell contains cadmium-plated negative collectors on which the zinc is deposited, a 9-10 M KOH electrolyte, and the CMG positive electrode constructed from thin nickel foils in a laminar structure.

TABLE XVII

CHARACTERISTICS OF NICKEL-OXIDE POSITIVES

Type	Ah/kg 8C/5	Ah/kg 9C/5	Swelling Factor[a]	Shedding Factor[b]	Rate Capability[c]	Overcharge Required at C/5 Charge Rate
Pocket	70	.17	A	XX	C/3	40%
Sintered Plaque	110	.38	A	XX	C/2	40%
Nickel Plated Steel Wool-Impregnated	135	.27	E	XXX	C/3	20%
Exide Plastic Bonded	145	.23	D	X	C/3	40%
CNG (Multi-Foil) INCO	193	.36	B	XX	C/2	40%

[a] A=Swells less than 10%
B=Swells 10-25%
C=Swells 25-50%
D=Swells 50-75%
E=Does not swell, but blisters occasionally

[b] X = Little or no shedding, XX = Moderate shedding requiring occasional clean-up, XXX = Excessive shedding

[c] Maximum discharge rate with acceptable nickel polarization for a 3mm-thick electrode, except the nickel-plated steel wool type for which the basis is a 5mm-thick electrode.

Source: Reference 29.

The baseline 6-volt Vibrocel^{TM} module design, as of September 1980, is a 6-volt (four cell) unit with a nominal capacity of 185Ah. Each cell has 7 positive and six negative electrodes. The first test module was made with two cells.(30)

Table XVIII compares the approaches and test results of the four zinc/nickel-oxide batteries reviewed. Figure 24 summarizes the NBTL test data on zinc/nickel-oxide batteries.

3.4 Alkaline Battery Supporting Research

Basic and applied research to help overcome the deficiencies of the alkaline batteries have been undertaken under the DOE program. As has been noted, the zinc electrode has been especially troublesome. One approach to overcome some zinc electrode problems (see Table VII) has been to use metal additives to the zinc plate. To better understand the effects of metal additives on surface morphology, McBreen and coworkers at the Brookhaven National Laboratory (BNL) have used various electrochemical techniques and scanning electron microscopy. Small amounts of additives, 2 to 4 weight % of mercuric oxide (HgO), thallic oxide (Tl_2O_3), lead monoxide (PbO), cadmium oxide (CdO), indium oxide (In_2O_3), indium hydroxide [$(In(OH)_3)$], indium metal (In), and gallium oxide (Ga_2O_3) were examined. Some of the additives, such as HgO and Tl_2O_3, were completely reduced prior to the deposition of zinc. CdO and PbO were approximately 20% reduced prior to zinc deposition. PbO, Tl_2O_3, and $In(OH)_2$ improved the current

TABLE XVIII

ZINC/NICKEL-OXIDE BATTERY DEVELOPMENT

System Features	ERC		Gould		ERADCOM		EXIDE	
Negative	Roll bonded, ZnO with additives, copper foil current collector, CdO-PbO additive		Proprietary construction		Zinc containing CdO and PbO on Ag- or Pb-plated copper grid		Zinc electrodeposited on a cadmium-plated steel substrate	
Positive	Roll bonded, pressed nickel hydroxide, graphite plastic binder		Thick, sintered porous nickel on thin nickel grid, chemically impregnated		Sintered plaque-nickel-standard			
Separator	Cellulose acetate coated Celgard K-306, asbestos electrolyte wrap		Electroporous separator with electrode wickers		Celgard[a] K 317, cellophane, Celgard 3,500 Aldex paper next to negative			
Electrolyte	Potassium hydroxide + 1% KOH		Potassium hydroxide with mobility suppressants					
Test Results	Cell	Battery[b]		Battery	Cell[c]	Battery[c]	Cell	Battery[d]
Voltage (V)	1.6	106	1.6	--	1.6	6.4		
Capacity Ah	250	250	225	225	5	5	300	250
Specific Energy(Wh/kg)	55.1	55	--	68	65	--	42	46.8
Energy density(Wh/l)	--	91	--	--	120	--	--	71.6
Specific power, W/kg								
Sustained								45
peak/50% DOD	--	--	--	131	--	--	--	128
Cycles/ to % DOD	150/80	100	200 400/5Ah	189/75	500	350/na	300/100	400
Energy efficiency (percent)	--	--	--	----		--	--	60

[a] See Appendix B for Celgard descriptions.

[b] Data from SR II.

[c] All data are not for the same cell configuration.

[d] Estimated for 1981.

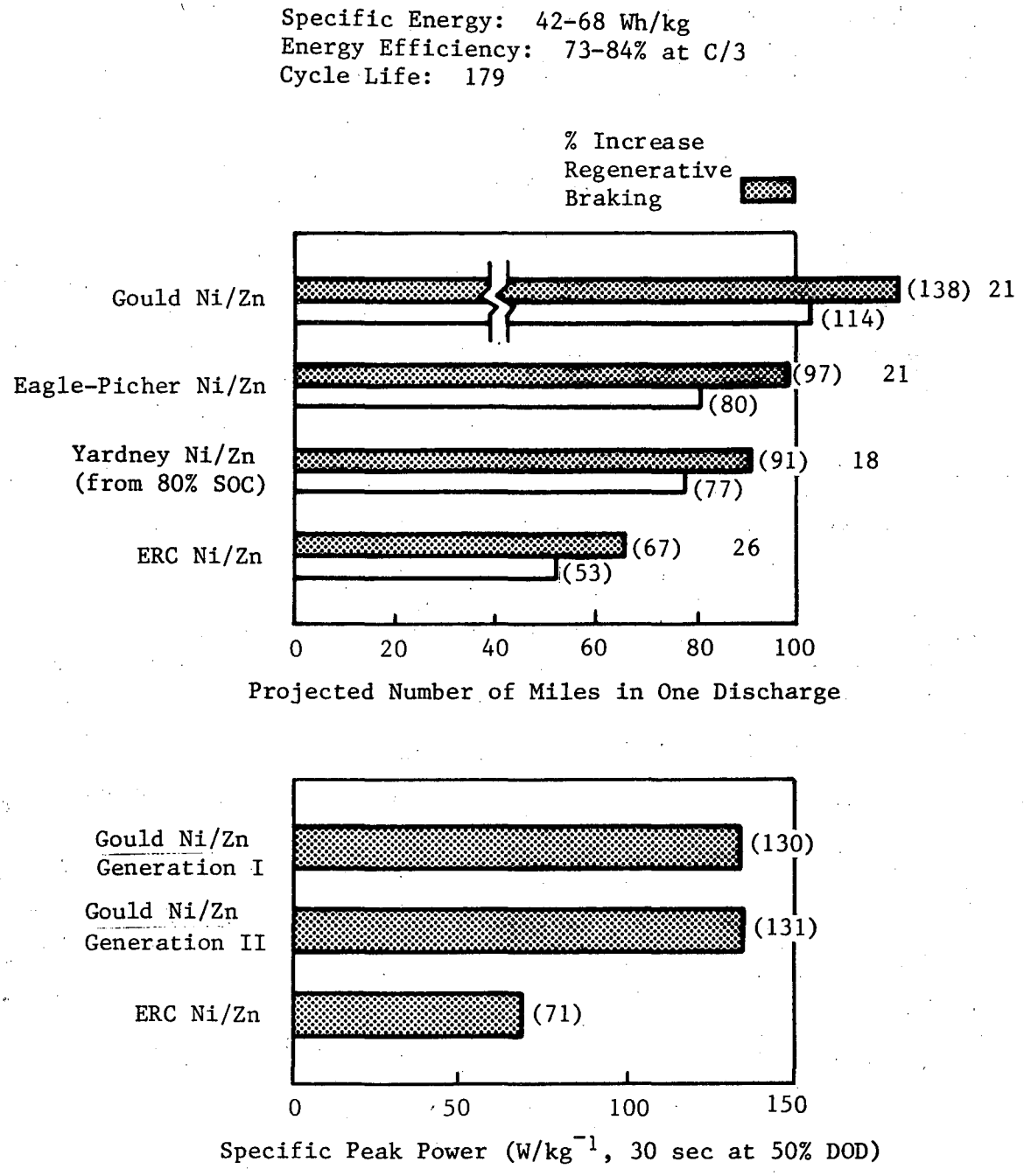

FIGURE 24
NBTL ZINC/NICKEL-OXIDE BATTERY TEST RESULTS

distribution. The PbO was more effective when it was added to the ZnO along with metallic zinc (93% ZnO, 5% Zn, 2% PbO). PbO and $In(OH)_2$ increased the density and polarizability of the zinc whereas Ga_2O_3 and CdO produced finely divided deposits of low polarizability. No tests were reported on the combination of PbO and CdO. It is of interest to note that, although they have opposite effects on deposit density and polarizability, their combination was beneficial in cells studied by ERC and ERADCOM. It was also concluded that additives of metals with atomic radii close to that of zinc resulted in zinc deposits oriented parallel to the basal plane. Additives of metals with larger atomic radii than zinc resulted in deposits that were oriented perpendicular to the basal plane. The general conclusion was that the additive effect was as a substrate rather than as a codeposited material. A general rule of thumb for selecting additives for long cycle life was proposed by McBreen:

> "[S]elect an oxide or hydroxide of a high hydrogen overvoltage metal with a reversible potential more positive to zinc and an atomic radius at least 15% greater than that of zinc."

Although this rule of thumb can explain the effect of single metal additives, it does not explain why cadmium and lead, which individually have opposite effects, combined to improve zinc positive performance in cells tested by ERC and ERADCOM.

Another approach to improving zinc electrode performance, decreasing the solubility of the discharge product, has also been

investigated by McBreen and coworkers. Zinc electrodes were prepared using a 1:1 paste of calcium hydroxide [$(Ca(OH)_2)$] and zinc oxide. The zinc utilization, in 20% KOH, was 48%. The addition of 8% of PbO increased the zinc utilization by 30%. Research on decreasing the solubility of zinc anodes is also under way at ERC but specific results were not available at the time of the BECC.

Katan and Carlen, of Lockheed Palo Alto Research Laboratory (LPA), have continued the use of a model single pore electrode for studying the morphological changes in zinc during cycling. The technique was described in SR-II and in the technical literature.[32] Katan and Carlen have recently shown that mossy zinc grows on the tips of zinc dendrites within seconds after switching to open circuit. The growth, in the direction of the counter-electrode, frequently bridges the interelectrode gap. The mossy zinc formed can lead to shorting. This observation is in accord with the concept of a zincate-ion rich, reduced-pH electrolyte arriving from the counter electrode at the tips of the dendrites closest to the counter electrode. This leads to the formation of a local cell at the zinc electrode with hydrogen evolution within the pore and zinc deposition at the dendrites.[33]

Liu, Cook, and Yao of ANL have been investigating the passivation of zinc anodes in potassium hydroxide. Based on their review of the literature, they concluded that three different

mechanisms have been proposed for passivation of the zinc electrode:[34]

- Dissolution-precipitation model--Precipitation of zinc hydroxide or zinc oxides occurs on the zinc surface following the buildup of a critical concentration of zinc moieties in solution leading to the formation of a layer of ZnO or $Zn(OH)_2$ on the surface. The surface layer decreases the effective zinc area leading to passivation.

- Adsorption model--Hydroxide ions are adsorbed on the zinc electrode to form a monolayer of $Zn(OH)_2$ which releases protons. This results in a passive zinc-oxide film which retards hydroxyl-ion diffusion to the zinc.

- Nucleation and crystal growth model--The zinc oxide initially formed on the anode surface acts as nucleation sites for the growth of zinc oxide. The surface becomes passivated when the zinc is covered by a layer of zinc oxide.

(For citations to the original literature see reference 33.)

Current density vs. time measurements were conducted on zinc microelectrodes (0.05 x 0.13 cm) set in acrylic plastic. Various concentrations of KOH were used and the current density vs. time curves for passivation were determined.[34] Based on these measurements, Liu and coworkers proposed the scheme for passivation shown in Figure 25. During the first step, t_a, the anodic reaction produces zincate ions which accumulate near the electrode surface because of the slowness of diffusion. The zincate ion builds up to a critical concentration at which point type I ZnO forms. The critical concentration is believed to be three to four times the solubility of ZnO in the KOH solution and independent of the initial zincate ion concentration. Reaction continues via the

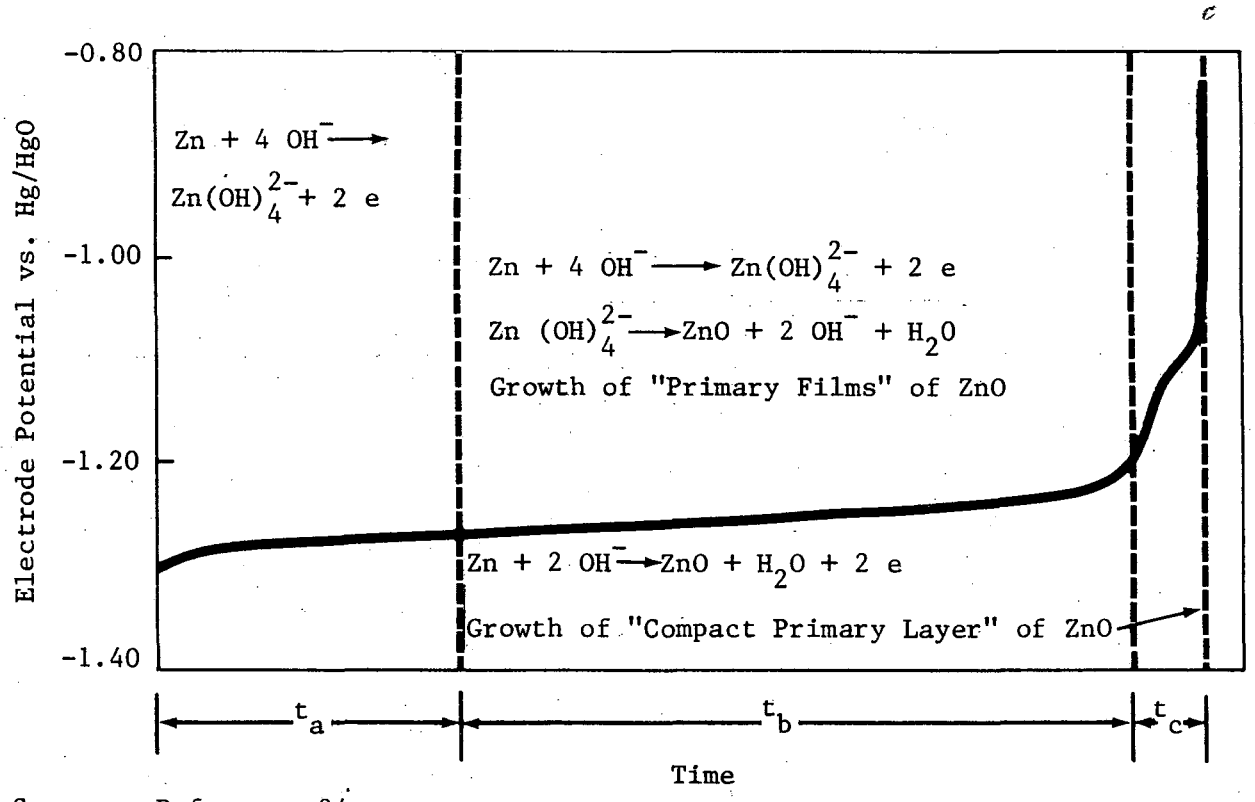

Source: Reference 34.

FIGURE 25
ZINC ELECTRODE PASSIVATION SCHEME

transport of hydroxyl ions through the ZnO layer initially formed, T_b. With the buildup of the ZnO I layer the supply of hydroxide ions becomes too slow for zincate ion formation, leading to type II ZnO formation and zinc passivation. Observations were made on a porous zinc electrode and it was concluded that simple passivation does not limit the utilization of a newly formed porous zinc battery electrode.

Yamazaki and Yao of ANL developed a mathematical model for the zinc/zincate ion electrode reaction in the pores of the zinc electrode.[35] The model makes use of Ohm's law for the pore and the relationship between the concentration gradient of the reacting species and the current density in the pore. The results of the calculation indicated that a considerable difference exists in the current distribution in the pore during charge and discharge. The physical origins for the difference were traced to a resistivity change in the electrolyte in the pore and a change in the interfacial reaction resistance at the electrolyte and pore matrix surface. The calculation also suggests that the pore structure of an alkaline zinc electrode will change during charge and discharge cycles even in a relatively small current region where no passivation film is formed.

The model discussed above was tested experimentally using a segmented porous electrode prepared by a photolithographic technique.[36] Figure 26 compares the theoretical curve and

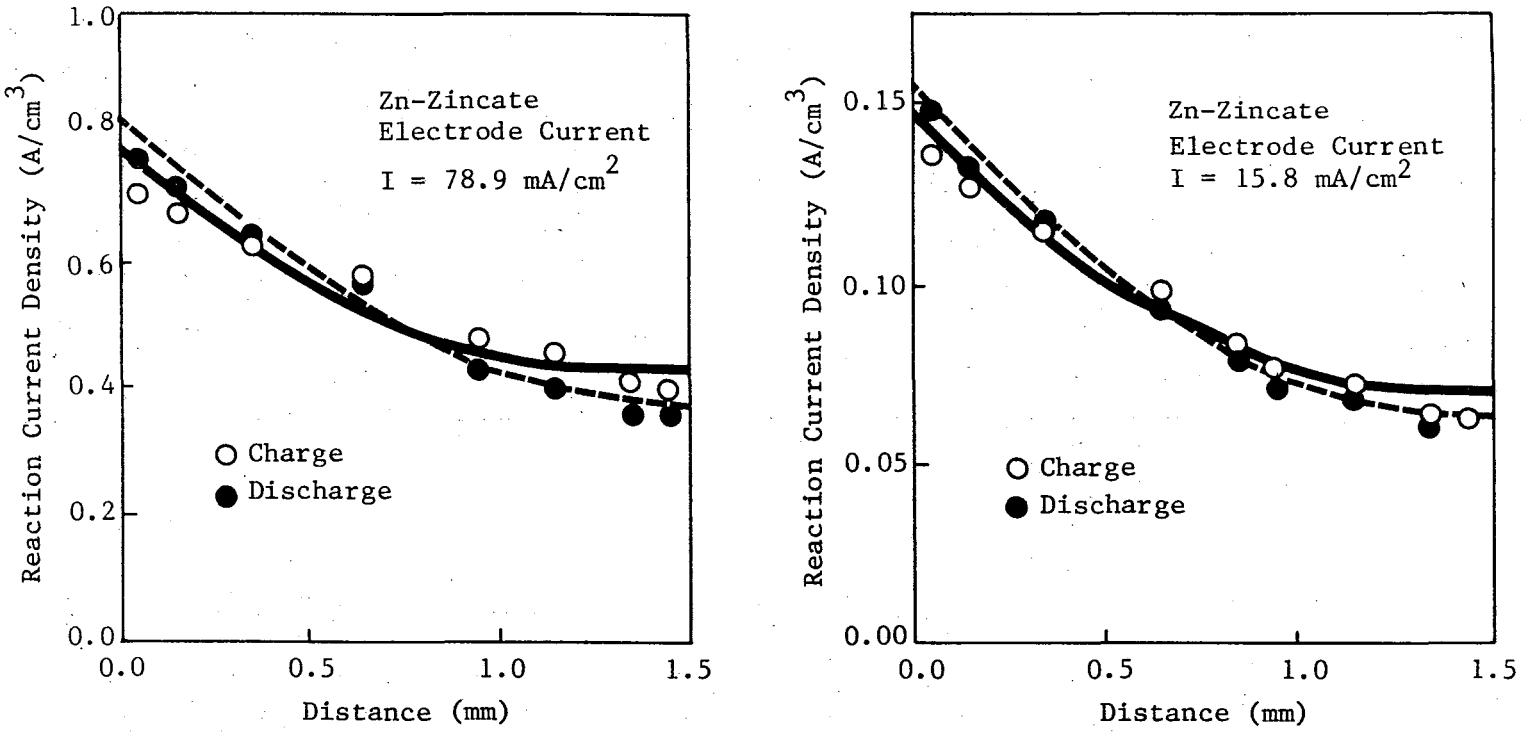

Source: Reference 36.

FIGURE 26
REACTION DISTRIBUTION IN ZINC PORES

observed data for reaction current densities at superficial current densities of 15.8 and 78.9mA/cm^2. The agreement is better at the lower current densities. The estimate of a difference in the current distribution between charge and discharge was confirmed and reasonable agreement was obtained between the theoretical and measured current distribution in the pores.

To aid in the engineering analysis of porous zinc electrodes, Liu et al. have measured the conductivity of 7.32M KOH containing from 0 to 1.5 M of zincate.[37] The conductivity was found to decrease with increasing zincate ion, consistent with predictions based on the mixture rule. The conductivity of the KOH-zincate ion mixture can be expressed by the equation:

$$k = k_o - C_{Zn(II)}$$

where: k_o = specific conductivity of the KOH electrolyte; y = proportionality constant; and $C_{Zn(II)}$ = molar concentration of zincate ion.

Liu and collaborators have undertaken the mathematical modeling of the zinc Vibrocel electrode performance.[38] The model considers the mass transport of zincate and hydroxide ions, the fluid dynamics, and the mechanism of zinc deposition. The fluid flows considered include free-convection due to concentration gradients, oscillatory bulk and boundary flows induced by the vibration, and a steady circulatory flow which is observed in fluids near vibrating bodies. The zinc deposition model is based on the

effect of polarization on the degree of interaction of the zincate ion with the electrode. Low polarization leads to weak interaction and mossy deposits; high polarization leads to strong interaction and dense deposits. The following are some of the conclusions resulting from the above considerations:

- The interelectrode spacing in the Vibrocel does not limit free convection mass transfer.
- Further experimental work is required to estimate mass transfer coefficients.
- Charging at current densitites of 100mA/cm^2 or more is favorable for the formation of dense deposits and avoiding mossy zinc.

Several studies have also been conducted on the changes which occur at the nickel-oxide electrode during cycling. Lenhart et al. at Ohio State have adopted a transmission line model for the porous nickel-oxide electrode.[39] Figure 27(a) shows a schematic of a porous electrode and Figure 27(b) an idealized schematic of a single pore as well as the sources of impedance used in establishing the model. The analysis of the equivalent circuit for the electrical characteristics of the pore showed that the total impedance of the electrode is a complex function of system variables. It was concluded that the resistance of the metal as a function of the charge/discharge cycle is of great importance. This resistance is a function of the extent of rupture of particle contact as a result of cycling.

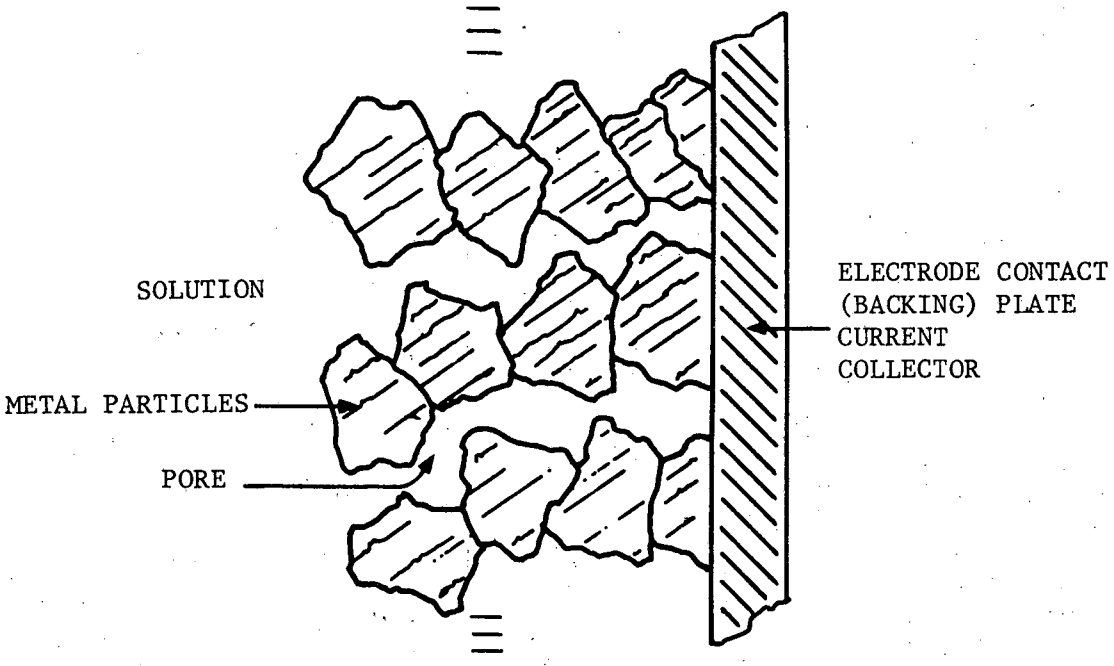

(a) SCHEMATIC OF A POROUS ELECTRODE OF FINITE THICKNESS

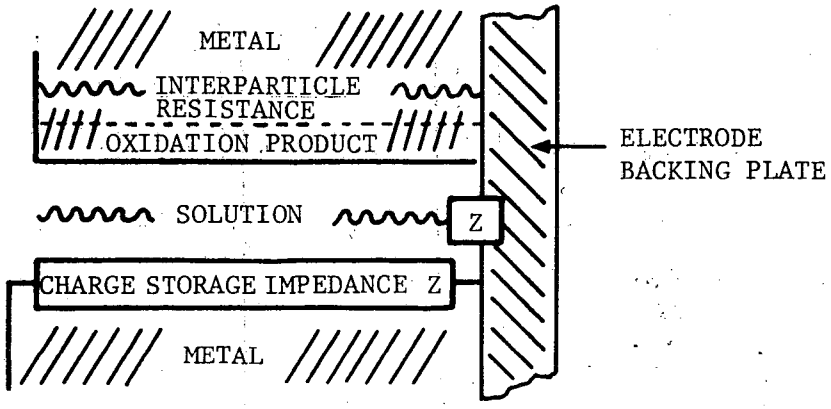

(b) IDEALIZED MODEL OF SINGLE PORE

Source: Reference 39.

FIGURE 27
MODEL OF A POROUS ZINC ELECTRODE

Experimental measurements of the charge transfer properties of the nickel-oxide electrode were conducted using a 0.32-cm^2 exposed end of a nickel rod mounted in a Teflon holder as the working electrode. An oxide film was formed on the electrode and its impedance measured at various frequencies. The oxide film thickness was measured ellipsometrically. Based on the observations, the diffusion of point defects is expected to be rate controlling for the charging of the nickel electrode.

The nickel-oxide film thickness influences the extent of porous electrode changes. Lenhart et al. measured the rate of film growth which followed the inverse logarithmic law:

$$1/L = AB \log t$$

where: L = film thickness; T = time (minutes); and A and B are constants. When the potential was lower than -51mV (vs Hg/HgO) only NiO, or its hydrated form, is stable. At higher potentials, higher oxides, species of Ni(III) and Ni(IV), are formed.

The group at Lockheed has continued studies on model nickel pores having dimensions of the same order as those in practical electrodes. This technique is detailed in reference 40. The most recent studies were on the effect of charging rate on the retained capacity of the nickel oxide formed. At low formation currents the nickel oxide coating the films was relatively stable. At high currents, the film capacity decreased with time. This effect of high current charging was consistent with the concept of decreased

stability of thicker films due to their greater ease of exfoliation.[41]

Greater detail on the structural changes of nickel oxide during charge and discharge has resulted from the spectroscopic studies of Jackovitz and Seidel of Westinghouse.[42] They have determined the infrared (IR) and Raman spectra of charged and discharged powders from nickel-oxide electrodes. To assist in resolving the spectra, deuterated potassium and lithium hydroxides in deuterium oxide were used as well as the normal hydrogen compounds. The spectra of the charged material was consistent with a hydrated NiO_2 species, not a peroxide, but very closely related in structure to $Ni(OH)_2$. This indicates a greater valence change in the $Ni(OH)_2$ than the generally written formula of NiO(OH). The authors estimate the change is of the order of 1.4 electrons/nickel atom in the active material.

Studies on the emission spectra of the active material cycled in a solution of KOH and LiOH indicated that the lithium ion is preferentially adsorbed in the interlayer. The interlayer concentration of both Li^+ and K^+ is significantly reduced in the fully discharged active material. This suggests the migration of the hydrated cations out of the interlayer during discharge.

Thermogravimetric analysis of active nickel-oxide materials indicated three types of water to be present: non-coordinated

water, hydrated K^+, and hydrated Li^+. All active powders showed an oxygen evolution peak at 250°C.

Jackovitz and Seidel concluded that their observations suggest a specific structure and stoichiometry for well cycled nickel electrode powders which, if synthesized and properly incorporated into a conducting matrix, can drastically reduce electrode swelling. Research is in progress to demonstrate this conclusion.

Sundarai et al. have reanalyzed the data on the activity of potassium hydroxide, sodium hydroxide, and water in alkaline solutions of interest to batteries. They have presented the results of their analysis of these activity coefficients as a function of concentration and temperature in both tabular and graphic form.(42)

3.5 Alkaline Battery Status Overview

The iron/nickel-oxide battery has met 1980 performance goals and promises to meet several 1984 goals. The specific energy and power goals may, however, be difficult to achieve as they require improved utilization of active material. The iron/nickel-oxide system has low round trip efficiency due to the low overvoltage of hydrogen on iron and the difficulty involved in recharging the nickel-oxide electrode. Low overvoltage impurities on the iron can further decrease this efficiency. The electrode cost is high; both the high-purity-iron and nickel-oxide electrodes contribute to this.

The various approaches to the zinc electrode problem show some hope for improving cycle life through forced electrolyte convection,

improved separator design, and the use of pulsed charging techniques (e.g., that of ERADCOM). The EXIDE Vibrocel has shown markedly improved cycle life, but with low round-trip energy efficiency. Whether or not a combination of some of the approaches, such as electrolyte forced convection, metallized separator, pulsed charging, and inorganic additives to the zinc, can overcome the performance deficiencies should be determined.

The cost of the nickel-oxide positive is a major deterrent to meeting the cost goals. As has been noted, Gould has elected to withdraw from the zinc/nickel-oxide battery program because of the estimated high cost of production for the positive electrode and the resultant high battery life-cycle cost due to the limited cycle life. Himy has reviewed the status of this battery and is very pessimistic with respect to achieving batteries with a low enough cost to make it economically attractive for the electric vehicle.[43] A detailed independent evaluation of the probability of achieving alkaline battery costs compatible with electric vehicle economics should provide valuable program guidance.

4.0 ADVANCED BATTERIES

The Advanced Batteries Subelement (ABS) is concerned with battery systems whose electrochemical characteristics have been shown to form a base for exploratory and engineering development of the battery system. Initially, the battery systems included were lithium/metal sulfide, sodium/sulfur, and zinc/chlorine. Several other battery systems, which have not been programmatically included in the ABS, are currently in the exploratory and/or engineering development phase for one or more of the application areas discussed in Section 2. These have been included in this section. Several of these batteries have one or more consummables fed to the electrode from an external storage source. These have been called semi-continuous and continuous feed batteries and include metal/air, hydrogen/nickel-oxide, metal/halogen, metal/redox, and iron/chromium redox batteries. The term "redox" is reserved for soluble reactants which produce soluble reaction products.

4.1 Metal/Air Semicontinuous Batteries

The two metal/air batteries included in the ongoing program are the iron/air electrically rechargeable battery and the aluminum/air mechanically rechargeable battery. No further work on the lithium/air and zinc/air cells, described in SR-II, was reported at the BECC or included in reference 4.

4.1.1 Iron/Air Battery

The general characteristics of the Westinghouse iron/air battery system were described in the two preceding reports, SR-I and SR-II. It consists of a sintered porous iron negative, a bifunctional oxygen electrode, and a 25 wt % potassium-hydroxide electrolyte. The electrolyte is circulated during charge.

Improvements have been made in the iron and air electrodes. Figure 28 compares the near-term and advanced cell polarization curves.[44] A life of over 500 cycles has been demonstrated for the cycle-life controlling air electrode. It has also been established that the air electrode can withstand more than 5,000 regenerative braking, i.e., high-current, short-duration, cycles, Table XIX lists the characteristics of a five-cell (5.8 volt) module.

Using the methodology developed at the LLNL, Demcyk and coworkers at Westinghouse have made an iron/air battery mission analysis.[44] Two- and five-passenger commuter vehicles, with and without regenerative braking, were evaluated. A proposed 40kWh battery system was estimated to give the larger vehicle a range of 120 km and the two passenger vehicle a range of 240 km. For the same ranges, vehicles with regenerative braking were found to require approximately 5% less battery capacity and 3% less total weight. It was also estimated that the iron/air battery would be comparable in weight to the lithium-aluminum/FeS_2 battery for the same performance. The estimated cost for the mass produced iron/air

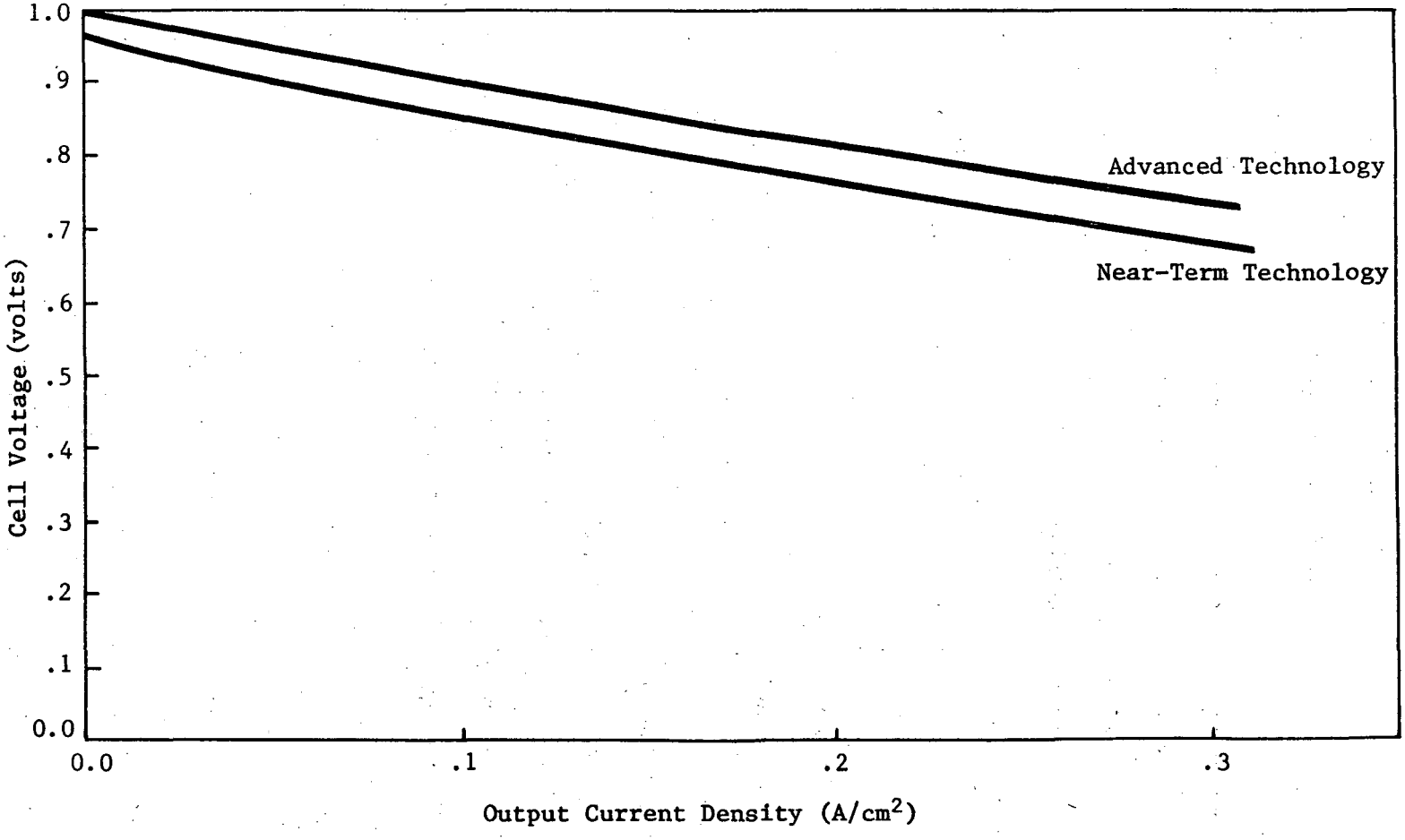

Source: Reference 43, Westinghouse.

FIGURE 28
IRON/AIR CELL POLARIZATION CURVES

TABLE XIX

IRON/AIR MODULE CHARACTERISTICS

	Near-Term
Five Cell Weight	2,350 g
Electrolyte-Gas Manifold	160 g
Interconnectors	50 g
Total Module Weight	2,570 g
Total Module Volume	2.12 l
Energy Content	352 Wh
Energy Density	352 Wh/kg
Power[a]	400 W
Power Density[a]	154 W/kg
Volumetric Energy Density	0.167 kWh/l

[a]At 150 mA/cm^2.

Source: Westinghouse Research and Development Center.

battery was $40/kWh in 1979 dollars. The Westinghouse estimates include an air scrubber to remove the carbon dioxide and the cooling of the electrolyte by heat exchange with the incoming air. Figure 29 is a schematic of the thermal management system.[45]

Additional details have been published on the preparation of the iron electrode.[46] These are produced by pressing and sintering a mixture of sponge iron powder and urea between perforated nickel current collectors. The urea acts as a pore former. Sintering is carried out in a hydrogen atmosphere at temperatures of 700 to 800°C. The density of the sintered iron in the electrode is approximately 22% of the theoretical iron density.

Although the oxygen electrode has been reported to achieve over 500 cycles, research is continuing to overcome its high degree of irreversibility and its tendency to erode and delaminate on cycling. The efforts to improve the bifunctional oxygen electrode are being conducted at Westinghouse, Case Western Reserve University, and the Lawrence Berkeley Laboratory.

The schematic structure of the Westinghouse air electrode is shown in Figure 30. Sintered-nickel-fiber grids are used as the current collectors. The active material is a silverized carbon powder which contains other additives such as tungsten carbide containing 12% cobalt, iron tungstate, and nickel sulfide along with fluorinated polymeric materials used to wet-proof the

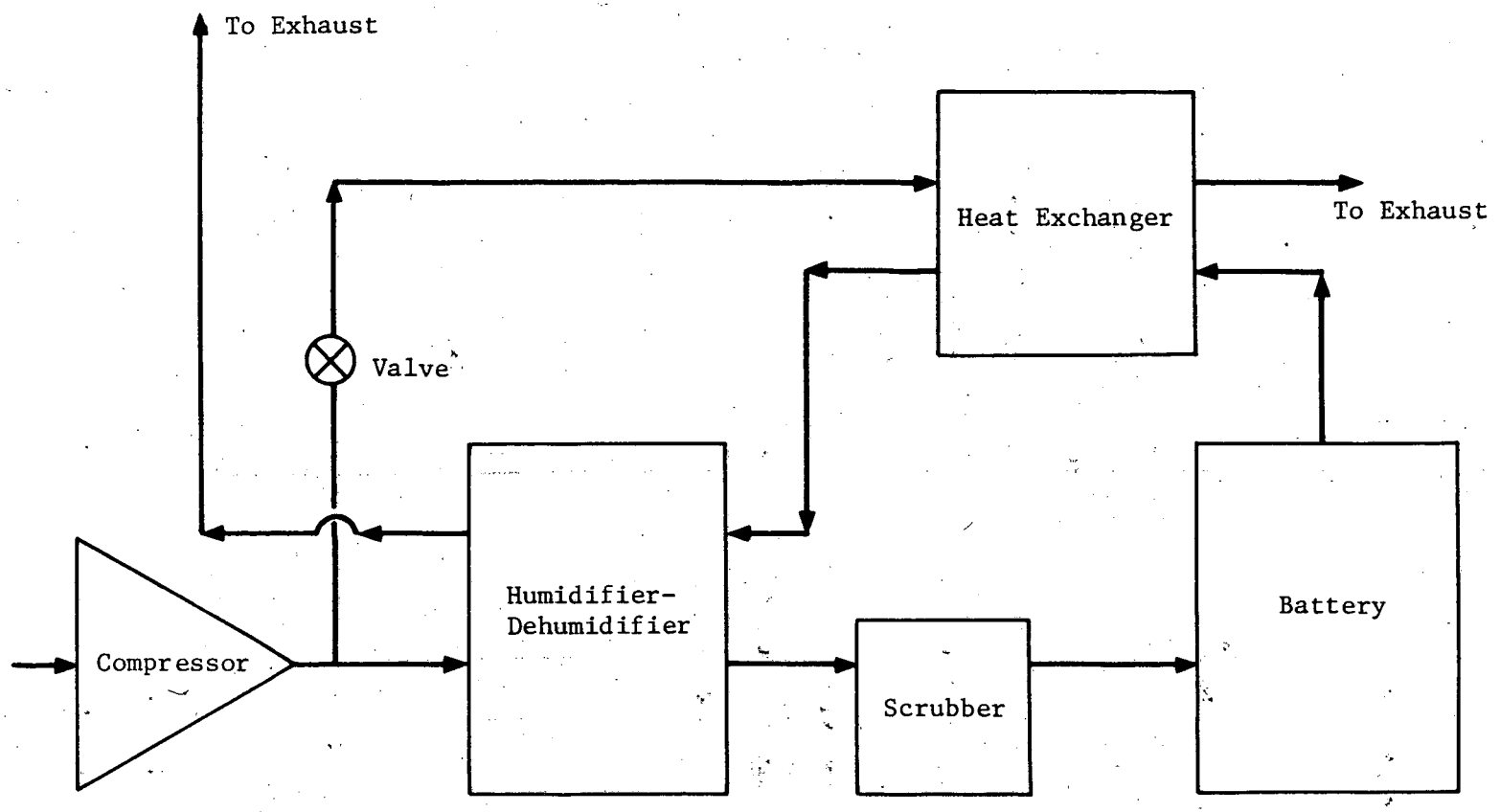

Source: Reference 44, Westinghouse.

FIGURE 29
SCHEMATIC ARRANGEMENT FOR IRON/AIR CELL THERMAL MANAGEMENT SYSTEM

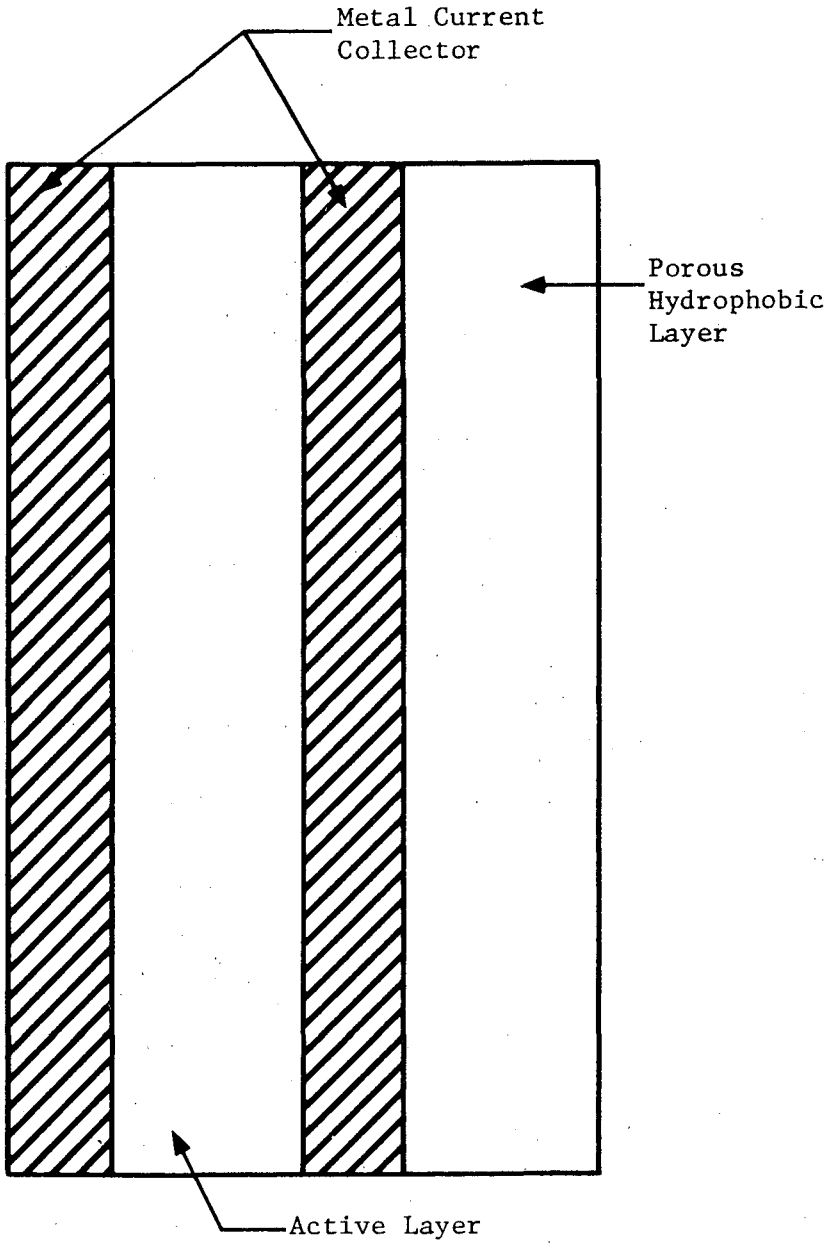

Source: Reference 45, Westinghouse.

FIGURE 30
AIR ELECTRODE CROSS SECTION

catalyzed portion of the electrode. The outer layer is also wet-proofed; it consists of a mixture of carbon powder and Teflon 30B. The electrode is prepared by pressing the materials to form the green electrode structure. The green electrode is then hot pressed at 370° C.

Westinghouse has recently reported that the inorganic additives present decrease the rate of silver loss from the electrode. The rate of silver loss in the presence of the additives is sufficiently low to assure effective catalytic activity over the projected cycle life of the battery.

The results of the research on oxygen electrocatalysis in bifunctional electrodes are also partly applicable to the monofunctional air electrode in mechanically rechargeable air cells, discussed in Section 4.1.2, fuel cells, and industrial electrochemistry, discussed in Section 6.0. The study at Case Western Reserve University investigated the extent of loss of the various components of the Westinghouse air electrode.[47] Failed Westinghouse electrodes showed a loss of the metallic constituents, Ag, Ni, Fe, W and Co, when compared with new electrodes. Scanning electron microscopy showed that the carbon morphology of some failed electrodes was similar to that of oxidized carbons. It was also observed that the structure of the Teflon in the hydrophobic layer changes markedly with heat treatment and with battery cycling.

Voltammetry studies were conducted on the various components of the Westinghouse air electrode. The results showed that the nickel-oxide coating formed on the nickel mesh current collector was an effective catalyst for oxygen generation. The single additives showed loss of material during cycling; however, electrodes containing all the additives experienced a lower rate of material loss. Yeager, of Case Western Reserve University, has noted that the loss of additives from the oxygen electrode can cause its deterioration through mechanical, thermal, and current distribution effects. Contamination of the iron electrode by the dissolution products from the air electrode can lead to increased hydrogen evolution at the negative electrode.

Short-term oxygen generation studies at Case Western Reserve University showed that the nickel oxide formed on the surface of the nickel-fiber grid was the critical component in the oxygen generation reaction. Of the various additives used, NiS was most effective in improving the anodic polarization of the oxygen electrode and also was effective in decreasing the rate of loss of silver.

The importance of NiO in the charging of the iron/air battery confirms the desirability of having different catalysts for the discharge and charge reactions. The following catalyst pairs have been evaluated by Ohzuku et al.:[48]

- Pt/NiO_x--Pt, although effective for O_2 consumption, is not effective for O_2 generation. In addition, dissolution of Pt and its deposition on the iron negative can lead to hydrogen evolution.

- Ag/NiO_x--This pair is in current use with other additives in the Westinghouse cell. Silver oxide shows some solubility and can deposit on the iron negative.

- The higher overvoltage of silver makes it less deleterious to the iron electrode than platinum.

- Active carbon/NiO_x--Some carbons are active for oxygen reduction but not for oxygen evolution. Although oxidizable under charging conditions, carbon does not affect the negative electrode and is inexpensive.

- Others--Macrocyclic complexes, underpotential deposited metals, and Li-doped Co_3O_4 appear promising as bifunctional oxygen electrode catalysts. Various mixed metal oxides are also candidates for catalysts for the oxygen electrode.

Ross's research at the Lawrence Berkeley Laboratory (LBL) emphasizes the following:

- The redistribution of electrolyte within multicomponent, multilayer electrode structures during charge and discharge.

- The use of C^{14} to measure corrosion rates of carbon black supporting materials.

- New concepts in catalytic materials and electrode structures.

Ruthenium and platinum-ruthenium alloy clusters dispersed on graphitized carbon black, similar to phosphoric acid fuel-cell oxygen electrodes, are being studied for bifunctionality. The use of a separate charging electrode also is to be explored.

Liu of Westinghouse has investigated gas transport in bifunctional air electrodes.[49] The objective of his studies was

to determine the uniformity of the electrodes and the effect of non-uniformity on performance of the iron electrode. The implications resulting from these studies were:

- Less uniform electrodes will generally have higher polarization characteristics.
- Loss in capacity of the iron electrode may be due to the uneven discharge of iron by the air electrode.
- Discharge of most of the oxygen formed during charge on the air side of the electrode indicates the extent of electrolyte penetration within the electrode. This penetration can eventually lead to leakage.

The improvements made in the iron/air battery, especially in the cycle life of the bifunctional air electrode, indicate that this couple offers promise for meeting electric vehicle performance goals. Continuing research on the bifunctional air/electrode catalyst system and performance can be expected to lead to further improvement.

The Westinghouse mission analysis concluded that the iron/air cell could meet near-term and intermediate electric vehicle performance goals. The cell does not have the performance capability equal to that of an internal combustion engine, since, like all other secondary batteries, it cannot meet the 15-minute refueling goal.

4.1.2 The Aluminum/Air Battery

The effort to develop the aluminum/air battery is centered at the Lawrence Livermore National Laboratory (LLNL). The earlier

research and development and the structure of the LLNL program, including the subcontractors and their tasks, were reviewed in SR-I and SR-II. The program participants, as of the fourth BECC, are listed in Table XX. A cross section of a planar aluminum/air cell and a simplified schematic for the aluminum/air battery system are shown in Figure 31.

Anode studies are being conducted on pure and alloyed aluminum. Morris and Tsai (Continental Group, Inc.) have reported on the anodic dissolution of aluminum and an aluminum-gallium alloy (RX 808) in sodium hydroxide and sodium hydroxide, sodium stannate solutions.[50] Earlier studies using rotating aluminum disk electrodes and chronopotentiometric measurements have been extended to cover a greater range of temperatures. Critical current densities were determined as a function of temperature. These data were used in an Arrhenius plot and an activation energy and preexponential factor were determined. The measured activation energy was compared with earlier values for the corrosion of aluminum and for the crystallization reaction of $Al(OH)_3$. The rate constant of the dissolution reaction was also determined.

The research at LLNL emphasizes the investigation of the electrode properties of a matrix of aluminum-alloy anodes/electrolyte combinations. Separate polarization curves have been obtained for the anode solution reaction and the hydrogen evolution reaction. The studies were undertaken to determine the effects of

TABLE XX

ALUMINIUM/AIR MAJOR CONTRACTORS AND TASKS

Task	Contractor
Overall Project Management	Lawrence Livermore National Laboratory
Anode Research and Development	Lawrence Livermore National Laboratory Reynolds Metals Co. University of Belgrade
Cathode Research and Development	Diamond Shamrock Lawrence Berkeley Laboratory
Reaction Product Handling	Alcoa
Safety and Environmental Analysis	IWG Corporation
Hardware Development	Continental Group/Lockheed Missiles and Space Co.

Source: Lawrence Livermore National Laboratory.

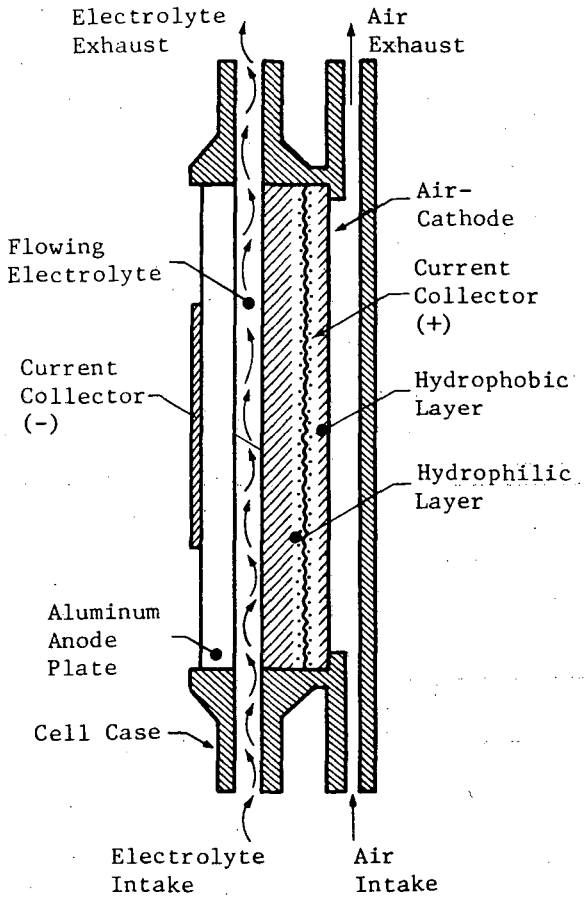

Source: Lockheed.

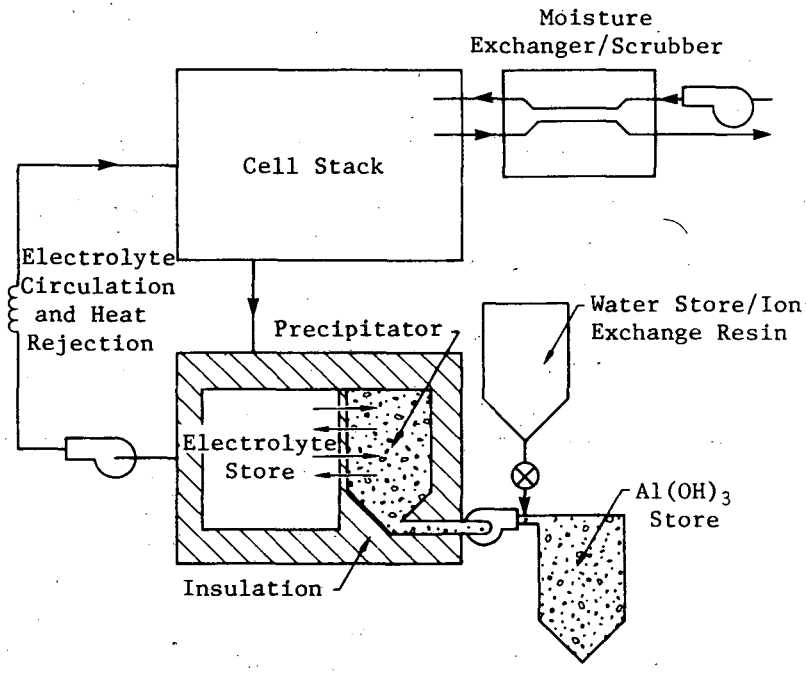

Source: Lawrence Livermore National Laboratory.

FIGURE 31
ALUMINUM/AIR BATTERY SYSTEM

low levels of Ga, Fe, Si, Mg, Mn, and Cu in caustic-aluminate and caustic-halide electrolytes. Some of the above listed impurities, such as iron, occur in the aluminum as recovered in the plant. The economic benefit of using pot-line aluminum has led to the investigation at Reynolds of the aluminum-gallium alloy RX 808 with iron and silicon impurity levels corresponding to Hall process aluminum. Using an impressed-current weight loss experiment with the impure alloys in 4M caustic (NaOH), it was shown that at high current densities the coulombic efficiency of the anode alloys was proportional to their iron content. At low current densities, the anodic dissolution did not show this relationship but was related to the grain structure of the alloy. Similar results were obtained at LLNL in alkali solutions containing stannate at high current density. There was a substantial improvement in efficiency at low current density in the presence of stannate ion. According to McNamara and coworkers at Reynolds, this suggests that tin from the stannate containing solution was plating out on the grain boundaries and preventing grain boundary attack.

The addition of 0.04% Mn to the alloy containing 0.04% Fe resulted in an improved coulombic efficiency. This is to be investigated in greater detail. This development has potentially important cost consequences as aluminum containing 0.04% Fe can be produced at low cost in carefully controlled smelters.

The unifunctional cathodes for the aluminum/air cell are being developed at the Diamond Shamrock Corp. Malkin and Barnes have noted that these electrodes differ from those being developed for use in chlor-alkali production, as shown in Figure 32. They also differ from the structure of the bifunctional air electrode (Figure 30). The major problem in the design of the cathode is the possibility of flooding of the electrode during standby as a result of corrosion of the carbon matrix or as a result of large changes in power demands with a vehicle going from idling to acceleration to cruise and back to idling.[51]

The present current collector is either silver-plated nickel mesh or nickel-plated copper mesh. The wet-proof layer must be conductive since it provides the contact to the current collector. This layer must have good tensile strength and good adhesion to the active layer to prevent delamination or blistering. The key variables in electrode preparation are the pressure and temperature at which the layer is formed.

The test electrodes supplied by Diamond Shamrock to LLNL contain 2.4 mg Pt/cm^2. Work is in progress on reducing the platinum content and substituting silver or certain macrocyclic complexes for platinum. Results of these studies are shown in Figure 33. The change in electrode performance with time under intermittent load is also being determined. The electrode containing 1.2 mg Pt/cm^2 met LLNL specifications after 175 hours

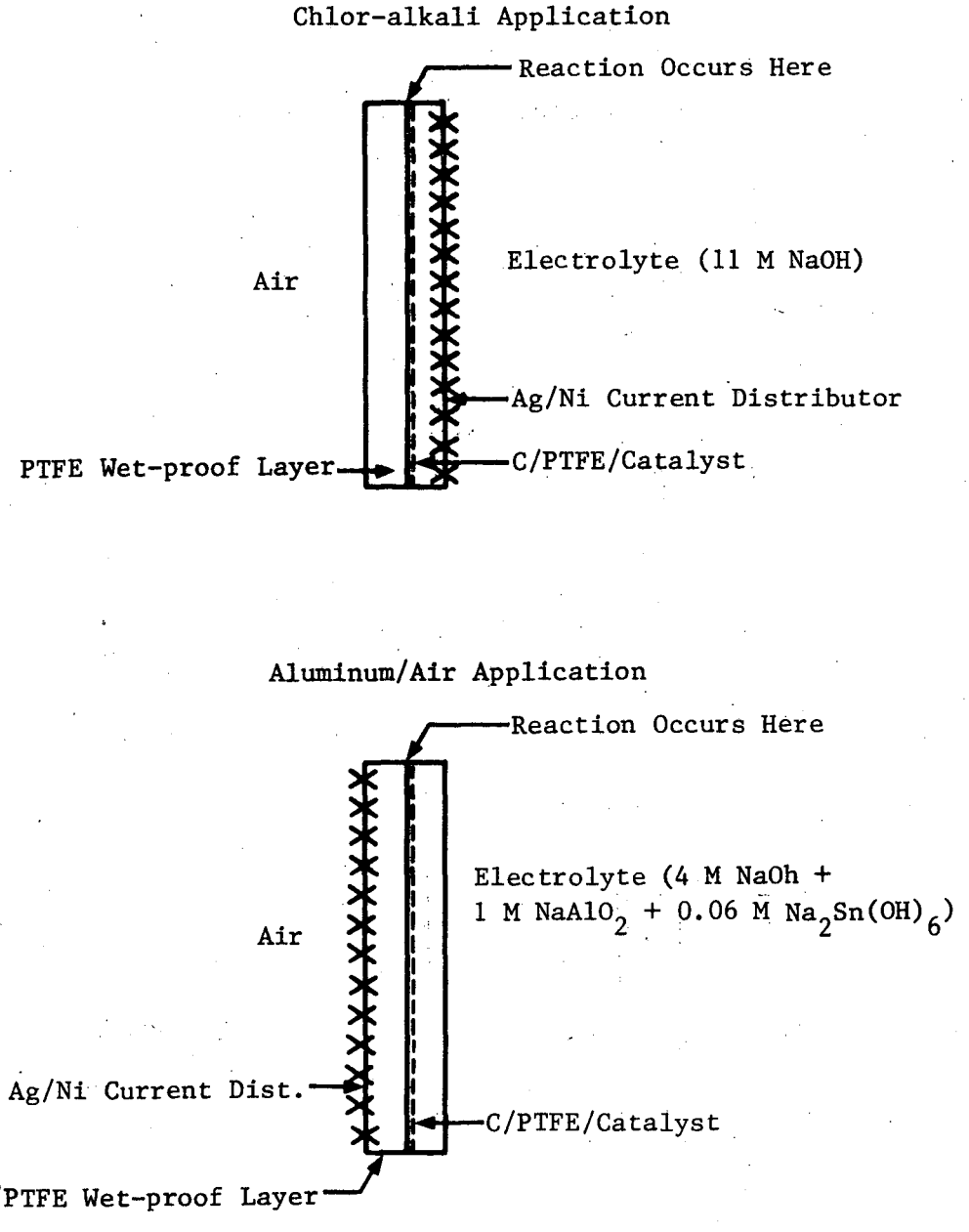

Source: Diamond Shamrock Corp.

FIGURE 32
COMPARISON OF ALUMINUM/AIR AND CHLOR-ALKALI CATHODES

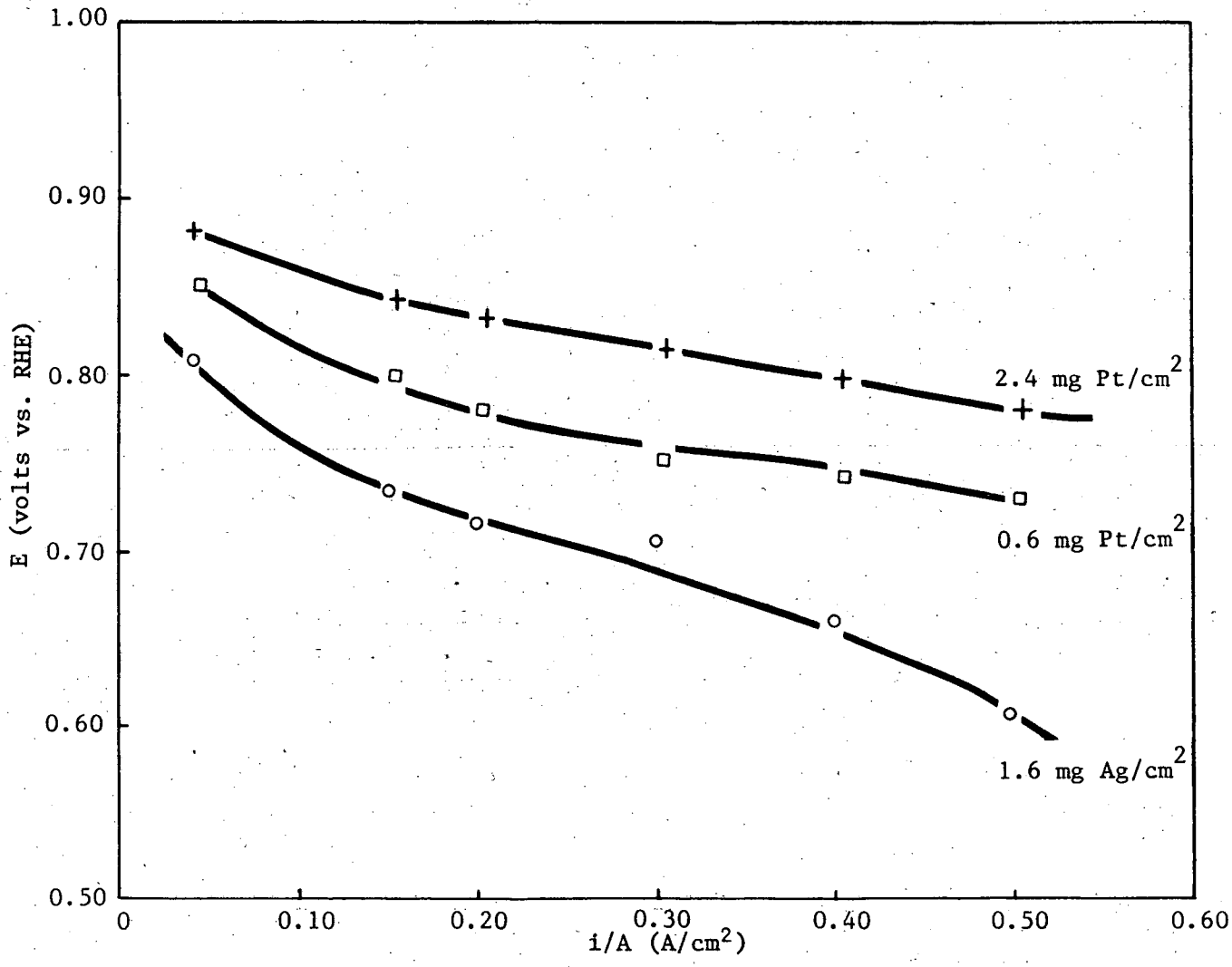

Source: Diamond Shamrock Corp.

FIGURE 33
AIR ELECTRODE CATALYSIS

of intermittent testing with a voltage decay of 76 millivolts at a current density of 0.5A/cm^2, the highest current density investigated.

Studies of the catalysis of the monofunctional air electrodes are reviewed in Section 6 below because much of this effort has been oriented toward the air electrode for industrial applications.

Scale-up and engineering of the aluminum/air cell is in progress. Figure 34 compares the performance of various experimental cells.

Rapidly refuelable batteries are being designed and tested. Figure 35 illustrates a Lockheed design for such a battery. The cell cover plates can be removed and aluminum anodes added without removal of the residual unspent anode. The design has been tested on single cells and the results were satisfactory.

As part of the battery operation, the spent aluminum is to be removed from the battery in the form of hydrargillite [$Al(OH)_3$] and reprocessed to aluminum. To test this concept, a cell has been operated with the control of the aluminate ion concentration in the electrolyte by precipitating the hydrargillite in a crystallizer unit. The decrease in aluminate ion concentration through the use of a crystallizer unit is shown in Figure 36.

The principal performance objectives for the system are:

Specific energy--350Wh/kg

Specific power--170W/kg

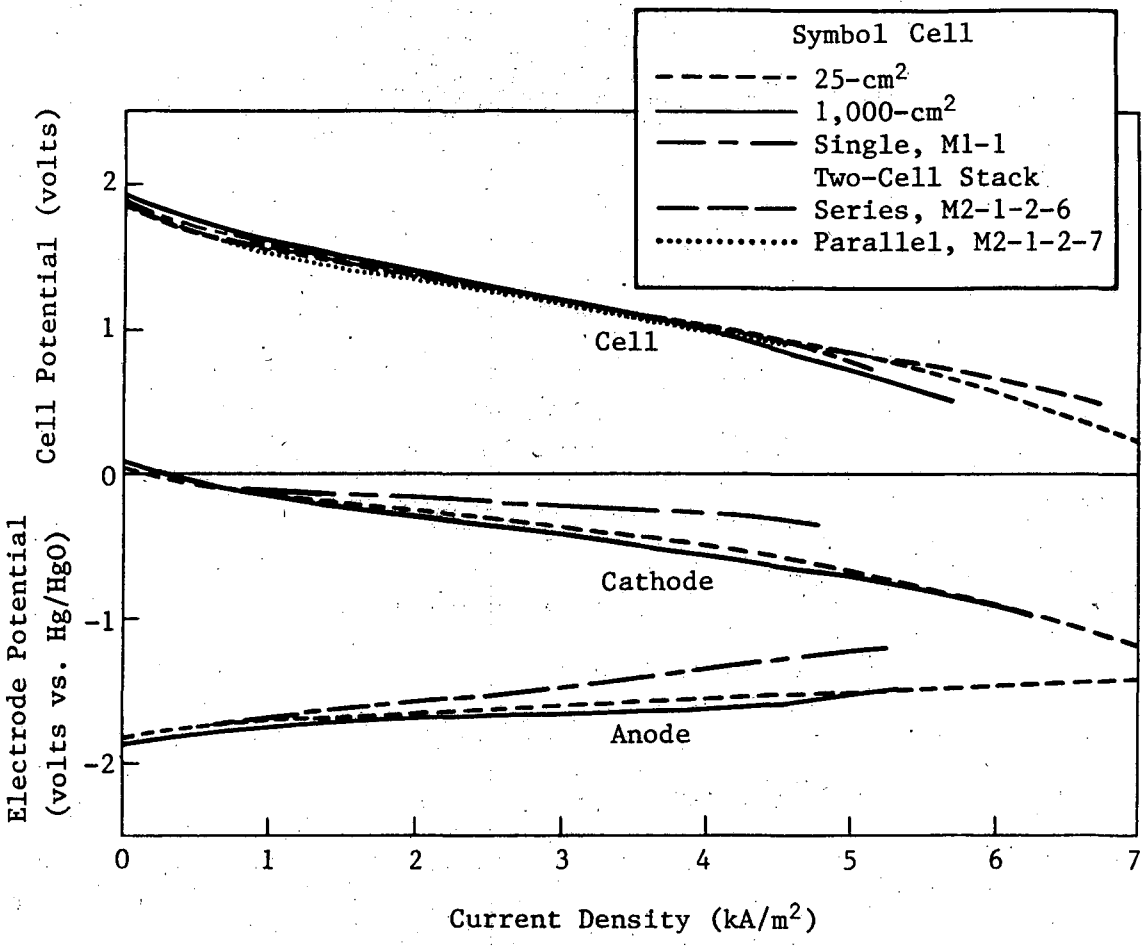

Source: Lawrence Livermore National Laboratory.

Polarization curves are provided for identical pairs of electrodes in small-scale cells (25 cm^2), large-scale cells (0.1 m^2), and in rapidly refuelable cells (M1 series, 167 cm^2) and refuelable bicells (M2 series). Displacement of the electrode potential curves (no correction for IR drop) for the M1 results from a change in the virtual position of the reference electrodes. Anode, Al-0.07 Ga; electrolyte, 4 M NaOH + 1 M $Al(OH)_{3,aq}$ + 0.06 M $Na_2Sn(OH)_6$; temperature, 60°C.

FIGURE 34
COMPARATIVE PERFORMANCE OF ALUMINUM/AIR CELLS AND BICELLS

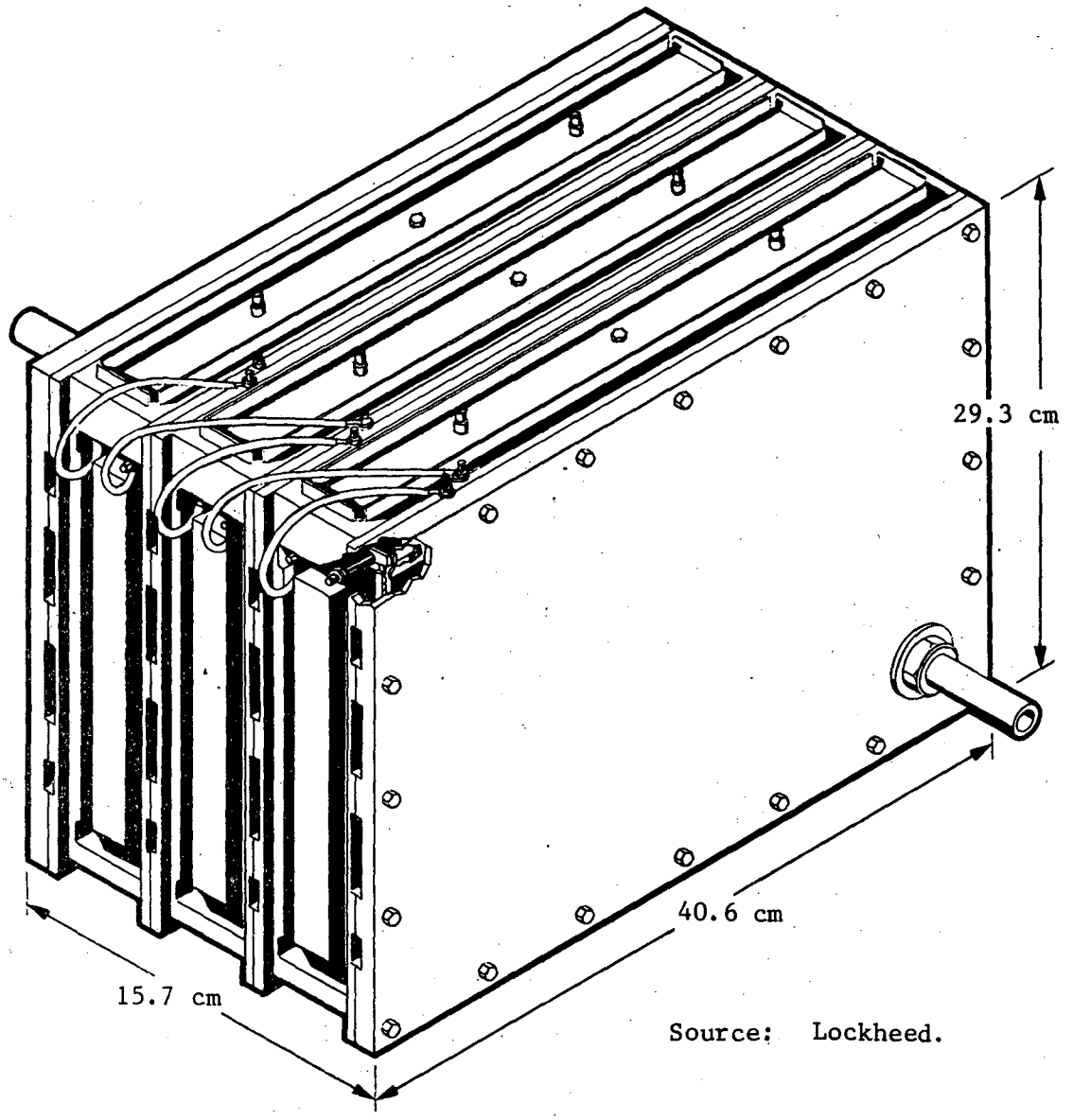

Source: Lockheed.

FIGURE 35
REFUELABLE ALUMINUM/AIR BATTERY

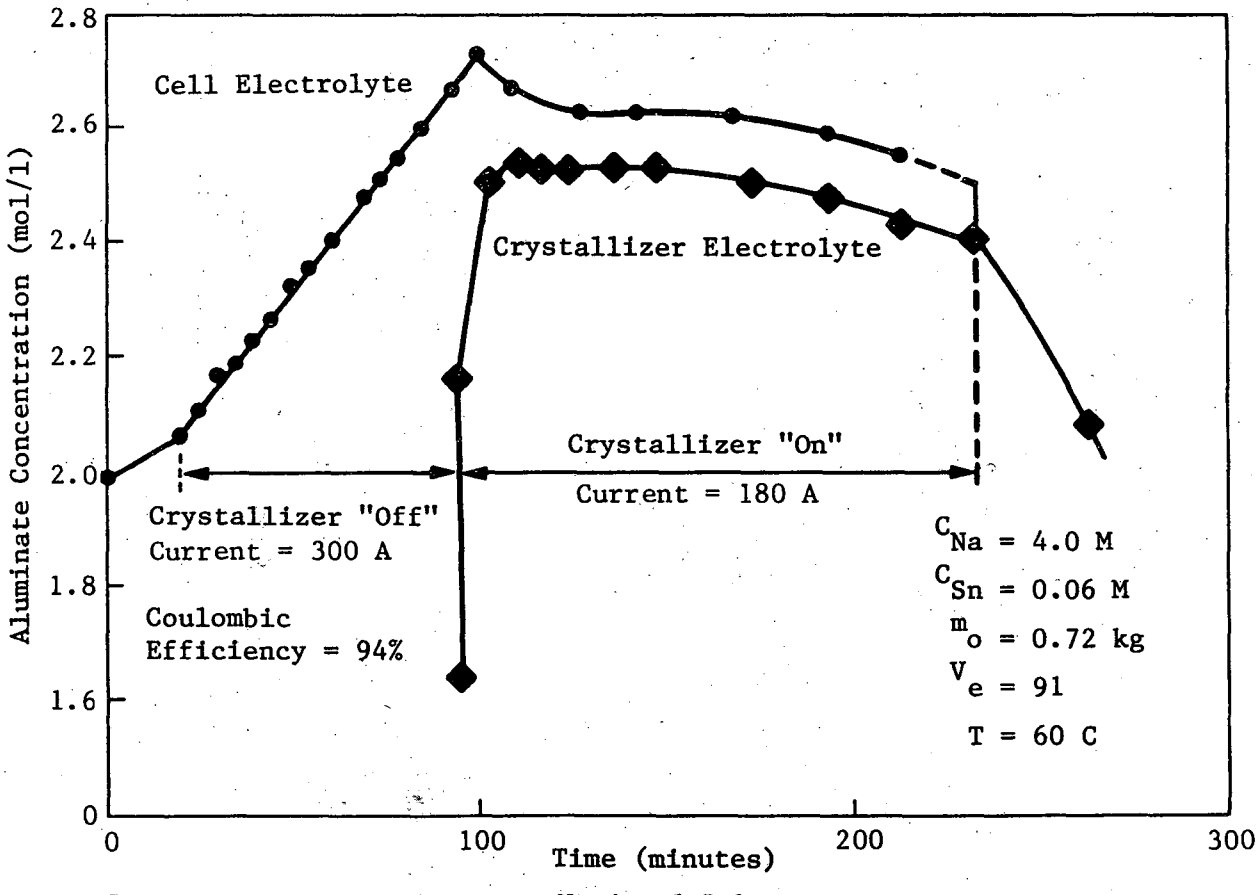

Source: Lawrence Livermore National Laboratory.

FIGURE 36
CONTROL OF COMPOSITION OF ALUMINUM/AIR CELL ELECTROLYTE WITH HYDRARGILLITE CRYSTALLIZER

These values are for the battery system as illustrated in Figure 31 above. Until complete units are operated so that system weight and size can be minimized, estimates of performance can only be based on design results. It is also important to develop data on the ratio of aluminum corrosion to faradaic aluminum to determine the magnitude of any potential hydrogen evolution problem as a function of power output.

4.1.3 Hydrogen/Nickel-Oxide

The hydrogen/nickel-oxide couple was included among the cells of potential interest for solar applications. This couple had not been considered in earlier reports; the cell has been developed for space applications. The cell reactions are:

Negative:

$$1/2\ H_2 + OH^- \underset{\text{Charge}}{\overset{\text{Discharge}}{\rightleftharpoons}} H_2O + e^-$$

Positive:

$$NiO(OH) + H_2O + e^- \underset{\text{Charge}}{\overset{\text{Discharge}}{\rightleftharpoons}} Ni(OH)_2 + OH^-$$

Net reaction:

$$1/2\ H_2 + NiO(OH) \underset{\text{Charge}}{\overset{\text{Discharge}}{\rightleftharpoons}} Ni(OH)_2$$

Theoretical Specific Energy: 336Wh/kg

The electrolyte for the cell is 30% KOH and asbestos separators are used.

The configuration of the cell developed by the Air Force is shown in Figure 37. The electrode stack assembly is contained in a

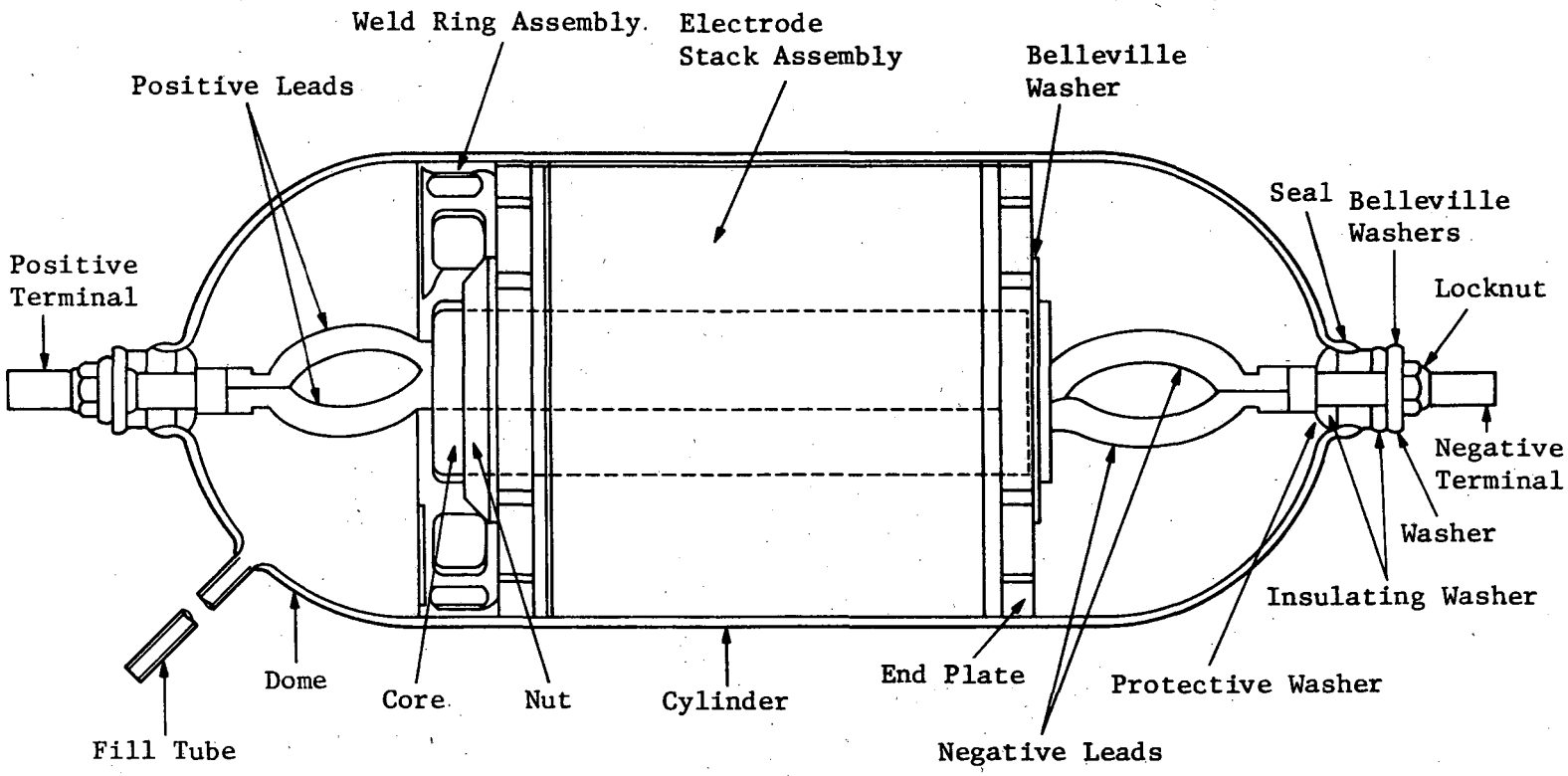

Source: Reference 52.

FIGURE 37
TYPICAL HYDROGEN/NICKEL-OXIDE CELL (AIR FORCE) DESIGN

hermetically-sealed, thin-walled, cylindrical pressure vessel. Dimensions for a 50Ah cell are: diameter 8.9 cm and length 21.3 cm (exclusive of terminals). The weight is 1.2 kg. The hydrogen pressure varies from 40 atm at full charge to 7 atm when discharged.(52)

The accumulation of oxygen during charge is prevented by the presence of a platinum catalyst on the negative electrode to catalyze the hydrogen oxygen recombination. The hydrogen/nickel-oxide cell has a built-in, state-of-charge indicator, the hydrogen pressure. One deficiency of this system is that it undergoes self-discharge via the direct reaction of H_2 and NiO(OH).

The hydrogen/nickel-oxide cell has shown long cycle-life (7,000 cycles) at 80% DOD and at high rates of charge. The cell can be maintained at full charge by trickle charging at the rate of self-discharge. It is capable of high rates of charge and has good energy efficiency (75-80%).

The cell is designed for space applications. Clifford and Brooman have estimated the performance characteristics of the cylindrical cells when packaged as a 25kWh hydrogen/nickel-oxide battery system for stationary terrestrial applications. The results are listed in Table XXI.

The major drawback for this cell, in its aerospace configuration, is its high cost. However, Clifford and Brooman report that various designs have projected costs ranging from

TABLE XXI

PRELIMINARY ESTIMATES FOR 25-kWh HYDROGEN/NICKEL-OXIDE BATTERY SYSTEM[a]

Parameter	Cell	Battery Module	Battery System
Number of cells	1	8	160
Voltage--nominal, volts	1.25	10	200
maximum, volts	1.50	12	240
minimum, volts	1.00	8	160
Rated Capacity, Ah	125	125	125
Wh	156	1250	25,000
Length, in (cm)	21 (54)	21 (54)	42 (108)
Width, in (cm)	3.5 (9)	14 (36)	28 (72)
Height, in (cm)	3.5 (9)	7 (18)	35 (90)
Volume, ft^3 (l)	0.15 (4.2)	1.3 (33.7)	28 (675)
Weight, lb (kg)	5.2 (2.4)	45 (22.7)	1000 (455)
Energy Density, Wh/in^3 (Wh/l)	0.6 (37)	0.55 (34)	0.5 (31)
Specific Energy, Wh/lb (Wh/kg)	30 (66)	28 (61)	25 (55)
Footprint, kWh/ft^2 (kWh/m^2)	1.8 (20)	1.8 (20)	3.2 (34)

[a]Based on aerospace cell design, includes container, does not include thermal control subsystem or power conditioner.

Source: Reference 52.

$50/kWh to $250/kWh. They estimate a minimum materials cost of $20/kWh, processing costs of $30 to $80/kWh, and a pressure vessel cost of $50 to $150/kWh. Their total battery cost estimate is $100 to $200/kWh (in 1980 dollars) with volume production.

When this report was prepared, Sandia National Laboratories was planning to initiate efforts leading to a low-cost hydrogen/nickel-oxide battery system for solar applications.

4.1.4 Metal/Continuous-Feed, Positive Batteries

Three couples are to be discussed in this section: the zinc/chlorine, zinc/bromine, and zinc/ferricyanide. The last of these has been included although it is less well developed and it is one of the exploratory couples included in the Electrochemical Systems Research Subelement. These cells involve the dissolution and redeposition of zinc during discharge and charge, respectively. All three systems are electrochemically reversible.

4.1.4.1 Zinc/Chlorine Battery. The major thrust of the zinc/chlorine development effort reported at the BECC was on the production of a battery for evaluation in the BEST facility. This effort is jointly sponsored by DOE, EPRI, and PSE&G, with EDA also sharing the cost.

The characteristics of the zinc/chlorine cell were described in SR-I and SR-II. As of June 1981, two 50kWh prototype models had been built and were undergoing cycling tests. The modules could be

charged and discharged without operator intervention although they were not under automatic control.

The design and analysis of the BEST installation were completed and a site-specific commercial battery has been designed. Submodule manufacture has been implemented in the pilot-plant facility at Greensboro, North Carolina. Development of module components, i.e., pumps, heat exchangers, and valves, is continuing in order to improve component reliability, efficiency, and manufacturability. Supporting investigations to improve battery performance are being conducted under EPRI sponsorship.

4.1.4.2 Zinc/Bromine Battery. The zinc/bromine battery, as reported in Section 2, is a candidate for application in solar-photovoltaic systems. It is also being evaluated for use in distributed energy systems. The two efforts are oriented toward fulfilling the requirements of specific applications: Exxon, solar photovoltaics; and Gould, distributed energy systems. The Exxon system may be suitable for mobile applications but this is outside the scope of the company's present contract. Although the investigation of the zinc/bromine couple for use in mobile applications has been deemphasized and was not covered in the fourth BECC, this application is the subject of considerable interest. Improvements in performance through the use of supported electrolytes and potential low cost provide the impetus for this renewed interest.

The general characteristics of these two systems and the approaches of the two contractors were reviewed in SR-II.

The bipolar arrangement of the cells in the zinc/bromine battery leads to the presence of shunt currents due to the use of a common electrolyte for the cells in series. The formation of zinc dendrites during charge has been partially attributed to the presence of the shunt currents. Zahn and others at Exxon have patented a method for the minimization of shunt currents.(53) As stated in the initial patent, "the method involves applying a protective current through at least a portion of said conductive bypass path in a direction which is the same as the shunt current through said shared electrolyte and of a magnitude which reduces said shunt currents." The improved method involves the use of "tunnels" between branched channels rather than passing a protective current through the common manifold, as in earlier patents. The tunnel and manifold arrangement is shown in Figure 38. Shunt current protection allows the repeated partial discharge of the battery without the need to completely discharge the battery at the end of each cycle. It is anticipated that this approach to shunt current minimization will reduce pumping and parasitic power in certain designs. Manifold shunt current protection has been demonstrated for over 100 cycles in a test battery.

Bellows of Exxon also reported that the selectivity of microporous membranes has been improved through a low-cost treatment

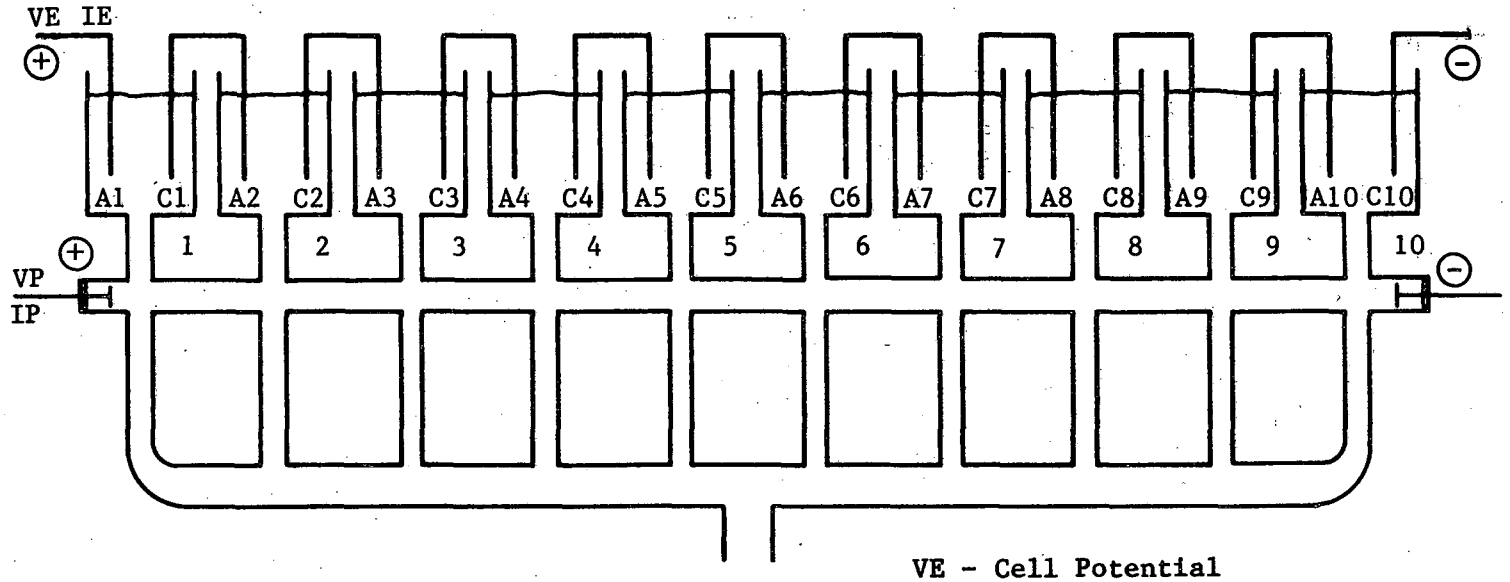

VE - Cell Potential
IE - Cell Current
VP - Parasitic Potential
IP - Parasitic Current

Source: Exxon.

FIGURE 38
SHUNT CURRENT PROTECTION VIA MANIFOLD INTERCONNECTS—
"TUNNELS"

involving polyelectrolyte additives. This treatment was reported to improve coulombic efficiencies, probably through decreased diffusion of bromine to the zinc negative. This is accomplished with no increase in resistivity.

The battery electrodes have been made using both injection molding and a novel co-extrusion technique. In a recent design, the co-extruded bipolar electrode is sandwiched between the microporous separators. The separator has molded supports on both surfaces to maintain uniform electrode spacing. The electrolyte flow manifolding is formed by injection molding of a flow network around the periphery of the separator.

Life testing of the electrodes and separators under use conditions has not identified any life-limiting mechanism in the system. The use of hydrogen-bromine recombination and excluding oxygen from the system enables maintenance of the pH level in the battery. Multi-kWh systems, with H_2-Br_2 recombination, have been deep-cycled for over 100 cycles.

Performance testing has been conducted on 500Wh and 3kWh batteries. Stable performance has also been demonstrated in 3 and 10kWh sub-modules. Current module performance characteristics, as well as projected performance characteristics, based on 500Wh test modules are listed in Table XXII.

Cost studies based on the demonstrated extrusion and injection molding techniques have shown that this battery, with plastic

TABLE XXII

ZINC/BROMINE BATTERY PERFORMANCE

	Unit	Exxon		Gould
		Present[a]	Projected[b]	Mod 2A
Electrochemical Efficiency	%	68-73	72-78	73
Voltaic Efficiency	%	85	85-90	87
Coulombic Efficiency	%	80-85	85-90	84
Energy Efficiency	%	65-70	70-75	70
Specific Energy	Wh/kg	55	65-70	40
Energy Density	Wh/l	70	80-85	--
Specific Power (20-sec)	W/kg	80	90-100	30
Power Density	W/l	90	105-110	--
Discharge Voltage	volts	80 (50 cells)	120 (75 cells)	--
Factory Cost--100,000 Units/yr	1981$	--	$28.05	$88.00

[a]Present electrode performance of X-3 modules in 20-kWh design.

[b]Present electrode performance of 500-W system in advanced 20-kWh design.

electrodes, bipolar stacks, bromine complexation, and circulating electrolytes, could be produced in 20kWh units at a rate of 100,000 units/year at a factory cost of $28/kWh (in 1980 dollars). This does not include return on investment and various indirect charges.

For the solar photovoltaics application, plans are to develop a microprocessor controller, extend cycle life, and scale-up the system to 20kWh. The delivery to Sandia National Laboratories of a 20kWh stand-alone system is scheduled for late 1983.

The Gould system has some features which differ from the Exxon cell; however, the overall systems are quite similar. Figure 39 shows the cell stack components for the Gould zinc/bromine cell. A feature of the cell, not clearly shown in the figure, is the presence of a carbon felt in contact with the positive electrode. This increases the effective surface area of the positive and decreases the polarization. The presence of the carbon felt increased the sub-module efficiency from 55-60% to 65-70%. The separator is microporous Daramic. The bipolar plate is a thin sheet of non-porous carbon. The electrolyte is zinc bromide and potassium chloride. An additive for improved zinc deposition is included in the anolyte. This enables zinc electrode capacities of 200 mAh/cm^2 without dendrite growth. Screening tests have shown the stability of the preferred bromine complexing agent. Figure 39 also shows the inlet and outlet ports for the circulating anolyte and catholyte.

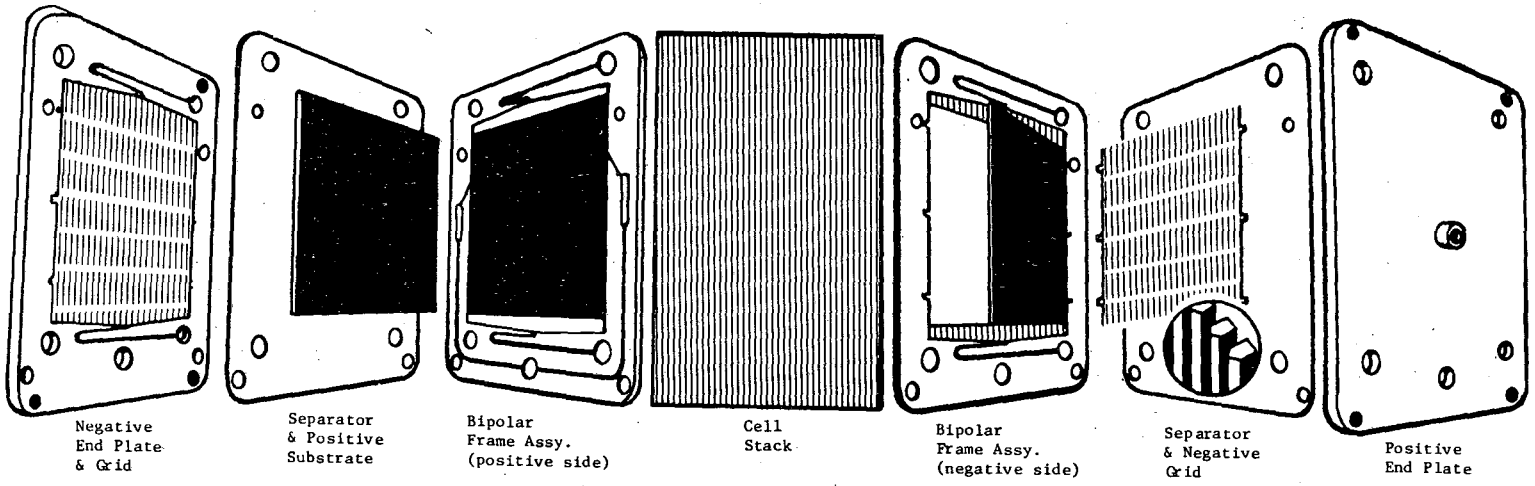

Source: Gould

FIGURE 39
ZINC/BROMINE CELL STACK COMPONENTS

The battery hardware program has focused on the design optimization of a 1kW, 5 to 8kWh sub-module of 1 ft^2 (30.5 cm^2) bipolar cells in a filter press stack. Three sub-modules have been built and tested. Design improvements have been incorporated in the sub-modules. One six-plate unit achieved 700 cycles in continuous automatic testing. Energy efficiencies of over 73% were obtained in initial cycling. A stand-alone, 10kW, 50 to 80kWh module, consisting of 10 sub-modules, is currently under construction. This is to be a subscale prototype of a much larger, e.g., 1MWh module for stationary storage applications.

Performance characteristics of the Gould battery are included above in Table XXII. It should be noted that the performance values for the Exxon and Gould systems are not completely comparable because the development status of the two systems is different.

Gould has carried out a cost study on its zinc/bromine system for large volume production (2,500MWh/yr) of 10kW modules.[54] The calculated costs were $188/kW for the stack components and $12/kWh for the chemicals. These costs applied to purchased materials and components in a ready-to-assemble condition. The balance of system components (pumps, plumbing, structures, etc.) totaled $194/kW for a module cost of $382/kW and $12/kWh. For a 5-hour discharge system, this results in a cost of $88/kWh.

Gould has also conducted supporting research related to the zinc/bromine battery. Thermodynamic data (enthalpies, entropies,

and free energies) were measured over the ranges of electrolyte concentrations and temperatures used in battery service. These were used to predict the reversible thermodynamic heat rate and heat rate due to irreversible losses. The sum of these two factors represents the design load on the heat exchanger during isothermal operation.

The kinetics of the bromine release from the liquid polybromide complex were determined for use in the design of the bromine storage system.

Both Exxon and Gould have made progress since late 1979 on development of the zinc/bromine battery. The cost estimates differ markedly, with Exxon reporting $28.80/kWh and Gould, $88/kWh. A detailed comparison of the two cost estimates appears desirable to resolve the large cost differences for two similar systems.

4.1.4.3 Zinc/Ferricyanide Battery. The initial DOE-supported studies on the zinc/ferricyanide system were reported in SR-II. The cell has some similarities to the zinc/halogen systems except that the positive reactant, the ferricyanide ion, remains in the catholyte solution and undissolved zinc oxide in the anolyte is accumulated in an external tank. On charge, the zinc oxide is dissolved in the circulating anolyte and redeposited and the ferrocyanide in the catholyte is reconverted to the ferricyanide. Separate pumps and filters are included in the anolyte and catholyte circulating systems.

The experimental electrode and cell studies used 60-cm^2 electrodes. The negative plate was cadmium-plated iron, copper, or brass. Copper and brass were the preferred materials as their voltaic and coulombic efficiencies are greater than that of the cadmium-plated iron over the range of alkali concentrations of interest. Zinc capacities as high as 3,000Ah/m^2 have been shown to be reversible under the cell operating conditions.

Tests of a cell consisting of a sintered-nickel electrode for the redox positive, a cadmium-plated iron substrate for the zinc negative, 5N NaOH electrolyte, and a NAFION N-114 separator were conducted at a current density of 350A/m^2 for 950 cycles.

Lower cost technology and cells are being investigated and the preferred configuration reported at the June 1981 BECC consisted of:

- Graphite-felt positive;
- Brass or copper as negative electrode substrate; and
- Use of RAI Permion P-1010 in place of NAFION N-114 as the membrane.

The performance of a cell based on the preferred configuration and using 2N NaOH as the supporting electrolyte is shown in Figure 40.(55)

An economic analysis at Lockheed, which assumed the development of low cost technology, suggested a battery selling price of $32/kWh, an installed price of $230/kW, and a footprint of 94 kWh/m, as realistic goals for a 20MW, 100MWh system.

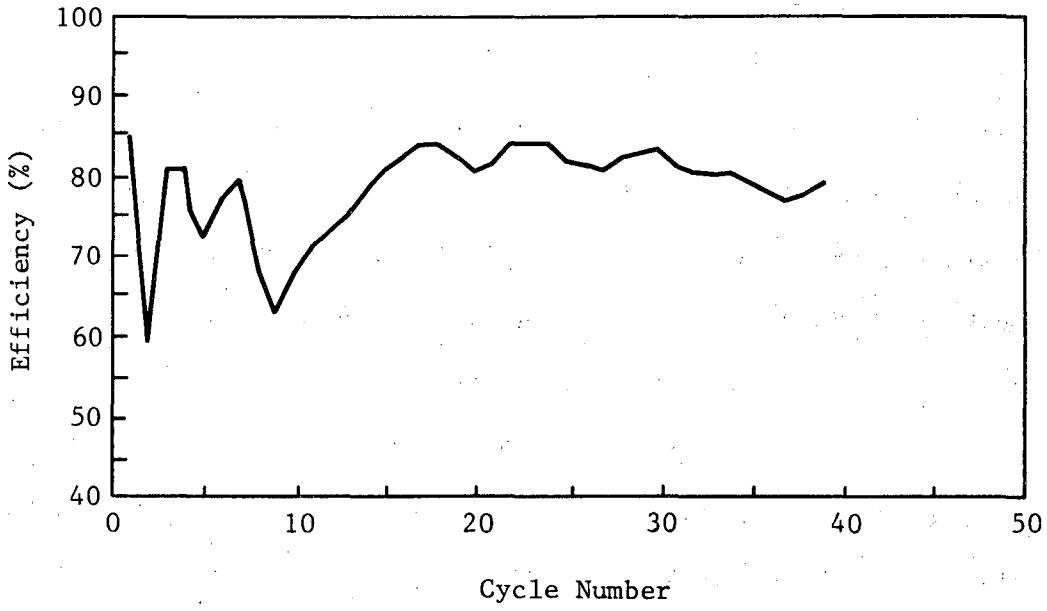

Brass Negative Plate
Permion P-1010 Separator
Graphite Felt Positive
2 M NaOH Supporting Electrolyte

Source: Reference 55.

FIGURE 40
PERFORMANCE OF ZINC/FERRICYANIDE CELL

The Lockheed investigators consider the following as the primary remaining issues in the establishment of the cell as a candidate system for use in dispersed, including solar, systems:

- Development of a low-cost bipolar electrode based on plastic carbon technology;
- Determination of scale-up criteria for 0.1-m^2 electrode single cells;
- Design and development of a five-cell, 300W multicell battery;
- Evaluation of applicability of batteries to solar photovoltaic and dispersed energy storage; and
- Engineering studies of materials selection.

4.1.5 NASA Redox Battery

Current emphasis on this battery system, described in SR-II, is as a storage system for solar energy systems. It has also been considered, and has potential, for distributed energy systems.

The battery system consists of a soluble anode couple chromous ion/chromic ion, and a cathode soluble couple of ferric ion/ferrous ion. It involves a circulating anolyte and a circulating catholyte, an ion exchange membrane separating the two electrolytes, external reactant storage, and trim, charge-indicator, and rebalance cells in addition to the cell stacks.(56) The trim cells are switched in or out of the load circuit to maintain the bus voltage. The charge-indicator cell is used as a reference cell to determine the state of charge in the power generating cells. The rebalance cells

are to convert products of side reactions back to cell reactants to maintain reactant concentrations.

Hagedorn has described in detail the NASA 1kW, 10kWh preprototype battery.[57] The design parameters for this battery are listed in Table XXIII. Figure 41 shows the polarization curves at three different states of charge. The sharp increase in voltage shown by the charge curve for 75% state of charge is accompanied by an increase of hydrogen evolution.

The 1kW preprototype system showed that the control concepts were valid and trouble free. The determination of loss mechanisms has provided direction for design changes which can decrease these losses. It is expected that pumping and shunt losses will be decreased when larger systems are built. The marked decrease in performance at low temperature, because of increased cell resistance, makes it desirable to employ passive temperature management, such as undergound storage, to prevent loss of performance.

Table XXIV shows the relationship between redox system characteristics, based on experience with the 1kW preprototype battery, and other systems investigated with regard to battery requirements for solar systems. The shortcomings of the NASA system relative to these requirements for deep-discharge applications are:

- Round trip energy efficiency;
- Operating temperature range; and

TABLE XXIII

NASA REDOX SYSTEM DESIGN PARAMETERS

Gross Power	1,260 W
Nominal Net Power	1,000 W
Voltage	120±5% volts-DC
Number of Stacks	4
Number of Cells per Stack	39
Number of Trim Packages (six cells each)	10
Depth of Discharge Range	80-20%
Reactant Volume (each)	700 l (186 U.S. gals)
Reactant Energy Density (end of life)	14.5 Wh/l
Cell Active Area	320 cm^2
Nominal Current Density	30 mA/cm^2
Reactants	1 M/1 $FeCl_3$, 2 M HCl 1 M/1 $CrCl_2$, 2 M HCl
Reactant Flow Rates per Cell (nominal)	100-150 cm^3/min
Parasitic Losses	
Pumps (15% pump efficiency)	120 W
Shunt Power	120 W
Number of Rebalance Cells	5
Number of Charge Indicator Cells	1

Source: Reference 57.

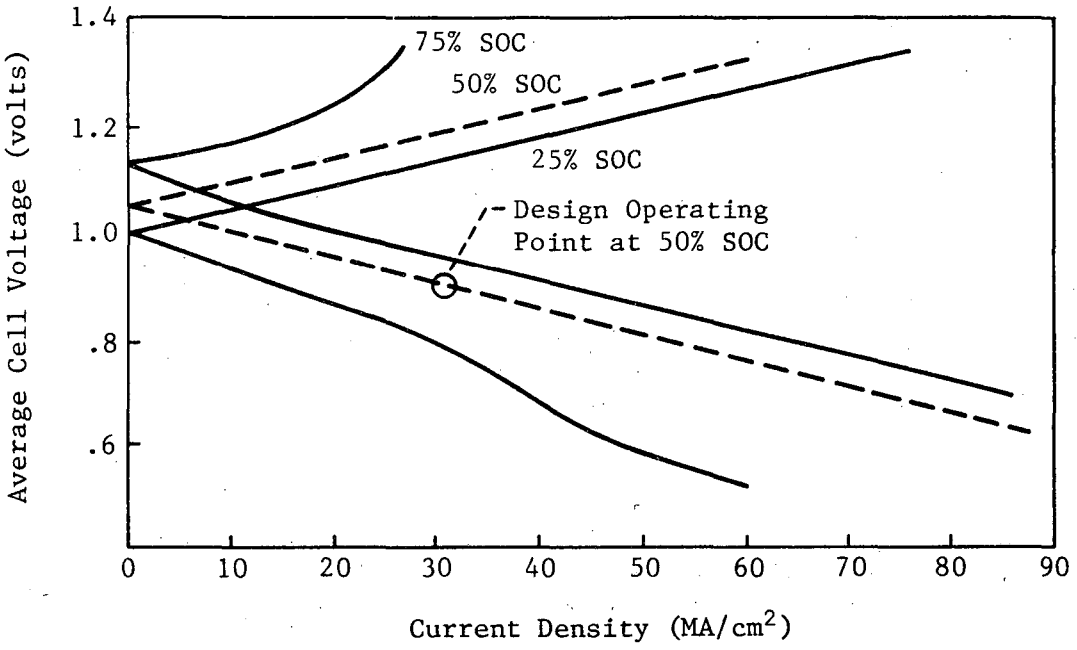

Source: Reference 57.

FIGURE 41
POLARIZATION CURVES, CHARGE AND DISCHARGE, FOR THE NASA 1-kW REDOX STORAGE SYSTEM

TABLE XXIV

COMPARISON OF NASA REDOX BATTERY CHARACTERISTICS AND SOLAR CELL SYSTEM REQUIREMENTS

CHARACTERISTIC	DEEP DISCHARGE			SHALLOW DISCHARGE	
	Requirement	4.0-kW/24-kWh System	8.0-kW/48-kWh System	Requirement	9.3-kW/2,245-kWh System
System Voltage	160 to 240 volts, nominal, 200 volts	200 volts	200 volts	12 to 120 volts	120 volts-DC
Capacity	15 to 50 kWh, nominal, 25 kWh	24 kWh nominal	48 kWh nominal	8-hr rate 25 to 2,500 Ah @25°C	N/A
Rate in Service	1 hr maximum, 6 hrs nominal	6-hr discharge	6-hr discharge	8 hrs maximum 250 hrs normal	250 hrs (design)
Duty Cycle	Daily discharge to 80% RC	20 to 80% DOD	20 to 80% DOD	Daily--5% RC Annual--100 to 20 to 100% RC	Daily--50%RC Annual--80 to 20 to 80% RC
Life	5 yrs minimum 20 yrs nominal	20 yrs nominal	20 yrs nominal	5 yrs minimum 20 yrs nominal	20 yrs
Energy Efficiency	80% minimum round trip	70.1% (64.8%)[a]	71.3% (67.0%)[a]	80% minimum round trip	76.2% at max pump and shunt power losses
Self-Discharge	1%/week maximum	1% Pumps not running	1%	1%/month maximum	0.05% pumps not running
Temperature Range	0°C to 50°C	20°C to 55°C	20°C to 55°C	-40°C to 60°C	20°C to 55°C
Maintenance	Minimum automatic desired	Periodic pump servicing		Yearly maximum, none desirable	Periodic pump servicing
Charge Rate		-	-	8 hrs maximum	46 hrs
Cost Goal	$100/kWh for 700 cycles, $50/kWh for 7,000 cycles	$134/kWh (115 kWh)[a] factory cost	$130/kWh (115 kWh)[a] factory cost	$100/kWh maximum $50/kWh desirable	$59/kWh, factory cost
Stand without Damage	Any SOC, 7 days minimum during any 3-month period	Yes	Yes	Operate 1 yr minimum at less than 100% SOC	Yes
Building Code	Acceptability	Low pressure, low temperature		Withstand environmental effects	Function of installation

Note: RC = Rated capacity; SOC = State of charge.

[a]For minimized system cost.

Source: National Aeronautics and Space Administration.

- Projected cost.

For shallow-discharge solar applications, the NASA system characteristics closely match the requirements.

Decreasing ionic membrane resistance and reactant crossover have been major research efforts for cell performance and life improvement. Recent advances in membrane technology have been reported by Ling and Charleston of the National Aeronautics and Space Administration.[58] The membranes investigated were made by Ionics, Inc., and are based on variations of a copolymer of vinylbenzyl-chloride and dimethylaminoethyl methacrylate (CD1L series). The best of the membranes examined showed a marked resistance to surface fouling. The area resistivity with Fe^{+3} flowing on both sides of the membrane was:

- o 3.6 Ω-cm^2 in 1.0M HCl
- o 3.9 Ω-cm^2 in 0.5M Fe^{+3}
- o 5.4 Ω-cm^2 in 1.0M Fe^{+3}
- o 10.3 Ω-cm^2 in 1.5M Fe^{+3}

All iron solutions contained 1.0M HCl. It was also shown that the surface fouling was primarily due to the ferric ion which forms complexes with the chloride ion present. Figure 42 shows the estimate of the effect on battery capacity of crossover of iron ions. The curve is based on measurements and the equation for the rate of crossover.

Average Current Density: 50 asf
Membrane Diffusion Parameter: 20 μgm Fe/hr/cm^2/M/1
Storage Time: 50 Hrs

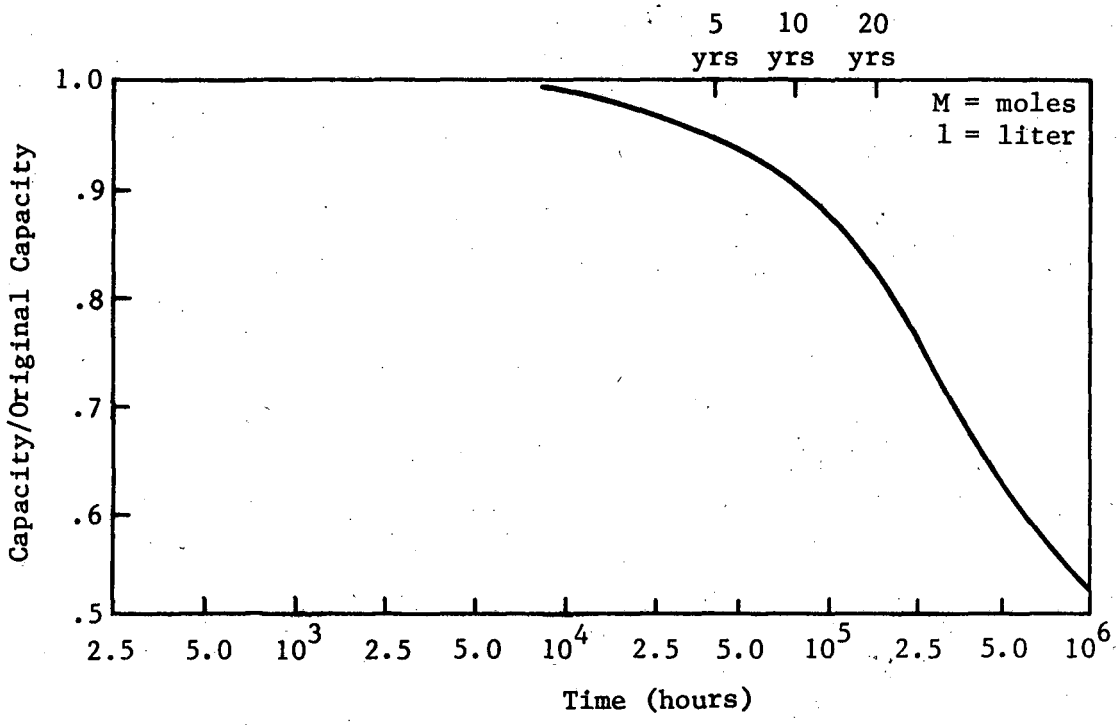

Source: Reference 58.

FIGURE 42
CAPACITY RETENTION ESTIMATE FOR NASA REDOX SYSTEM

The study of pumping losses in NASA redox cells has shown that these are derived from two sources:[59]

- Interelectrode spacing; and
- Compression of the carbon felt structure which forms part of the electrode.

It was estimated that the pumping power losses constitute less than 5% of the overall parasitic losses in the system.

Gahn and Thaller have reported on an accelerated test of the gold and lead catalyzed positive electrode, which they consider to be cell life determining.[60] The basic assumption of this accelerated test was that the voltage swings taking place during the course of the discharge are more important than the ampere-hour capacity of the fluids that are being discharged. This enables the use of short duration testing. The testing was carried out automatically using approximately 100 rapid cycles per day. The hydrogen evolution tendency of the negative plate, which is a measure of the catalyst condition, was determined. Cell current voltage characteristics were checked after 500 rapid cycles. The electrodes were tested for 20,000 rapid cycles, with anolyte and catholyte changed every 2,000 cycles to avoid the possible effects of cross-over. This test was equivalent to one cycle per day for 50 years. Using the same electrode and flowing solutions, another 3,000 cycles between 10 and 90% depth-of-discharge (DOD) were obtained. At that time the hydrogen evolution rose sharply, leading

to ampere-hour efficiencies of 90 to 95% and the test was terminated. The reliability of these tests as predictive tools is still to be established.

The efforts to date show a continuing improvement in the performance of the redox cell. The scale-up of the redox batteries and their evaluation in solar photovoltaic systems is planned.

4.2 Lithium-Alloy/Iron-Sulfide Battery

Research and development on the lithium-alloy/iron-sulfide battery is under the technical management of the Argonne National Laboratory (ANL). The organization of the program is shown in Figure 43. The status of battery research and development, as of the third BECC, was described in SR-II. The current performance goals for the lithium-alloy/iron-sulfide electric vehicle (EV) battery are shown in Table XXV. Although stationary batteries for distributed energy systems are an objective of the program, current developmental effort is focused on the EV battery. The research and development for the Mark II battery emphasizes:

- Improved cycle life;
- Demonstration of cell reliability; and
- Building and testing 10-cell battery modules based on demonstrated cell improvements.

The following sections discuss the status of the technology for the Mark II battery and the results of research on cell chemistry and cell components.

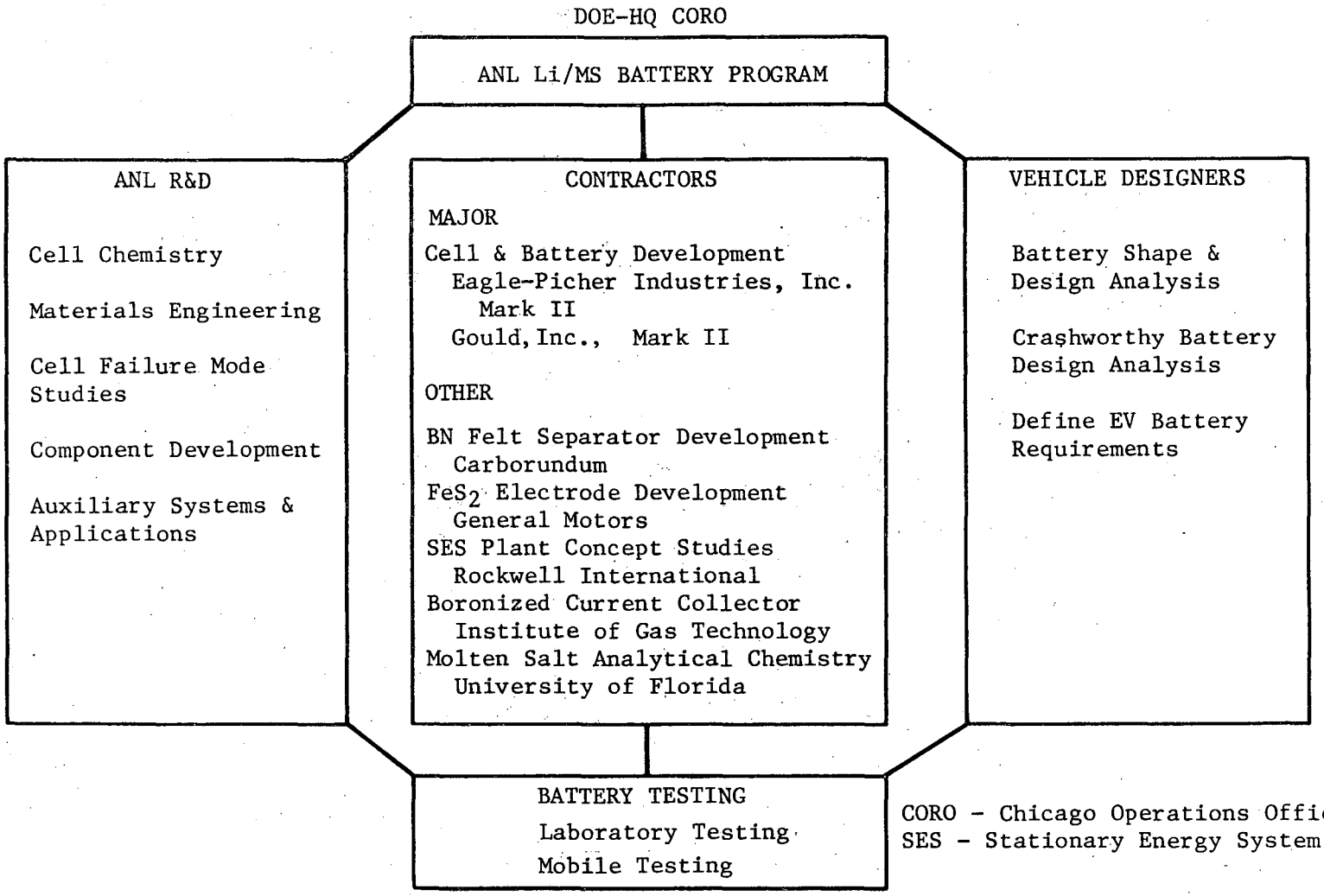

Source: Argonne National Laboratory.

FIGURE 43
LITHIUM-ALLOY/IRON-SULFIDE BATTERY PROGRAM ORGANIZATION

TABLE XXV

PROGRAM GOALS FOR THE LITHIUM-ALLOY/IRON-SULFIDE ELECTRIC VEHICLE BATTERY

	Mark II	Mark III
	FeS	FeS_2
Specific Energy (Wh/kg)		
Cell (average)[a]	125	160
Battery	100	130
Energy Density (Wh/l)		
Cell (average)	300	400
Battery	150	200
Peak Power (W/kg)[b]		
Cell	185	320
Battery	150	260
Jacket Heat Loss (W)[c]	75-150	75-150
Lifetime		
Deep Discharges	500	1,000

[a]For a 4-hr discharge rate (120 mile range on J227 a/D cycle).

[b]Peak power sustainable for up to 30 secs at 0 to 50% of battery discharge; at 80% discharge, peak power is to be 70% of value shown.

[c]Heat loss to be optimized based upon vehicle duty cycle.

Source: Argonne National Laboratory.

4.2.1 Lithium-Alloy/Iron-Sulfide Cell and Battery Studies

The failure of one of the two modules of the Mark IA EV battery, reported in SR-II, led to a concerted effort to better understand the causes of cell failure. Both the failed and unfailed modules were subjected to a detailed examination and the failure was attributed to leakage of electrolyte, which resulted in short circuits among the cells and between the cells and the cell tray. Battles et al. have described the facilities developed at ANL for post-test examination and failure analysis of Li-Al/FeS_x cells.[62]

Post-test examinations were conducted at ANL on 46 multiplate cells and 47 bicells. The major cause of failure for the cells tested was extrusion of active material from the electrodes which results in a short circuit. This indicated a need for strengthening the electrode structures.

Cell swelling, which requires that the cells be restrained mechanically during cycling, was found to be caused by gas pressure and electrode expansion. The gas pressure effects were minimized by modifying the cell filling procedure. Studies are continuing on the effect of electrode loading and other factors on cell swelling.

The diagnosis of Mark IA modules formed part of the input to the design and testing of cells for the Mark II battery. To measure the progress in meeting the Mark II performance goals, the Status Cell Program was instituted. The program consists of testing groups of 12 identical status cells fabricated by ANL, Eagle Picher, and

Gould. The ultimate goal of the test of the status cells is to predict cell reliability. The results of the tests are to be analyzed using statistical analysis in order to predict the cycle life of the cells.

At the time of the fourth BECC, five groups of Mark II status cells had been tested. The distribution of the test results of 12 ANL cells included in the status cell studies is shown in Figure 44. Table XXVI lists the results of the statistical analysis of the cells examined. Mark II status cells with specific energies of 92 to 99Wh/kg and with peak specific powers ranging from 55 to 100W/kg were reported. These are below the Mark II goals of 125Wh/kg and 185W/kg for specific energy and specific power, respectively. However, ANL reported the fabrication of an experimental multiplate cell with a specific power of 192W/kg at 50% state-of-charge (SOC). The specific energy and cycle life of this cell were not given. Another reported accomplishment was a decrease in the rate of capacity loss from 0.3%/cycle to 0.03%/cycle.

The main goals of the Eagle Picher Mark II development program were:

- The incorporation of boron nitride (BN) felt into the cell design;
- Elimination of material extrusion from the electrodes;
- Reduction/elimination of capacity fade;
- Increased cycle life; and
- Delivery of a 10-cell module to ANL.

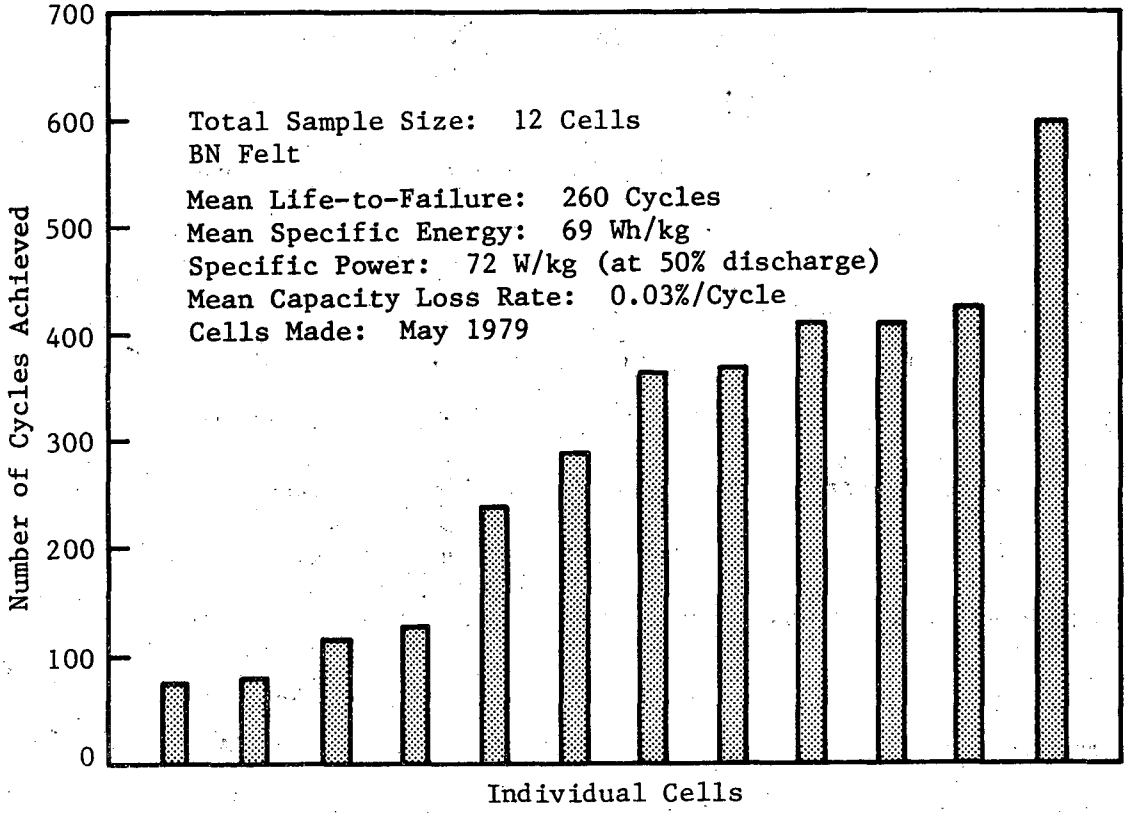

End of life defined by 20% loss of capacity or 5% loss of coulombic efficiency.

Source: Argonne National Laboratory.

FIGURE 44
LIFE TEST, ANL MARK II STATUS BICELLS

TABLE XXVI

STATISTICS FOR POPULATION BASED ON SAMPLING OF LITHIUM-ALLOY/FERROUS-SULFIDE CELLS

Designation of Cells in Sample	Number of Cells in Sample	Weibull Slope (90% confidence)		Mean Life to Failure (cycles)[b]		Cycles at Which Indicated Failures May Occur[b]					
						5%		10%		20%	
		Low	High	Low	High	Low	High	Low	High	Low	High
EPI Group III Status Cells	12	0.7	2.1	197	525	11	147	22	205	50	285
EPI Group I Development Cells	14	2.0	3.8	295	510	95	280	130	330	180	390
Gould Mark II (Bn felt type) Status Cells (Group 0)	12	1.8	3.8	58	106	19	60	26	70	36	82
ANL Mark II Status Bicells	12	1.0	2.2	171	425	15	122	36	180	64	243

[a] Cycle life data were analyzed using the Weibull distribution and suspended testing approach.
[b] Confidence level of 95%.

EPI = Eagle-Picher, Inc.
ANL = Argonne National Laboratory.

To accomplish the above, Eagle Picher fabricated and tested successive iterations of cell designs. This involved the fabrication and testing of approximately 150 cells, including 1 cell that achieved 900 cycles. This effort resulted in a 10-cell, 4kWh module which was delivered to ANL for testing. The testing was initiated shortly before the BECC and only 10 cycles had been completed at that time.

During the past year, the Gould program has developed a new design concept for the rechargeable Li/MS system. The change resulted from the poor cycle life of the Gould Group 0 status cells (see Table XXVI), which were of the conventional boron-nitride separator-flooded electrolyte design. These cells, like previous BN separator cells, failed due to shorting caused by one of the following:

- The positive FeS electrode has negligible mechanical strength when operated in a flooded electrolyte condition. Therefore, the volume changes which occur in the electrode during cycling result in extrusion of electrode material through openings in the particle retainer system, causing internal shorting.
- The negative electrode grows during repeated cycling and develops protrusions which, despite the use of a particle retainer system, penetrate the fragile BN felt separator and cause shorting.
- The electrolyte creeps up into the positive feedthrough seal with time and results in a short between the positive terminal and cell container which is at negative potential.

The new design concept utilizes a magnesium oxide powder separator operated in an immobilized electrolyte condition. This

new design evolved from earlier work at Gould on the development of a thermal battery. The advantages envisioned for the powder separator-immobilized electrolyte design are as follows:

- Improved mechanical stability of the electrodes and separator during cycling.
- Elimination of the expensive honeycomb electrode support structure.
- Simplified cell fabrication; electrodes and separator layers can be pressed at room temperature in a dry room environment and the electrolyte vacuum fill step is eliminated.
- Increased specific energy by the use of more energetic active materials for the negative electrode.
- Operation independent of cell orientation.
- Reduction in the separator cost, from about $1,600/kWh for BN felt to about $1/kWh for magnesia powder.

Because of the success of the pressed ceramic powder separator-immobilized electrolyte and anticipated improvements, it was logical to evaluate this approach in the rechargeable Li/MS system.

Performance data from approximately 70 200Ah engineering cells of this new design have been most encouraging with some cells achieving 300 to 400 deep discharge cycles. A group of 10 identical cells completed over 170 cycles without any failures. A cell design producing 100Wh/kg has also been demonstrated.

In addition to the engineering size cell work at Gould, a 6Ah cylindrical pellet cell containing a reference electrode (see Figure

45) has been developed to characterize the performance of the individual electrodes in relation to their chemical composition and physical parameters. This is proving to be a valuable tool in guiding design improvements. Figure 46 is representative of the data from a 6Ah Li-Al/FeS pellet cell with an MgO powder separator; it shows the effect of current density (discharge rate) on the positive electrode utilization. This cell also had an excess of negative electrode capacity.

Additional studies on MgO powder separators are discussed in Section 4.2.2; however, there are major differences between the two systems. The Gould technology is based on a pressed high surface area magnesia powder layer operating in a starved electrolyte environment. On the other hand, the Rockwell studies were conducted on a vibratory loaded, sieve-size, magnesia powder layer operated in a flooded electrolyte condition. Consequently, results from the two systems are markedly different.

Kaun et al. of ANL have investigated the effect of excess negative capacity on the rate of capacity decline.[63] It was shown that as the negative:positive capacity ratio increased, the rate of capacity decline decreased. Similar results were obtained when "D" cells with a negative:positive capacity ratio of 1.1:1 operated below their rated capacity of 420Ah. This is shown in Figure 47. The cell, designated EPRE-2, had a negative:positive capacity ratio of 3, whereas the Mark IA design has a ratio of 1.

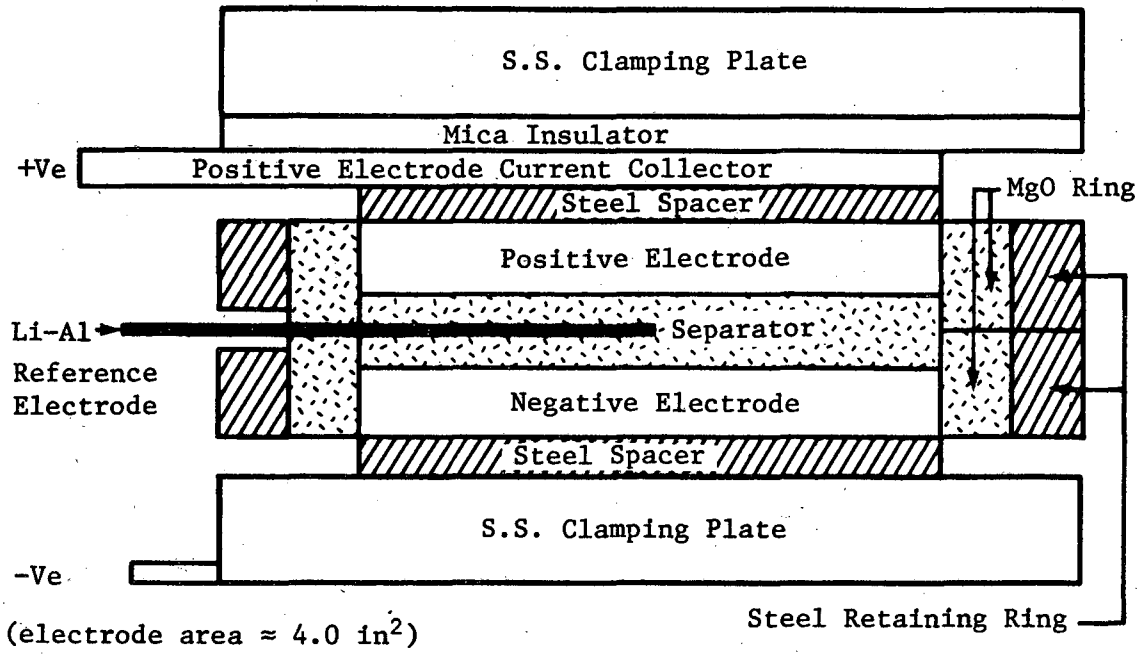

Source: Gould.

FIGURE 45
PELLET BICELL FOR REFERENCE ELECTRODE STUDIES

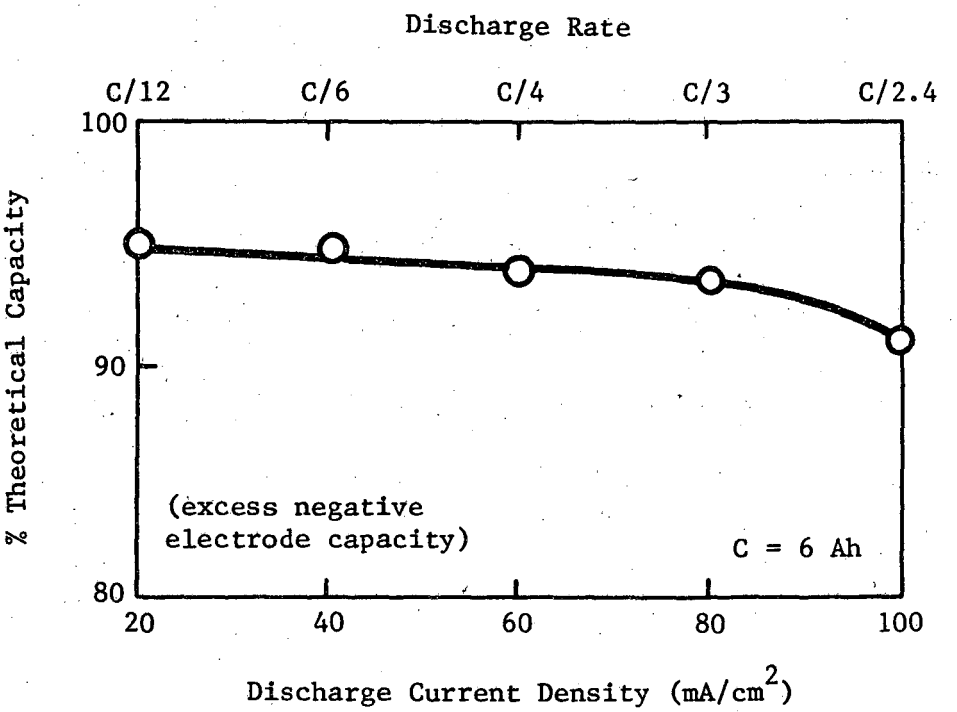

Source: Gould.

FIGURE 46
EFFECT OF CURRENT DENSITY OF THE CAPACITY OF A MAGNESIUM OXIDE SEPARATOR CELL

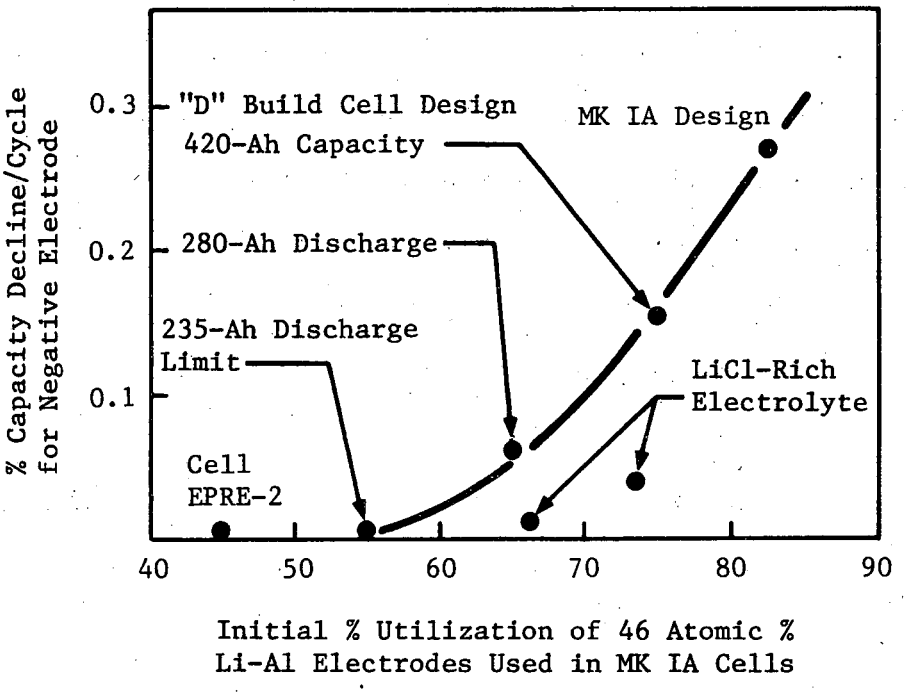

Source: Argonne National Laboratory.

FIGURE 47
LITHIUM-ALLOY ELECTRODE CAPACITY STABILITY TEST

Farahat and coworkers at ANL have investigated the feasibility of rapidly recharging the Li-Al/FeS battery. Two different full-scale EV-battery cells were charged at high rates and the heat generation rate was determined.[64] The charge replacement varied from 32% in 0.3 hours using a 200A current to 93% in 2.6 hours using a 100A current for batteries with standard capacities of 200 and 285Ah, respectively. The heat generation rate during the 200A charge was 16W and during the 100A charge was 7W. These were less than the heat generation rates during discharge. These and the other data obtained showed that these cells could be operated at high rates of charge without thermal overload.

All the battery systems to be used in EVs and stationary energy storage systems require thermal control. Figure 48 shows the relationship between specific energy and the adiabatic temperature rise that would occur if all the battery energy were converted to heat, as in the case of a short circuit. Thus, high specific energy batteries such as lithium-alloy/iron-sulfide have larger thermal balance problems. In addition to the control of the heat generated, in the case of high temperature batteries, heat loss must be prevented during idle and standby to avoid solidification of the electrolyte.

Heat generation in the cell has been mainly attributed to two factors:

- Cell overpotential (irreversible heat generation); and
- Entropy change (reversible heat generation).

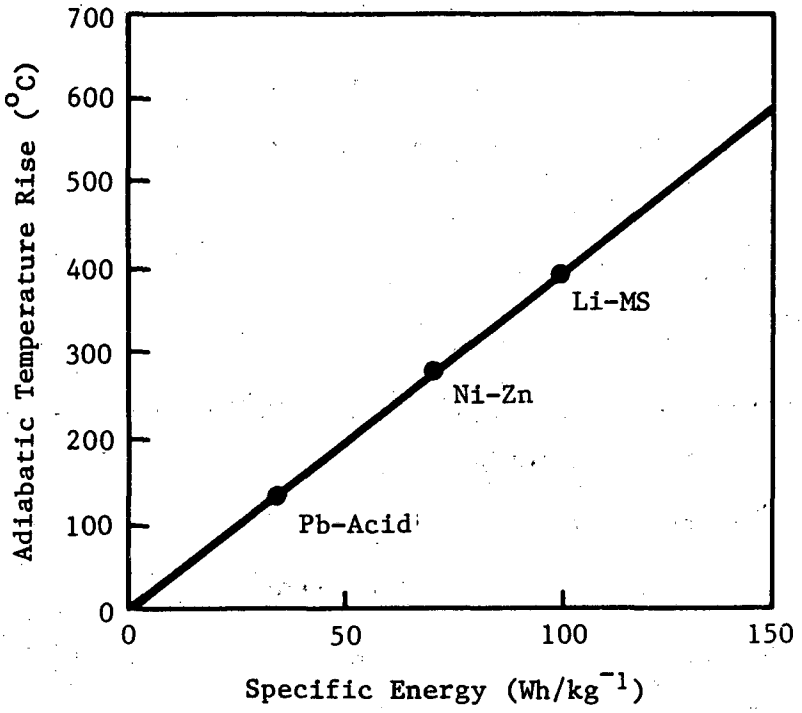

Source: Gould.

FIGURE 48
DEPENDENCE OF ADIABATIC TEMPERATURE RISE ON SPECIFIC ENERGY OF SYSTEM

The heat generation is the sum of these; the effect of overpotential is always exothermic while the entropy will have one sign on charge and the opposite sign on discharge.[65] The average rate of heat generation, $\dot{Q}$, is due to these and other lesser effects, is shown in Figure 49. The discharge rate was 70A (C/4) and the charge rate was 40A (C/7) for a 280Ah cell. To be noted is the marked increase in the heat generation rate after 200Ah of discharge. The results of measured heat loss showed good agreement, within about 1.3% or 6°C, of the values calculated based on a heat loss model for the cell.

Gibbard and coworkers at Gould have determined the thermal energy generation by Li-Al/FeS batteries indirectly and directly.[66] The indirect method consisted of thermodynamic calculations based on the combined use of precise measurements of the cell potential as a function of temperature and SOC and measurements of cell voltage during discharge at various constant current drains. Direct measurements of heat generation were made in a specially designed isothermal-conduction battery calorimeter. Results from the two approaches were in agreement.

The effective thermal conductivity of the battery was determined using a discharged battery which was heavily insulated on all sides, except the ends parallel to the plates. The cell, first heated to a uniform temperature, was subjected to heating on one of the two non-insulated faces and the time-dependent temperature

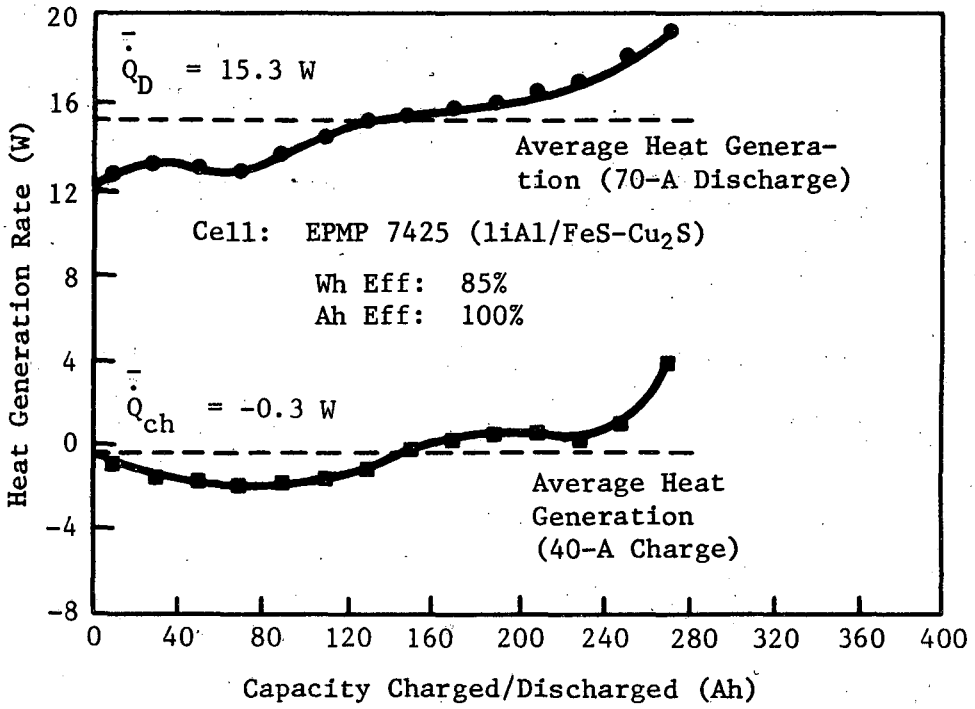

Source: Reference 65.

FIGURE 49
LITHIUM-ALLOY/IRON SULFIDE CELL HEAT GENERATION RATE DURING CYCLING

profiles were measured at the cell center and its surface. From the measurement of the thermal diffusivity, the mean density of the cell, and the cell heat capacity, the thermal conductivity was calculated. The experimentally determined thermal conductivity was of an order of magnitude less than that estimated based on the fresh constituent materials. Although the reasons for this are not understood, some possible sources of this discrepancy are the existence of void volume in the cell due to the porous mixture of the materials used, changes in properties resulting from changes in the discharged-shorted cell, and contact resistances between cell components.

Based on the thermal studies, the Gould workers concluded that, when a full-scale Li-Al/FeS battery of 100 cells is discharged, the average rate of heat loss will be 1.5W/cell and the battery temperature will rise from 450°C to 500°C during a 50A discharge.

Attempts to control the temperature of a 2.5kWh battery, consisting of 10 200Wh cells, by direct air cooling showed this method may be inadequate for a full size EV battery. Although the average battery temperature dropped about 20°C after 30 minutes of cooling, the temperature gradient in the battery increased by about a factor of three, from a maximum temperature difference of 5°C to 15°C. This indicates a need for the use of more direct means of cell cooling to control the temperature of large batteries.[67]

4.2.2 Lithium-Alloy/Ferrous-Sulfide Cell Research and Component Studies

The agglomeration of Li-Al electrodes is considered as a possible cause for the loss in negative electrode capacity with cycling. To determine some of the factors leading to agglomeration Fisher and Vissers of ANL constructed an $\alpha+\beta$ Li-Al/LiCl-KCl eutectic/Al cell.[68] The reference electrode was $\alpha+\beta$ Li-Al. The cell was operated at 450°C using a current density of 48 mA/cm^2 and a cut-off voltage of 0.2 volts in both directions. The cell was cycled for 1 week.

During cycling the capacity of the Li-Al electrode declined showing that the loss of capacity was not due to the iron sulfide electrode of the Li-Al/FeS cell. It was further observed that polarization of the negative electrode occurs more rapidly during discharge than charge.

Examination of Li-Al electrodes from engineering cells using iodine vapor etching showed a structure with prominently aligned pores. This indicated pore localization along grain boundaries as a result of agglomeration. Cadmium and magnesium were added to the Li-Al electrode as possible agglomeration inhibitors. Neither was effective.

It has been observed that the corrosion of positive current collectors can limit the life of the Li-Al/FeS cells. Bicells were constructed for the examination of positive current collector corrosion.[69] These cells were cycled at the 4-hour discharge rate and with discharges simulating the urban driving cycle. An

8-hour charge rate was used. Both carbon steel and nickel current collectors were used. These two materials showed excellent corrosion resistance over the test period. The unexpectedly low corrosion was explained as due to the passivation of the low carbon steel electrode by sulfidation leading to a thin film of J Phase ($LiK_6Fe_{24}S_{26}Cl$), X phase (Li_2FeS_2), or FeS on the steel.

Metallographic studies of the nickel current collector showed that a film of iron deposited on the nickel surface caused the passivation of the nickel. Because of the passivation, both the low carbon steel and nickel electrodes were judged to be satisfactory as current collectors.

Braunstein et al. have conducted experiments to examine their earlier prediction of composition gradients induced in the molten salt electrolyte during battery operation (see SR-II). The Li-Al/FeS cell was rapidly quenched after cycling to minimize convective transport of the electrolyte.[70] The distribution of Li and K across the cell was determined by sectioning the solidified electrolyte and the retaining material, followed by analysis of the Li:K ratio in the sections. It was shown that the mol fraction of potassium at the cathode was greater than that at the anode. The observed composition changes were consistent with the predictions of the model.

Sudar and coworkers at Rockwell International are investigating improved separator materials. It had been previously reported[2]

that lithium tetrachloroaluminate ($LiAlCl_4$) acted as a wetting agent for the boron nitride (BN) felt. The work at Rockwell has shown that the incorporation of submicron magnesium oxide (MgO) into the BN felt had advantages. Concentrations of 3 to 20 mg of MgO per cm^2 of felt were found to be effective. The inclusion of MgO gave a separator with greater stability than with the addition of LiAlCl . Moreover, the additive concentration required was less critical in the case of MgO.

Sudar and coworkers have also investigated the use of MgO powder as a replacement for the BN felt separator (see Section 4.2.1 for other MgO separator work at Gould). It was found that an MgO particle density of greater than 50% of MgO solid density was required for successful cell operation. The preferred particle size range was approximately 100 to 200 mesh with close control of the particle size range necessary. Both larger and smaller particle sizes were found to be less satisfactory. Tests also showed that 96% pure commercial MgO was satisfactory. Figure 50 compares the utilization of the FeS in cells with MgO or BN felt separators. It was concluded that the MgO separator was satisfactory for utility applications but the BN felt was superior for EV applications.

Efforts to reduce the cost of producing BN felt separators are continuing at the Carborundum Division of the Kennecott Corporation. Commercial papermaking/felt forming technology is being adapted to BN felt preparation. A slurry of BN and B_2O_3

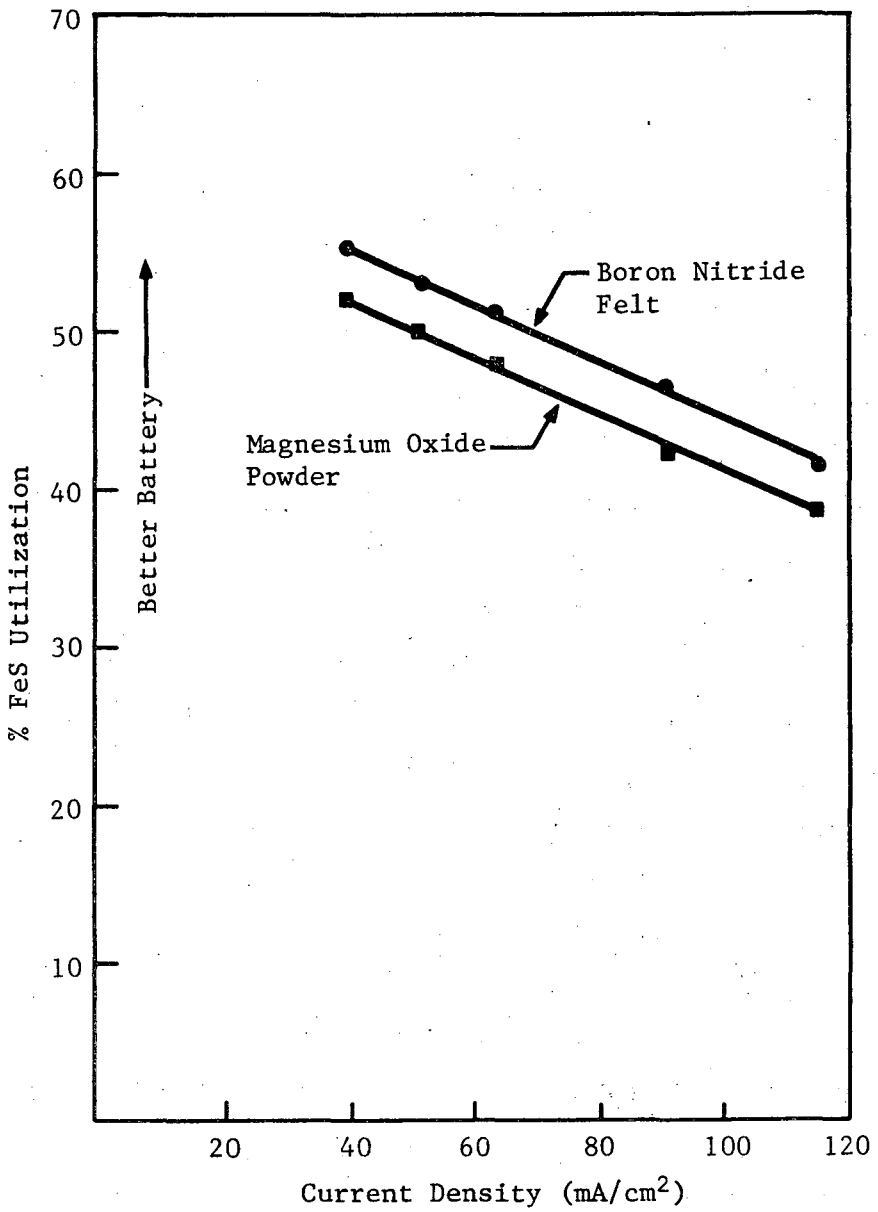

Source: Rockwell.

FIGURE 50
COMPARISON OF BORON NITRIDE AND MAGNESIUM OXIDE SEPARATORS

in a nonaqueous carrier and higher temperatures than those used in papermaking are required for processing the ceramic fiber system. Following formation of the BN/B_2O_3 felt, it is converted to BN by nitriding with ammonia.

Pollard and Newman have developed a set of governing differential equations for the description of the discharge behavior of the Li-Al/LiCl-KCl/FeS cell.[71] These equations have been modified to study the changes taking place in the cell during relaxation and charge.[72] Composition profiles across the cell after current interruption at the end of the discharge have been calculated. At the negative electrode, the back becomes cathodic with respect to the front establishing local concentration cells:

$$\text{Li-Al} \rightleftharpoons \text{Li}^+ + \text{Al} + e^-$$

These concentration cells promote a uniform electrolyte composition but accentuate the nonuniform utilization of reactants. At the positive electrode adjacent to the current collector, the FeS reacts with lithium ions, and, near the front of the electrode, Li_2S reacts anodically with the iron. Heat is not generated during cell relaxation and the cooling of the cell can lead to electrolyte precipitation.

During charge, the region of the negative electrode closest to the electrode/separator interface is recharged first and the reaction front moves back through the electrode reconverting the alloy to Li-Al. Relaxation of the electrolyte composition during

stand between discharge and charge results in a greater nonuniformity in the utilization of reactants compared with no relaxation between discharge and charge. At the positive electrode, in both the relaxed and unrelaxed cases, a sharp reaction front moves through the electrode, consuming the Li_2FeS_2 formed during discharge.

The above conclusions are sensitive to the heat balance in the cell. This suggests a need for precise thermal management of Li-Al/FeS battery modules. The non-uniformity in the utilization of negative electrode reactants agrees with observations on the morphological changes in the Li-Al electrode on cycling.

Nowobilski and coworkers have continued their efforts on the development of light-weight vacuum insulation with good load-bearing capability (15 psi plus battery loading). The goal is a rectangular enclosure 0.91 m long x .46 m wide x .41 m high. Three types of insulation construction, shown in Figure 51, have been investigated. Table XXVII compares insulation characteristics of the three types of construction. Both the peg-supported multifoil and the Linde IDLAS insulation fulfill the heat loss goal and the density goal of 288 kg/m^3 (18 lb/ft^3) for Mark II and Mark III batteries.

4.2.3 Lithium-Alloy/Ferric-Sulfide Cells

The Li-Al/FeS_2 cell had been considered early in the studies of the Li-alloy/FeS_x system as the one with the potential for the

- Compressed Multi-Layer

  Load Carried Over Total Area

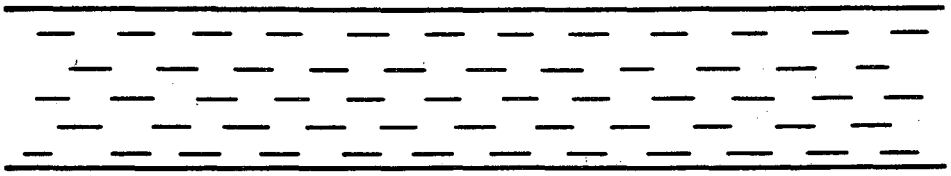

- Peg-Supported Super Insulation

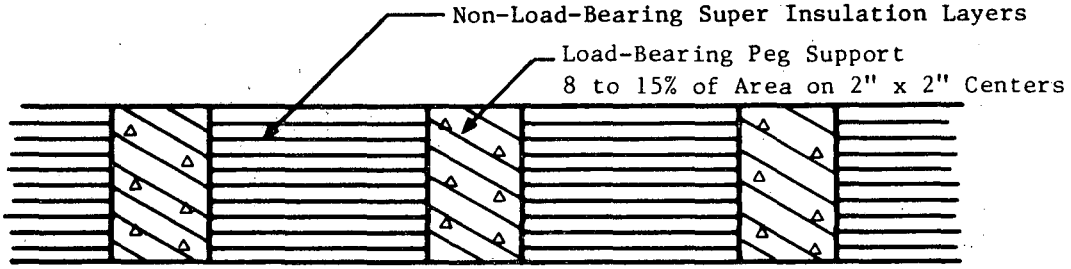

- Linde IDLAS Insulation

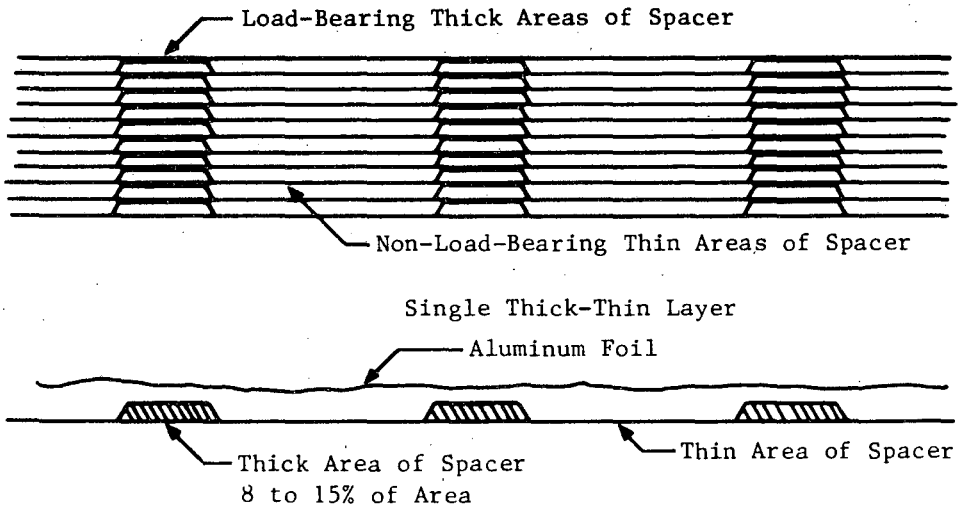

Source: Linde Division, Union Carbide.

FIGURE 51
INSULATION CONSTRUCTION

TABLE XXVII

LOAD-BEARING INSULATION COMPARISON

Insulation Type	1979 Program: Thermal Conductivity X 10^{-5} Btu/hr-ft-^{0}F (W/m-^{0}K) Th=850^{0}F TC=75^{0}F 454^{0}C 24^{0}C	1979 Program: Density lbs/ft^3 (kgs/m^3)	1980 Program: Thermal Conductivity X 10^{-5} Btu/hr-ft-^{0}F (W/m-^{0}K) Th=850^{0}F TC=75^{0}F 454^{0}C 24^{0}C	1980 Program: Density lbs/ft^3 (kgs/m^3)	Projected 1981 Program: Thermal Conductivity X 10^{-5} Btu/hr-ft-^{0}F (W/m-^{0}K) Th=850^{0}F Tc=75^{0}F 454^{0}C 24^{0}C	Projected 1981 Program: Density lbs/ft^3 (kgs/m^3)
Glass Board	224 (.00038)	22 (352)	160 (.0027)	18 (288)	140 (.0024)	20 (320)
Peg-Supported	101 (.0017)	11 (176)	93 (.0016)	13 (208)	90 (.0015)	13 (208)
IDLAS	95 (.0016)	15 (240)	95 (.0016)	15 (240)	95 (.0016)	15 (240)
Commercial State of the Art Min-K 2000, Produced by John-Manville Co.	900 (.013)	20 (320)				

Calculated thermal conductivity required to meet heat loss and volume goals: Mark II 140 x 10^{-5} Btu/Hr-FT- F
Mark III 100 x 10^{-5} Btu/Hr-Ft- F

Th = high temperature.
Tc = cold temperature.

Source: Linde Division, Union Carbide.

best energy density characteristics. However, problems of finding inexpensive cathode current collectors and capacity loss led to emphasis on the Li-Al/FeS system to provide an advanced EV and dispersed storage system battery.

Dunning et al. have investigated the discharge behavior of the FeS_2 electrode as it is affected by construction variables, such as: electrode thickness, porosity, current collection, and electrolyte composition.[73] The small, 2 cm^2, test electrodes were prepared by hot pressing mixtures of Fe, Li_2S, FeS_2, electrolyte, and current collector at 27MPa and 325°C in a graphite die. Constant current discharges and a current limited (100 mA/cm^2) constant voltage (2.0 volts) charge were used. The following are some of the results in terms of the variables tested:

- Electrode thickness--At 400°C electrodes thinner than 2 mm would have higher specific energies; at 450°C the specific energy is maximum in electrodes in the range of 2.5 to 3.5 mm thick.

- Electrode porosity--Increasing the porosity of 3 mm electrodes from 30 to 50 v/o increased the utilization of active material in both voltage plateaus.

- Current collection--Performance was best with 3 to 4 v/o of conductive graphite powder. The electrodes showed a marked improvement at 450°C in the utilization of active material in the lower plateau region.

- Electrolyte composition--Three electrolyte compositions (53, 58, and 68 m/o LiCl-KCl) were investigated at 450°C. For 30 v/o porosity electrodes the rate of capacity loss in the upper plateau increased with LiCl content. The lower plateau had a much higher capacity utilization in LiCl-rich salts, reaching 85% at the 4 hour rate.

Overall, the utilization of the lower plateau was improved by the presence of the current collector and excess LiCl. The upper plateau was not as strongly affected by these factors.

Studies were also conducted at General Motors on the causes of capacity loss in the upper plateau region.[74] Variables included in the experiments were: electrolyte composition and volume, charging procedures, operating temperatures, additives to the FeS_2 electrode, and restricted cycle operations. The loss rate of the positive upper plateau capacity and of active material was found to decrease with decreased electrolyte volume. The extent of loss was greater than could be accounted for by the solubility of Li_2S and it was concluded that a single mechanism did not suffice to explain the observations. The loss rate was inhibited by the presence of an excess of KCl in the electrolyte, but this also markedly decreased the lower plateau capacity. Studies are being continued to overcome the shortcomings in the performance of FeS_2 electrodes.

Earlier studies, briefly reviewed in SR-II, on phase relationships in positive electrodes of Li-Al/FeS cells have been extended by Tomczuk and coworkers at ANL to FeS_2 positive cells.[75] X-ray diffraction and metallographic examinations have been used to examine the phases and to supplement the data obtained by potential measurements. As reported in SR-II, the phases found in the cycling of Li-Al/LiCl-KCl eutetic/FeS cells were:

FeS, J($LiK_6Fe_{24}S_{26}Cl$), X (Li_2FeS_2), and Fe

The replacement of FeS by FeS_2 in the positive leads to a more complex situation. The phases found in the case of FeS_2 cycled in LiCl-KCl eutectic were:

FeS_2, $Li_3Fe_2S_4$, Y ($Li_7Fe_2S_6$), $Fe_{1-x}S$,

Li_2FeS_2, $KFeS_2$, J Phase, Li_2S, and Fe

Ceramic coated materials, as positive current collectors for the FeS_2 electrode, are being studied at ANL.[75] Static corrosion tests of metal nitrides, borides, and carbides were carried out in mixtures of FeS_2 and LiCl-KCl at 500°C. Both the isolated compounds and iron-based alloys coated with these compounds by chemical vapor deposition (CVD) were studied. CVD-TiC and -TiN coatings showed promise and were further tested in cells. Both monolithic TiN and TiN-coated AlSi type 304 stainless steel were completely stable in a Li-Al/FeS_2 cell after approximately 30 days of operation. Based on these results TiN and TiN-coated stainless steel were considered sufficiently promising for use in cell testing.

Sammells and coworkers are investigating the reaction of FeS_2 with iron borides FeB and Fe_2B. If these borides prove to be corrosion resistant, they will be tested in cells.

4.2.4 Overview of Lithium-Alloy/Iron-Sulfide Cells

The present effort to better understand the causes of inconsistent performance of Li-Al/FeS cells has led to improved and more uniform cycle life in the status test cells. Agglomeration of the negative electrode and the improved performance with a large

excess of negative electrode capacity indicate that the negative electrode is an important contributor to the observed loss of capacity on cycling. Improved cell design, which will avoid electrolyte loss and provide better intercell insulation will help in building batteries with the desired lifetime. The reported results on the use of MgO powder separators indicate that this will help in overcoming some of the earlier cycle life difficulties. The continued effort to obtain reproducible cell and module performance could permit the design and construction of battery units with the desired lifetime.

The development of the Li-Al/FeS_2 cell still requires materials development, especially for the positive electrode. The proof of satisfactory components and good cell cycle life are prerequisites to module battery design, construction, and testing.

4.3 Sodium/Sulfur Batteries

The two approaches to the sodium/sulfur cell by Ford Aerospace and Communications Company (FACC) and Dow were described in SR-I and SR-II. The essential features of the Ford cell are: sodium metal negative/β''-alumina ceramic electrolyte/sulfur cathode. The ceramic electrolyte acts as a sodium-ion conductor. The cell operates at 300 to 350°C, a temperature range at which both the sodium and sulfur are molten. The major problems have been the reproducible preparation of the β''alumina electrolyte and sealing between the negative and positive current collectors. These seals must be able

to withstand temperature cycling yet remain intact in spite of the differences in the coefficients of expansion of the current collectors and the insulating glass and ceramic seals. As of the third BECC, utility size β'' alumina tubes, 33 mm in diameter and 260 mm long, had been evaluated and shown to have sufficient reproducibility for module construction and testing. Higher reproducibilty was desired for battery production.

The features of the Mark II cell being developed for utility load-leveling are listed in Table XXVIII. Cell performance characteristics are listed in Table XXIX. Note that the achieved average performance of the 12 cells included exceeds the performance goals. The capacity retention of Mark II Na/S cells is shown in Figure 52. The reproducibility of the cells is shown in Figure 53 for a group of 64 cells.

One question which has been raised is that of safety of the Na/S battery in case of failure or accident leading to the direct reaction of the molten sodium and sulfur. To determine its safety, failures were induced in nine-cell groups by mechanical crushing, electrically inducing failures, exposing cells to open flame, drop tests, and drop tests plus exposure to flames. It was found that, on reaction after cell damage, a temperature rise of 100°C occurred. It was also shown that "dead" cells can be safely shorted. A schematic showing the fusing system for bypassing the

TABLE XXVIII

MARK-II SODIUM/SULFUR CELL FEATURES

Design:	Electrolyte: Li_2O - Stabilized β" Alumina 33 mm X 260 mm (OD X L)	
	Container: Chromium-Plated Stainless Steel	
	Sodium-Core, Vertical Orientation 2.0 kgs, 0.9 l, 54 mm (OD X 430 mm (L)	
Ratings:	135 Ah 225 Wh 75% Wh Eff 5-hr Discharge, 7-hr Charge Life: 10 yrs, 2,500 Cycles	End of Life
Features:	Radial Compression Ring Seal Simple Cylindrical Components Ambient Assembly and Storage Reactants Restricted for Safety	

Source: Ford Aerospace and Communications Company.

TABLE XXIX

MARK II SODIUM/SULFUR CELL PERFORMANCE

Cell Performance	Achieved[a]	Phase-IV Goals
Energy (Wh)	280	240
Efficiency (100 (Wh_o/Wh_i)%)	81	75
Capacity (Ah)	156	140
Utilization (% of theoretical capacity)	81.1	75
Specific Energy (Wh/kg)	140	120
Energy Density (Wh/l)	280	220

[a]12-Cell Average; 7-hr Charge, 5-hr discharge.

Wh_o = Wh discharge
Wh_i = Wh charge

Source: Ford Aerospace and Communications Company.

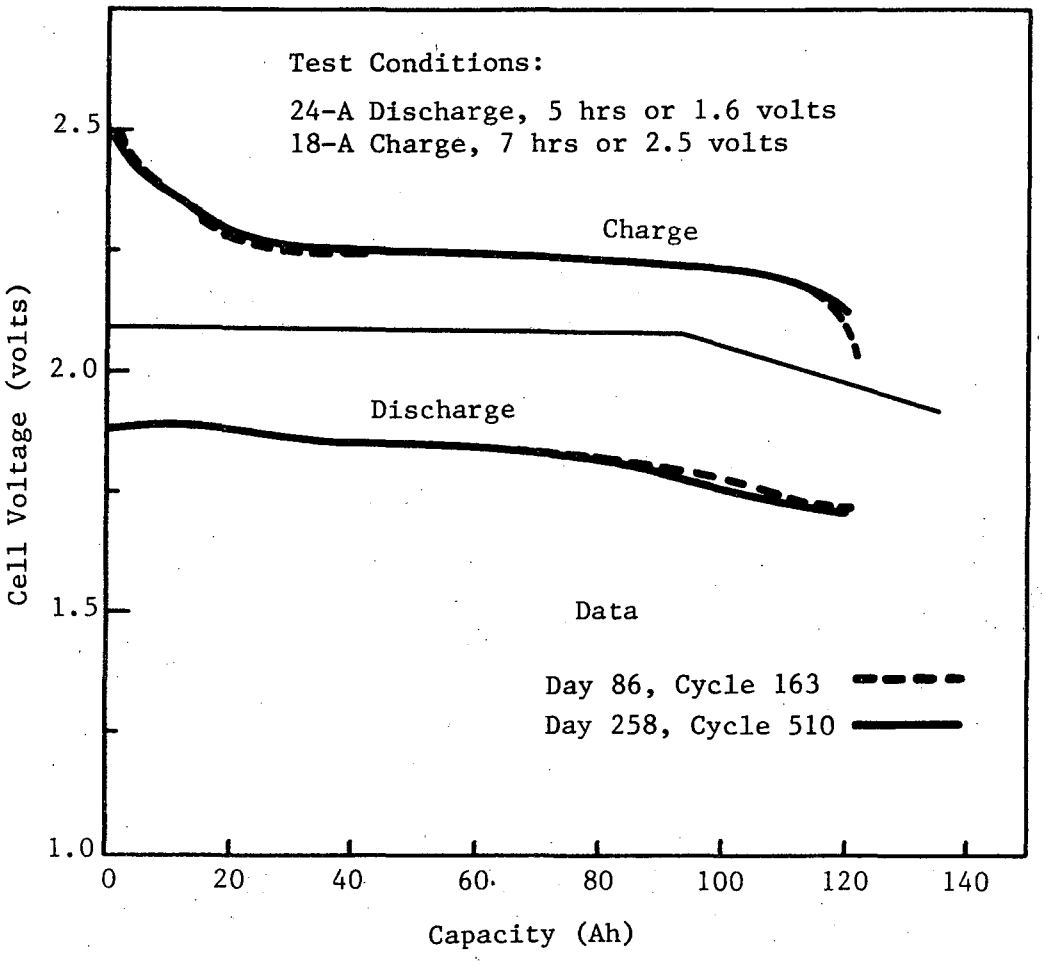

Source: Ford Aerospace and Communications Company.

FIGURE 52
MARK II SODIUM/SULFUR CAPACITY RETENTION

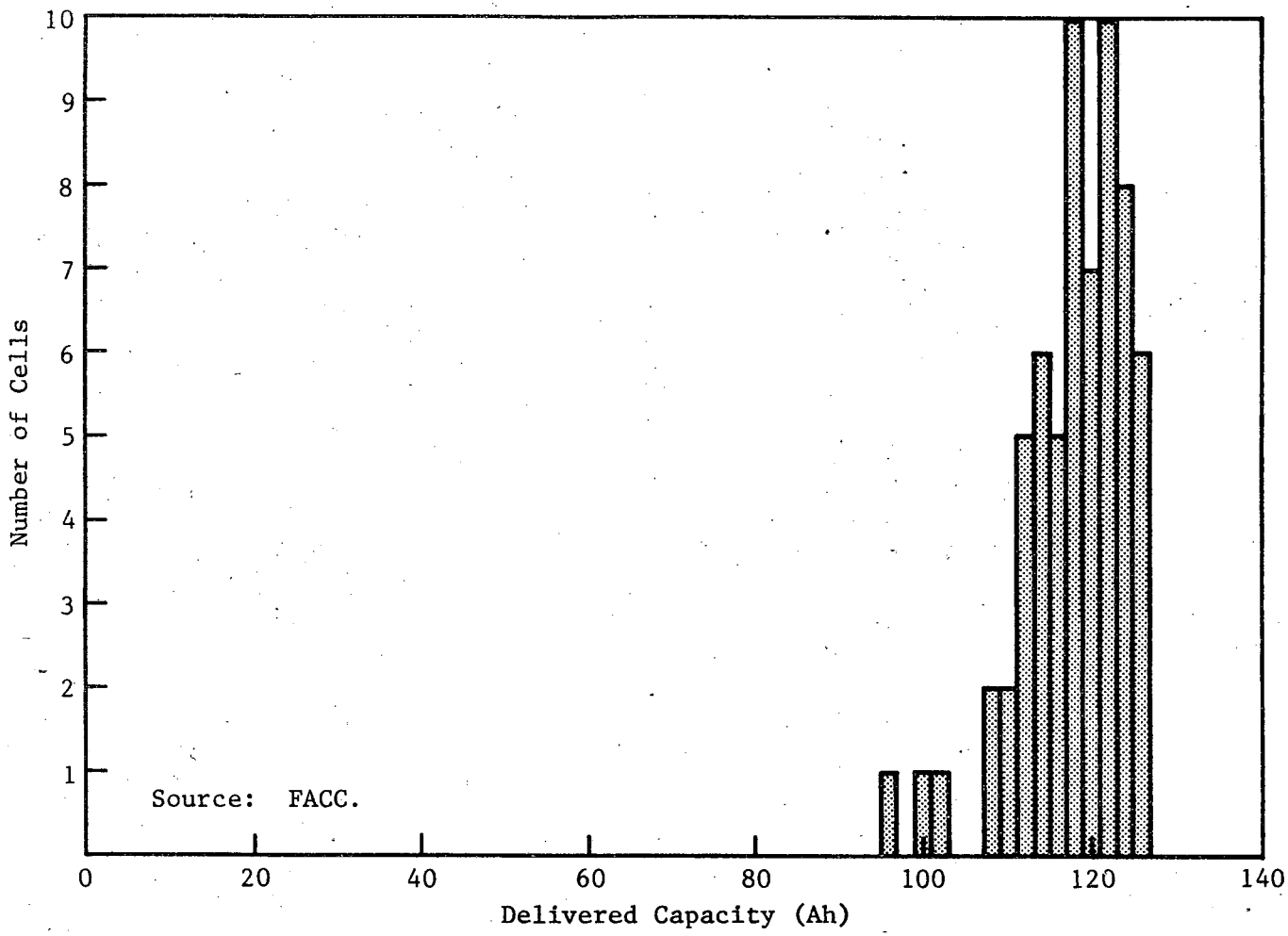

FIGURE 53
MARK II SODIUM/SULFUR CELL RESULTS REPRODUCIBILITY

dead cells is shown in Figure 54.[77] Failure of seals or case rupture rarely occurred during the induced failure tests.

A performance map of cells with various diameter-to-length ratios of the β"alumina tube is shown in Figure 55. The lower diameter:length aspect ratio tubes gave the higher powers. The cell capacity increased with the volume of the ceramic electrolyte tubes.

Figure 56 shows the performance of a 25kWh module for a load leveling battery. The actual capacities shown are in excess of those required to meet the design energy output. Four modules were assembled in series to construct a 100kWh battery which was operated. The battery demonstrated the design performance, safety, and maintenance features of the system.

Batteries have also been designed and tested for electric vehicles. The relative volumes and weights of various cell configurations considered for the EV application are shown in Figure 57. The multi-plate and concentric electrolyte configurations gave the lowest volumes and weights. An Na/S battery was assembled, using the load-leveling configuration, for demonstration in a battery powered truck. Table XXX provides a vehicle description and compares the performance characteristics of the Na/S and lead-acid battery.

Haskins and Domaszewicz have evaluated the sodium/sulfur battery for its application to solar systems.[77] The advanced high energy cell was used in the conceptual design of a 1MWh solar

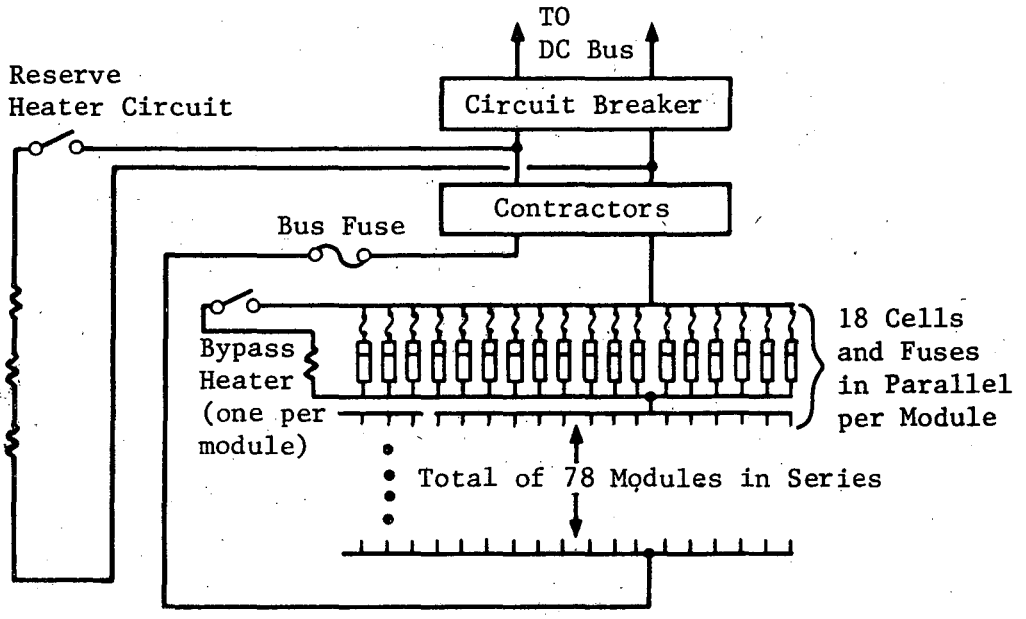

Source: Reference 77.

FIGURE 54
SIMPLIFIED BATTERY ELECTRICAL SCHEMATIC

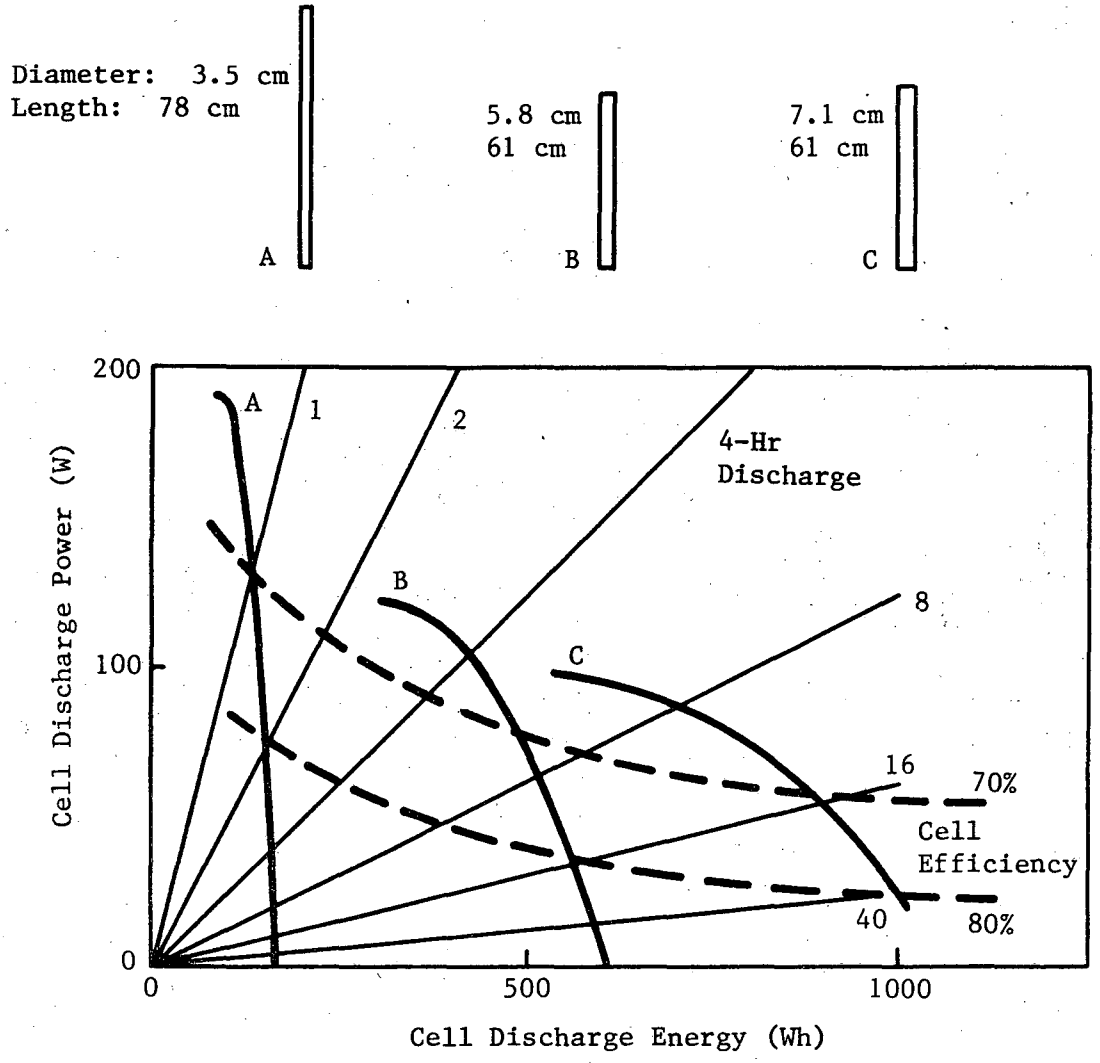

FIGURE 55
SODIUM/SULFUR CELL PERFORMANCE MAP

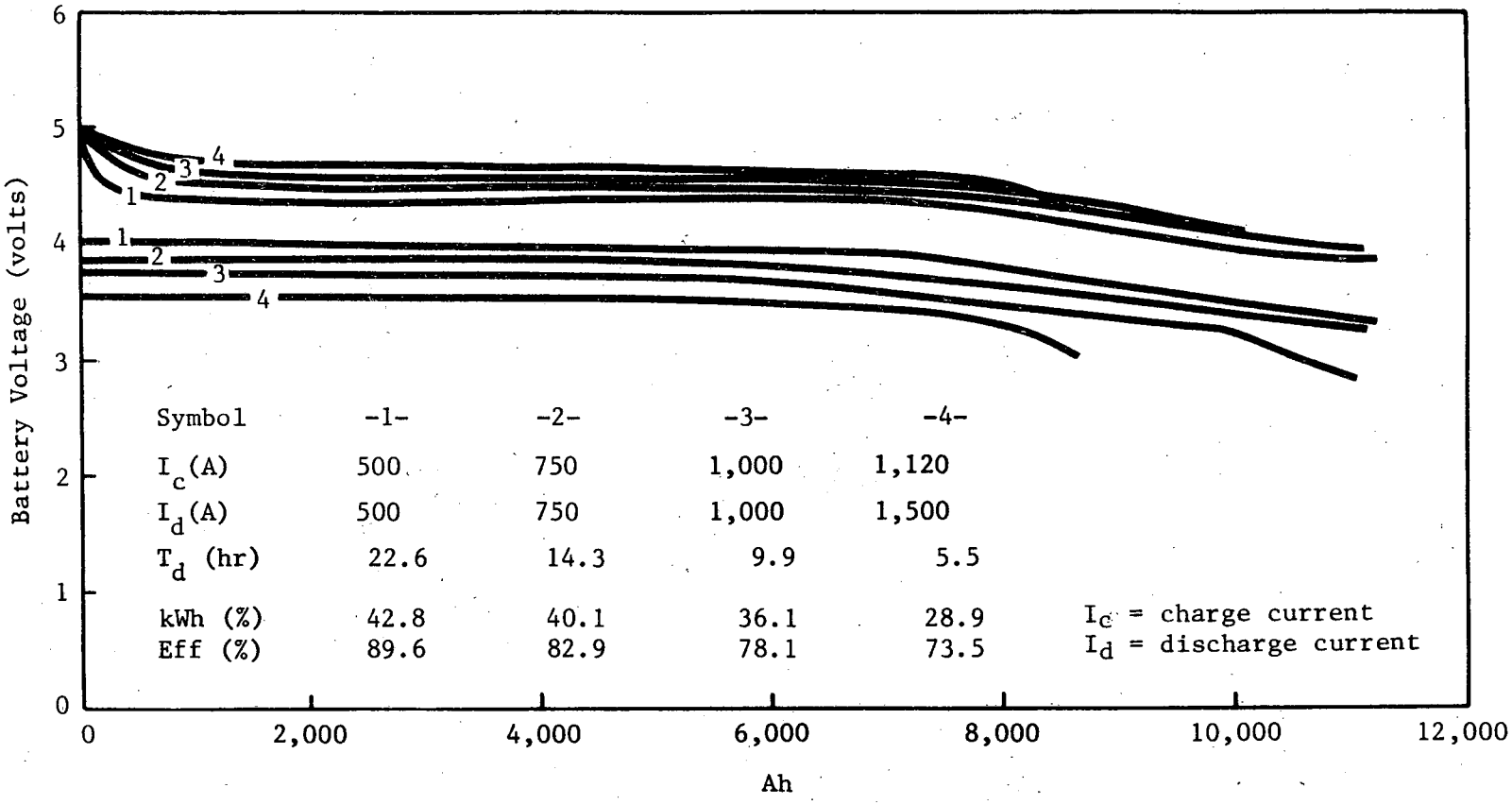

Source: Ford Aerospace and Communications Company.

FIGURE 56
PERFORMANCE OF A 25-kWh SODIUM/SULFUR MODULE

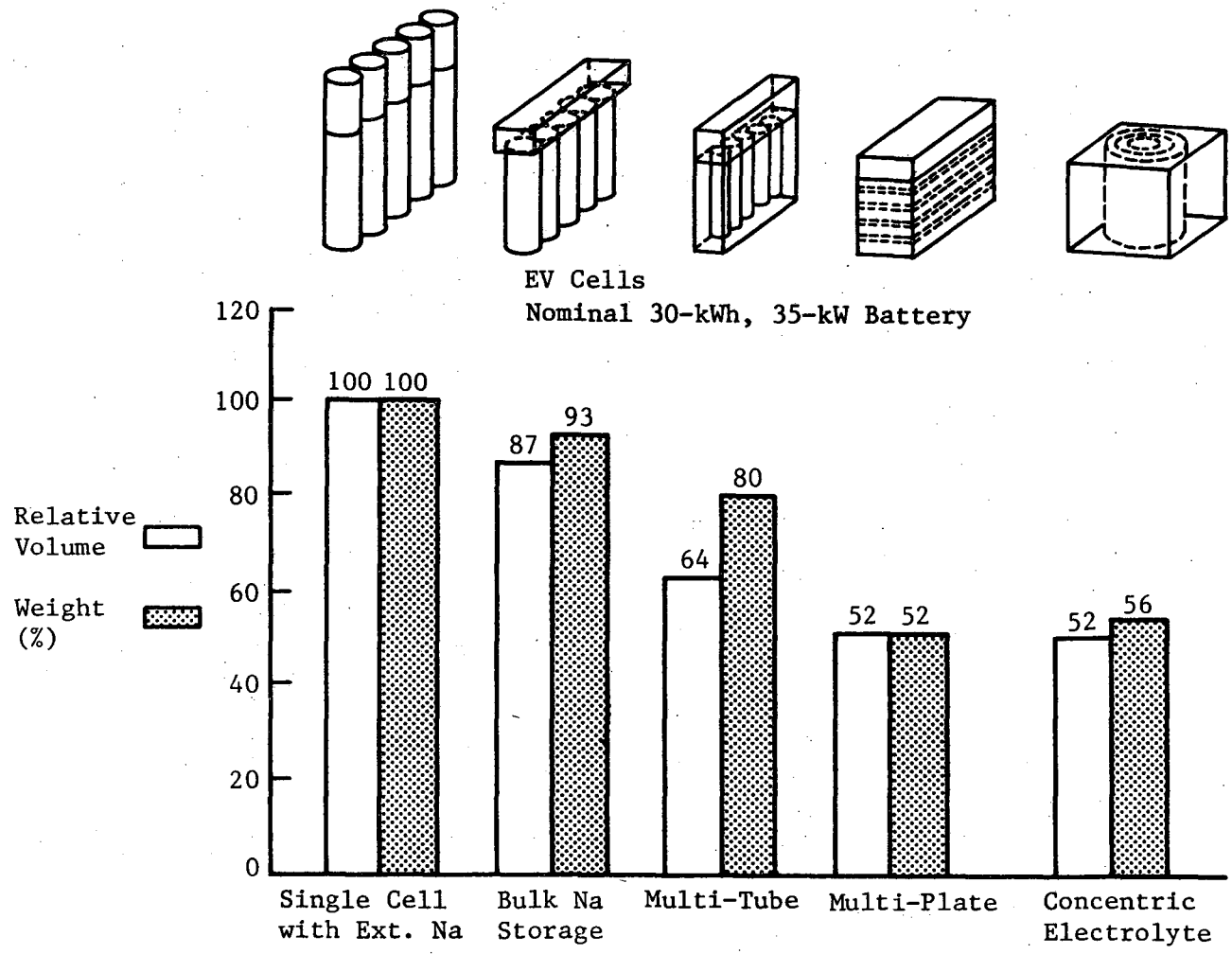

FIGURE 57
RELATIVE VOLUMES AND WEIGHTS OF SODIUM/SULFUR CELLS

TABLE XXX

SODIUM/SULFUR BATTERY FOR TRUCK DEMONSTRATION

Vehicle:	Taylor-Drum Model BO-012-48, four wheel
Dimensions:	119 in long 45 in wide 69 in cab height 25 in bed height 55 in wheel base
Gross Vehicle Weight:	Empty--1,475 lb (with batteries)
Maximum Speed:	10 mph
Motor:	24/36 volts, 95 A, 2¼/3½ HP

Battery Comparison:

	Pb-Acid Supplied	Sodium/Sulfur[a]
Ah:	115 (90 mins)	600 (8 hrs)
Wh:	2,800	14,400
Weight:	250 lbs	400 lbs
Cost:	$250	$600 future
Life:	100-500 cycles	2,500 cycles (goal)
Range (miles):	15 (10 mph)	80 (10 mph)

[a]Constructed with cells designed for load leveling; not optimum for this application.

Source: Ford Aerospace and Communications Company.

photovoltaic or wind energy storage system. The performance of this cell is compared with the Mark II cell in Table XXXI. The battery design was for a small, 15kW, stand-alone system which incorporates 1,400 of the higher energy Na/S cells. They are connected in a parallel-series network to provide a discharge voltage of 120 volts-DC, and with sufficient redundancy for a 10-year life. Based on their performance estimates, these authors conclude that the Na/S battery has the potential for good performance and reliability in small, stand-alone power systems.

Ceramatec, Inc., has established facilities for manufacturing a range of sizes of β"alumina tubes. Approximately 100 Mark II electrolytes can be batch sintered daily. The process has a 60% yield of acceptable electrolyte tubes. In addition, Ceramatec has the capability of manufacturing α-alumina seal header components for the various cell sizes being assembled by Ford Aerospace and Communications Company.

As an alternative to pressing the mixture for β"alumina, a slurry-solution spray drying process, which also eliminates the calcining and milling operations required for the pressing process, is being examined.

The status of reproducibility of cells prepared in a large facility capable of producing 50 β"alumina electrolytes and cells per week is provided in Table XXXII for 512 cells of a single battery.

TABLE XXXI

COMPARISON OF MARK-II AND HIGH ENERGY SODIUM/SULFUR CELL PERFORMANCE CHARACTERISTICS

	Mark II	High Energy
Theoretical Capacity	192 Ah	580 Ah
Coulombic Utilization	0.8	0.8
Cell Impedance:		
Beginning of life	10 Ω	12.5 Ω
End of life	10 Ω	17.5 Ω
Cell Life	10 yrs	10 yrs
Cell Failure Rate (Uniform)	0.5 %/yr	0.5 %/ yr
Cell Diameter	5.4 cm	7.9 cm
Cell Length	40 cm	42 cm
Cell Weight	2.0 kgs	3.6 kgs

Source: Reference 71, Ford Aerospace and Communications Company.

TABLE XXXII

SODIUM/SULFUR BATTERY PRODUCTION/ASSEMBLY EXPERIENCE

512-Cell Battery	Number of Defects	Mfg Yield
Defects Replaced During Assembly	2	99.61%
Failures During Early Operation	8	98.44%
Overall	-	98.06%

Mfg = manufacturing

Source: Ford Aerospace and Communications Company.

DeJonghe has investigated the factors which contribute to the mechanisms for the initiation and propagation of failures in β and β"alumina.[78] Two modes of failure have been identified. Mode I failure involves a cathodic plating of sodium in a preexisting crack of 1 to 20 micrometers. Once the crack becomes filled with sodium, current focusing occurs, leading to crack propagation. The results tend to favor contribution to the crack propagation by small fissures connected to the crack in which the failure was initiated by current focusing. The Mode II failure involved sodium precipitation internal to the ceramic body and possible microfracture. Mode II can be activated when a gradient in transport number ratios results from the chemical reduction of the sodium electrode.

Based on these studies, DeJonghe has suggested approaches to improved cell performance. The suggestions include:

- Improved sulfur electrode design;
- Improved corrosion resistance of materials; and
- Cell cycle management that avoids interface polarization.

The Dow Na/S cell differs from the Ford cell in the choice and construction of the electrolyte. The Dow electrolyte consists of hollow fibers of a sodium conducting glass. These fibers are attached to a glass header in contact with the sodium reservoir. To obtain a high cell capacity, several thousand glass fibers are used.

A large number of cells of varying capacity have been constructed and operated. The cell production technology has improved to 70% cell acceptance, i.e., the ratio of cell assemblies approved for filling with reactants and testing to the total number of assemblies (glass fiber plus metal foil) fabricated. Actual cell lives show a great variation. These have been reported to vary from a few weeks to over 1 year. This lack of reproducibilty makes it premature to construct modules and batteries requiring a large number of cells. The effort at Dow, as reported at the fourth BECC, concentrates on improving the predictabilty and lifetime of the glass fiber electrolyte cells.

The glass fibers have been found to break either along the length of the fiber or directly under the tubesheet.[79] In studies of fiber fracture, it was observed that most fractures started at some surface flaw. Breaks initiated at the inner wall and in the bulk of the fiber have also been identified. Micro-crystals in the glass were observed to be an important source of weak spots. The strength of the fibers was improved by over 15% by redesigning the melting furnace so the total melt was above the crystal melting point of any of the glass components.

Platinum inclusions have been observed in about 3% of the fibers tested. The platinum came from the crucibles used for melting the glass.

The use of a molybdenum layer on the aluminum cathode foil has been shown to improve the foil lifetime. The molybdenum is slowly converted to molybdenum sulfide. After several months of operation aluminum migrates through the molybdenum sulfide layer. Neither sulfidation of molybdenum nor migration of aluminum increases the cell resistance.

Work is continuing to better understand the source of the flaws and to improve the techniques for making highly reproducible glass fibers.

In summary, progress has been made in the fabrication of the ceramic electrolyte Na/S battery. Further improvement in electrolyte reproducibility or in the ability to detect defects prior to cell assembly can lead to the capability of producing highly reliable modules and batteries. The development of fusing to bypass shorted cells enables the use of replacement cells or building into the system sufficient redundancy to give the battery the required cycle life. This increased reliability will make it opportune to build large batteries for evaluation for EVs or stand-alone batteries for distributed or solar energy storage.

5.0 EXPLORATORY BATTERY AND SUPPORTING RESEARCH

This part of the ECS program is monitored by the Lawrence Berkeley Laboratory (LBL) of the University of California. Professor Cairns and Dr. McLarnon are the technical managers.

This effort constitutes the applied research base for the ECS program. The first aspect is the exploration of new electrochemical couples to determine their promise for use in high-performance battery systems. The second aspect is supporting research leading to better understanding of the electrochemistry, materials problems, and engineering principles of batteries and electrochemical technologies.

Investigations related to specific industrial electrochemical processes are discussed in Section 6. Supporting studies and research on particular cell systems under development are included in the appropriate sections of this report.

5.1 Exploratory Battery Research

The exploratory research includes studies concerning the use of lithium negative cells in non-aqueous electrolytes as well as the use of lithium or calcium in molten salt and solid electrolyte systems. Early studies on some of the exploratory cells were reviewed in SR-I or SR-II. The zinc/ferricyanide, semicontinuous-feed battery, formerly a part of this effort, is discussed above in Section 4.1 since it is being considered for the electrical storage component of photovoltaic and wind power systems.

5.1.1 Organic and Polymeric Electrolyte Cells

The EIC Corporation has recently summarized its efforts, briefly described in SR-I and SR-II, on lithium/organic electrolyte cells and batteries.[80] The general cell configuration is:

Li	LiX	Organic solvent Supporting electrolyte Dissolved Li_2S_n $X = ClO_4^-$, AsF_6^-, etc.	Carbon current collector

The solubility of Li_2S_n in various solvents was determined. The best solvents found were tetrahydrofuran and dimethylsulfoxide which dissolved the equivalent of 10M sulfur (as Li_2S_n) per 1. Investigation of the performance of small cells showed tetrahydrofuran to be the preferred solvent. The supporting electrolyte was 1M $LiAsF_6$. The cells showed a deteriorating capacity when cycled.

Based on an experimental investigation of this decrease in capacity, it was concluded that two problem areas needed to be addressed to overcome this deficiency:

- Reduce the self-discharge rate and delay Li_2S formation on the anode; and
- Discover a method for the solubilization of Li_2S without increasing the self-discharge reaction.

As an alternative to the use of Li_2S_n as the cathodic reactant, insoluble sulfide positive electrodes were investigated. The calculated specific energies of the reactants considered are listed in Table XXXIII. In the potential calculations it was

TABLE XXXIII

SPECIFIC ENERGIES OF INSOLUBLE SULFIDE POSITIVE ELECTRODES

Compound	Eq.Wt.[a]	No. of Electrons	E^{o}[b]	Wh/lb
A. Complete Reduction				
NiS	52.32	2	2.022	470
CuS	54.74	2	2.231	496
FeS	50.89	2	1.98	473
MnS	50.44	2	1.39	335
MnS_2	66.47	4	0.759	138
Ag_2S	130.84	2	2.28	212
VS	48.44	2	1.523	382
CoS	52.44	2	2.056	477
B. Partial Reduction to Monosulfide				
SiS_2	53.10	2	4.54	1,037
TiS_2	63.00	2	3.73	720
MnS_2	66.52	2	5.29	967
FeS_2	66.98	2	5.69	1,033

[a] Includes weight of required Li.

[b] The cell potentials were computed from the free energies of formation at 25°C tabulated by Gibson and Sudworth in Specific Energies of Galvanic Reactors, cited in reference 80.

Source: Reference 80.

assumed that the discharge products were the monosulfide of the cathode metal and lithium sulfide (Li_2S). Actual cells are expected to give a product intermediate between the monosulfide and a higher valent sulfide.

Several of the sulfides included in Table XXXIII were examined in cells. Of these, copper sulfide and titanium disulfide, which had been previously studied, showed the best performance. The Li/CuS cell with a cathode loading of $85mAh/cm^2$ averaged well over 0.8 equivalents/M over the first 100 cycles. The output dropped to approximately 0.25 eq/M around the 300th cycle. The reasons for the decline are not understood. Other candidate positive electrodes are V_6O_{13}, MoS_3, and Cr_3O_8.

Diethyl ether, neat or blended with other ethers, with $LiAsF_6$ as the supporting electrolyte, has shown the least activity toward the Li electrode.[81] Of the mixed electrolytes studied, the most desirable one was $(C_2H_5)_2O$ (90 v/o):tetrahydrofuran (10 v/o) with 2.5M $LiAlF_6$. Stored cells, with TiS_2 cathodes, showed stable open circuit voltages for up to one month. (The work at EIC on mixed ether solvents was partially supported by the Office of Naval Research.)

The studies of the Li/TiS_2 and Li/V_6O_{13} cells have led to projected performances as follows:[82]

- 130Wh/kg;
- 50W/kg;

- 100-200 cycles; and
- $100/kWh.

The work of Eisenberg at Electrochimica, as reported in SR-II, emphasizes the cell system:

Li	organic solvent Li salt	Chalcospinel $M_1M_2X_4$

where M_1 is a divalent metal, M_2 a trivalent metal, and X is S, Se, or Te.

Cells of Li	Tetrahydrofuran $LiClO_4$	$CuCoS_4$

were investigated. Some of the cells used a solvent mixture of tetrahydrofuran (THF) and dioxolane (DIOX)[83] and delivered 109 cycles at 70% DOD. During cycling, the lithium electrode became capacity limiting. The $CuCoS_4$ operated reversibly with a three-electron change per mole.

Recent investigations have emphasized techniques for the study of morphological changes in the lithium.[84] An aluminum substrate for investigating lithium stripping efficiency was found to give reproducible results and the lithium reversibly alloyed with the aluminum. Scanning electron microscopy and other techniques were used to study the lithium deposits. It was observed that electrocrystallization and other morphological effects vary as a function of cathode substrate, the solvent system including the anions present, additives, and the applied current density.

In the study of solvents, DIOX was found to be desirable, but it required the addition of polymerization inhibitors. Additions of 1,2-dimethoxyethane (DME) to the DIOX gave the best overall results for Li reversibility. $LiAsF_6$ was found to be more satisfactory than $LiClO_4$ as the supporting electrolyte giving denser deposits and a safer system.

Schwager and Muller of the Lawrence Berkeley Laboratory have investigated film formation on Li in an electrolyte consisting of 1M $LiClO_4$ or 1M $LiAsF_6$ in propylene carbonate (PC).[85] The techniques used were:

- Ellipsometry;
- Auger electron spectroscopy;
- Ion etching; and
- Secondary-ion mass spectroscopy.

The ellipsometer measurements were made over a 14-day period using a flat, optically smooth, lithium-foil electrode and 1M $LiClO_4$ in PC as the electrolyte. The measurements showed that the method could be applied to the Li/PC-$LiClO_4$ system. The larger film thickness measured by ellipsometry as compared to capacitance measurements was accounted for by a multi-layer film structure involving porous layers.[86] The data also indicated the presence of Li_2O or possibly LiCl in the film.[85]

Argon-ion etching and auger spectroscopy confirmed the film thickness derived by ellipsometry. These observations were

consistent with the presence of Li_2O rather than LiCl in the film on the lithium. The observed presence of carbon throughout the film may indicate Li_2CO_3 as a component of the film. Secondary-ion mass spectroscopy partly confirmed the presence of Li_2CO_3.

The factor of five difference in film thickness estimated from capacitance and ellipsometric methods led to the suggestion of an inner compact film which reaches a steady state and an outer porous layer which continued to grow.

Law and Tobias at the Lawrence Berkeley Laboratory have investigated the stability of potassium in propylene carbonate containing 0.5M of $KAlCl_4$.[87] Cyclic voltammetry and chronopotentiometry were used in this study. The response of the potassium electrode to two consecutive pulses showed the potassium to be activated by either an anodic or cathodic current. Electroplated potassium remains shiny in the electrolyte for extended periods of time. Cyclic voltammograms of the stored material indicate that the potassium may be protected by a thin film. Impurities in the electrolyte can lead to passivation as a result of reaction with the potassium. Among the likely reactions are:

$$2K + H_2O \longrightarrow K_2O + H_2$$

$$K + ROH \longrightarrow KOR + 1/2\ H_2$$

$$K + PC \longrightarrow CO_2 + C_3H_5OK + 1/2\ H_2$$

$$PC + 2K \longrightarrow K_2CO_3 + C_3H_6$$

$$PC + 2e^- + 2K^+ \longrightarrow K_2CO_3 + C_3H_6$$

The reactions with water and alcohols, the primary impurities in PC, are considered the most probable. Corrosion rates were established for potassium in PC-$KAlCl_4$ electrolyte.

Dey of Duracell, Inc., is investigating the chemistry of charging and discharging of the $Li/SO_2/C$ cell.[88] The following results have been reported:

- A hermetically sealed Li/SO_2 rechargeable cell, incorporating a reference electrode, has been developed
- $Li_2S_2O_4$ has been shown to be the discharge product of the cell.
- $Li_2B_{10}Cl_{10}$ has been demonstrated as a scavenger for electrically isolated Li and $Li_2S_2O_4$ in the cell.

Dey and his coworkers at Duracell have determined that $Li_2B_{10}Cl_{10}$ is oxidized at 3.6 volts vs. Li. This is a one-electron reaction giving $LiB_{10}Cl_{10}$ as the product. $LiB_{10}Cl_{10}$ can oxidize both Li and $Li_2S_2O_4$, preventing loss of active material in the cell.

$LiB_{10}Cl_{10}$ was prepared chemically by oxidizing $Li_2B_{10}Cl_{10}$. $LiB_{10}Cl_{10}$ can be further oxidized at a potential of 4.3 volts vs. Li. Although the oxidation product was unstable in acetonitrile, it could be studied by pulsed polarography. The following summarizes the reactions of $Li_2B_{10}Cl_{10}$, including the reaction of Li and $Li_2S_2O_4$ with $LiB_{10}Cl_{10}$.

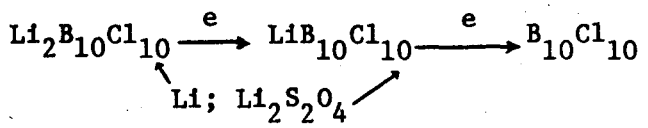

Farrington and Worrell of the University of Pennsylvania are exploring the use of polymeric electrolytes in ambient temperature lithium cells. Efforts have concentrated on polyethylene-oxide (PEO) complexes with lithium-ion salts. Examples of these complexes are shown in Figure 58. Nuclear magnetic studies have shown Li^+ to be the dominant charge carrier.

Thin films of the PEO complex have been used as a solid electrolyte in cells of the type:

$$Li \;\Big|\; \begin{matrix} PEO \\ \\ Li\ Salt \end{matrix} \;\Big|\; TiS_2$$

The cell open circuit voltage varied with the amount of lithium in the cathode, i.e., the state of charge, similar to organic electrolyte cells with the same electrodes.

Alternative membranes to the PEO-LiX complexes are being explored by Litt at Case Western Reserve University. Tri-block polymers are being synthesized in which polyethylene glycol (molecular weight 1,000) is to be the central block. A high-pressure gel permeation chromatogram has been constructed to obtain polyethylene glycol polymers with a narrow molecular weight distribution.(89)

Polyethylene Oxide - Salt Complexes

$\{ CH_2-CH_2-O \}_n$

PEO - LiSCN
PEO - KSCN
PEO - NaI

$\sigma \sim 10^{-5} \sim (\Omega\,cm)^{-1}$ at 45-75°C

PEO - LiTFA

$\sigma \sim 10^{-11}$ $(\Omega\,cm)^{-1}$ - 30°C

$\sigma \sim 10^{-4}$ $(\Omega\,cm)^{-1}$ - 140°C

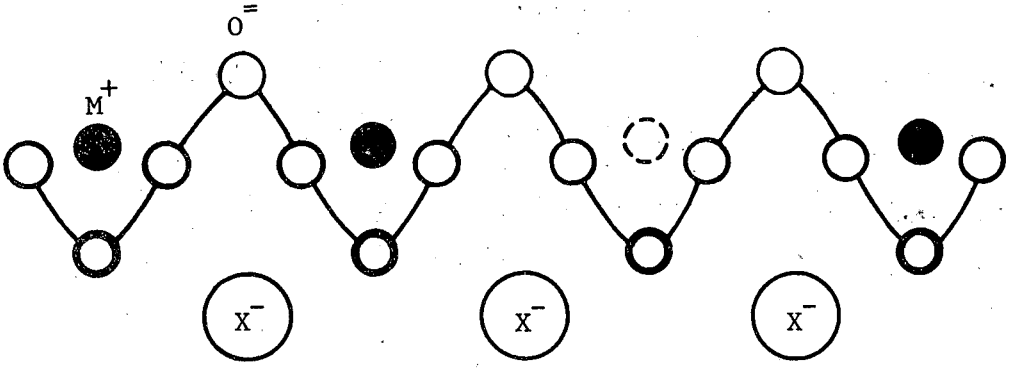

LiTFA - Lithium trifluoracetate

FIGURE 58
POLYMERIC SOLID ELECTROLYTES

5.1.2 Molten Salt Electrolyte Cells

The Ca-alloy/molten salt/FeS_2 cell was described in SR-I and SR-II. Roche and coworkers at ANL are continuing to explore this cell as an alternative to the Li-Al/LiCl-KCl/FeS cell. Post-test examination of the cells reported in SR-II showed that the BN separator had been degraded by reaction with the Ca_2Si negative. Lowering the calcium activity in the anode by the use of a ternary alloy, Ca-Al-Si, was shown to markedly decrease the rate of attack on the BN. Cells with these alloys gave voltages 0.24 volts less than the Ca_2Si cells. The negative electrode composition selected was a mixture of $CaAl_2$ and CaSi.

Based on cyclic voltammetry measurements, finely divided carbon (E-Coke Flour) was selected as the current collector for the FeS_2 electrode. Cyclic voltammetry experiments were also used to examine the effects of electrolyte composition on the performance of the FeS_2 electrodes. Bicells (two negative and one positive electrode), $CaAl_{1.2}Si_{0.4}$/LiCl-NaCl-$CaCl_2$-$BaCl_2$/FeS_2, were cycled. Figure 59 shows voltage-time curves for two different discharge rates and one charge rate. Both the charge and discharge curves show the two steps in the reaction of FeS_2. The cells showed a decline in capacity with cycling. The cells did show improved cycle life when compared with the Ca-Si negative cells; however, cell reproducibility, based on cycle life, was not high.

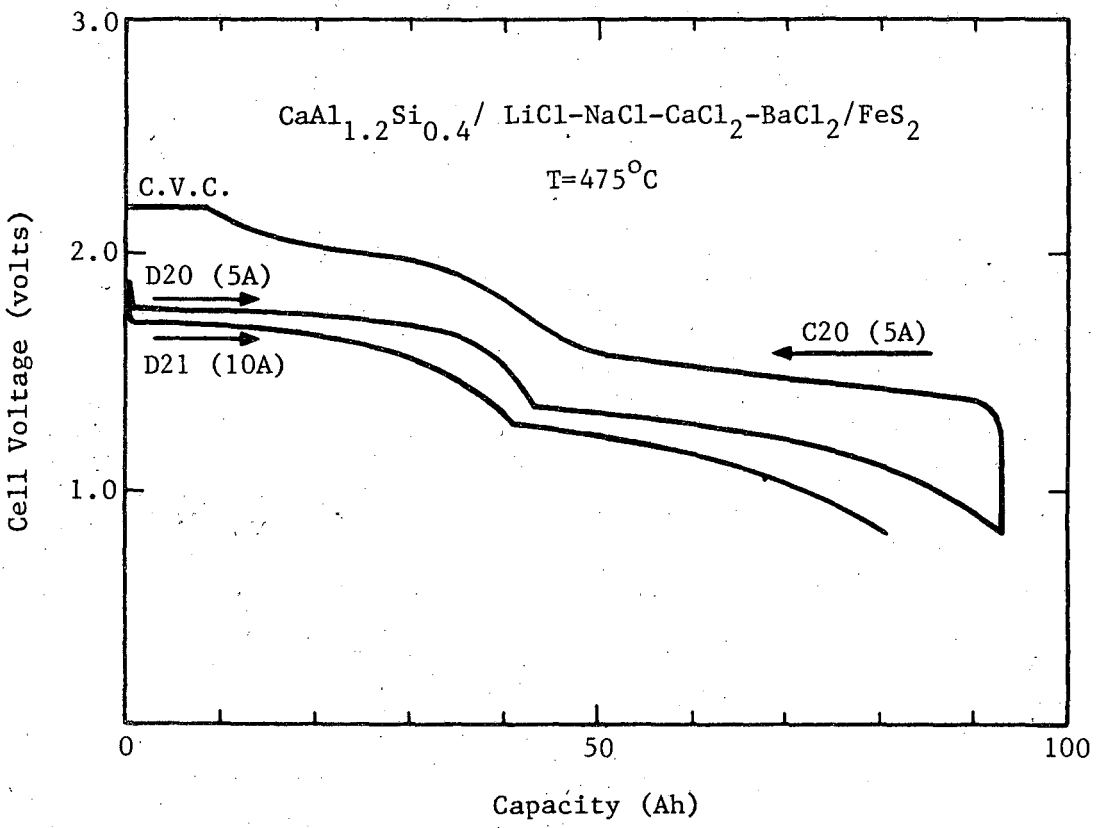

FIGURE 59
DISCHARGE PLATEAUS CHARACTERISTIC OF THE IRON SULFIDE ELECTRODE

Efforts to overcome the declining capacity with cycle life, which limits the useful cycle life, are continuing. The goal of the studies is a multiplate Ca-Al-Si/FeS_2 cell with the following characteristics:

- Specific energy, 160Wh/kg;
- Specific power, 200W/kg; and
- Cycle life, 1,000 cycles.

Earlier studies by Mamantov and coworkers on the cell:

Na/Na^+ ion conductor/SCl_3^+ in molten chloroaluminates

were described in SR-II. The sodium ion conductor, β"alumina, acts as both a separator and ion conductor. The cathode reactant is prepared by the electrochemical oxidation of elemental sulfur or introduced as SCl_3AlCl_4. The cell is operated in the temperature range of 180 to 250°C, the lower temperature being determined by the decreasing conductivity of the β"alumina with temperature. The electrochemistry of the cell reactions has recently been reviewed.(90)

The simplified cell reaction can be written in two steps based on the following assumptions:(91)

- S(IV) is present as SCl_4 even though SCl_4 is not stable under normal conditions.
- Elemental sulfur is written as S rather than S_8.

Step 1: $SCl_4 + 4Na \longrightarrow S + 4NaCl$

Step 2: $S + 2Na \longrightarrow Na_2S$

The actual reactions are much more complex involving melt species such as $AlCl_4^-$ and $Al_2Cl_7^-$ and the compounds formed by their interaction with sulfur species. The cell capacities and specific energies are a function of the $NaCl:AlCl_3$ ratio. The calculated capacities and specific energies for various cells are listed in Table XXXIV.

The two reaction steps are shown in Figure 60. They were determined by constant current discharge and charge. The two-step discharge permits almost 90% utilization of the sulfur capacity; the first step accounts for 60%. This agrees with a four-electron change in the first discharge step and a two-electron change in the second step for an overall change of six electrons. The effect of temperature on cell performance is shown in Figure 61. A cycle life of over 1,350 has been obtained in one cell and another cell has been cycled 476 times in a 10-month period. The cell has also withstood several temperature cycles.

The excellent capacity and cycling of the Na/SCl_3^+ cell, along with its much lower operating temperature than the Na/S cell, make it worthy for further evaluation in practical cell structures. The lower operating temperature should decrease the sealing and current collection material problems.

5.1.3 All Solid State Cell

Initial studies and the construction of the solid state cell,

Li alloy/$LiI.Al_2O_3$/metal sulfide,

TABLE XXXIV

CALCULATED CAPACITY AND SPECIFIC ENERGIES FOR SEVERAL CELL REACTIONS

Case A: The discharge stops when the solvent composition in the cathode compartment reaches the Al(III)/Na(I) mole ratio of 1:1.

Overall Cell Reaction	Cell Voltage (volts)	Ah/g	(10^{-2})	Specific Energy (Wh/kg)	
		63/37[a]	70/30[a]	63/37[a]	70/30[a]
$SCl_4 + 4Na = S + 4NaCl$	4.17[b]	5.67	7.80	236.4	325.2
$SCl_4 + 6Na = Na_2S +$ $4NaCl$	4.17[b] 3.37[c]	5.85	8.14	228.3	317.9
$SCl_4 + 2Al + 2NaAlCl_4 =$ $Na_2S + 4AlCl_3$	2.57[b] 1.77[c]	7.19	9.35	-	-

Case B: The four electron process occurs until the solvent composition becomes equimolar; the two electron process occurs in NaCl saturated melts.

Overall Cell Reaction	Cell Voltage (volts)	Ah/g	(10^{-2})	Specific Energy (Wh/kg)	
$SCl_4 + 6Na = Na_2S +$ $4NaCl$	4.17[b] 2.75[c]	8.30	11.32	306.8	418.5

[a]Initial mole ratio of total Al(III) to Na(I).

[b]First step.

[c]Second step.

Source: Reference 90.

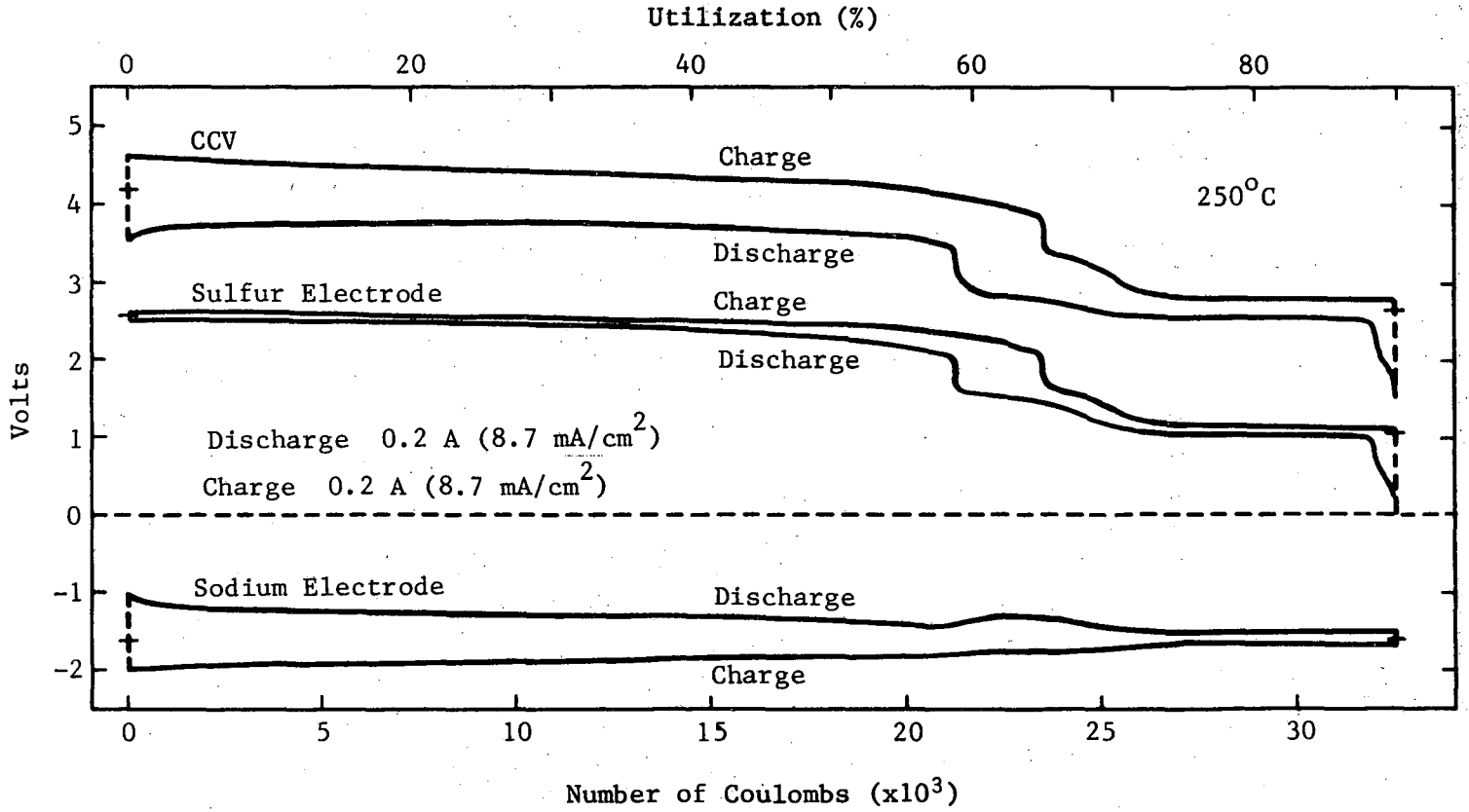

Reference Electrode: Al III/Al in NaCl Sat. Melt

Source: University of Tennessee.

FIGURE 60
Na/SCl_3^+ CELL CHARGE-DISCHARGE CURVES

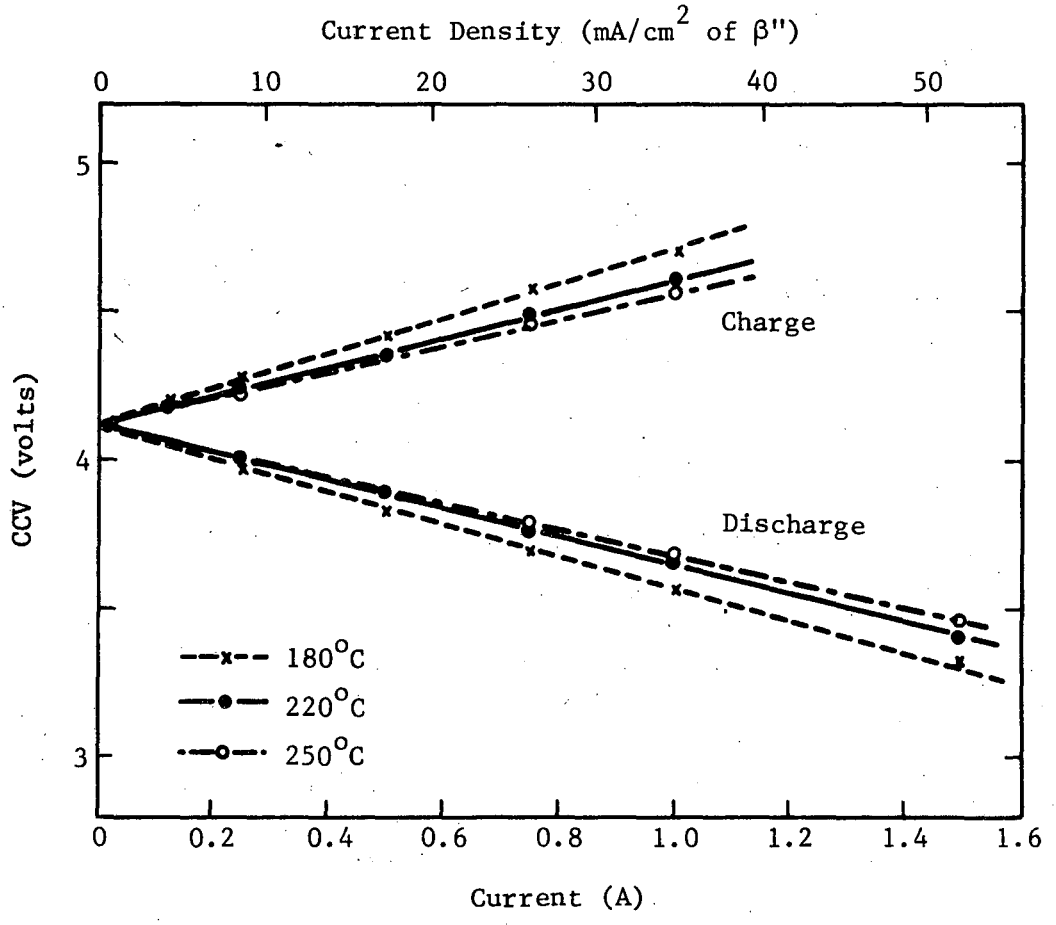

CCV - Closed Circuit Voltage at Midpoint of Discharge

Source: Reference 91.

FIGURE 61
CURRENT DEPENDENCE OF THE Na/SCl_3^+ CELL VOLTAGE

are reviewed in SR-II. This cell is being investigated by Rey of Duracell and operates at 350°C.[92] The Li-Si/TiS_2 couple has been shown to be capable of the following performance (packaging not included):

- Energy efficiency:

  84 to 87% at 5mA/cm^2 (C/10)

  78 to 81% at 10mA/cm^2 (C/5)

- Specific energy:

  110 to 140Wh/kg (C/10)

  60 to 100Wh/kg (C/5)

- Peak specific power (15 second pulse):

  360W/kg (full charge)

  100 to 180W/kg (half charge)

The investigators at Duracell have developed a hermetic glass-to-metal feedthrough for can cells and have fabricated 5-cm diameter cells. The cells can withstand deep thermal cycling and long-term, open-circuit storage at operating temperature. To enable a more detailed study of electrode polarization characteristics, a three-electrode cell has been developed.

5.2 Electrolyte, Materials, and Cell Engineering Research

The collection of systematic data on aqueous electrolytes is the goal of studies by Goldberg and Staples at the National Bureau of Standards. SR-II noted the computational methods for evaluating the activity and osmotic coefficients of sulfuric acid. The

computational schemes have been extended to the evaluation of the relative molal enthalpies and apparent molal heat capacities of aqueous systems. Activity and osmotic coefficients have been evaluated for the bivalent compounds of cadmium and zinc and for the univalent-bivalent aqueous solutions of Li_2SO_4 and Na_2CO_3.

Studies on the activity coefficients of alkaline electrolytes by Macdonald and coworkers are noted above in Section 3.4.

SR-I and SR-II described the discovery and initial evaluation of Nasicon ($Na_{1+x}Zr_2Si_xP_{3-x}O_{12}$, where x = 2.0 to 2.4) as a possible alternative solid electrolyte to β and β"alumina. Gordon and coworkers at Ceramatec have been exploring alternative methods of fabricating Nasicon electrolyte tubes. The procedures developed involve the following steps:

1. Mechanical mixing of raw materials ($Na_3PO_4.12H_2O$, SiO_2, ZrO_2 or $ZrSiO_4$, and Na_3PO_4);
2. Calcination at 1,160°C;
3. Dry milling;
4. Isostatic pressing; and
5. Sintering at 1,230 to 1,260°C.

Electrolyte tubes with x=2, prepared by the above method, showed poor static corrosion resistance in sodium at 200 to 300°C and low endurance in sodium-sodium test cells. Improved electrolyte tubes were prepared by hot isostatic pressing or by changing the composition to x=2.4. Alternative procedures to obtain more durable

electrolyte tubes such as sol-gel and slurry-solution spray drying were reportedly under investigation.[93]

Studies of Nasicon have also been undertaken by DeJonghe at the Lawrence Berkeley Laboratory.[94] Compositions with x=2 and x=2.3 were prepared. The samples with x=2.3 showed less degradation in 300°C sodium. Crack patterns, which markedly decreased the strength of the Nasicon, were observed. Further evidence of crack formation was the increased resistance following exposure to sodium. X-ray analysis showed that an unidentified compound, possibly a phosphate, was severely attacked by molten sodium. The Nasicon lattice parameter was also increased during sodium exposure. The Nasicon compositions prepared to date have been shown to be unsatisfactory for a practical electrolyte.

Wuensch at the Massachusetts Institute of Technology is investigating the mechanism of fast ion conduction in Nasicon-like and other fast ion conductors.[95] Synthesis, x-ray diffraction analysis, and AC conductivity measurements at 1 kHz have been completed for more than 50 solid solution phases in 10 different Nasicon-related systems:

$Na_4Zr_2Si_{3-x}Ge_xO_{12}$

$Na_3Zr_2PSi_{2-x}Ge_xO_{12}$

$A_{1+x}Zr_2V_{3-x}T_xO_{12}$ (A=Na and K, T=Ge and Si)

$Na_xX_2S_{3-x}P_xO_{12}$ (X=Al and Y)

$Li_{1-x}Ti_{2-x}Ta_xP_3O_{12}$

$K_{2-x}Mg_{2-x}Y_xS_3O_{12}$

A complete series of Nasicon-like solid solutions is formed for $0<x<3$ in the system $Na_4Zr_2Si_{3-x}Ge_xO_{12}$. Conductivity is not strongly dependent upon composition. Upon substitution of the larger Ge ion, the c axis of these hexagonal solid solutions rises through a maximum and then anomalously decreases. A similar effect was reported near the compositions of maximum conductivity in Nasicon, per se, $Na_3Zr_2PSi_2O_{12}$, and was attributed to repulsive interactions between the mobile Na ions as their number and site occupancies changed with composition. In $Na_4Zr_2Si_{3-x}Ge_xO_{12}$, however, the concentration of Na is not only fixed, but all sites are fully occupied. Earlier explanations of the anomaly cannot, therefore, be valid.

An appreciable range of solid solution extends between Nasicon and its Ge analogue, $Na_3Zr_2PSi_{2-x}Ge_xO_{12}$. The c axis decreases anomalously upon substitution of the larger Ge ion. Conductivity at 300°C changes little with composition but the activation energy displays an apparent decrease with Ge content. Upon substitution of a smaller octahedral cation in the framework, improved Li conductivity was obtained: the conductivity of $LiTi_2(PO_4)_3$, $\sigma_{300} = 7 \times 10^{-3}$ reciprocal Ω-cm, is an order of magnitude higher than the Li analog of Nasicon, $Li_3Zr_2PSi_2O_{12}$, and 50% higher than Li βalumina. Sodium and

potassium analogs of the Ti-substituted phase had σ_{300} of 4.6 x 10^{-6} and $<10^{-7}$ reciprocal Ω-cm, respectively, demonstrating the importance of the match between size of the mobile ion and the Nasicon framework.

Tuller at the Massachusetts Institute of Technology has continued his work on glasses in the system Li_2O-B_2O_3, which was briefly reviewed in SR-II. Recent studies have involved the substitution of chlorine for oxygen in these glasses through the substitution of LiCl for Li_2O. This resulted in systematically increasing the lithium ion conductivity and decreasing the glass transition temperature as well as the density. Conductivities as high as 2 x $10^{-2}\Omega^{-1}cm^{-1}$ at 300°C have been attained.

Glasses in the Li_2O-B_2O_3 system were exposed to attack by molten lithium. They remained coherent and did not dissolve. However, a black reaction product formed on the surface. The rate of formation of the black product decreased with increasing lithium content of the glass. Similar black films were formed on $Li_2O(LiCl)$-B_2O_3 glasses. Studies have been initiated on the corrosion resistance of these glasses and the effects of imposed current flow on their properties. Initial results are encouraging.

Huggins and coworkers at Stanford are continuing their studies on the thermodynamics, structure, and electrochemistry of lithium-based systems as they relate to possible use in secondary

batteries. The emphasis has been on the relationship of microscopic properties of the materials to their behavior in battery systems.

The studies at Stanford on the Li-Sn system were summarized in SR-II. These have led to a different approach to lithium-alloy negatives. An all-solid composite microstructure which may be able to overcome some of the life-limiting processes of the Li-Al electrode, noted in Section 4.2.1, has been postulated. The compound for the matrix phase of the composite should have the following characteristics:

- Good electronic conductivity in order to act as the current collector;
- High diffusion constant for the electroactive species (e.g., Li);
- Stable over the operating range of potentials; and
- Capable of maintaining the microstructural morphology of the reactant phase.[97]

The above concept has been demonstrated using $Li_{2.6}Sn$ as the matrix and Li_ySi as the reactant. Experiments were performed using an initial matrix composition of $Li_{1.56}Sn$. Silicon powder was added to this material. The lithium was added electrochemically to form the $Li_{2.6}Sn$ matrix and the two-phase $Si\text{-}Li_{1.71}Si$ reactant.

The material was studied in a cell using Al/Li-Al counter and reference electrodes. Representative charge and discharge curves, showing the electrode polarization as a function of the cell's

state of charge, appear in Figure 62. Curve A shows the disappearance of the nucleation-related dips and peaks when the cell was not cycled to the ends of the plateau. The total capacity over the discharge range was 0.93Ah/cm^3.

Although the theoretical capacity of the matrix-reactive alloy system is less than the Li-Al or Li-Si negatives being evaluated for the Li-alloy/FeS cell, the Li-Sn, Li-Si system may have some advantages. One is a kinetic advantage due to the higher diffusivity of Li in the matrix compared with the fused-salt matrix combination of the ANL cell. This system also avoids the possibility of electrolyte freezing within the pores of the electrode matrix. The major advantage would be the retention of capacity on cycling. As noted above in Section 4.2.2, the Li-Al system tends to lose capacity on cycling and an excess of the negative plate may be needed to obtain the desired cycle life with capacity retention. Under these circumstances a lower energy density electrode may be a better choice for meeting the lifetime goals for the molten salt systems.

The group at Stanford has also investigated alternative positive electrodes for lithium molten-salt batteries.[98] These studies have focused on ternary lithium, transition metal-oxide systems. The phase equilibria of lithium-metal oxide (Li-MeO) systems have been examined to select useful positive active materials. The electrochemical reduction of Li_xFeO_2 in galvanic cells of the type:

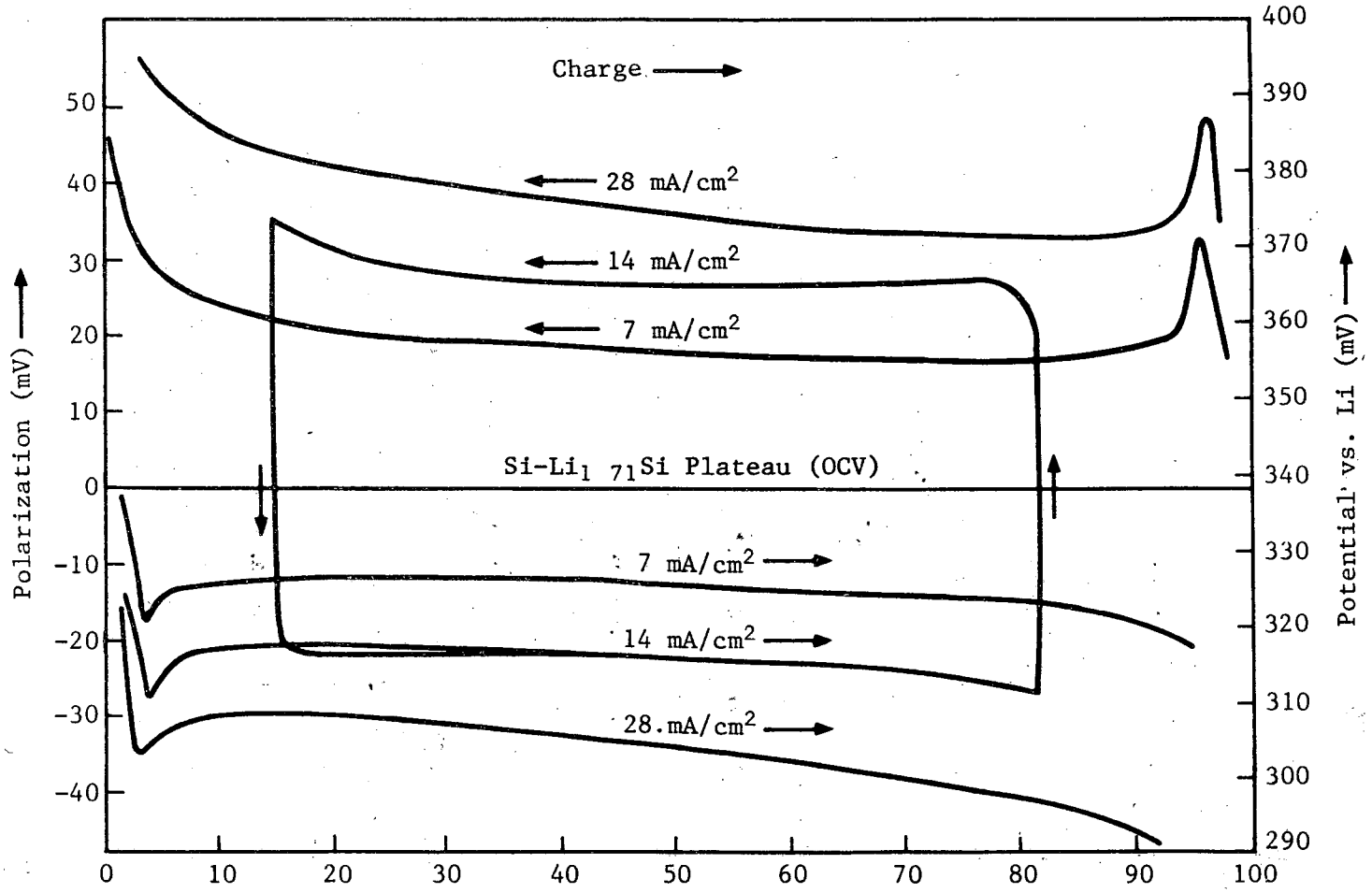

Source: Reference 97.

FIGURE 62
POLARIZATION OF Li-Si IN Li-Sn MATRIX

Al, Li-Al/LiCl-KCl/Li_xFeO_2

was investigated. The equilibrium potential curve for the positive of the above configuration is illustrated in Figure 63. Note the flat value of E over x values from ~ 1.1 to 3.8. This has led to the estimation that, for the cell described above, the theoretical specific energy is 413Wh/kg. Simple cells were also shown to be operable at 10 to 12mA/cm^2 with low overvoltage. These cells were shown to be reversible.

Raistrick and Poris, working with Huggins at Stanford, have examined the use of alkali nitrate molten salts as electrolytes in intermediate temperature lithium batteries. These authors note the importance of the formation of a protective film in those cases where the lithium potential is below the reduction limit of the electrolyte. Such a protective film of Li_2O forms in the molten nitrate salt eutectic $LiNO_3$-KNO_3 at 150°C. This layer is very thin and has a resistance of only a few ohms for a 1 cm^{-2} lithium electrode. The Li_2O layer formed acts as a second electrolyte in series with the molten salt electrolyte.

V_2O_5 and $LiCoO_2$ have been examined as positive electrodes with a lithium negative and a molten $LiNO_3$-KNO_3 electrolyte. The V_2O_5 had the better characteristics and discharge and charge curves are shown in Figure 64.

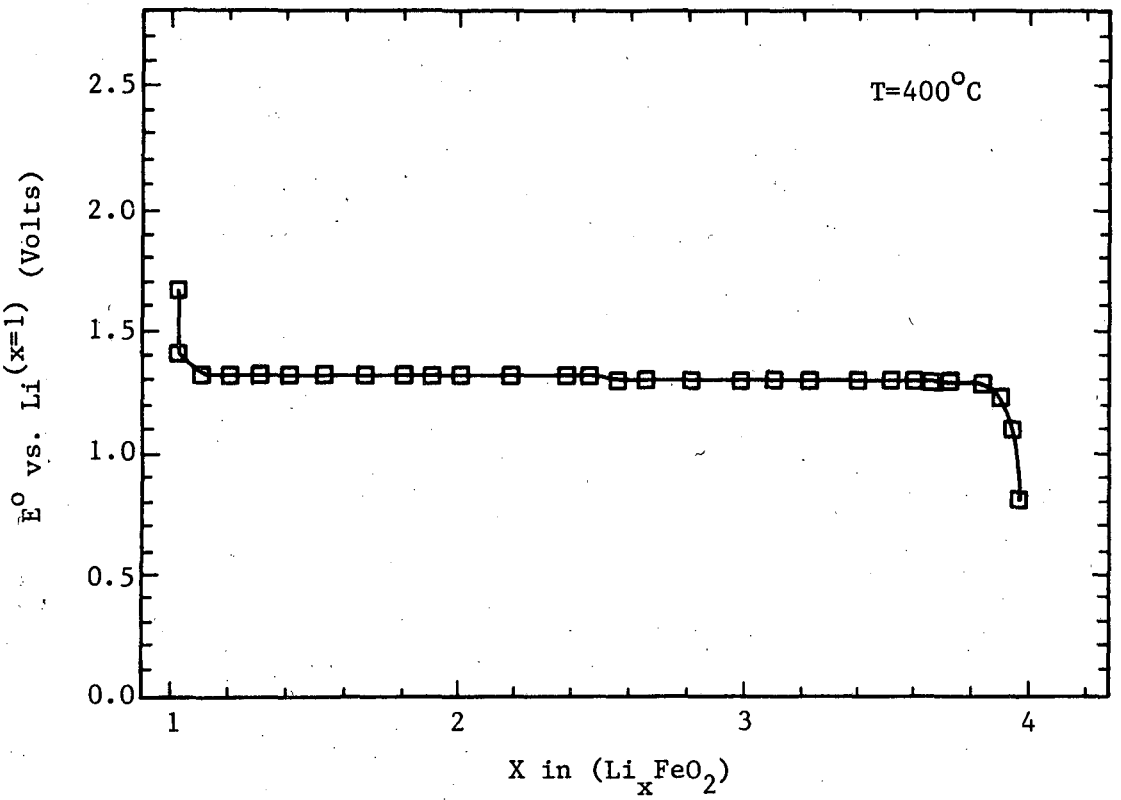

Source: Reference 98.

FIGURE 63
EQUILIBRIUM POTENTIAL CURVE FOR (Li_xFeO_2)

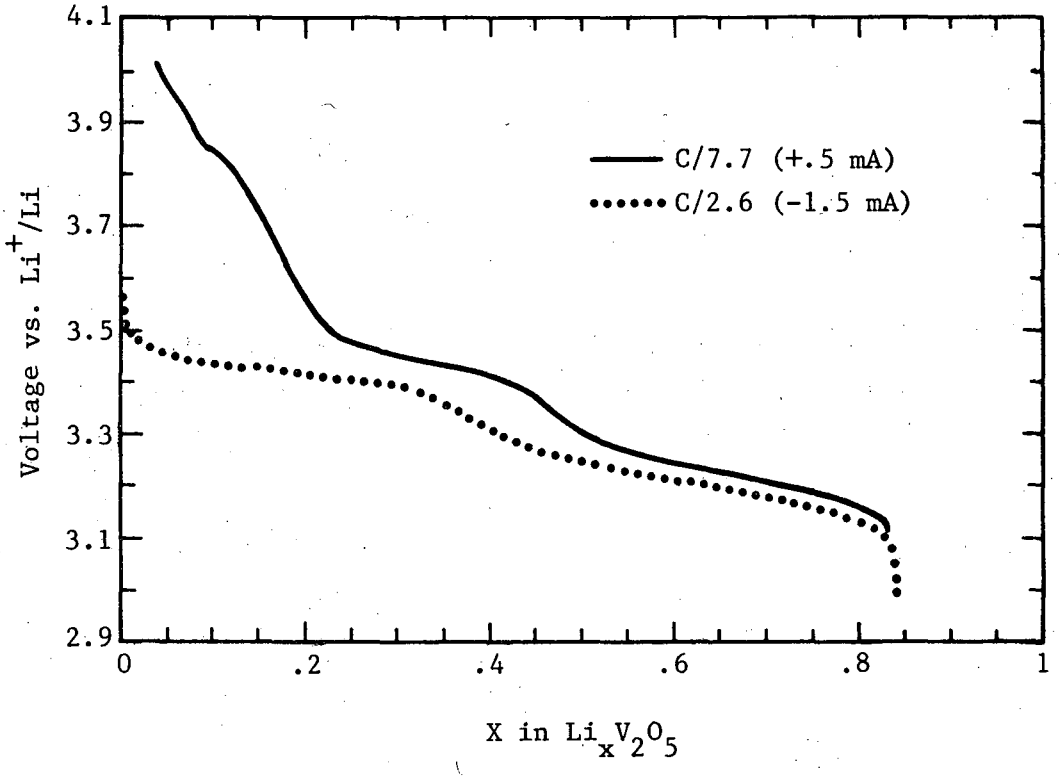

Source: Reference 99.

FIGURE 64
VANADIUM PENTOXIDE DISCHARGE AND CHARGE CURVES

The research on alternative approaches to high energy cells is continuing and potential new couples will continue to be evaluated.

Specific cell modeling studies have been reviewed with other aspects of research and development of the specific cells. Tobias and coworkers at LBL are investigating the general problem of the hydrodynamics and structure of electrodeposition. The results are applicable to batteries with a soluble anode product, such as zinc, electrowinning of metals, and electrodeposition.

A current density regime, below the limiting density, has been identified in which spiral like striations form on a rotating electrode.[100] Within this regime, an increase in current density leads to an increased number of spirals and decreases their formation time.

Based on studies with $ZnCl_2$ and $ZnSO_4$ solutions, it was concluded that complex formation and electrolyte conductivity do not influence spiral formation. Other studies indicate that spiral formation was associated with the speed of rotation of the electrode on which deposition was occurring.

Variable-current step and AC pulse techniques were used to relate the original substrate surface conditions to the structure of the electrodeposit. A close relationship between surface defects, nucleation density, and the formation of spirals was observed.

Prentice and Tobias have developed a model for simulating transient behavior of electrodes undergoing deposition or

dissolution.[101] The model accounts for ohmic drop, charge-transfer overpotential, and mass-transport effects. Finite difference techniques were used in computer simulations. Convergence has been attained and general guidelines for determining the computational parameters have been established.

Experimental testing of the model was carried out using carefully controlled electrodeposition conditions. The working electrodes were two contoured rotating cylinders with different sinusoidal profiles. A range of Wagner numbers (W_{no}):

$$W_{no} = \frac{\eta_\epsilon}{\eta_\Omega} \quad \frac{\text{(Charge transfer resistance)}}{\text{(Ohmic resistance)}}$$

was investigated. At low W_{no}, the current density variation on the profile of the electrodeposit was greatest. When W_{no} was high, the current density and the electrodeposit were more uniform. Deposition kinetic parameters were determined from overpotential behavior on smooth, copper, rotating cylinders. These were incorporated in the model simulations of the electrodeposit profiles. The simulated and experimental profiles generally agreed to within 10%.

6.0 ELECTROLYTIC TECHNOLOGIES

The electrolytic technology subelement has the objective of increased energy efficiency and materials savings in industrial electrochemical processes. SR-II reviewed the results of a series of process studies on the electrowinnng and recovery of metals, inorganic electrochemical synthesis, battery materials recovery, and the potential for energy savings in organic electrochemical synthesis. Laboratory efforts on process improvements and the understanding of process-related phenomena were also reviewed in SR-II. This report covers the continuing efforts on conservation in electrochemical technologies which were reported at the BECC.

6.1 Electrochemical Winning of Metals

The potential for energy savings in the electrochemical winning and recovery of metals was reviewed in SR-II. Based on the results of these studies specific topics were selected for emphasis between December 1979 and June 1981. The studies reported at the BECC centered on the electrowinning of aluminum and zinc, with brief mention of the ANL studies on the recovery of copper via the electrolysis of solutions of the cuprous ion.

6.1.1 Electrowinning of Aluminum

The winning of aluminum, because of its high electricity usage, has been one area of emphasis under the program. SR-II described the work at Argonne National Laboratories concerning alternatives to the Hall-Heroult process. The alternative process selected for

investigation at ANL was the electrolysis of Al_2S_3 rather than of Al_2O_3. Three reaction paths to Al_2S_3 considered were:

$$Al_2O_3 + 3C + 3S \xrightarrow{\text{high temperature}} Al_2S_3 + 3CO \quad (1)$$

$$Al_2(SO_4)_3 + 6SS_2 \xrightarrow{700^\circ C} Al_2S_3 + 6CO_2 + 6S_2 \quad (2)$$

$$Al_2O_3 \text{ (in melt)} + 3COS \xrightarrow{850^\circ C} Al_2S_3 \text{ (in melt)} + \quad (3)$$

Experimental work has been conducted at ANL on reactions (2) and (3). Table XXXV lists the results of the effect of the flow rate of carbon disulfide and reaction time on the conversion of aluminum sulfate to the sulfide, reaction (2). The percent conversion increased with the time of flow.

The results of the study of reaction (3) are listed in Table XXXVI. The conversion of Al_2O_3 to Al_2S_3 in the melt increased with the flow rate of the carbonyl sulfide, COS. The conversions were low and the maximum final concentration given in Table XXXVI was 0.39 wt % of Al_2S_3 in the melt. Separate measurements determined the solubility of Al_2S_3 in the melt to be 3 wt %. However, the solubility was increased to 7.5 wt % by the addition of aluminum chloride to the melt. The Al_2S_3 in the presence of $AlCl_3$ formed AlSCl in the melt.

Electrolysis experiments were conducted with three different Al_2S_3 concentations. The electrolysis voltage was from 1.4 to 1.6 volts at current densities of 200mA/cm^2. The current

TABLE XXXV

PRELIMINARY RESULTS OF THE SULFURIZATION OF ANHYDROUS $Al_2(SO_4)_3$ WITH CS_2

Sample Number	Conditions	% Conversion of $Al_2(SO_4)_3 \longrightarrow Al_2S_3$
R-24	700°C, 1 hr, CS_2/He flow of 134 cc/min	46.7
R-25	700°C, 1-1/2 hrs, CS_2/He flow of 100 cc/min	55.0
R-26	700°C, 30 mins, CS_2/He flow of 103 cc/min	29.0
R-27	700°C, 80 mins, CS_2/He flow of 98 cc/min	47.8
R-28[a]	700°C, 100 mins, CS_2/He flow of 127 cc/min	55.6

[a] -325 mesh $Al_2(SO_4)_3$ was used. All other samples were mixtures of + 325 mesh $Al_2(SO_4)_3$.

Source: Argonne National Laboratory.

TABLE XXXVI

CONDITIONS OF IN-SITU Al_2S_3 PREPARATION AT 850°C AND ANALYTICAL RESULTS OF REACTION PRODUCTS[a]

	Sample Number			
	MS-1	MS-2	MS-3	MS-4
Wt% of Al_2O_3	6.29	4.98	6.00	4.3
COS Flow Rate (cc/min)	68	102	108	120
Reaction Time (hrs)	2	2	1.5	1
Al_2S_3 Concentration ($M \times 10^2$)	0.93	2.50	2.90	5.28
Al_2S_3 Concentration (wt%)	0.065	0.185	0.215	0.39

[a]Eutectic chloride salts with the composition of $MgCl_2$:NaCl:KCl = 50:30:20 mol %.

Source: Argonne National Laboratory.

efficiency was over 80%. These results indicate the feasibility of the Al_2S_3 electrolysis method for preparing aluminum.

ANL has also initiated studies to improve the preparation of $AlCl_3$. This compound is used in a new process for aluminum electrolysis being evaluated by Alcoa. Studies are in progress on liquid-liquid extraction of $AlCl_3$ from an aqueous solution or from a suspension of aluminum hydroxide, $Al(OH)_3$. The following reactions outline the approach under investigation:

$$Al(OH_3)\ (Aqueous) + 3HX(org) \xrightarrow{80^\circ C} AlX_3\ (org) + H_2O$$

$$AlX_3(org) + (Li,Na,K)Cl(s) + 3HCl(g) \xrightarrow{125^\circ C} (Li,Na,K)\ AlCl_4(l) + 3HX(org)$$

where HX(org) is a carbon- or phosphorous-based extractant. No specific results were reported.

Modeling studies, reported in SR-II, of the electrolysis of alumina in cryolite, have shown that the dissolution and recirculation of the aluminum in the molten salt can lead to current inefficiencies. Magnetic field effects, which induce recirculation in the electrolyte, have been suggested as one of the factors requiring control to improve the energy efficiency. A mathematical model to determine the changes in cell design that can reduce the magnetic field effects has been undertaken at Lawrence Berkeley Laboratory.(102)

By applying the model to cells with various arrangements of busbars, the cryolite velocity contours in the cells were calculated. These were used for calculating the electrolysis

efficiency of various cell designs. As a result of these calculations, researchers plan to experimentally evaluate alternative configurations which may lead to higher cell efficiencies.[103]

6.1.2 Electrowinning of Zinc

The Battelle study, reported in SR-II, concluded that the alkaline leach and electrolysis process was a lower energy route to zinc, in selected cases, than the commonly used sulfate process.[104] Further study of zinc recovery has been conducted at ANL and Prototech.

Meisenhelder et al. at ANL have further analyzed the conclusions of Battelle and have concurred with the energy savings potential of the alkaline process.[105] However, they have concluded that the realizable energy savings will probably be less than the savings projected by Battelle--10% vs. 33%. ANL also concurred in the Battelle conclusion of the potential for cost savings through the use of the alkaline zinc process.

The ANL analysis of the zinc industry production projections was not encouraging with respect to the introduction of new processes. However, the alkaline process is highly compatible with the lower grade ores which will constitute a major source of the future U.S. zinc supply. Thus, if additional capacity should become necessary the alkaline process represents a promising alternative.

The recovery of zinc from scrap, which is practiced more extensively outside the United States, and from zinc flue dusts presents an additional potential application for the alkaline process. The evaluation of the process by the EIC Corporation was also summarized in SR-II.

A potential need for zinc recovery would be the introduction into the marketplace of one or more of the zinc negative batteries discussed in Sections 3 and 4. For example, the introduction of the zinc/nickel-oxide battery in EVs has been projected to reach one million cars by the year 2000. Assuming a 5-year battery life, this would lead to a potential of 100,000 metric tons of zinc being available for recovery in 2005.

Based on this evaluation, Meisenhelder et al. have made the following recommendations for additional studies:

- Further economic assessments of the alkaline vs. acid processes for the primary and secondary recovery of zinc.
- Laboratory research on the operation of the alkaline electrolysis process.

The Prototech approach to reducing the energy requirements in the acid electrolysis of zinc is through the use of a Prototech hydrogen anode to replace the oxygen evolving lead anode. The standard hydrogen electrode being used in these studies is a platinum-catalyzed gas diffusion anode containing 0.3 mg of Pt/cm^2. Modifications of this electrode to obtain improved performance have been evaluated by comparing the anode working

potentials. Anodes have been tested in 15 x 15 cm cells. A saving of 1.69kWh/kg of zinc (i.e., 50%) was obtained when compared with the energy used with the standard lead anode. Endurance tests of 1,000 hours have been carried out with hydrogen anodes having 0.4 or 0.09 mg Pt/cm^2. The higher platinum content electrode was less polarized.

Meisenhelder et al. have evaluated the use of the hydrogen anode in the alkaline zinc electrolysis process.[105] Their estimate of a saving of 1.41kWh/kg of zinc in the acid process is somewhat lower than that reported above (1.69kWh/kg). In the case of the alkaline zinc recovery they estimate a saving of 1.14kWh/kg, a 56% energy saving.

Both the Prototech and ANL studies show marked electrical energy savings in the electrochemical recovery of zinc by the use of a hydrogen anode.

Prototech[106] reports an overall energy saving due to the H_2 process (including estimated energy inefficiency due to producing hydrogen from petroleum coke) of about 40%. In 1979, Prototech Company estimated the combined amortization plus operating cost saving[106] due to the H_2 process (at 50 ASF, 40-60°C) at 4.2-5.6¢/kg zinc. More recent estimates based on improved performance indicate a saving of 5.9¢/kg zinc.

Preliminary studies by the EIC Corporation concerning metal recovery from spent batteries were reported in SR-II. This work has been extended by Castle Technology Corporation to include six battery systems: zinc/nickel-oxide, iron/nickel-oxide, zinc/chlorine, zinc/bromine, sodium/sulfur, and lithium-aluminum/iron sulfide.

Flow sheets, such as those included in SR-II for the Zn/NiO(OH) and Li-Al/FeS batteries, were developed for the various battery systems. For the Zn/NiO(OH) and Fe/NiO(OH) cells, ammonical and acid leach and pyrometallurgical processes were evaluated. The process evaluation concluded that, for the Zn/NiO(OH) battery with pressed nickel oxide electrodes, a hydrometallurgical (leaching) route is best. In the same batteries with sintered-nickel positive electrodes, the pyrometallurgical carbonyl process producing zinc oxide and powdered nickel was preferred.[107] However, batteries in which the positive electrode is made by the deposition of nickel on an iron substrate may require either an additional step for iron removal or they may need to be recycled hydrometallurgically.

The zinc chloride and zinc bromide from their respective batteries can be recycled following solution purification. The spent reactants in the Na/S battery can be recovered by dissolution

in dimethylacetamide followed by conversion to Na_2S_3 by reacting with sulfur.

A flow sheet for the recovery of material from the Li-Al/FeS_x battery was included in SR-II. An alternative method for lithium recovery, suggested by Pemsler and Spitz, is the leaching of the Li_2S from the spent battery with water.[107] The lithium is then precipitated as the carbonate and reconverted to the sulfide.

Estimated capital and operating costs for the various processes are listed in Table XXXVII. The table indicates that, of the materials included, the recovery of nickel yields the greatest economic benefit. However, until one or more of the alternative batteries is commercialized, pilot plant evaluation of recovery processes would be premature.

6.2 Electrochemical Production of Inorganic Chemicals

Energy conservation efforts in the electrochemical industry have included an overview of inorganic electrosynthetic processes and a continuing experimental program concerned with lower energy chlor-alkali (chlorine and sodium hydroxide) processes. The latter includes both fundamental and process investigations.

6.2.1 Electrochemical Production of Inorganic Chemicals

A survey of the electrochemical production of inorganic chemicals was completed during 1980.[108] This study by the Castle Technology Corporation had as its objective the identification of electrochemical technologies applicable or

TABLE XXXVII

RECYCLE PROCESS CAPITAL AND OPERATING COSTS FOR LARGE ELECTRIC VEHICLE BATTERY PLANTS

Process	Product	Tons/Yr	Capital Cost ($1,000)	Operating Cost ($1,000/yr)	Recycled Material Cost (¢/lb of product)	New Material Cost (¢/lb of product)
Zinc - Acid Leach	ZnO	5,282	4,830	7,300	69	45
Zinc - Ammonia Leach	ZnO	4,090	5,470	4,590	56	45
Zinc - Pyrometallurgical	ZnO	4,090	4,770	2,800	34	45
Nickel Solution - Acid Leach	$NiSO_4$	9,929	4,670	5,590	28	103
Nickel Solution - Ammonia Leach	$NiSO_4$	9,930	5,010	6,270	32	103
Nickel Powder - Acid Leach	Ni Powder	8.107	11,310	9,190	57	250
Nickel Powder - Ammonia Leach	Ni Powder	8,780	11,050	9,870	56	250
Nickel Powder - Pyrometallurgical	Ni Powder	8,167	6,440	3,940	24	250
Combined Nickel and Zinc - Acid Leach	ZnO	5,507	9,290	9,710	30	83
	$NiSO_4$	10,454				
Combined Nickel and Zinc - Ammonia Leach	ZnO	4,266	9,900	7,840	27	86
	$NiSO_4$	10,454				
Zinc/Chlorine	$ZnCl_2$	8,423	1,620	2,330	14	25
Zinc Bromine	$ZnBr_2$	10,218	2,240	2,620	13	41
Sodium Sulfur	Na_2S_3	46,640	10,610	8,460	9	12
Lithium-Aluminum/Sulfide	Li_2S	8,560	7,830	9,190	54	125-155

[a]Plants handling 100,000 electric vehicle batteries/yr.

[b]Cost of combined product

potentially applicable to the production of inorganic chemicals, excluding chlorine/caustic and metals. Emphasis was placed on energy conservation. The study included inorganic chemicals that are:

- Currently produced electrochemically.
- Not currently produced by electrochemical technology but ones for which electrosynthesis may offer advantages.
- Used captively within a process and can be regenerated electrochemically.

It was estimated that currently 6×10^{12} kcal/yr (3×10^{6} barrels of oil equivalent) are used for inorganic synthesis (excluding chlorine/caustic). Of this, 67% is used for the production of chlorates and perchlorates.

Sodium chlorate is produced by the electrolysis of sodium chloride at a pH of 6.4 to 6.8 (maintained by the addition of hydrochloric acid). The anodes used have generally been graphite, however, these are being replaced by titanium coated with a noble metal or metal oxide (Pt, RuO_2). The newer anodes permit higher operating temperatures, better current efficiency, and lower energy consumption, 4,700-5,500kWh/ton $NaClO_3$ compared with 5,100 to 6,000 kWh/ton for graphite.

The study noted recent improvements in cell design and operation. These can result in small decreases in energy consumption but do not overcome the large voltage loss at the hydrogen evolving cathode. Pemsler and Spitz note that the

development of improved catalytic coatings can reduce cathodic overpotentials by 0.2 to 0.5 volt. This corresponds to a 5 to 14% energy savings. They further suggest that electrocatalysts developed for other electrochemical systems be tested in the chlorate cell. In addition, the air depolarized cathode, discussed below as part of chlor/alkali cell development, may also be applicable to the chlorate cell. This would decrease the voltage by 0.8 volt. Another suggested energy saving approach is to use the hydrogen evolved as the anode reactant in the fuel cell.

The preparation of other inorganic compounds currently manufactured electrochemically, but involving less energy than sodium chlorate production, was also reviewed. The compounds considered were: sodium perchlorate, sodium hypochlorite, and manganese dioxide.

Hydrogen peroxide and zinc were suggested as industrial chemicals, currently manufactured by non-electrochemical methods, for which energy saving electrochemical processes may become available. Hydrogen peroxide, once manufactured electrochemically, is presently manufactured by the oxidation of organic intermediates. Pemsler and Spitz suggest combining the cathodic reduction of oxygen to hydroperoxide ion in alkaline solutions with the anodic oxidation of sulfate ion to the peroxydisulfate ion:

Cathode:

$$O_2 + H_2O + 2e \longrightarrow HO_2^- + OH^-$$

Anode:

$$2SO_4^{2-} \longrightarrow S_2O_8^{2-} + 2e$$

The conversion of the peroxydisulfate ion to hydrogen peroxide was the method for peroxide production used prior to the introduction of the organic oxidation routes. The use of both anodic and cathodic pathways to hydrogen peroxide permits the synthesis of 2 moles of peroxide with the use of two faradays, thus halving the classical current requirements. A flow sheet based on this process is shown in Figure 65.

Electrochemical approaches were outlined for the production of ozone and for the regeneration of sodium hydroxide from sodium sulfate produced when sodium hydroxide solutions are used for sulfur dioxide removal from the stack gases of coal burning systems.

The production projections for the year 2000 for the chemicals considered in the Castle Technology Corporation study and their energy requirements are summarized in Table XXXVIII.

6.2.2 Chlor-Alkali Production

The chlor-alkali industry is the second largest electricity consumer in chemical and metal production. A lower energy path for the manufacture of chlorine and sodium hydroxide has been a major thrust of the ECS program and earlier studies were reviewed in SR-I and SR-II.

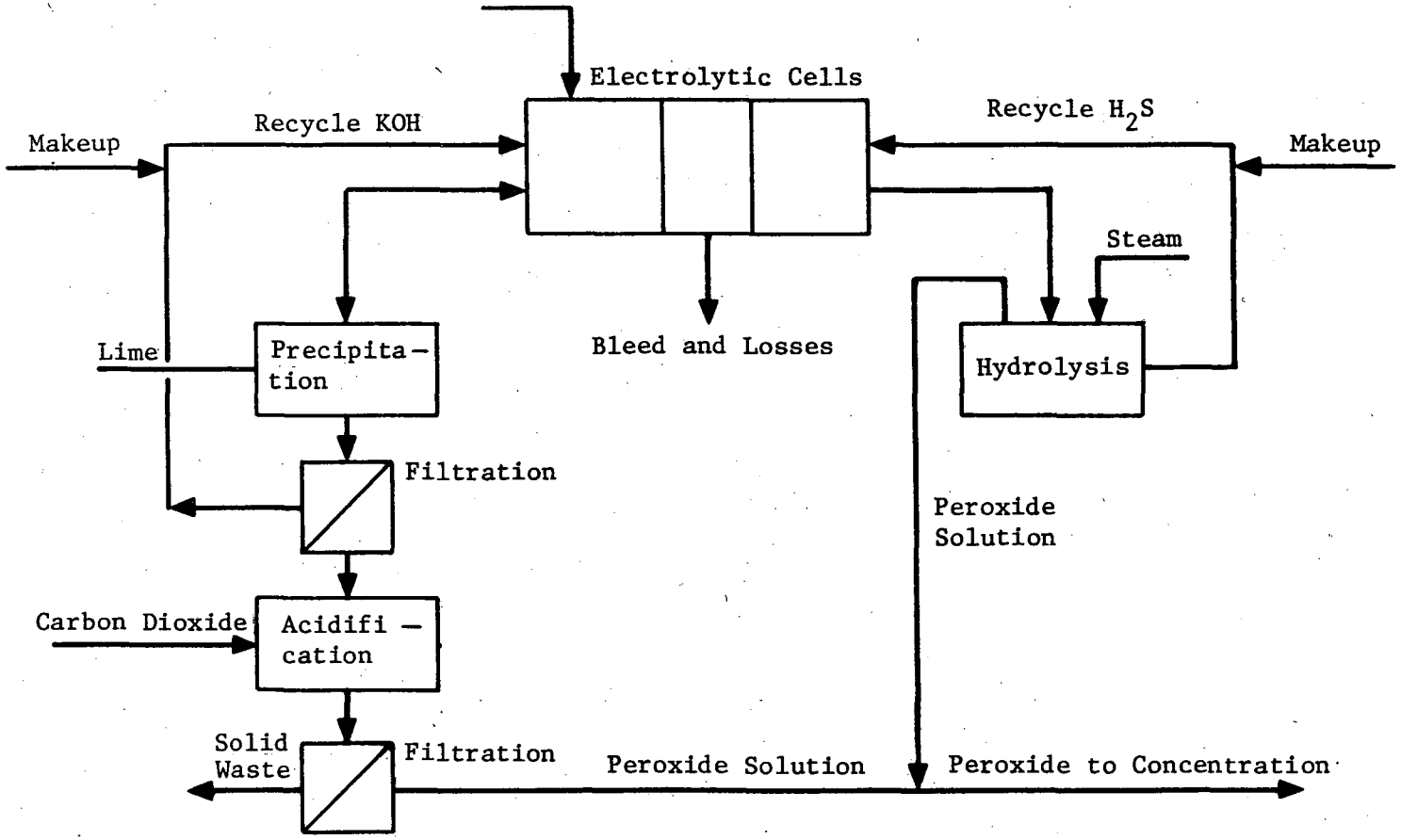

Source: Reference 107.

FIGURE 65
SIMPLIFIED FLOWSHEET FOR HYDROGEN PEROXIDE BY CONCEPTUAL PROCESS

TABLE XXXVIII

PRODUCTION AND ENERGY CONSIDERATIONS FOR THE ELECTROCHEMICAL GENERATION OF INORGANIC CHEMICALS IN THE YEAR 2000

	Chemical	Growth Rate (%)	Production in Year 2000 (thousands of short tons)	Energy Content		Annual Energy Requirements	
				Total (10^6 Btu)	Electrolytic (10^6 Btu)	Total (10^{12} Btu)	Electrolytic (10^{12} Btu)
Produced Electrochemically	Chlorate	5.6	840	58.1	54.5	48.8	45.7
	Perchlorate	4	75	32.6	30.8	2.4	2.3
	Electrolytic Hypochlorite	6	100	53.6	47.4	5.4	4.7
	Electrolytic Manganese Dioxide	6.5	80	75.5	44.3	6.0	3.5
	Fluorine	4	4.5	100	100	0.45	0.45
Alternate Electrochemical Route	Hydrogen Peroxide, Chemically Produced	6	400	45.6	-	18.2	-
	Ozone Produced by Silent Discharge	-	240[a]	63-190	-	15.1-45.6	-
Regenerated Electro-chemically	Caustic from Sodium Sulfate	-	350[b]	34.7	34.7	12.1	12.1

[a] Ozone production taken as 10% of the chlorine production used for water treatment; chlorine growth rate estimated as 6%/yr.

[b] Caustic recycle from sodium sulfate based on sulfate formed in caustic scrubbers; caustic scrub estimated to be used in 10% of scrubbing systems.

Abam Engineers, Inc., has conducted a study comparing the process engineering and economics of the diaphragm and membrane chlor-alkali technologies.[109] Some emphasis was placed on the membrane type cells as they are considered to be most readily adapted to the new technology. The status of the oxygen cathode technology is described in the review of the Diamond Shamrock Corp. studies which follows. The specific technologies compared in the Abam Engineers study were:

- Conventional diaphragm cell plant;
- Membrane cell plant with current commercial technology;
- Membrane cell plant with catalytic cathodes; and
- Membrane cell plant with oxygen depolarized cathodes.

The study found that the diaphragm cell plant, at the size of 544 metric tons per day, may have a small economic advantage over other technologies. The membrane cells, however, consume less energy with the oxygen (air) cathode cell. These are promising, as lower energy chlor-alkali cells, when there is no market for hydrogen.

The Abam Engineers' evaluation of alternative, but highly developed, technologies concluded that the solid polymer electrolyte cell, the coupling of diaphragm cells with fuel cells, and the dynamic gel diaphragm offer technologies for reducing chlor-alkali industry energy requirements. The Abam Engineers' study projects that the electrical energy required to produce a unit of chlorine in 1990 will be 50% to 60% of that required in 1970.

The research and development effort concentrates on the reduction of energy consumption in the membrane process. The approach is the use of an air cathode to reduce the operating voltage of the cell. To achieve this end, emphasis has been placed on high performance oxygen electrodes. This effort consists of a developmental program at the Diamond Shamrock Corporation and fundamental studies at Case Western Reserve University. Related investigations at Case Western concerning bimodal oxygen electrodes are discussed above in Section 4.1.1.2. A comparison of the structure of the oxygen electrode for use in the Al/air battery and chlor-alkali cell is included above in Figure 32.

The joint effort has shown definite promise of energy conservation. A reduction of the chlor-alkali cell operating voltage by 0.9 volt, with an air cathode, has been achieved. Assuming no change in current efficiency, this represents a 22% energy decrease when operated on air and a 31% decrease on oxygen. This is illustrated in Figure 66 which compares the pilot plant cell performance with air and oxygen with that of a hydrogen evolving cell. The electrodes in the pilot plant cell were 550 cm^2. Prototype production cell electrode fabrication, leading to prototype cell operation, has been successful. The test program was to be initiated in the second quarter of 1981, but no data were presented at the BECC. However, a section of the prototype

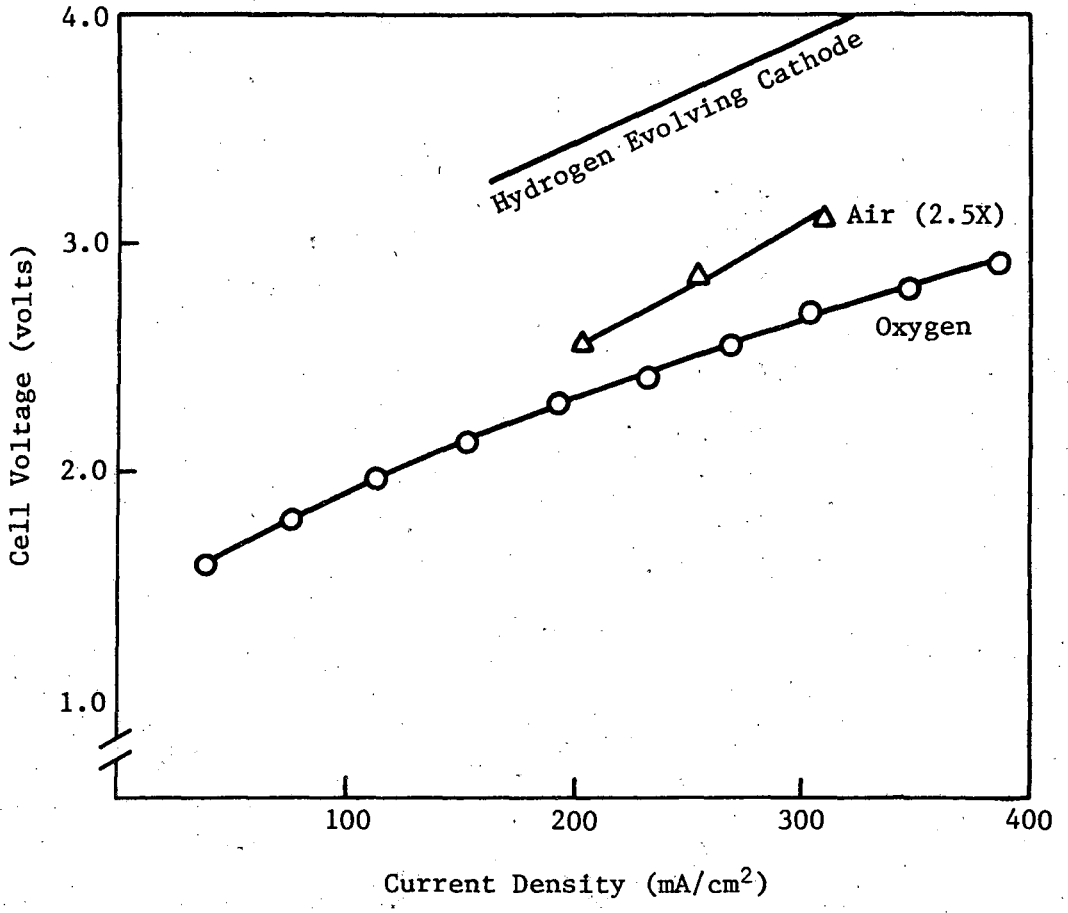

FIGURE 66
PILOT CELL PERFORMANCE

electrode has been life tested for over 40 days with little to no change in performance after the first 5 days.

The approach at Case Western to improved electrodes for the chlor-alkali cell has several aspects:

- Development of a predictive base for identifying oxygen electrocatalysts;
- Mechanistic studies on specific electrocatalysts;
- Studies of surface properties of specific electrocatalysts;
- Short-term polarization measurements on gas-fed cathodes; and
- Peroxide decomposition measurements.

A broad array of catalytic materials is being investigated at Case Western Reserve, as indicated in Table XXXIX. Some of these are noted above in Section 4.1.1.

The results of studies on oxygen reduction on the various catalysts is briefly summarized:

- Pt and its alloys--These have the highest sustained overall activity on carbon supports (10^3-10^4 h).
- Silver--This is an attractive air electrode for intermediate performance, but it slowly goes into solution during extended operation.
- Underpotential deposited metals--The adsorption of metal species, e.g., Tl and Pb, on metal catalysts, e.g., Pt and Au, increases the catalytic activity and offsets the inhibiting effects of some impurities (See Figure 67).
- Transition metal oxides--The spinels, e.g., Co_3O_4 and $NiCo_2O_4$, are effective as hydrogen peroxide elimination catalysts and can be used to suppress peroxide in air cathodes catalyzed by Pt.

TABLE XXXIX

CATALYSTS INVESTIGATED AT CASE WESTERN RESERVE UNIVERSITY

METALS
Pure
Alloys
Underpotential Deposited Layers
OXIDES
Spinels
Perovskites
Others (mixed oxides of manganese, nickel, silver; passivation layers; pyrochlores)
INTERCALATION COMPOUNDS
Graphite
TRANSITION METAL COMPLEXES
Phthalocyanines: monomeric, polymeric
porphyrins
Tetraazannulenes
Naphthocyanines
Others, including dimetal
CARBONS AND GRAPHITES
Pure
Doped
Surface Treated

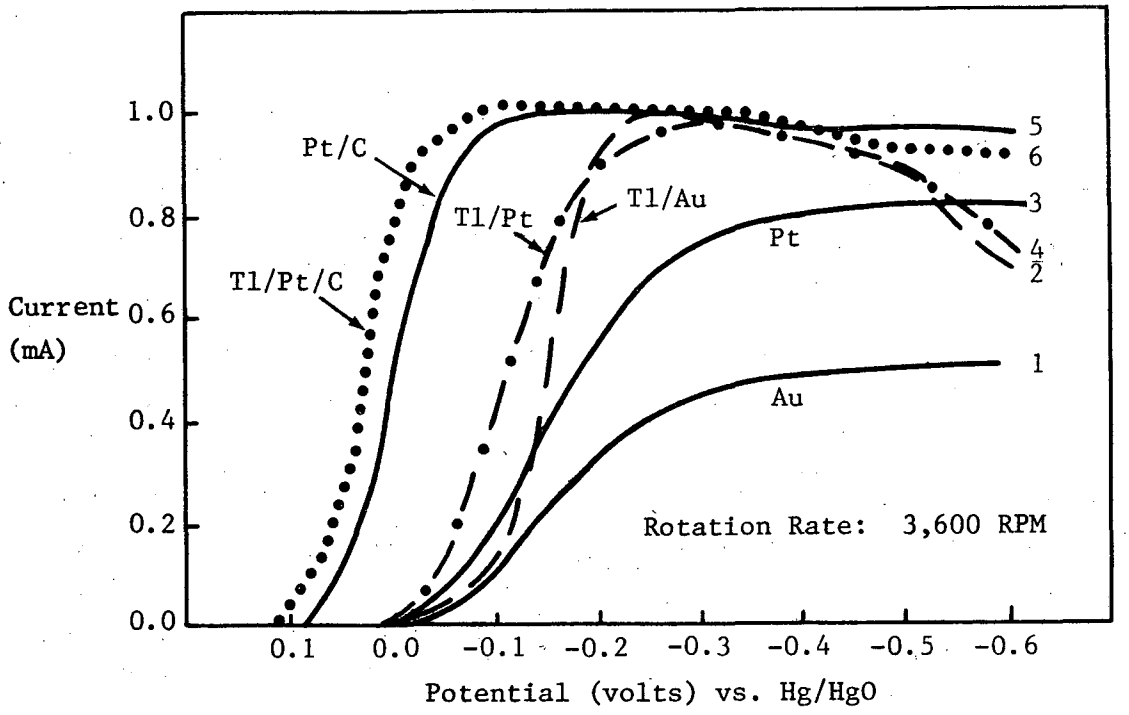

Polarization curves for O_2 Reduction with rotating disk electrode:

1) Gold in 1 M NaOH
2) Gold in 1 M NaOh + 6.6 x 10^{-6} M Tl (I)
3) Platinum in 1 M NaOH
4) Platinum in 1 M NaOH + 3.2 x 10^{-6} M Tl (I)
5) Dispersed Pt/carbon in 1 M NaOH
6) Dispersed Pt/carbon in 1 M NaOH + 1.1 x 10^{-5} M Tl (I)

Scan rate: 10 mV/s (except for dispersed Pt, obtained at steady state).

Electrodes area: 0.196 cm^2. Dispersed Pt/carbon supported as a thin coating on ordinary pyrolytic graphite ($\sim$0.05 mg Pt/cm^2).

FIGURE 67
EFFECT OF UNDERPOTENTIAL DEPOSITED THALLIUM ON OXYGEN REDUCTION

- Perovskites--These, e.g., $La_{0.5}Sr_{0.5}CoO_3$, have substantial activity for oxygen reduction as well as peroxide decomposition but show less overall activity than Pt.

- Macrocyclic catalysts--Several transition metal macrocyclics, e.g., phthalocyanines and porphyrins, have short-term activity comparable to or greater than Pt.

The results of the findings of Case Western Reserve University are being incorporated into test electrodes for Diamond Shamrock Corporation evaluation in the chlor-alkali process.

Ross at the Lawrence Berkeley Laboratory is also studying the electrode kinetics of oxygen reduction on various electrocatalysts. Emphasis is on the following topics:

- The effects of pH on the kinetics of oxygen reduction on Pt.

- The relative kinetics of reduction on clusters vs. bulk metal.

- The effect of the structure of metallic surfaces, including underpotential deposited surfaces, on electrocatalyst reactivity.

- Dual functionality in metal oxide/activated carbon catalysts.

Oxygen reduction on platinum was found to be much more sensitive to the structure of the metal in alkaline than in acid media. Small clusters of platinum, 20 to 30 Å in diameter, were shown to be 10 times more active than similar sized clusters of ruthenium.[110] All other metal clusters of this size studied were less active than ruthenium. Intermetallic cluster catalysts,

such as Pt_3Ti and Ag_3Ti, had improved polarization characteristics relative to the pure metallic clusters. Two reasons were given for this improvement:

- An improved dispersion of the metal on the carbon support; and
- Alteration of the catalytic properties of the noble metal via a ligand effect.

Ross and coworkers are also investigating the reaction kinetics of oxygen reduction on platinum and silver using rotating ring-disc experiments. The reaction pathway used for analyzing the results is shown in Figure 68. The two different pathways generally considered applicable to oxygen reduction are shown--the four- and two-electron catalytic surface reduction steps. These workers have reported a new chronopotentiometric technique which permits the direct measurement of the kinetics of reaction step 4 (k_4).[111]

The initial results confirm other experimental work showing that the four-electron pathway, k_1, is predominant on platinum. On silver only the two-electron path occurs. The importance of recycling via peroxide decomposition on silver was also confirmed. Ross and coworkers indicate that free peroxide in the porous electrode could accelerate its corrosion and loss of hydrophobicity.

6.3 Organic Electrochemical Synthesis

The study by Beck and associates on the potential for energy savings by the electrochemical synthesis of organic compounds was summarized in SR-II. During the period between the third and fourth

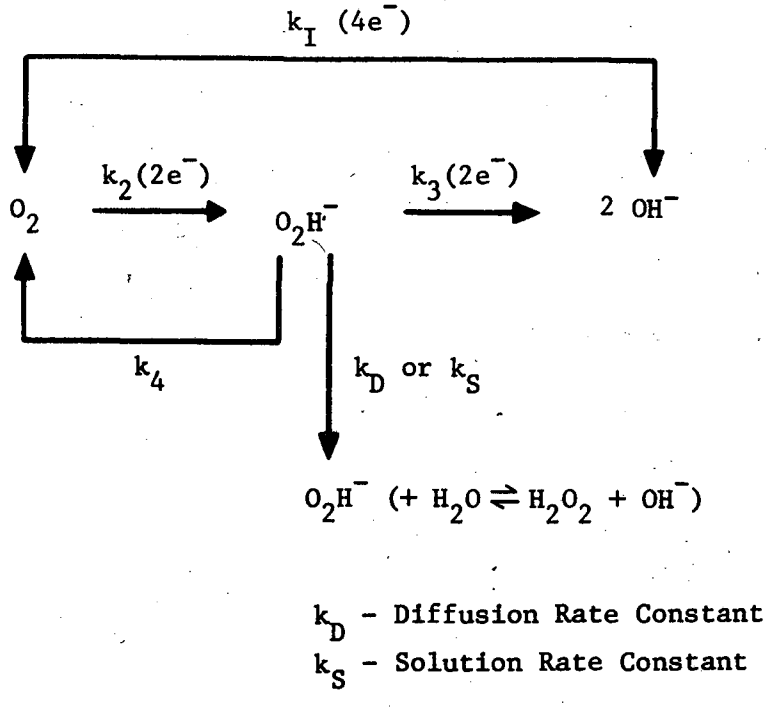

Source: Reference 111.

FIGURE 68
GENERAL REACTION SEQUENCE FOR OXYGEN PATHWAYS IN ALKALINE ELECTROLYTE

BECCs, an experimental program was initiated under the direction of Baizer at the University of California at Los Angeles (UCLA).

This research is emphasizing paired organic reactions, i.e., anode and cathode processes lead to two products or moieties generated at each electrode interact to produce the final product. Examples of each type are shown in Figure 69. In reaction (1) benzene is oxidized at the anode to quinone. In the absence of a membrane the quinone is transported to the cathode becoming hydroquinone. In reaction (2) the acrylic ester is dimerized at the cathode and the dialkyl malonate ester is oxidized at the anode and dimerized to the tetraalkyl ester of tetracarboxyethane. The electrode reactions can be either direct (with the electron transfer to or from an adsorbed organic moiety) or indirect (with the electron transfer to a species which in turn reacts with the organic substrate).

As a model of the paired reaction, Baizer and coworkers are investigating the reactions of glucose. The ring form of glucose, Figure 70, is converted to the aldehyde form at high pH. The latter is reducible to sorbitol and mannitol (not shown). The aldehyde form also can be oxidized by hypobromite ion to gluconic acid in an indirect anodic reaction, as shown in Figure 71. The periodic reversal of the current reduces the bromate formed at the anode to reduce the bromine loss. The simultaneous carrying out of the two reactions enables the production of two products, sorbitol-mannitol

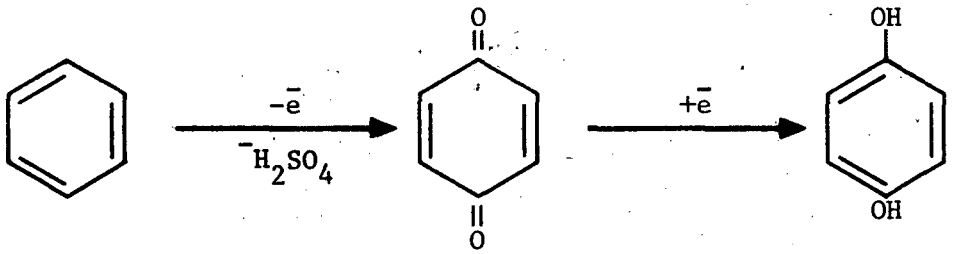

(1)

U.K.
B.R.D.

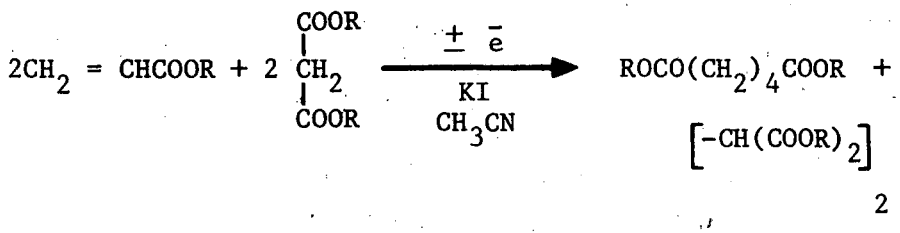

(2)

Source: University of California at Los Angeles.

FIGURE 69
PAIRED ELECTROCHEMICAL REACTIONS

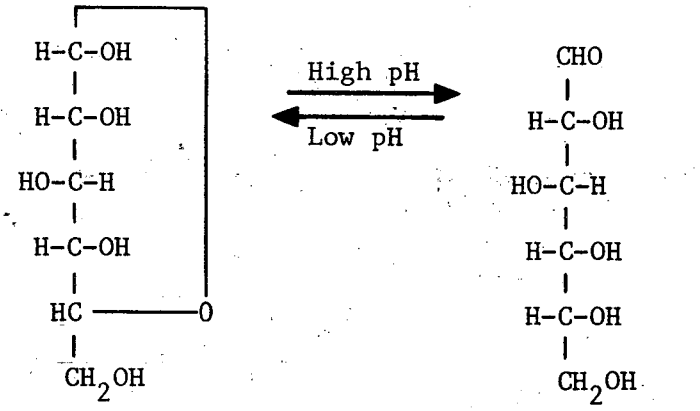

Not Electroreducible Electroreducible

Source: University of California.

FIGURE 70
STRUCTURES OF α-D-GLUCOSE

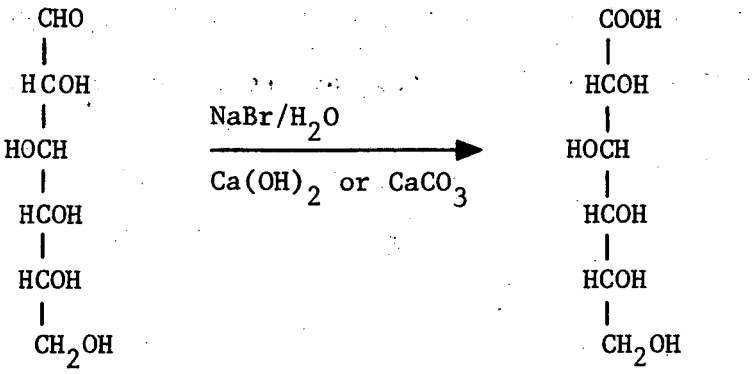

Gluconic Acid
(as Ca salt)

Reported

Yield: > 95%

C.E.: 89-90%*

Mechanism

Indirect via BrO^-

*Bromine "loss" (as BrO_3^-) reduced by imposing 60 cycle A.C. periodically.

Source: University of California at Los Angeles.

FIGURE 71
ELECTROOXIDATION OF GLUCOSE

and gluconic acid, using half the number of Faradays required for the independent electrochemical preparation of the products.

This work is in its initial phases. It should be noted that paired reactions producing two desired products can increase the commercial attractiveness of this approach to electrochemical synthesis.

APPENDIX A

PROGRAM FOR THE FOURTH U.S. DEPARTMENT OF ENERGY
BATTERY AND ELECTROCHEMICAL CONTRACTORS' CONFERENCE

June 2-4, 1981
Washington, D.C.

TUESDAY, JUNE 2

OPENING SESSION

9:30 a.m.	INTRODUCTORY REMARKS Rufus Shivers, U.S. Department of Energy
9:35 a.m.	WELCOME Maxine Savitz, U.S. Department of Energy
9:50 a.m.	OVERVIEW John Brogan, U.S. Department of Energy
10:10 a.m.	OVERVIEW OF DOE'S ELECTROCHEMICAL SYSTEM PROGRAM Al Landgrebe, U.S. Department of Energy
10:45 a.m.	OVERVIEW OF THE EHV PROGRAM Paul Brown, U.S. Department of Energy
11:15 a.m.	OVERVIEW OF DOE'S PHOTOVOLTAIC PROGRAM Richard F. Santopietro, U.S. Department of Energy
11:30 a.m.	OVERVIEW OF DOE'S ELECTRIC ENERGY SYSTEMS Leonard Rogers, U.S. Department of Energy
11:45 a.m.	APPLICATION OF THE "TECHNOLOGY INFORMATION SYSTEM" TO BATTERY AND ELECTROCHEMICAL DATA REQUIREMENTS V.E. Hampel, R.A. Kawin, and L.R. Spogen, Lawrence Livermore Laboratory
SESSION 2	NEAR-TERM BATTERIES
Chairman	N.P. Yao, Argonne National Laboratory

TUESDAY, JUNE 2 (continued)

SESSION 2 (continued)

1:30 p.m.	2.1 NEAR-TERM EV BATTERY PROJECT--OVERVIEW N.P. Yao, C. Christianson, T.S. Lee, J.F. Miller, and J. Rajan, Argonne National Laboratory
1:55 p.m.	2.2 GLOBE LEAD-ACID BATTERY, D.E. Bowman, Johnson Controls, Inc.
2:10 p.m.	2.3 EXXIDE LEAD-ACID EV BATTERIES--A PROGRESS REPORT, D.T. Ferrell and H.A. Guggiti, Exide Management and Technology Co.
2:25 p.m.	2.4 EXPANDED METAL GRIDS FOR ELECTRIC VEHICLE BATTERIES--A PROGRESS REPORT, H.R. Cash and C.J. Venuto, Eltra Electric Vehicles Group
2:40 p.m.	2.5 WESTINGHOUSE NICKEL-IRON TECHNOLOGY FEATURES, R. Rosey, Westinghouse Electric Co.
2:55 p.m.	2.6 NICKEL-IRON TECHNOLOGY FEATURES, E. Broglio and R. Hudson, Eagle-Picher Industries, Inc.
3:25 p.m.	2.7 GOULD NICKEL-ZINC BATTERY, H.R. Espig, Gould Laboratories
3:40 p.m.	2.8 DEVELOPMENT OF LOW-COST NiZn ELECTRIC VEHICLE BATTERIES, A. Leo, M. Klein, and A. Charkety, Energy Research Corporation
3:55 p.m.	2.9 EXIDE LONG LIFE NICKEL-ZINC VIBROCEL™ BATTERY, E. Pearlman, Exide Management and Technology Company
4:10 p.m.	2.10 BATTERY TESTING RESULTS AT THE NATIONAL BATTERY TEST LABORATORY, F. Hornstra, E. Berrill, P. Cannon, D. Corp, W. Deluca, D. Fredrickson, L. Singer, C. Swoboda, C. Webster, C. Christianson, and N.P. Yao, Argonne National Laboratory
4:30 p.m.	2.11 ORGANIZATION OF THE NATIONAL BATTERY ADVISORY COMMITTEE, C.E. Larson, Energy Consultant

TUESDAY, JUNE 2 (continued)

SESSION 3	SOLAR APPLICATIONS
Chairman Co-Chairman	Albert Landgrebe, U.S. Department of Energy Robert Clark, Sandia National Laboratory
1:30 p.m.	INTRODUCTORY REMARKS Albert Landgrebe, U.S. Department of Energy
1:35 p.m.	3.1 BATTERIES FOR SPECIFIC SOLAR APPLICATIONS--PROGRAM OVERVIEW, R. Clark, Sandia National Laboratories
1:45 p.m.	3.2 BATTERY REQUIREMENTS ANALYSIS, D. Caskey, Sandia National Laboratories
2:05 p.m.	3.3 STUDY OF CUSTOMER VERSUS UTILITY LOCATION, OWNERSHIP AND CONTROL OF ELECTRICAL STORAGE, G. Ferrell, Research Triangle Institute
2:20 p.m.	3.4 ELECTRIC RATE ANALYSIS FOR SOLAR PHOTOVOLTAIC/BATTERY ENERGY SYSTEMS, R. Mueller, B. Cha, R. Giese, and S. Nelson, Argonne National Laboratory
2:35 p.m.	3.5 INITIAL LABORATORY EVALUATION OF BATTERIES FOR SOLAR APPLICATIONS, A. Verardo, P.C. Butler, D.M. Bush, and D.W. Miller, Sandia National Laboratories
3:00 p.m.	DISCUSSION
3:20 p.m.	3.6 BATTERIES FOR SOLAR ENERGY STORAGE: RESEARCH AND DEVELOPMENT PROGRAM OVERVIEW, J. Chamberlin, Sandia National Laboratories
3:30 p.m.	3.7 A REDOX BATTERY FOR SOLAR STORAGE, A.W. Nice, NASA Lewis Research Center
3:45 p.m.	3.8 RECENT PROGRESS ON EXXON'S CIRCULATING ZINC BROMINE BATTERY SYSTEM, R.J. Bellows, Exxon Research and Engineering Company
4:00 p.m.	3.9 SEALED BATTERY DEVELOPMENT PROGRAM: OVERVIEW, D.M. Bush, Sandia National Laboratories
4:10 p.m.	3.10 DEVELOPMENT OF A MAINTENANCE-FREE 100 AMPERE-HOUR LEAD-ACID BATTERY FOR DEEP DISCHARGE PHOTOVOLTAIC APPLICATIONS, C. Farris, Eagle-Picher Industries, Inc.

TUESDAY, JUNE 2 (concluded)

SESSION 3 (concluded)

4:25 p.m.	3.11 DEVELOPMENT OF A TOTALLY MAINTENANCE-FREE, DEEP DISCHARGE LEAD-ACID BATTERY FOR PHOTOVOLTAIC APPLICATIONS, J. Szymborski, Gould, Inc.
4:40 p.m.	3.12 ASSESSMENT OF NICKEL-HYDROGEN BATTERIES FOR PHOTOVOLTAIC ENERGY STORAGE, J.E. Clifford, Battelle, Columbus Laboratories
4:55 p.m.	DISCUSSION

WEDNESDAY, JUNE 3

SESSION 4	ADVANCED BATTERIES: SOLID ELECTROLYTES
Chairman	William Frost, U.S. Department of Energy, Chicago
9:00 a.m.	4.1 STATUS OF THE DOE/FORD SODIUM-SULFUR BATTERY DEVELOPMENT PROGRAM, R.A. Harlow, M.L. McClanahan and R.W. Mink, Ford Aerospace and Communications Corp.
9:30 a.m.	4.2 "THE STATUS OF BETA"-ALUMINA ELECTROLYTE DEVELOPMENT, R.S. Gordon and G.R. Miller, Cermatec, Inc.
9:50 a.m.	4.3 THE STATUS OF DOW Na/S BATTERY RESEARCH, C. Nielson and J. Ramos, Dow Chemical Co.
SESSION 5	ADVANCED BATTERIES: FUSED SALT ELECTROLYTES
Chairman	William Frost, U.S. Department of Energy, Chicago
10:30 a.m.	5.1 OVERVIEW OF LITHIUM/IRON SULFIDE BATTERY PROGRAM, D. Barney, Argonne National Laboratory
10:40 a.m.	5.2 LITHIUM/IRON SULFIDE STATUS CELLS PROGRAM, E.C. Gay, Argonne National Laboratory
10:50 a.m.	5.3 RESEARCH AND DEVELOPMENT PROGRAM ON LITHIUM/IRON SULFIDE BATTERIES, R. Steunnberg, Argonne National Laboratory
11:00 a.m.	5.4 LITHIUM/IRON SULFIDE BATTERY DEVELOPMENT, B.A. Askew, Gould Inc.

WEDNESDAY, JUNE 3 (continued)

SESSION 5 (concluded)

11:10 a.m.	5.5 LITHIUM/IRON SULFIDE BATTERY DEVELOPMENT, E. Cupp and R. Hudson, Eagle-Picher Industries, Inc.
11:20 a.m.	5.6 DEVELOPMENT OF BORON NITRIDE FELT SEPARATOR FOR LITHIUM/IRON SULFIDE BATTERIES, F.C. Tompkins, The Carborundum Company
11:30 a.m.	5.7 CAPACITY RETENTION IN FeS_2 ELECTRODES, J.S. Dunning and R.N. Seefurth, General Motors Research Laboratory
11:40 a.m.	5.8 SEPARATOR DEVELOPMENT FOR LITHIUM/IRON SULFIDE BATTERIES, L. McCoy, R.C. Saunders, and S. Sudar, Rockwell International
11:50 a.m.	5.9 DEVELOPMENT OF THERMAL INSULATION FOR HIGH TEMPERATURE BATTERY CASES, J. Nowobilski and A. Acharya, Union Carbide Corporation

SESSION 6	DISPERSED BATTERY APPLICATION
Chairman	Rufus Shivers, U.S. Department of Energy
Co-Chairman	Mohamed Zahid, U.S. Department of Energy, Chicago
9:00 a.m.	INTRODUCTORY REMARKS Rufus Shivers, U.S. Department of Energy
9:05 a.m.	6.1 EVALUATION OF CUSTOMER SIDE OF THE METER BATTERY STORAGE, F.J. Bates, J.E. Clifford, M.L. Duchi, T.R. Martineau, and J.C. Skelton, Battelle, Columbus Division
9:25 a.m.	6.2 BATTERY STORAGE ON NEW YORK CITY SUBWAY SYSTEM, F.V. Strnisa, New York State Energy Research and Development Authority
9:40 a.m.	6.3 DEVELOPMENT OF ADVANCED LEAD-ACID CELL DESIGN FOR LOAD-LEVELING APPLICATIONS, A.M. Chreitzberg, Exide Management and Technology Company
9:55 a.m.	6.4 ADVANCED LEAD-ACID LOAD-LEVELING BATTERY, R.M. Meighan and D.R. Green, C&D Batteries/Allied Chemical Corporation

WEDNESDAY, JUNE 3 (continued)

SESSION 6 (concluded)

10:10 a.m.	6.5 HYDROGEN OXYGEN RECOMBINATION DEVICE (HORD) FOR LOAD-LEVELING LEAD-ACID BATTERIES, K. Ledjeff, VARTA Batteries AG

SESSION 7 — ELECTROLYTIC TECHNOLOGY

Chairman	Stan Ruby, U.S. Department of Energy
Co-Chairman	Bryan Freeman, U.S. Department of Energy, Chicago
10:45 a.m.	7.1 FUEL CELL ELECTRODES IN ELECTROCHEMICAL INDUSTRIES: RECENT DEVELOPMENTS IN ZINC ELECTRO-WINNING, W. Juda, A.B. Ilan, and B. Finnigan, Prototech Company
11:00 a.m.	7.2 OXYGEN ELECTRODES FOR ENERGY CONVERSION AND STORAGE, L.J. Gestaut and I. Malkin, Diamond Shamrock Corporation
11:20 a.m.	7.3 ARGONNE NATIONAL LABORATORY--ELECTROCHEMICAL TECHNOLOGY RESEARCH PROGRAM, R. Loutfy, A. Brown, N.Q. Minh, C.C. Hsu, J. Meisenhelder, and N.P. Yao, Argonne National Laboratory
11:45 a.m.	7.4 PAIRED ORGANIC ELECTROCHEMICAL SYNTHESES IN CONTINUOUS FLOW CELLS, M. Baizer, D. Johnson, and K. Park, University of California, Los Angeles

SESSION 8 — FLOW SYSTEMS BATTERY

Chairman	Al Landgrebe, U.S. Department of Energy
Co-Chairman	Irv Weinstock, The Aerospace Corporation
1:30 p.m.	8.1 COST EFFECTIVE GOALS FOR BATTERY RESEARCH, W. Walsh, R.C. Elliot, R. McAlvey, S.H. Nelson, H.N. Steiger, and P.C. Symons, Argonne National Laboratory
2:00 p.m.	8.2 NASA-REDOX STORAGE SYSTEM PROJECT STATUS--JUNE 1981, A.W. Nice, NASA Lewis Research Center
2:30 p.m.	8.3 RECENT TECHNOLOGY IMPROVEMENTS IN EXXON'S CIRCULATING ZINC-BROMINE BATTERY SYSTEM, R. Bellows, Exxon Research and Engineering Company

WEDNESDAY, JUNE 3 (continued)

SESSION 8 (concluded)

3:00 p.m.	8.4 DEVELOPMENT OF ZINC-BROMINE BATTERIES FOR STATIONARY ENERGY STORAGE, R.A. Putt, Gould, Inc.
3:45 p.m.	8.5 ZINC CHLORIDE ENERGY STORAGE SYSTEM, Energy Development Associates
4:15 p.m.	8.6 RECHARGEABLE ALKALINE ZINC/FERRICYANIDE HYBRID REDOX BATTERY, G.B. Adams, R.P. Hollandworth, and E.L. Littauer, Lockheed Palo Alto Research Laboratories
4:45 p.m.	SUMMARY A.R. Landgrebe, U.S. Department of Energy
5:00 p.m.	DISCUSSION
SESSION 9	ELECTROCHEMICAL RESEARCH
Chairman	Stan Ruby, U.S. Department of Energy
Co-Chairman	Frank McLarnon, Lawrence Berkeley Laboratory
1:30 p.m.	9.1 OVERVIEW OF THE APPLIED BATTERY AND ELECTROCHEMICAL RESEARCH PROGRAM, F.R. McLarnon, Lawrence Berkeley Laboratory
1:45 p.m.	9.2 ELECTRODE KINETICS AND ELECTROCATALYSIS, P.N. Ross, Lawrence Berkeley Laboratory
2:15 p.m.	9.3 FACTORS AFFECTING THE PERFORMANCE OF SOLID ELECTROLYTES, L.C. DeJonghe, Lawrence Berkeley Laboratory
2:45 p.m.	9.4 POTENTIAL USE, FABRICATION AND CHARACTERIZATION OF NASICON SOLID ELECTROLYTES, R. Gordon and G.R. Miller, Ceramatec Inc.
3:30 p.m.	9.5 SODIUM-SULFUR (IV) CHLOROALUMINATE CELL, G. Mamantov, A. Katagiri, K. Tanemoto, Y. Ogata, and R. Marassi, University of Tennessee
4:00 p.m.	9.6 CALCIUM/METAL SULFIDE CELL DEVELOPMENT, M.F. Roche, Argonne National Laboratory

WEDNESDAY, JUNE 3 (concluded)

SESSION 9 (concluded)

4:30 p.m. — 9.7 POLYMERIC ELECTROLYTES FOR BATTERY APPLICATIONS, G. Farrington, W.L. Worrell, F. Tanzella, W. Bailey, D. Frydrych, and W. Johnson, University of Pennsylvania

THURSDAY, JUNE 4

SESSION 10 — ADVANCED BATTERIES: METAL/AIR

Chairman — Stan Ruby, U.S. Department of Energy
Co-Chairman — Erv Behrin, Lawrence Livermore Laboratory

9:00 a.m. — 10.1 THE DOE METAL-AIR PROGRAM, E. Behrin, Lawrence Livermore Laboratory

9:10 a.m. — 10.2 IRON-AIR BATTERY DEVELOPMENT, E.S. Buzzelli, Westinghouse Research and Development Center

9:20 a.m. — 10.3 BIFUNCTIONAL OXYGEN ELECTRODES FOR OXYGEN REDUCTION AND GENERATION, E.B. Yeager, D. Tryk, T. Ohzuku, and W. Aldred, Case Western Reserve University

9:30 a.m. — 10.4 BIFUNCTIONAL AIR ELECTRODES FOR THE Fe-AIR BATTERY, P.N. Ross, Lawrence Berkeley Laboratory

9:40 a.m. — DISCUSSION

9:45 a.m. — 10.5 THE ALUMINUM-AIR BATTERY PROGRAM, J.F. Cooper, Lawrence Livermore Laboratory

9:55 a.m. — 10.6 ALUMINUM/AIR BATTERY HARDWARE DEVELOPMENT AT LOCKHEED MISSILES AND SPACE COMPANY, E.L. Littauer, Lockheed Palo Alto Research Laboratory

10:05 a.m. — 10.7 UNIFUNCTIONAL AIR-ELECTRODE DEVELOPMENT AND TESTING, I. Malkin and A.L. Barnes, Diamond Shamrock Corporation

10:15 a.m. — 10.8 ALUMINUM ANODES FOR ALUMINUM-AIR BATTERY, C. McMinn, D. Scott, and P. McNamara, Reynolds Metals Company

THURSDAY, JUNE 4 (continued)

SESSION 10 (concluded)	
10:25 a.m.	10.9 CRYSTALLIZER RESEARCH, F.S. Williams, Alcoa Laboratories
10:35 a.m.	DISCUSSION
SESSION 11	FUEL CELLS FOR EVs
Chairman Co-Chairman	Al Landgrebe, U.S. Department of Energy Brian McCormick, Los Alamos National Laboratory
11:00 a.m.	11.1 FUEL CELLS FOR ELECTRIC VEHICLES--BACKGROUND, J. Huff, Los Alamos National Laboratory
11:15 a.m.	11.2 FUEL CELL/BATTERY VEHICLE SIMULATION PROGRAM, D. Lynn, Los Alamos National Laboratory
11:30 a.m.	11.3 FUEL CELL POWER PLANTS FOR ELECTRIC VEHICLES: ELECTROCHEMICAL ASPECTS, S. Srinivasan, E.R. Gonzalez, K-L. Ksueh, and C. Derouin, Los Alamos National Laboratory, D-T. Chin, Clarkson College
11:45 a.m.	11.4 FY81 ANNUAL OPERATING PLAN FOR FUEL CELLS FOR TRANSPORTATION, B. McCormick, Los Alamos National Laboratory
SESSION 12	ELECTROCHEMICAL RESEARCH
Chairman	Frank McLarnon, Lawrence Berkeley Laboratory
9:00 a.m.	12.1 THE THERMODYNAMICS AND KINETICS OF DEGRADATION ALKALINE BATTERY ELECTRODES, D.D. Macdonald, Ohio State University
9:30 a.m.	12.2 DEVELOPMENT OF A HIGH RATE INSOLUBLE ZINC ELECTRODE FOR ALKALINE BATTERIES, H. Vaidyanathan, A. Charkey, and C. Hargrave, Energy Research Corporation
SESSION 13	ANALYSES AND SYSTEMS STUDIES
Chairman Co-Chairman	Rufus Shivers, U.S. Department of Energy Joe Asbury, Argonne National Laboratory

THURSDAY, JUNE 4 (concluded)

SESSION 13 (concluded)

10:15 a.m.	13.1 LIFE CYCLE ENERGY ANALYSES OF ELECTRIC VEHICLE AND LOAD-LEVELING STORAGE BATTERIES, D. Sullivan, Hittman Associates
10:30 a.m.	13.2 BATTERY RESOURCE ASSESSMENT, D. Sullivan, Hittman Associates
10:45 a.m.	13.3 RECYCLE OF BATTERY MATERIALS, J.P. Pemsler and R.A. Spitz, Castle Technology Corporation
11:05 a.m.	13.4 NICKEL SUPPLY FOR ELECTRIC VEHICLE BATTERIES, G.W. Tuffnell, International Nickel Company
11:25 a.m.	13.5 HAZARD ASSESSMENTS FOR ELECTRIC VEHICLE BATTERIES, R. Zalosh and V. Hwa, Factory Mutual Research Corporation
11:45 a.m.	13.6 HEALTH AND ENVIRONMENTAL EFFECTS OF NEAR-TERM BATTERY CYCLES, M.H. Bhattacharyya and R.K. Sharma, Argonne National Laboratory

APPENDIX B

ABBREVIATIONS

For the reader's convenience, this appendix lists acronyms and abbreviations that appear frequently throughout the text. An alphabetized list of acronyms is followed by a list of abbreviations for units of measure and periods of time. Finally, there is a table listing the characteristics of Celgard separators mentioned in the report.

ACRONYMS

AC - Alternating Current

ANL - Argonne National Laboratory

BECC - U.S. Department of Energy Battery and Electrochemical Contractors' Conference

BEST Facility - Battery Energy Storage Test Facility

BNL - Brookhaven National Laboratory

CE - Counter Electrode

CMG - Controlled Micro-Geometry

DC - Direct Current

DOD - Depth of Discharge

DOE - Department of Energy

ECPS - Electrochemical Storage Systems Program Summary

ECS - Electrochemical Energy Storage Branch

EDA - Energy Development Associates

EDI - Energy Density Index

EES - Electrical Energy Systems Program (within DOE)

EPRI - Electric Power Research Institute

ERADCOM - Energy Research and Development Command

ERC - Energy Research Corporation

ETV - Electric Test Vehicle

EV - Electric Vehicle

FACC - Ford Aerospace and Communications Company

ISOA - Improved State of the Art

JPL - Jet Propulsion Laboratory

LLNL - Lawrence Livermore National Laboratory

LRS - Laser Raman Scattering

NASA - National Aeronautics and Space Administration

NBTL - National Battery Test Laboratory

NY ERDA - New York Energy Research and Development Administration

PAFC - Phosphoric Acid Fuel Cell

PSE&G - Public Service Electric and Gas Company

PV - Photovoltaic

SIMSTOR - Simulated Storage Computer Program

SNL - Sandia National Laboratories

SOC - State of Charge

SOLSTOR - Solar Energy Storage Computer Program

SR-I - "Status Report-1," Reference 1

SR-II - "Status Report-II," Reference 2

SSA - Specific Solar Applications

TIS - Technical Information System

TOD - Time of Day

UNITS OF MEASURE AND TIME

A - Amp

Ah - Ampere-hour

Atm - Atmosphere

cm - Centimeter

gm - Gram

HP - Horsepower

kcal - Kilocalories

kg - Kilogram

km - Kilometer

kW - Kilowatt

kWh - Kilowatt-hour

M - Mole

A - Milliamp

mm - millimeter

mV - Millivolt

mW - Milliwatt

MW - Megawatt

Sp gr - Specific Gravity

W - Watt

CHARACTERISTICS OF SEPARATORS
DEVELOPED BY THE CELANESE FIBER COMPANY[a]

Material	Description	Resistance ($m\Omega$-in^2 in 34% KOH)
Celgard 2400	1-mil microporous and polypropylene with an average pore size of 200 A in length and 20 A in width (porosity, 38%)	Rather high
Celgard 2500	1-mil microporous polypropylene with an average pore size of 400 A in length and 40 A in width (porosity, 45%)	Rather high
Celgard 3400	Celgard 2400 treated with wetting agents	.007 - .010
Celgard 3500	Celgard 2500 treated with wetting agents	.006 - .007
Celgard K307	Celgard 3400 coated on both faces with a 0.1-mil layer of cellulose acetate	.010 - .012

[a]Table lists Celgard materials discussed in this document that are being evaluated in the Army Electronics Research and Development Command nickel-zinc program.

Source: U.S. Army Electronics Research and Development Command, 1981. High Cycle Life, High Energy Density Nickel-Zinc Batteries, Report No. 4. PSD-4C. Fort Monmouth, New Jersey.

REFERENCES

1. Roberts, R., 1979. Status of the DOE Battery and Electrochemical Technology Program. MTR-8026. The MITRE Corporation, McLean, Virginia. August.

2. Roberts, R., 1980. Status of the DOE Battery and Electrochemical Technology Program II. MTR 80W15. The MITRE Corporation, McLean, Virginia. December.

3. U.S. Department of Energy, 1981. Fourth U.S. Department of Energy Battery and Electrochemical Contractors' Conference: Abstracts and Visual Presentations. The Aerospace Corporation, Germantown, Maryland. June.

4. U.S. Department of Energy, 1981. Electrochemical Storage Systems Program Summary: DOE Battery and Electrochemical Contractors' Conference. The Aerospace Corporation, Germantown, Maryland. June.

5. Savitz, M., 1981. "Welcoming Remarks before Fourth DOE Battery and Electrochemical Contractors' Conference." U.S. Department of Energy, Washington, D.C. 2 June.

6. Sharma, R.K., M.F. Bender, P. Benioff, M.H. Bhattacharyya, C.D. Brown, M.G. Chasanov, J.R.B. Curtiss, D.P. Peterson, L.F. Soholt, and R.W. Vocke, 1980. Ecological and Biomedical Effluents from Near-Term Electric Vehicle Storage Battery Cycles. ANL/ES-90. Argonne National Laboratory, Argonne, Illinois. May.

7. Roberts R., 1971. "Fuel and Continous-Feed Cells." The Primary Battery, pp. 331-332. G.W. Heise and N.C. Cahoon (eds.). J. Wiley and Sons, New York.

8. McCormack, B., J. Huff, S. Srinivasan, R. Bobbert, 1979. Application Scenario for Fuel Cells in Transportation. LA-7643PMS. Los Alamos Scientific Laboratory informal report, Los Alamos, New Mexico.

9. Caskey, D.L. (ed.), 1981. Batteries for Specific Solar Applications: Annual Report, May 1979-December 1980. SAND 81-0329. Sandia National Laboratories, Albuquerque, New Mexico. April.

10. Johnson Controls, Inc., 1981. Annual Report for 1980 on Research, Development, and Demonstration of Lead-Acid Batteries for Electric Vehicle Propulsion. ANL/OEPM-80-12. Globe Battery Division, Milwaukee, Wisconsin.

11. Exide Management and Technology Co., 1981. Annual Report for 1980 on Research, Development, and Demonstration of Lead-Acid Batteries for Electric Vehicle Propulsion. ANL/OEPM-80-11. Argonne National Laboratory, Argonne, Illinois. March.)

12. C&D Batteries Division of Eltra Corp., 1981. Annual Report for 1980 on Research, Development and Demonstration of Lead-Acid Batteries for Electric Vehicle Propulsion. ANL/OEPM-80-10. Argonne National Laboratory, Argonne, Illinois. March.

13. Wierschem, G.L., and W.H. Tiedemann, 1980, Battery Division Extended Abstracts. The Electrochemical Society Inc., Pennington, New Jersey. Fall Meeting, 5-10 October.

14. Chreitzberg, A.M., T.M. Noveske, and W.P. Sholette, 1981. Battery Division Extended Abstracts, p. 13. The Electrochemical Society, Inc., Pennington, New Jersey. Fall Meeting, 11-16 October.

15. Noreske, T.M., and A.M. Chreitzberg, 1981. Battery Division Extended Abstracts, p. 13. The Electrochemical Society, Inc., Pennington, New Jersey. Fall Meeting, 11-16 October.

16. Varma, R., G. Cook, and N.P. Yao, 1978. Monitoring Stibine and Arsine in Lead-Acid Battery Charge Gas and in Ambient Air: Development and Testing of a Field Kit. ANL/OEPM-78-4. Argonne National Laboratory Argonne, Illinois. November.

17. Sklarchuk, J.C., and A.M. Chreitzberg, 1981. Battery Division Extended Abstracts, p. 16. The Electrochemical Society, Inc, Pennington, New Jersey. Fall Meeting, 11-16 October.

18. Varma, R., G. Cook, and N.P. Yao, 1981. J. Electrochem. Soc. 128:(5):1165.

19. Walls, C.P., G.M. Caulder, and A.C. Simon, 1981. J. Electrochem. Soc.128(2):236.

20. Mahato, B.K., 1980. J. Electrochem. Soc.127(8):1979.

21. Mahato, B.K., 1980. J. Electrochem Soc.128(7):1416.

22. Eagle-Picher Industries, Inc., 1981. Annual Report for 1980 on Research, Development, and Demonstration for Electric Vehicle Propulsion. ANL/OEPM-80-16. Argonne National Laboratory, Argonne, Illinois. March.

23. Westinghouse Electric Corp., 1981. Annual Report for 1980 on Research, Development, and Demonstration of Nickel-Iron Batteries for Electric Vehicle Propulsion. ANL/OEPM-80-17. Argonne National Laboratory, Argonne, Illinois. March.

24. Energy Research Corp., 1981. Annual Report for 1980 on Research, Development, and Demonstration of Nickel-Zinc Batteries for Electric Vehicle Propulsion. ANL/OEPM-80-13. Argonne National Laboratory, Aronnne, Illinois. March.

25. Gould, Inc., 1981. Annual Report for 1980 on Research, Development, and Demonstration of Nickel-Zinc Batteries for Electric Vehicle Propulsion. ANL/OBDM-80-14, Contract No. 31-109-38-4200. Argonne National Laboratory, Argonne, Illinois. March.

26. Wagner, O.C., 1981. High Cycle Life, High Energy Density Nickel-Zinc Batteries: Report No. 4. ERADCOM Report No PSD-4C. Electronics Research and Development Command, Fort Manmouth, New Jersey. January.

27. Ferrando, W.A., and R.A. Sutula, 1980. U.S. Patent 4,215,190

28. Pickett, D.F., 1975. Fabrication and Investigation of Nickel-Alkaline Cells, Part 1, Fabrication of Nickel Hydroxide Electrodes Using Electrochemical Impregnation Techniques. AFAPL-TR-75-34(1975). Air Force Aero Propulsion Laboratory, Wright Patterson Air Force Base, Ohio.

29. Thornell, S., and E. Pearlman, 1981. Battery Division Extended Abstracts, p. 103. The Electrochemical Society, Inc., Fall Meeting, 11-16 October.

30. Exide Management and Technology Corp., 1981. Annual Report for 1980 on Research, Development, and Demonstration of Nickel-Zinc Batteries for Electric Vehicle Propulsion. ANL/OEPM-80-15. Argonne National Laboratory, Argonne, Illinois. March.

31. McBreen, J., G. Adzic, D.T. Chin, M.G. Chu, E. Gammon, R. Sethi, 1980. "Investigation of the Zinc Electrode Reaction." Brookhaven National Laboratory Annual Report: October 1, 1979-September 30, 1980. BNL 51370. Upton, New York. December.

32. Katan, T., P.J. Bergeron, and S. Szpak, 1979. Extended Abstracts, vol. 79-2., p. 430. Electrochemical Society, Inc., Pennington, New Jersey.

33. Katan, T. and P.J. Carlen, 1981. Battery Division Extended Abstracts, p.163. The Electrochemical Society, Inc., Pennington, New Jersey. Fall Meeting, 11-16 October.

34. Liu, M.B., G.M. Cook, and N.P. Yao. 1980. Galvanostatic Polarization of Zinc Microanodes in KOH Electrolytes. ANL/OEPM-80-1. Argonne National Laboratory, Argonne, Illinois. May. Also J. Electrochem. Soc.128(8):1663).

35. Yamazaki, Y., and N.P. Yao, 1981. J. Electrochem. Soc. 128(8):1655-1658.

36. Yamazaki, Y., and N.P. Yao, 1981. J. Electrochem. Soc. 128(8):1658-1662.

37. Liu, M.B., B.R. Faulds, G.M. Cook, and N.P, Yao. 1981. J. Electrochem. Soc.128(10):2049.

38. Liu, M.B., G.M. Cook, N.P. Yao, and J.S. Selman (in press). "Vibrating Zinc Electrodes in Ni/Zn Batteries." Argonne National Laboratory, Argonne, Illinois.

39. Lenhart, S.J., C.Y. Chao, and D.D. Macdonald, 1981. 16th Intersociety Energy Conversion Engineering Conference, 9-14 August, paper no. 819325, p. 663. The American Society of Mechanical Engineers, New York, New York.

40. Katan, T., J. Savory, and J. Perkins, 1979. J. Electrochem. Soc.126:1836.

41. Jackovitz, J.F., and J. Seidel, 1981. Battery Division Extended Abstracts, p. 66. The Electrochemical Society, Inc. Pennington, New Jersey. Fall Meeting, 11-16 October.

42. Sanderaj, B.K., R.P. Singh, and D.D. Macdonald, 1981. 16th Intersociety Energy Conversion Engineering Conference, 9-14 August, paper No. 819324, p. 658. The American Society of Mechanical Engineers, New York, New York.

43. Himy, A., 1981. 16th Intersociety Energy Conversion Engineering Conference, 9-14 August, paper no. 819321, p. 645. The American Society of Mechanical Engineers, New York, New York.

44. Demczyk, B.B., P.L. Ulerich, and E.S. Buzzelli, 1981. 16th Intersociety Energy Conversion Engineering Conference, 9-14 August, paper no. 819323, p. 653. The American Society of Mechanical Engineers, New York, New York.

45. Buzzelli, E.S., 1981. Extended Abstracts, vol. 81-2, p. 298. The Electrochemical Society, Inc., Pennington, New Jersey. Fall Meeting, 11-16 October.

46. Buzzelli, E.S., C.T. Liu, and W.A. Bryant, 1980. Iron-Air Battery Development Program. Final Report for 1979. DOE/ET/13390-TI. Westinghouse R&D Center, Pittsburgh, Pennsylvania. May.

47. Yeager, E., D. Tryk, T. Ohzuker, and W. Aldred, 1981. Bifunctional Oxygen Electrodes. Quarterly Report No. 2, 1 January 1981 to 31 March 1981. BOR. No. A1-05-10-10. Case Western Reserve University, Cleveland, Ohio. April.

48. Ohzuka, T., D.A. Tryk, and E.B. Yeager, 1981. Extended Abstracts, vol. 81-2, p. 293. The Electrochemical Society, Inc., Pennington, New Jersey. 11-16 October.

49. Liu, C.T., 1981. Extended Abstracts, vol. 81-2, p. 292. Electrochemical Society, Inc., Pennington, New Jersey. Fall Meeting, 11-16 October.

50. Morris, J.L., and K.C. Tsai, 1981. Extended Abstracts, vol. 81-2, p. 318. The Electrochemical Society, Inc., Pennington, New Jersey. Fall Meeting, 11-16 October.

51. Malkin, I, A.L. Barnes, and F. Solomon, 1981. Extended Abstracts, vol. 81-2, p. 270. The Electrochemical Society, Inc., Pennington, New Jersey. Fall Meeting, 11-16 October.

52. Clifford, J.E., and E.W. Brooman. 1981. Assessment of Nickel-Hydrogen Batteries for Terrestrial Solar Applications. SAND 80-7191. Final Report Sandia National Laboratories, Albuquerque, New Mexico. February

53. Zahn M., P.G. Grimes, and R.J. Bellows, 1980. U.S. Patent 4,197,169. April 8.

54. Putt, R.A., 1981. 16th Intersociety Energy Conversion Engineering Conference, 9-14 August, paper no. 819381, p. 793. American Society of Mechanical Engineers, New York, New York.

55. Adams, G.B., R.P. Hollandsworth and E.L. Littover, 1981. 16th Intersociety Energy Conversion Engineering Conference, 9-14 August, paper no. 81934, p. 812. American Society of Mechanical Engineers, New York, New York.

56. Thuller, L.H., 1979. Redox Flow Cell Energy Storage Systems. NASA-TM-79143, DOE/NASA/1002-79/3. National Aeronautics and Space Administration, Cleveland, Ohio.

57. Hagedorn, N.H., 1981. 16th Intersociety Energy Conversion Engineering Conference, 9-14 August, paper no. 819383, p. 805. American Society of Mechanical Engineers, New York, New York.

58. Ling, J.S., and J. Charleston, 1980. Advances in Membrane Technology for the NASA Redox Energy Storage System. NASA TM-82701, DOE/NASA TM-82701. National Aeronautics and Space Administration, Cleveland, Ohio. September.

59. Hoberecht, M.A., 1981. Pumping Power Considerations in the Design of NASA-Redox Flow Cells. NASA TM-82598, DOE/NASA/12726-7. National Aeronautics and Space Administration, Cleveland, Ohio. June.

60. Gahn, R.F., and L.H. Thaller, 1981. Extended Abstracts, vol. 81-2, p. 28. The Electrochemical Society, Inc., Pennington, New Jersey. Fall Meeting, 11-16 October.

61. Kolba, V.M., J.E. Battles, J.D. Geller, and K. Gentry, 1980. Failure Analysis of Mark IA Lithium/Iron Sulfide Battery. ANL 80-44. Argonne National Laboratory, Argonne, Illinois. October.

62. Battles, J.E., F.C. Mrazek, and N.C. Otto, 1980. Post-Test Examinations of Li-Al/FeSx Secondary Cells. ANL-80-130. Argonne National Laboratory, Argonne, Illinois. December.

63. Kaun, T.D., W.E. Miller, and J.D. Arnzten, 1980. Extended Abstracts of Battery Division, p. 202-205. The Electrochemical Society, Inc., Pennington, New Jersey. Fall Meeting, 5-10 October.

64. Farahat, M.M., A.A. Chilenskas, and D.L. Barney, 1981. 16th Intersociety Energy Conversion Engineering Conference, paper no. 819360, p. 744. American Society of Mechanical Engineers, New York, New York, 9-14 August.

65. Farahat, M.M., A.A. Chilenskas, and D.L. Barney, 1980. Battery Division Extended Abstracts, p. 234. The Electrochemical Society, Inc., Pennington, New Jersey. Fall Meeting, 5-10 October.

66. Gibbard, H.F., D.M. Chen, C.C. Chen, and T.W. Olszanski, 1981. 16th Intersociety Energy Conversion Engineering Conference, paper no. 819362, p. 752. American Society of Mechanical Engineers, New York, New York, 9-14 August.

67. Chen, C.C., T.W. Olszanski, and H.F. Gibbard, 1981. Battery Division Extended Abstracts, p. 126. The Electrochemical Society, Inc., Pennington, New Jersey. Fall Meeting, 11-16 October.

68. Fisher, A.K., and D.R. Vessers, 1980. Battery Division Extended Abstracts, p. 240. The Electrochemical Society, Inc., Pennington, New Jersey. Fall Meeting, 5-10 October.

69. Bartholme, L.G., E.C. Gag, and H. Shimotake, 1980. Battery Division Extended Abstracts. The Electrochemical Society, Inc., Pennington, New Jersey. Fall Meeting, 5-10 October.

70. Braunstein, J., S. Cantor, and C.E. Vallet, 1981. 16th Intersociety Energy Conversion Engineering Conference, 9-14 August, paper no. 819363, p. 757. American Society of Mechanical Engineers, New York, New York.

71. Pollard, R., and J. Newman, 1980. LBL 10420. January. (As cited in reference 72).

72. Pollard, R., and J. Newman, 1981. Applied Battery and Electrochemical Research Program for Fiscal Year 1980, LBL-12514 UC-94c, p. 48. E. Cairns, L. DeJonghe, J. Evans, F. McLarnon, R. Muller, J. Newman, P. Ross, and C. Tobias (eds.). Lawrence Berkeley Laboratory, Berkeley, California. April.

73. Dunning, J.S., R.N. Seefurth, and R.A. Marie, 1980. Battery Division Extended Abstracts, p. 206. The Electrochemical Society, Inc., Pennington, New Jersey. Fall Meeting, 5-10 October.

74. Seefurth, R.N., and J.S. Dunning, Battery Division Extended Abstracts, p. 237. The Electrochemical Society, Inc., Pennington, New Jersey. Fall Meeting, 5-10 October.

75. Tomczuk, Z., M.F. Roche, and D.R. Vissers, 1980. Battery Division Extended Abstracts, p. 209. The Electrochemical Society, Inc., Pennington, New Jersey. Fall Meeting, 5-10 October.

76. Bandyopadhyay, G., and T.M. Galvin, 1980. Battery Division Extended Abstracts, p. 305. The Electrochemical Society, Inc., Pennington, New Jersey. Fall Meeting, 5-10 October.

77. Haskins, H.J., and A.G. Domaszwicz, 1981. 16th Intersociety Energy Conversion Engineering Conference, 9-14 August, paper no. 819393, p. 836. American Institute of Mechanical Engineers, New York, New York.

78. DeJonghe, L.C., 1980. Improved Beta-Alumina Electrolytes for Advanced Storage Batteries. Progress Report. LBL-12357 UC-94cc. Lawrence Berkeley Laboratory, Berkeley, California. September.

79. Levine, C.A., 1981. "Recent Progress on the Development of the Dow Hollow Fiber Sodium-Sulfur Battery." 16th Intersociety Energy Conversion Engineering Conference, 9-14 August, p. 823. American Society of Mechanical Engineers, New York, New York.

80. Brummer, S.B., R.D. Rank, K.M. Abraham, V. Subrahmanyam, G.F. Pearson, J.K. Surpredant, and J.M. Bugby, 1980. Low Temperature Alkali Metal-Sulfur Batteries. Final Report, COO-2520-7. EIC Corp., Newton, Massachusetts. March.

81. Abraham, K.M., M.W. Rupich, L. Pitts, and C.J. Mattos, 1981. Extended Abstracts, vol. 81-2, p. 1232. The Electrochemical Society, Inc., Pennington, New Jersey. Fall Meeting, 11-16 October.

82. Brummer, S.B., 1980. "Study of the Status of Ambient Temperature Secondary Lithium Batteries" Applied Battery and Electrochemical Research Program: Report for Fiscal Year 1981, p. 5. LBL-12514. E. Cairns, L. DeJonghe, J. Evans, E. McLarnon, R. Muller, J. Newman, P. Ross, and C. Tobias (eds.), Lawrence Berkeley Laboratory, Berkeley, California. April

83. Eisenberg, M., 1980. Battery Division Extended Abstracts, p. 133. The Electrochemical Society, Inc., Pennington, New Jersey. Fall Meeting, 5-10 October.

84. Eisenberg, M., 1981. Study of the Secondary Li Electrode in Organic Electrolyte. LBL-13263. Lawrence Berkeley Laboratory, Berkeley, California. April.

85. Schwager, F., and R.H. Muller., 1981. "Ellipsometric Studies of Lithium in Propylene Carbonate Solutions." Applied Battery and Electrochemical Research Program: Report for Fiscal Year 1980, p. 41. LBL-12514 UC-94c. E. Cairns, L. DeJonghe, J. Evans, F. McLarnon, R. Muller, J. Newman, P. Ross, and C. Tobias, (eds.). Lawrence Berkeley Laboratory, Berkeley, California. April.

86. Geronov, Y., and R.H. Muller, 1981. "Transient Electrochemical Measurements on Lithium in Propylene Carbonate Solutions." Applied Battery and Electrochemical Research Program: Report for Fiscal Year 1980, p. 44. LBL-12514 UC-94c. E. Cairns, L. DeJonghe, J. Evans, F. McLarnon, R. Muller, J. Newman, P. Ross, and C. Tobias (eds.). Lawrence Berkeley Laboratory, Berkeley, California. April.

87. Law, H.H., R. Atanasoski, and C.W. Tobias, 1980. Battery Division Extended Abstracts, p. 106. The Electrochemical Society, Inc. Pennington, New Jersey. Fall Meeting, 5-10 October.

88. Dey, A.N, 1980. "All-Inorganic Ambient Temperature Lithium Battery." Applied Battery and Electrochemical Research Program: Report for Fiscal Year 1980, p. 13. LBL-12514 UC-94c. E. Cairns, L. DeJonghe, J. Evans, F. McLarnon, R. Muller, J. Newman, P. Ross, and C. Tobias, (eds.). Lawrence Berkeley Laboratory, Berkeley, California. April.

89. Litt, M., 1980. "Research on Novel Membranes for Lithium Batteries." Applied Battery and Electrochemical Research Program: Report for Fiscal Year 1980, p. 131. LBL-12514 UC-94c. E. Cairns, L. DeJonghe, J. Evans, F. McLarnon, R. Muller, J. Newman, P. Ross and C. Tobias, (eds.). Lawrence Berkeley Laboratory, Berkeley, California. April.

90. Mamantov, G., R. Marassi, M. Matsunaga, Y. Ogata, J. P. Wiaux, and E.J. Frazer, 1980. J. Electrochem. Soc. 127(11):2319.

91. Mamantov, G., R. Marassi, Y. Ogata, M. Matsunaga, and J.P. Wiaux, 1980. 15th Intersociety Energy Conversion Engineering Conference, 18-22 August, p. 569. American Institute of Aeronautics and Astronautics, New York, New York.

92. Rey, R., 1981. "Performance Characterization of a Solid-State Storage Battery." Applied Battery and Electrochemical Research Program: Report for Fiscal Year 1980, p. 11. LBL-12514 UC-94c. E. Cairns, L. De Jonghe, J. Evans, F. McLarnon, R. Muller, J. Newman, P. Ross and C. Tobias, (eds.). Lawrence Berkeley Laboratory, Berkeley, California. April.

93. Gordon, R., and G. Miller, 1981. "Fabrication and Characterization of Polycrystalline Nasicon Ceramic Electrolytes." Applied Battery and Electrochemical Research Program: Report for Fiscal Year 1980, p. 120. LBL-12514 UC-94c. E. Cairns, L. De Jonghe, J. Evans, F. McLarnon, R. Muller, J. Newman, P. Ross and C. Tobias, (eds.). Lawrence Berkeley Laboratory, Berkeley, California. April.

94. Hitchock, D.C., C.P. Cameron, H.K. Schmid, and L.C. DeJonghe, 1981. "Properties of Nasicon." Applied Battery and Electrochemical Research Program: Report for Fiscal Year 1980, p. 65. LBL-12514 UC-94c. E. Cairns, L. DeJonghe, J. Evans, F. McLarnon, R. Muller, J. Newman, P. Ross and C. Tobias, (eds.). Lawrence Berkeley Laboratory, Berkeley, California. April.

95. Wuensch, B., 1980. "Principles of Superionic Conduction." Applied Battery and Electrochemical Research Program: Report for Fiscal Year 1980. LBL-12514 UC-94c. E. Cairns, L. DeJonghe, J. Evans, F. McLarnon, R. Muller, J. Newman, P. Ross and C. Tobias, (eds.). Lawrence Berkeley Laboratory, Berkeley, California. April.

96 Tuller, H., and D. Uhlmann, 1981. "Electrical Conduction and Corrosion Processes in Fast Lithium Ion Conducting Glasses." Applied Battery and Electrochemical Research Program: Report for Fiscal Year 1980, p. 122. LBL-12514 UC-94c. E. Cairns, L. DeJonghe, J. Evans, F. McLarnon, R. Muller, J. Newman, P. Ross and C. Tobias, (eds.). Lawrence Berkeley Laboratory, Berkeley, California. April.

97 Boukamp, B.A., G.C. Lesh, and R.A. Huggins, 1981. J. Electrochem. Soc. 128(4):725.

98. Godshall, N.A., I.D. Raistrick, and R.A. Huggins, 1981. "Thermodynamic Aspects of the Reactions of Lithium with Ternary Positive Electrode Systems." 16th Intersociety Energy Conversion Engineering Conference, 9-14 August, paper no. 819371, p. 769. American Institute of Mechanical Engineers, New York, New York.

99. Raistrick, I.D., J. Poris, and R.A. Huggins, 1981. 16th Intersociety Energy Conversion Engineering Conference 9-14 August, paper no. 819372, p. 774. American Institute of Mechanical Engineers, New York, New York.

100. Kindler, A., and C.W. Tobias, 1981. "Microstructural Development During Mass Transfer Controlled Deposition." Applied Battery and Electrochemical Research Program: Report for Fiscal Year 1980, p. 41. LBL-12514 UC-94c. E. Cairns, L. De Jonghe, J. Evans, F. McLarnon, R. Muller, J. Newman, P. Ross and C. Tobias, (eds.). Lawrence Berkeley Laboratory, Berkeley, California. April.

101. Falteomier, J.L., V. Kommenic, T. Tsuda, and C.W. Tobias, 1981. "Effects of Hydrodynamic Flow on the Electrocrystallization of Zinc from Acid Electrolytes." Applied Battery and Electrochemical Research Program: Report for Fiscal Year 1980, p. 41. LBL-12514 UC-94c. E. Cairns, L. DeJonghe, J. Evans, F. McLarnon, R. Muller, J. Newman, P. Ross and C. Tobias, (eds.). Lawrence Berkeley Laboratory, Berkeley, California. April.

102. Evans, J.W., 1981. "Improvements in Efficiency of Aluminum Reduction Cells." Applied Battery and Electrochemical Research Program: Report for Fiscal Year 1980, p. 57. LBL-12514 UC-94C. E. Cairns, L. DeJonghe, J. Evans, F. McLarnon, R. Muller, J. Newman, P. Ross, and C. Tobias, (eds.). Lawrence Berkeley Laboratory, Berkeley, California. April.

103. Lympany, S., and J.W. Evans, 1981. "Current Inefficiencies in Aluminum Reduction Cells." Applied Battery and Electrochemical Research Program: Report for Fiscal Year 1980, p. 59. LBL-12514 UC-94c. E. Cairns, L. De Jonghe, J. Evans, F. McLarnon, R. Muller, J. Newman, P. Ross, and C. Tobias, (eds.). Lawrence Berkeley Laboratory, Berkeley, California. April.

104. Battelle Columbus Laboratories, 1979. A Survey of Electrochemical Metal Winning Processes. ANL/DEPM 79-3. Argonne National Laboratory, Argonne, Illinois. March.

105. Meisenhelder, S.H., A.P. Brown, R.O. Loutfy, and N.P. Yao, 1981. An Evaluation of the Alkaline Electrolysis of Zinc. ANL/DEPM-81-2. Argonne National Laboratory, Argonne, Illinois. May.

106. Prototech Co., 1979. "Energy Savings by Means of Fuel Cell Electrodes in Electrochemical Industries." Prototech Company Annual Report, pp. 163, 164. 31 October.

107. Pemsler, J.P., and R.A. Pitz, 1981. Battery Division Extended Abstracts, p. 50. The Electrochemical Society Inc., Pennington, New Jersey. Fall Meeting, 11-16 October.

108. Castle Technology Corporation, 1980. Survey of Electrochemical Production of Inorganic Compounds: Final Report. ANL/DEPM-80-3. Argonne National Laboratory, Argonne, Illinois. October.

109. Abam Engineers, Inc., 1980. Process Engineering and Economic Evaluations of Diaphragm and Membrane Chloride Cell Technologies: Final Report. ANL/DEPM-80-9. Argonne National Laboratory, Argonne, Illinois. December.

109. Ross, P.N., and L.R. Johnson, 1981. "Oxygen Reduction with Carbon Supported Metallic Cluster Catalysts in Alkaline Electrolyte." Applied Battery and Electrochemical Research Program: Report for Fiscal Year 1980, p. 70. LBL-12514 UC-94c. E. Cairns, L. DeJonghe, J. Evans, F. McLarnon, R. Muller, J. Newman, P. Ross, and C. Tobias, (eds.). Lawrence Berkeley Laboratory, Berkeley, California. April.

110. Ross, P.N., and D.A. Scherson, 1981. "Rotating Ring-Disc Studies of Oxygen Reduction of Pt and Ag in Alkaline Electrolyte." Applied Battery and Electrochemical Research Program: Report for Fiscal Year 1980, p. 75. LBL-12514 UC-94c. E. Cairns, L. DeJonghe, J. Evans, F. McLarnon, R. Muller, J. Newman, P. Ross, and C. Tobias, (eds.). Lawrence Berkeley Laboratory, Berkeley, California. April.

This report was done with support from the Department of Energy. Any conclusions or opinions expressed in this report represent solely those of the author(s) and not necessarily those of The Regents of the University of California, the Lawrence Berkeley Laboratory or the Department of Energy.

Reference to a company or product name does not imply approval or recommendation of the product by the University of California or the U.S. Department of Energy to the exclusion of others that may be suitable.

TECHNICAL INFORMATION DEPARTMENT
LAWRENCE BERKELEY LABORATORY
UNIVERSITY OF CALIFORNIA
BERKELEY, CALIFORNIA 94720